EIC and quarkonia

Charlotte Van Hulse
University of Alcalá

AdT

Comunidad de Madrid

Quarkonia as Tools 2024
January 08 – 13, 2024
Aussois, France

The electron-ion collider (EIC)

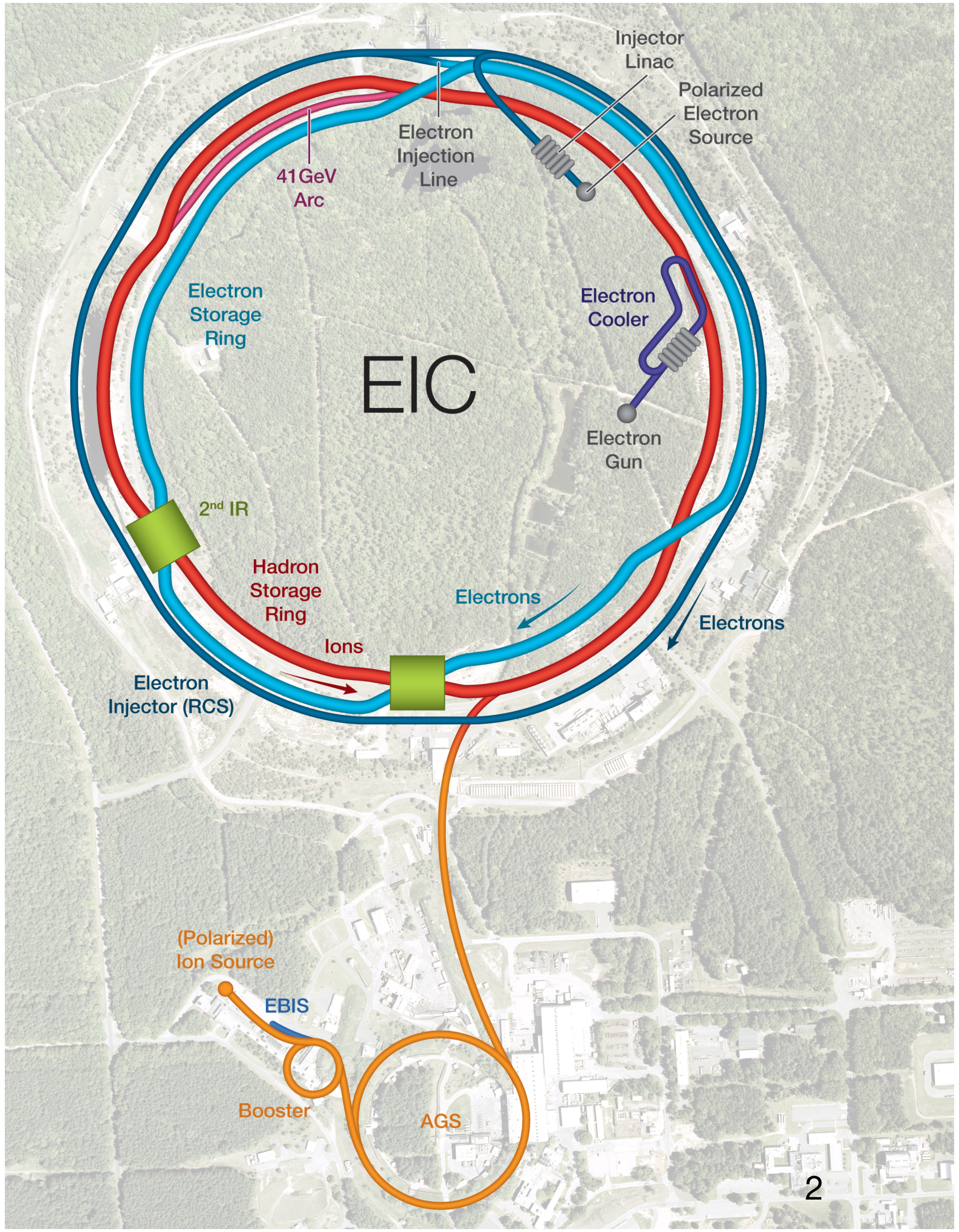

- Based on RHIC:
  - use existing hadron storage ring energy: 41–275 GeV
  - add electron storage ring in RHIC tunnel energy: 5–18 GeV

  $\rightarrow \sqrt{s_{NN}} = 29 - 141\ (90)$ GeV

The electron-ion collider (EIC)

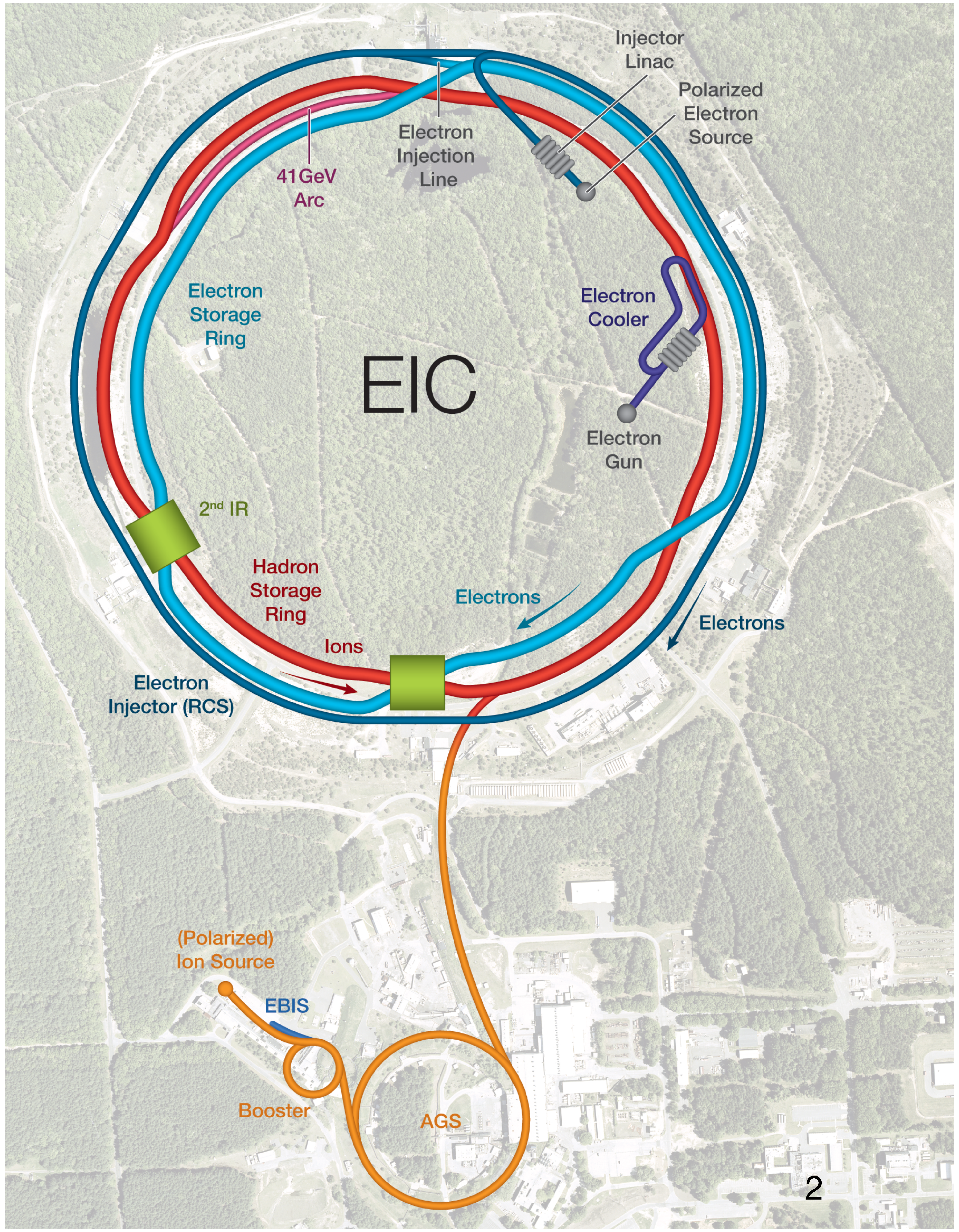

- Based on RHIC:
  - use existing hadron storage ring energy: 41–275 GeV
  - add electron storage ring in RHIC tunnel energy: 5–18 GeV

  $\rightarrow \sqrt{s_{NN}} = 29 - 141\ (90)$ GeV

- $\overrightarrow{e} + \overrightarrow{p}^{\uparrow}, \overrightarrow{d}^{\uparrow}, \overrightarrow{He}^{\uparrow}$, unpolarised ions up to U

  ~ 70% polarisation

The electron-ion collider (EIC)

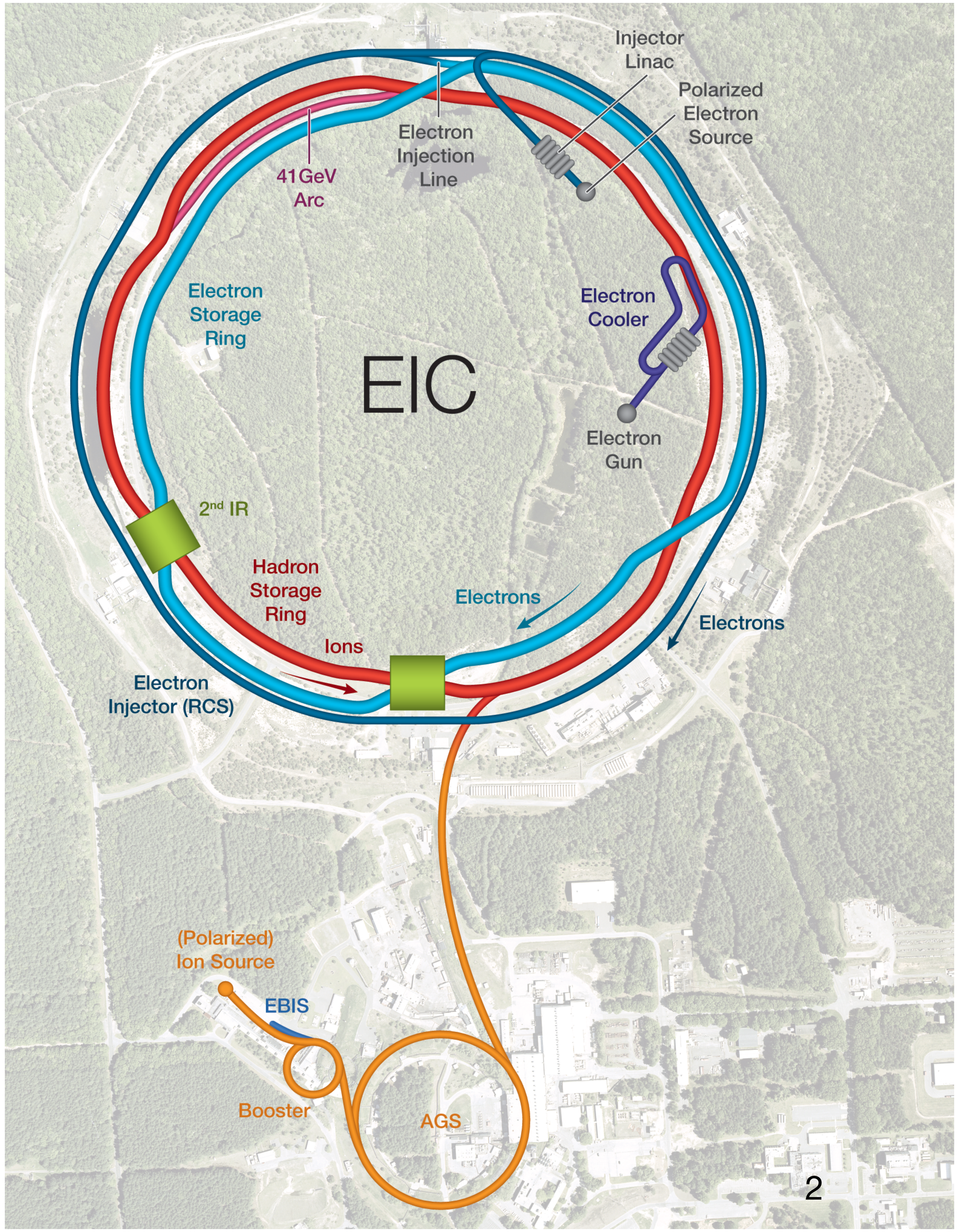

- Based on RHIC:
  - use existing hadron storage ring energy: 41–275 GeV
  - add electron storage ring in RHIC tunnel energy: 5–18 GeV

  $\rightarrow \sqrt{s_{NN}} = 29 - 141\ (90)$ GeV

- $\vec{e} + \vec{p}^{\uparrow}, \vec{d}^{\uparrow}, \vec{He}^{\uparrow}$, unpolarised ions up to U

  ~ 70% polarisation

- $\mathscr{L} = 10^{33-34}$ cm^{-2} s^{-1}

  $\leftrightarrow \mathscr{L}_{\text{int}} = 10 - 100$ fb^{-1}/year

Luminosity and centre-of-mass energy: ep collisions

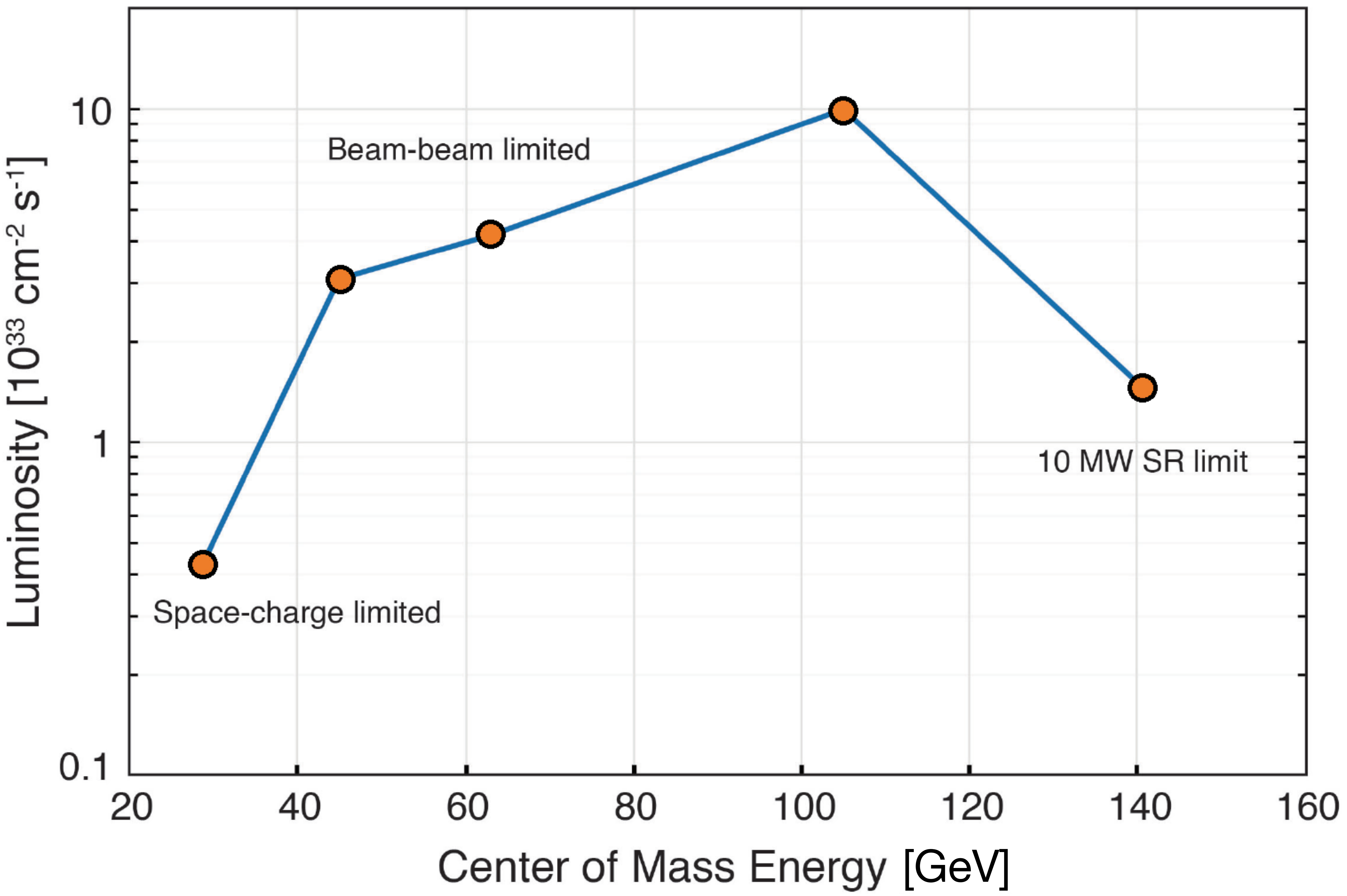

Luminosity for eA similar within factor 2–3

The electron-ion collider (EIC)

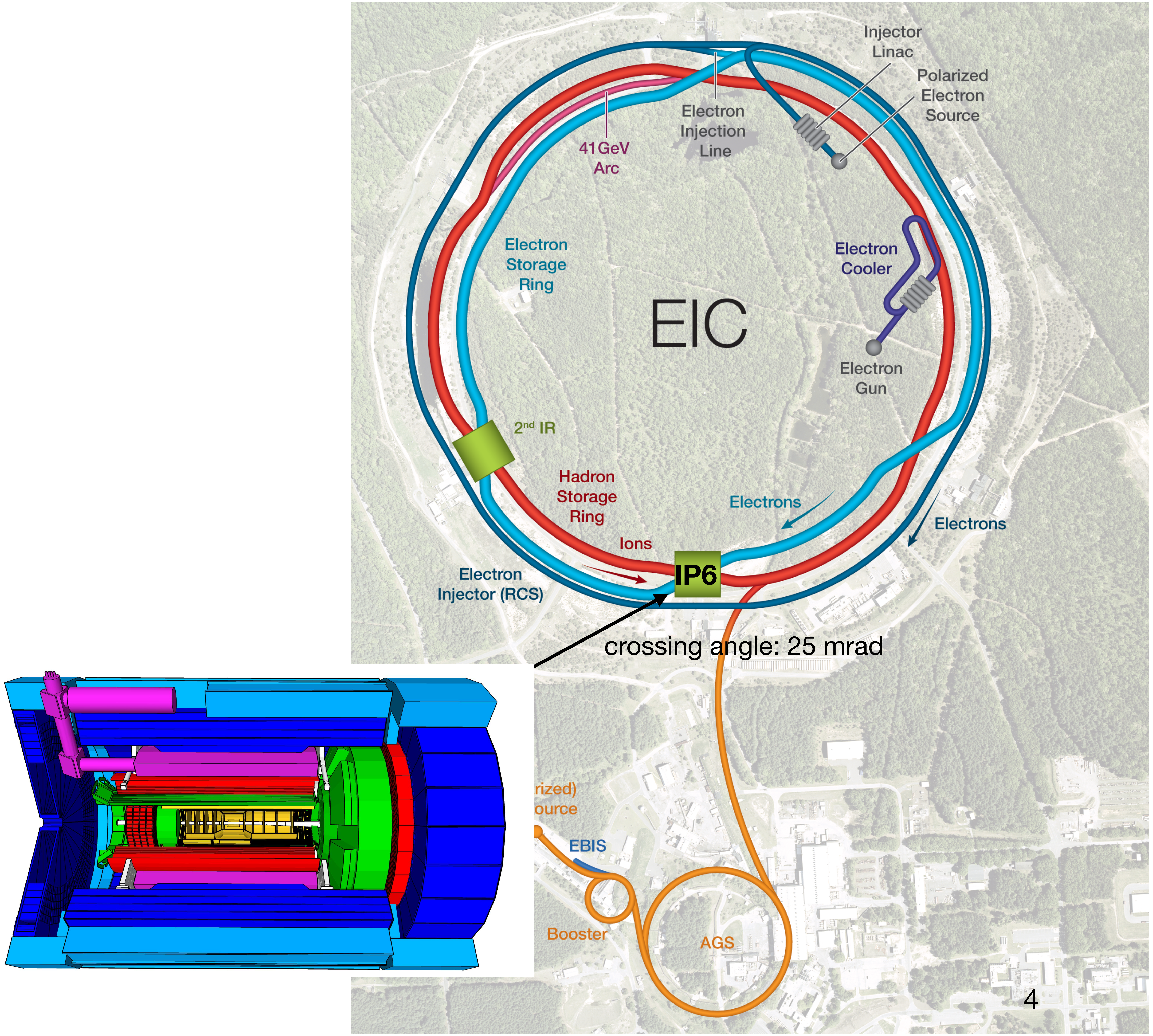

- Based on RHIC:
  - use existing hadron storage ring energy: 41–275 GeV
  - add electron storage ring in RHIC tunnel energy: 5–18 GeV

  $\rightarrow \sqrt{s} = 29 - 141$ GeV

- $\vec{e} + \vec{p}^{\uparrow}$, $\vec{d}^{\uparrow}$, $\overrightarrow{He}^{\uparrow}$, unpolarised ions up to U

  ~ 70% polarisation

- $\mathscr{L} = 10^{33-34}$ cm^{-2} s^{-1}

  $\leftrightarrow \mathscr{L}_{\text{int}} = 10 - 100$ fb^{-1}/year

The electron-proton/ion collider (ePIC) detector

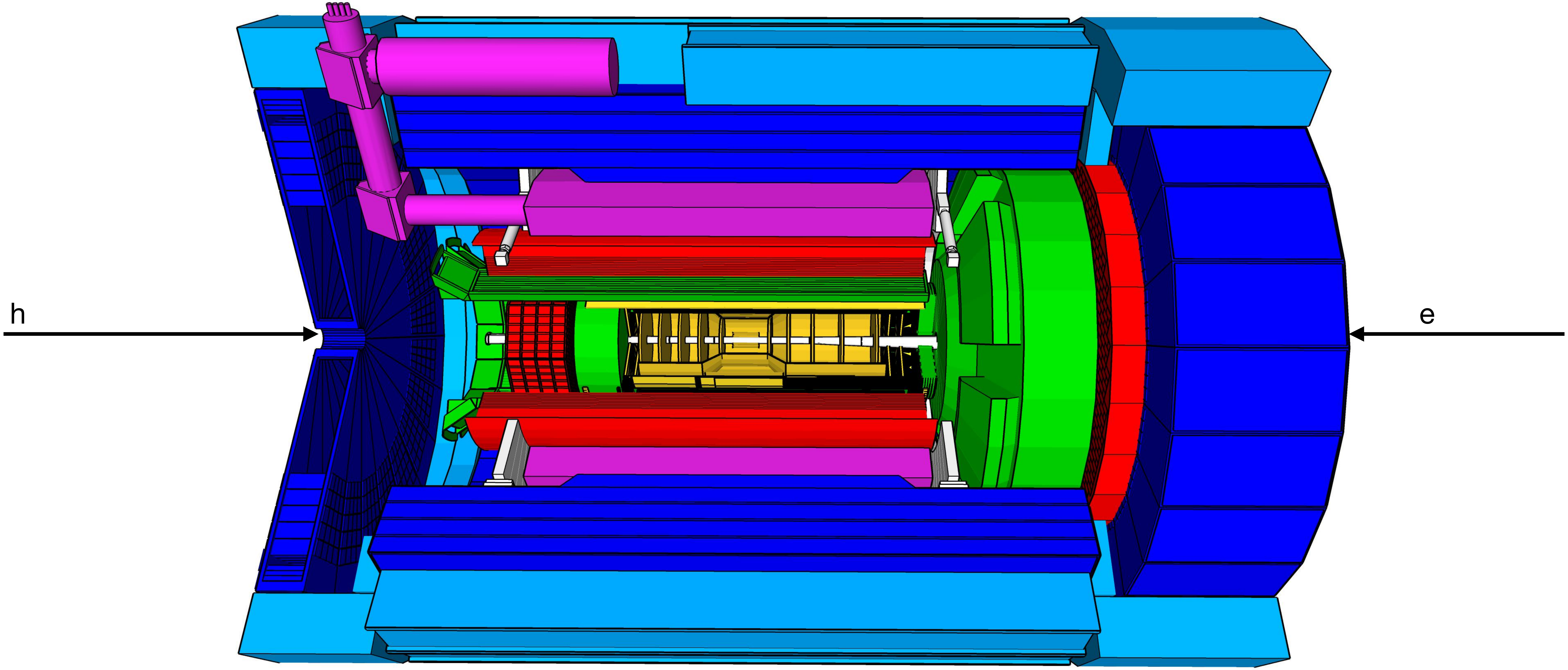

The electron-proton/ion collider (ePIC) detector

hermetic coverage:
0º≤ϕ≤360º
2º≤θ≤178º ⟺ -4<η<4

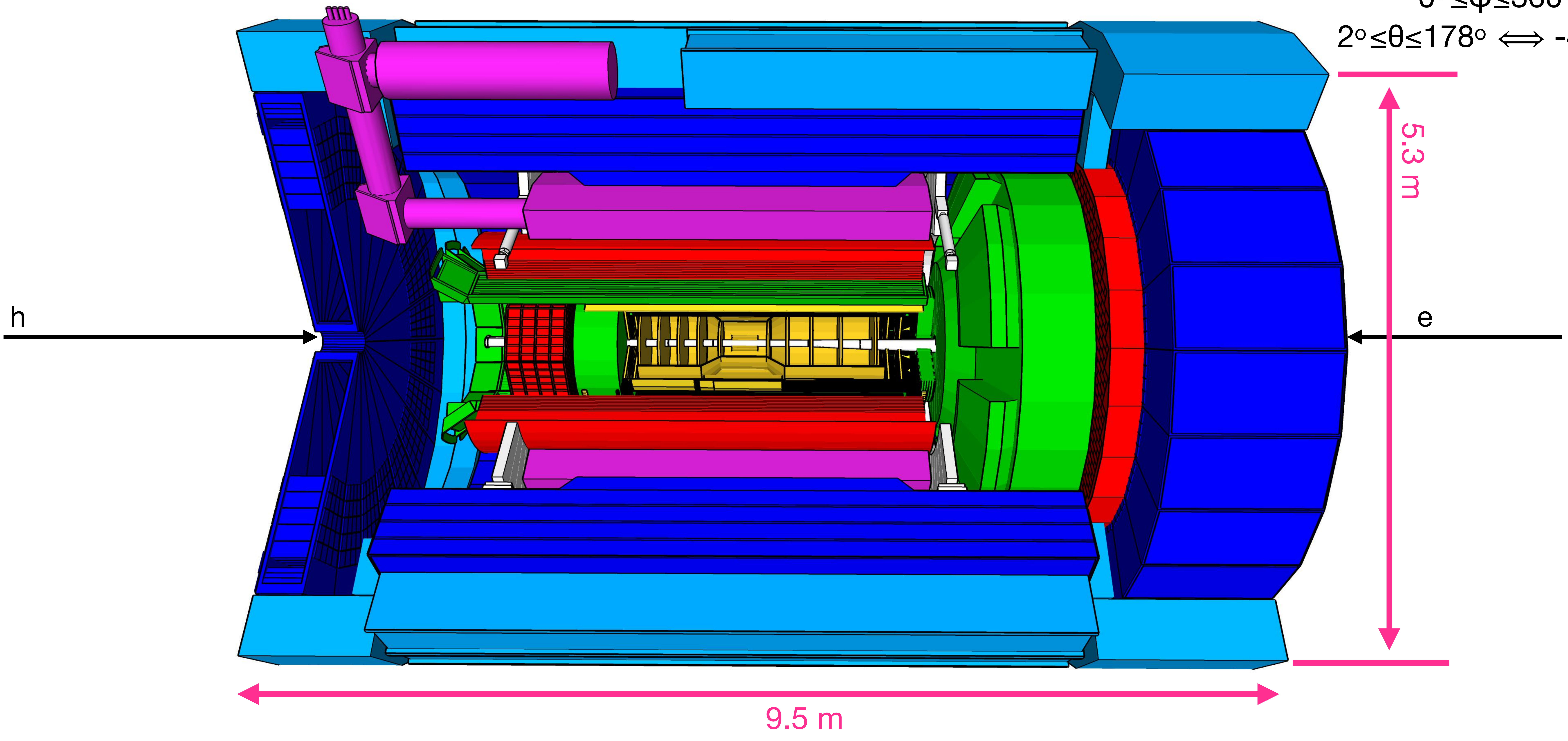

The electron-proton/ion collider (ePIC) detector

hermetic coverage:
$0^o \leq \phi \leq 360^o$
$2^o \leq \theta \leq 178^o \Longleftrightarrow -4 < \eta < 4$

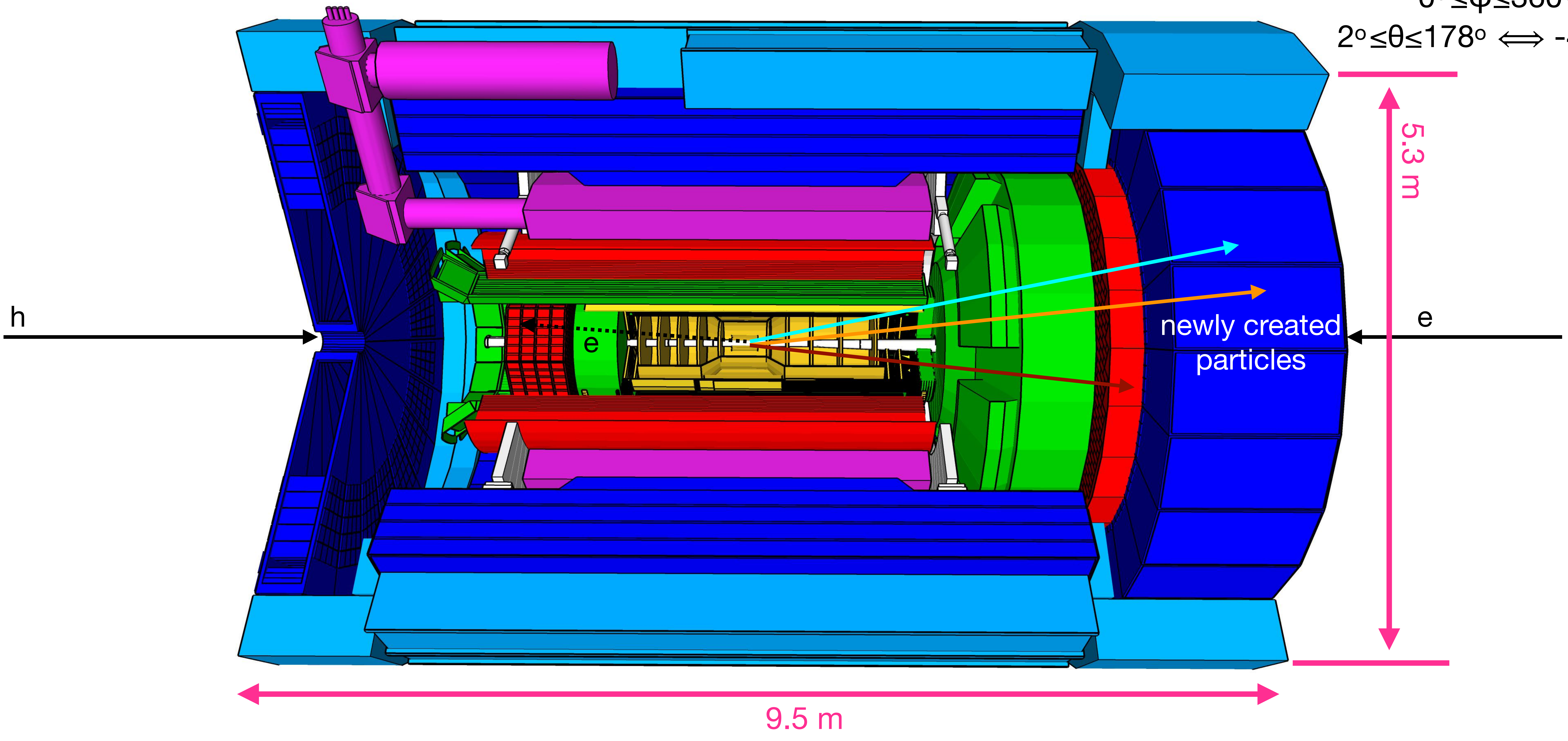

The electron-proton/ion collider (ePIC) detector

- Tracking
- PID
- Electromagnetic calorimeter
- Hadronic calorimeter

hermetic coverage:
$0^o \leq \phi \leq 360^o$
$2^o \leq \theta \leq 178^o \iff -4 < \eta < 4$

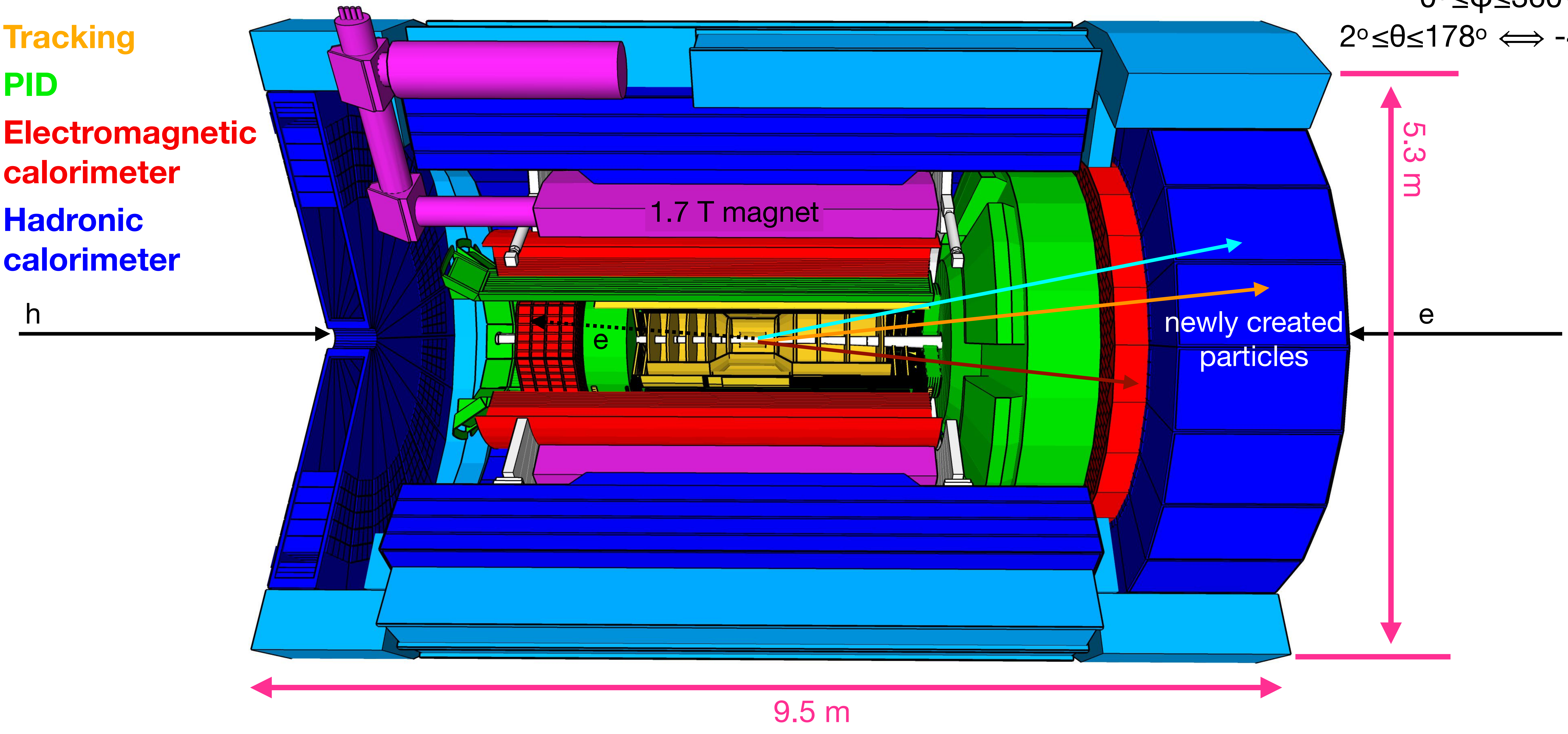

The electron-proton/ion collider (ePIC) detector

hermetic coverage:
0°≤ϕ≤360°
2°≤θ≤178° ⟺ -4<η<4

+ far backward

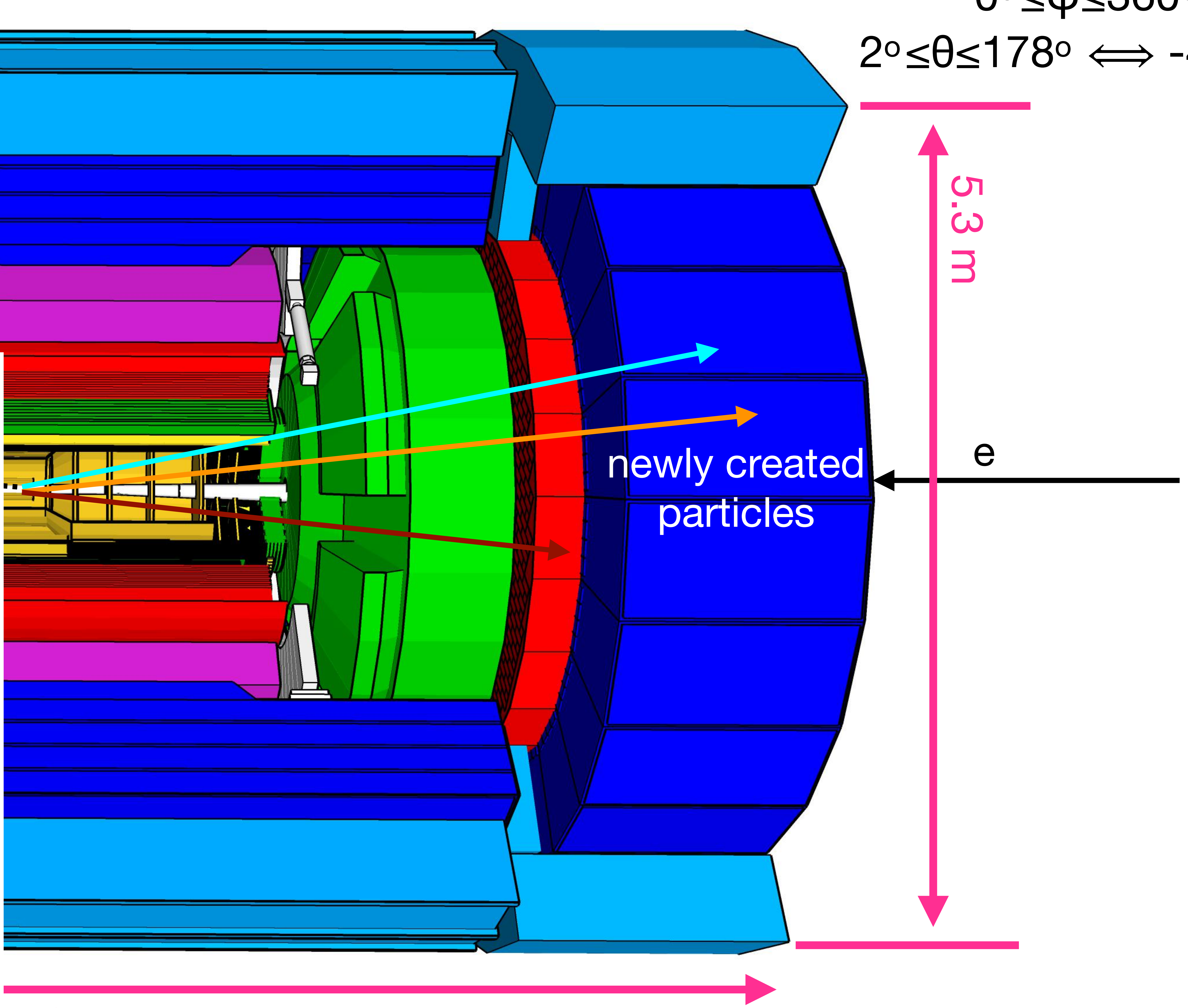

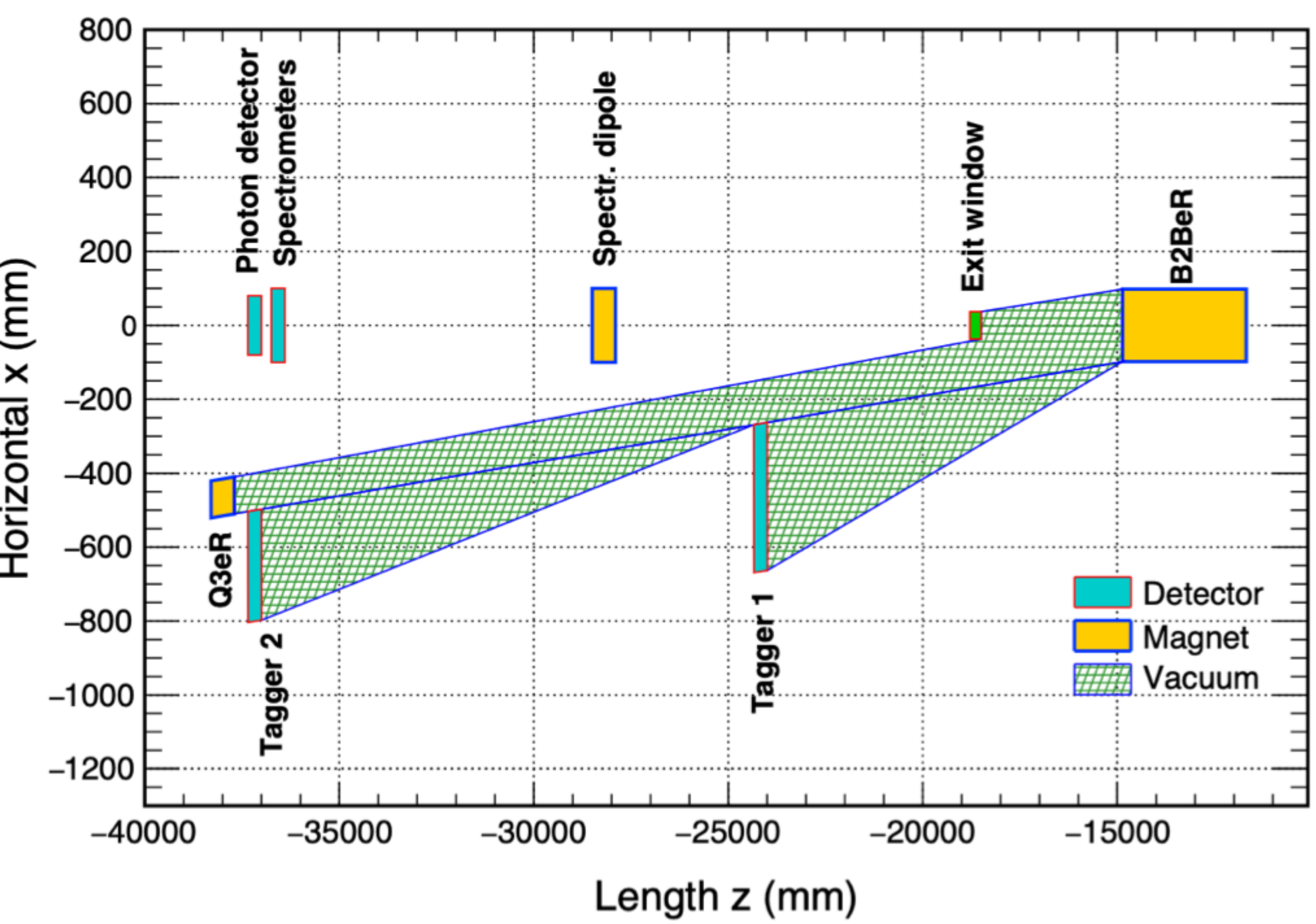

The electron-proton/ion collider (ePIC) detector

+ far backward

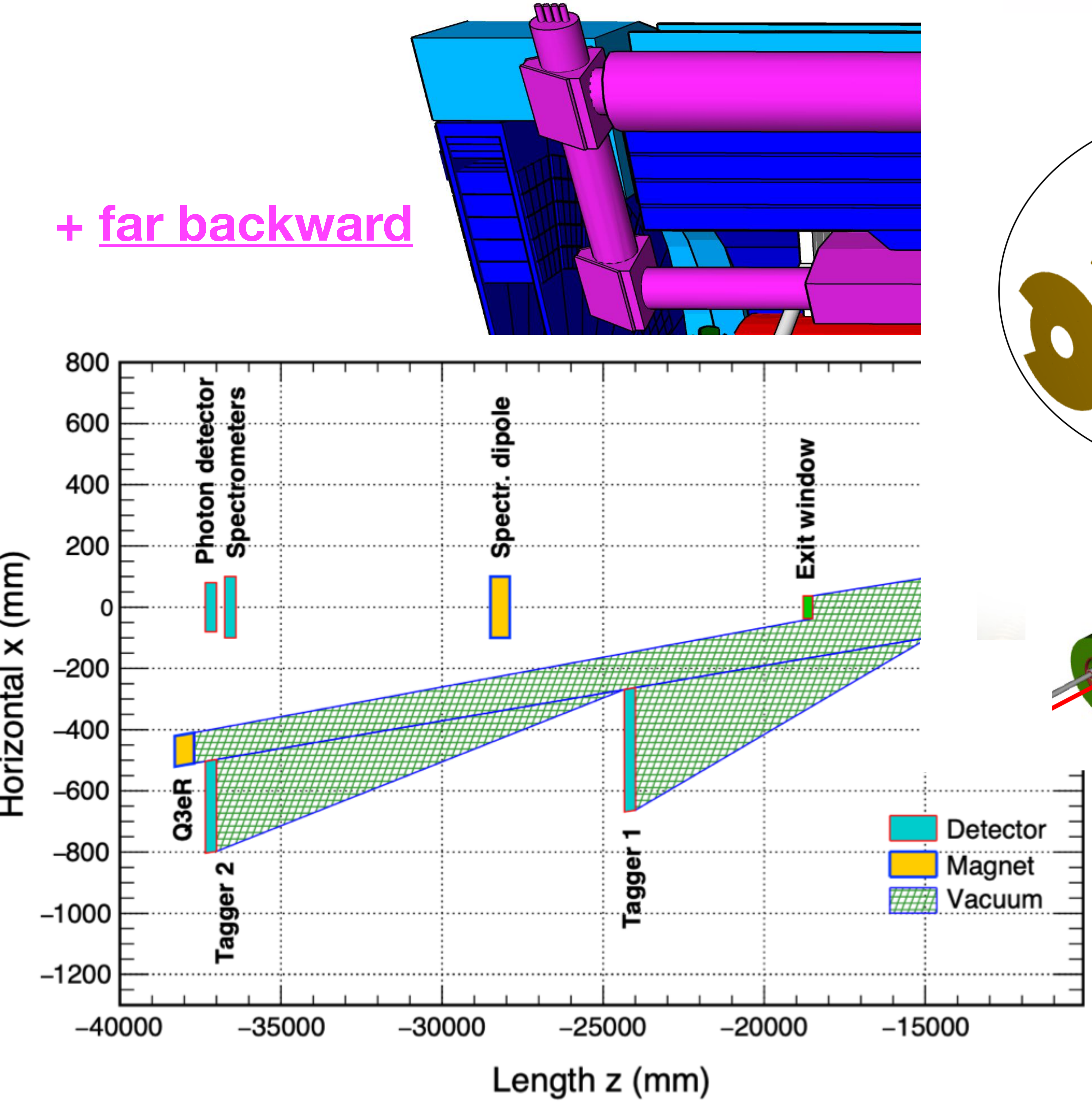

+ far forward

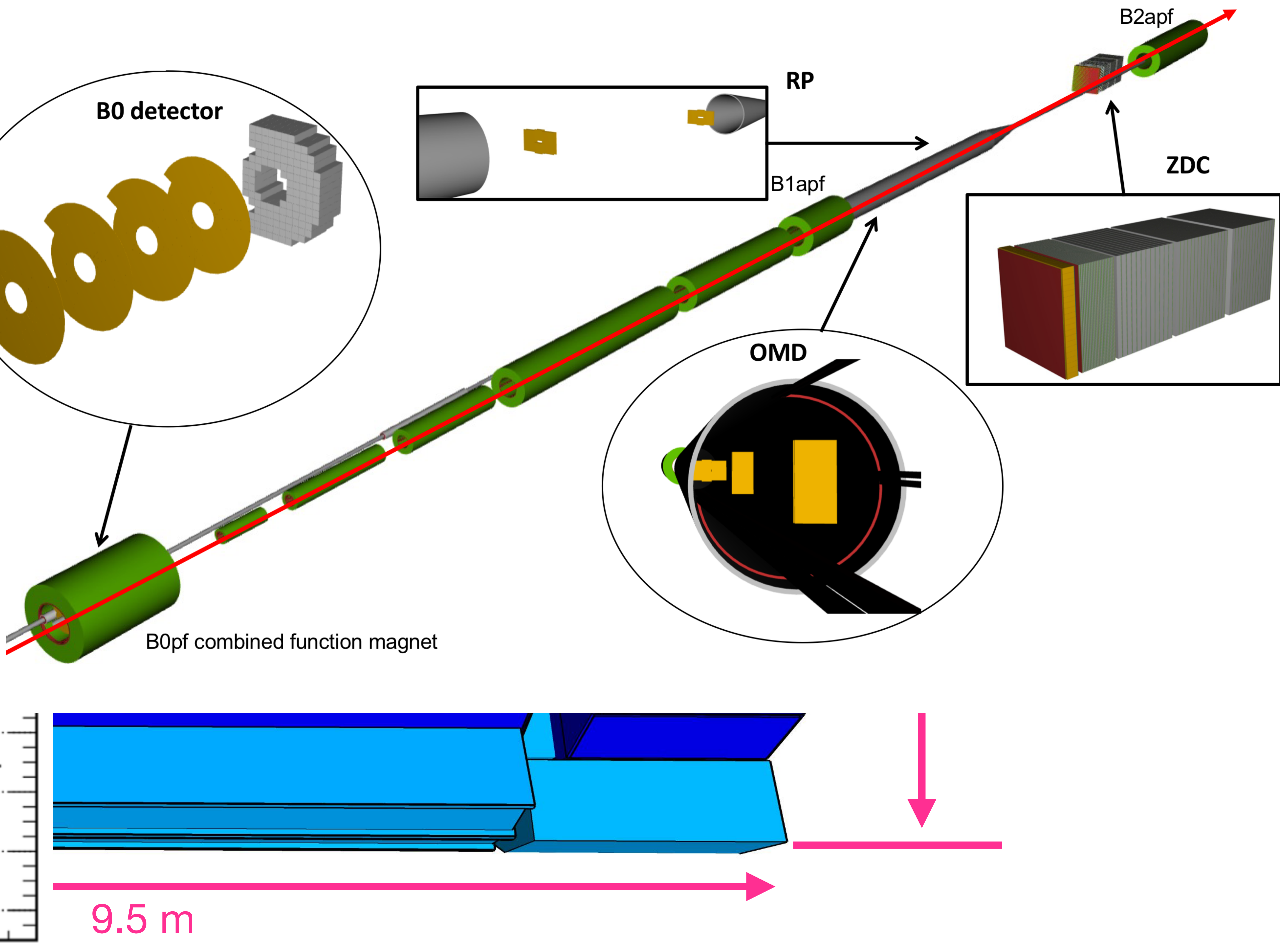

The electron-proton/ion collider (ePIC) detector

+ far forward

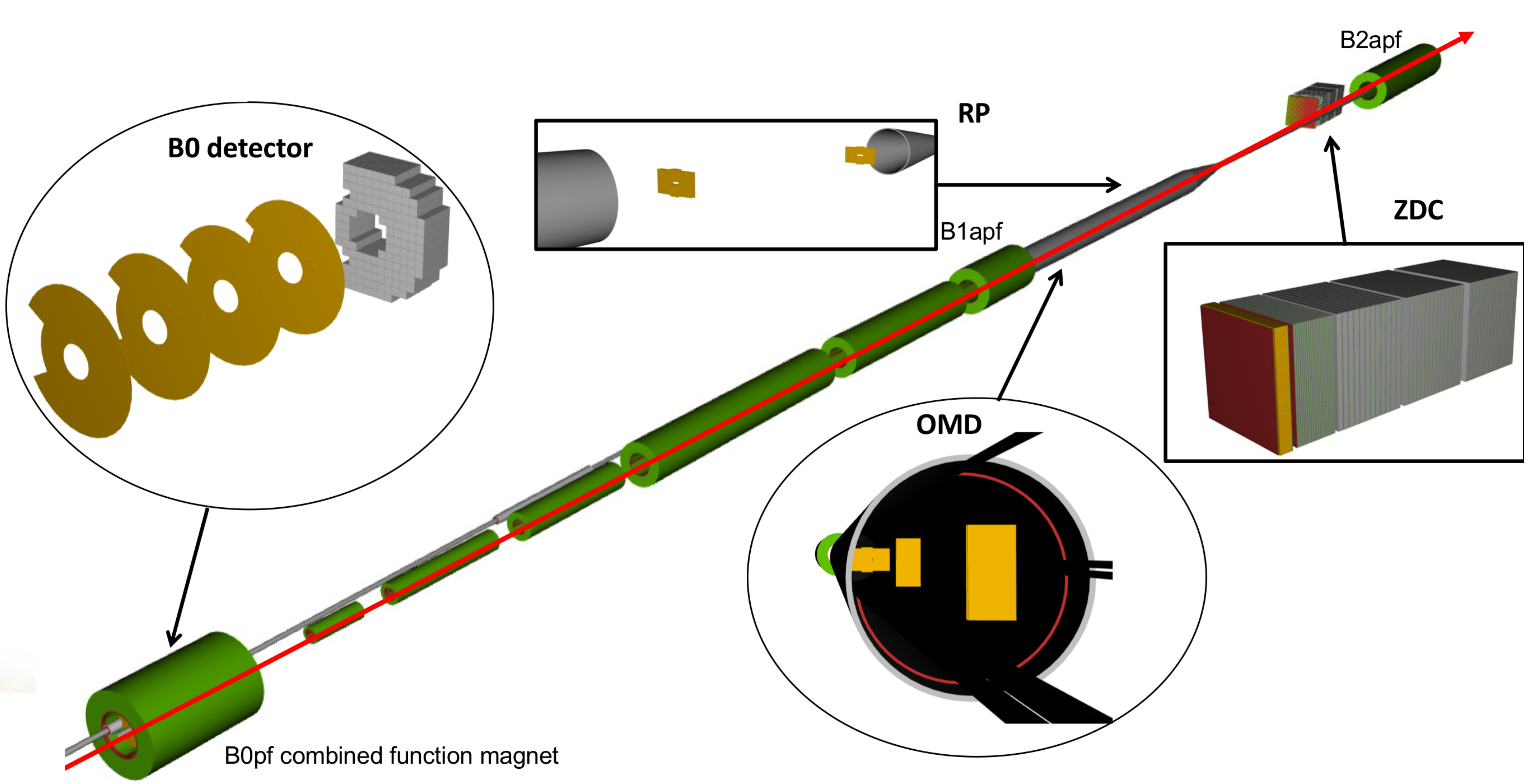

+ far backward

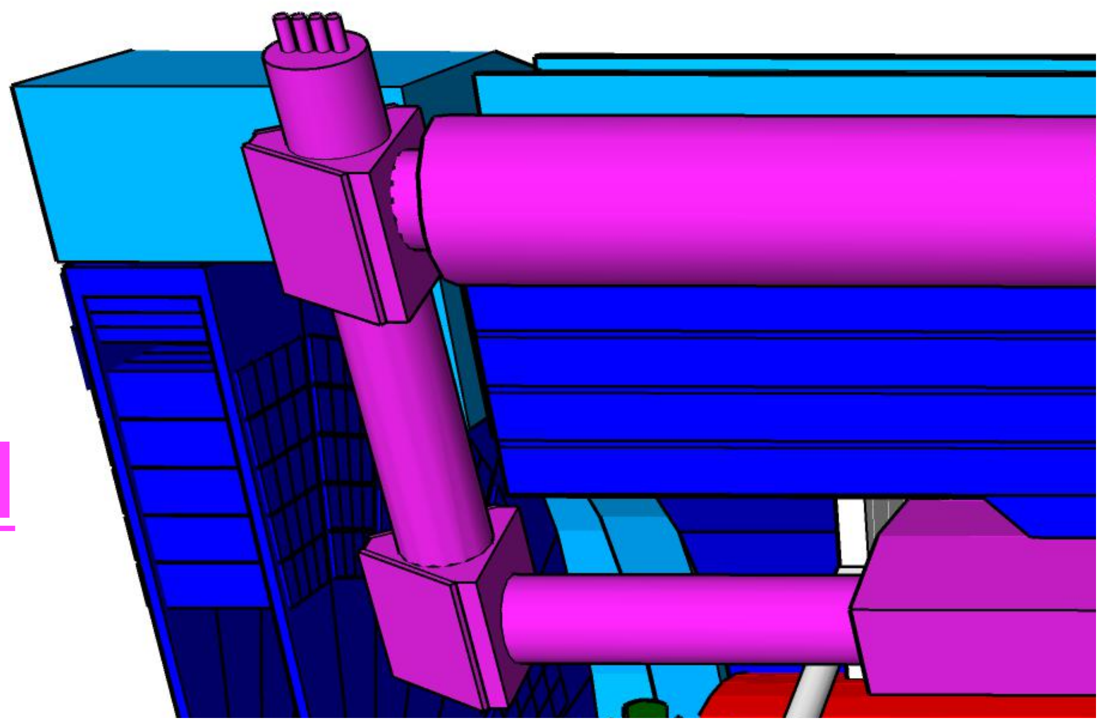

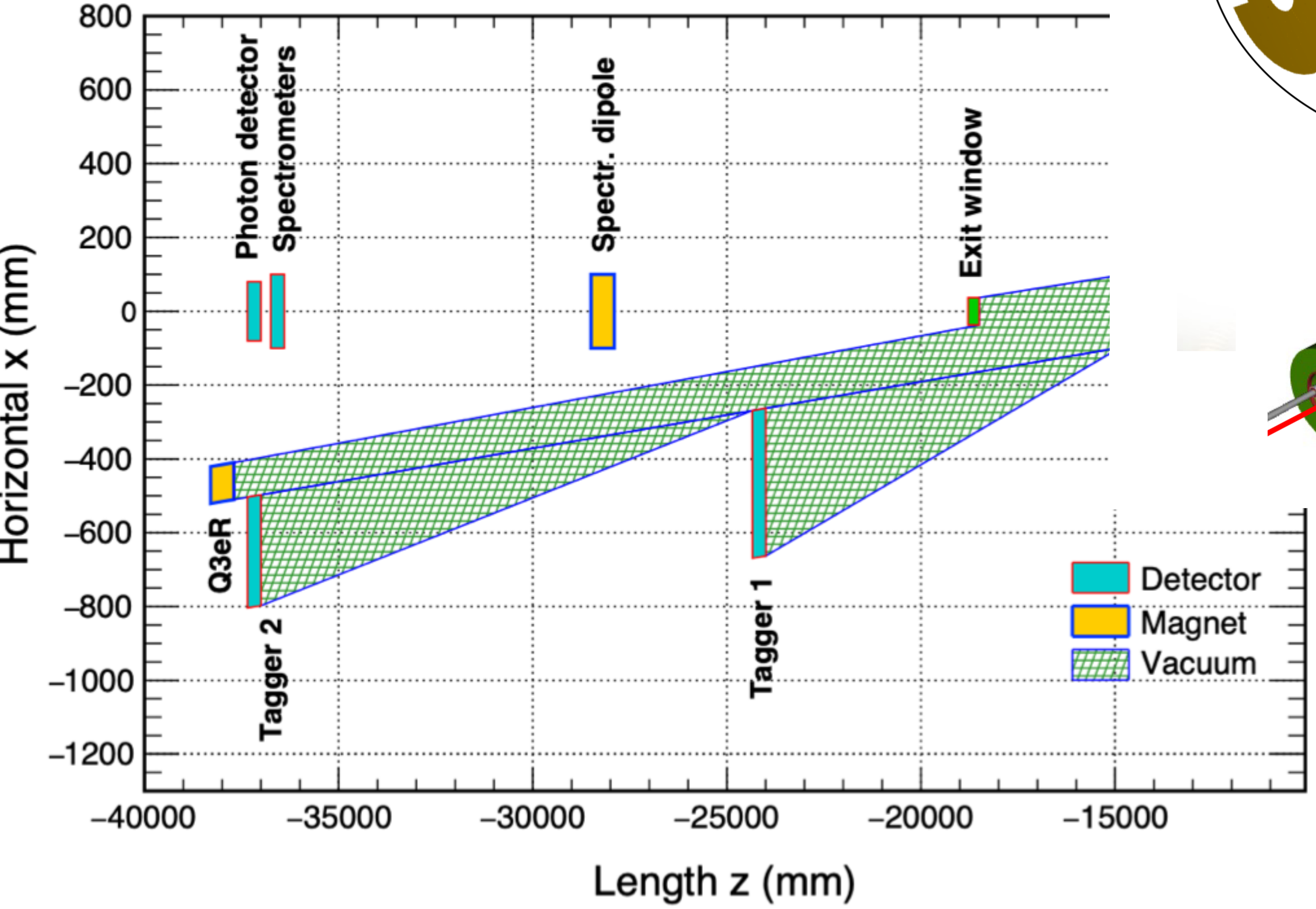

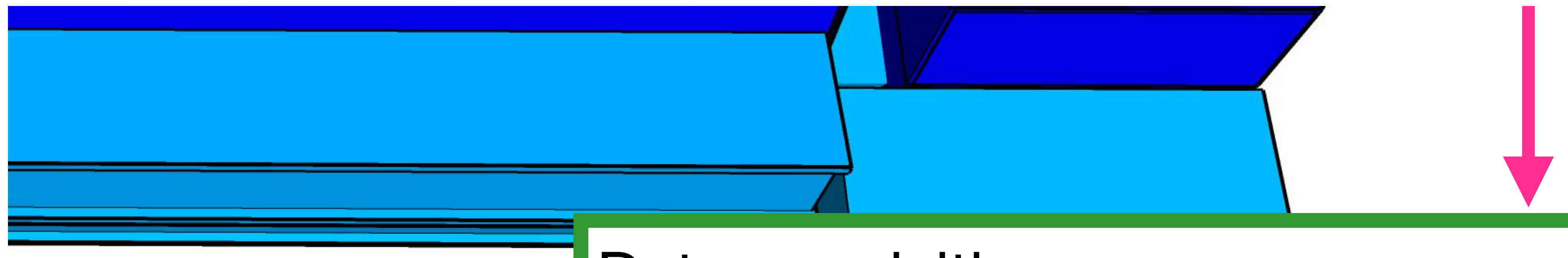

9.5 m

Data acquisition:
- no trigger
- all collision data is digitised
- with strong zero-suppression at front-end electronics

Tracking system

1.7 T magnet

- Monolithic Active Pixel Sensor (MAPS) Silicon vertexing/inner tracker
- Micro-pattern gaseous detectors

  μRWELL/microMegas:
  timing & pattern recognition
- AC-LGAD based TOF:
  PID & additional tracking point

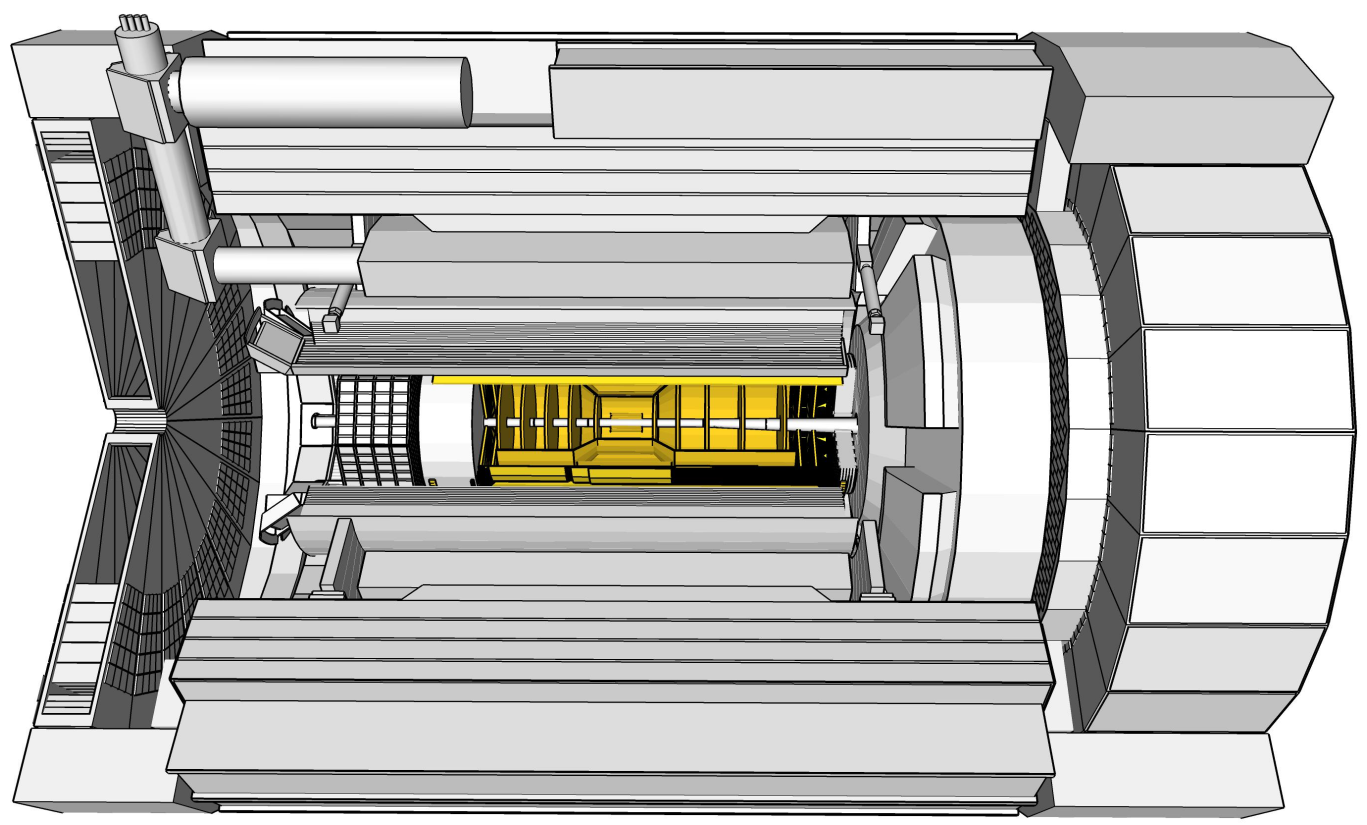

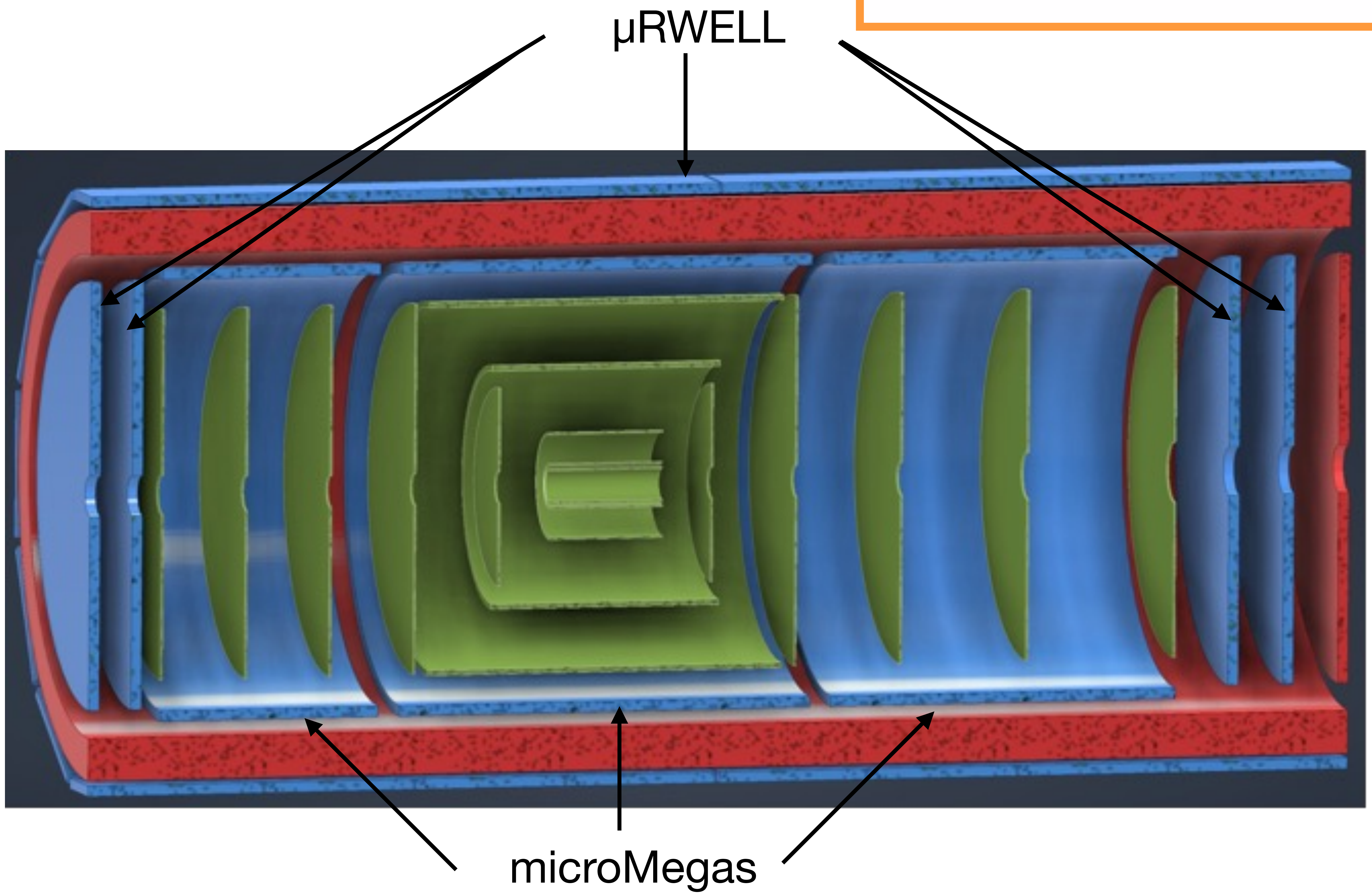

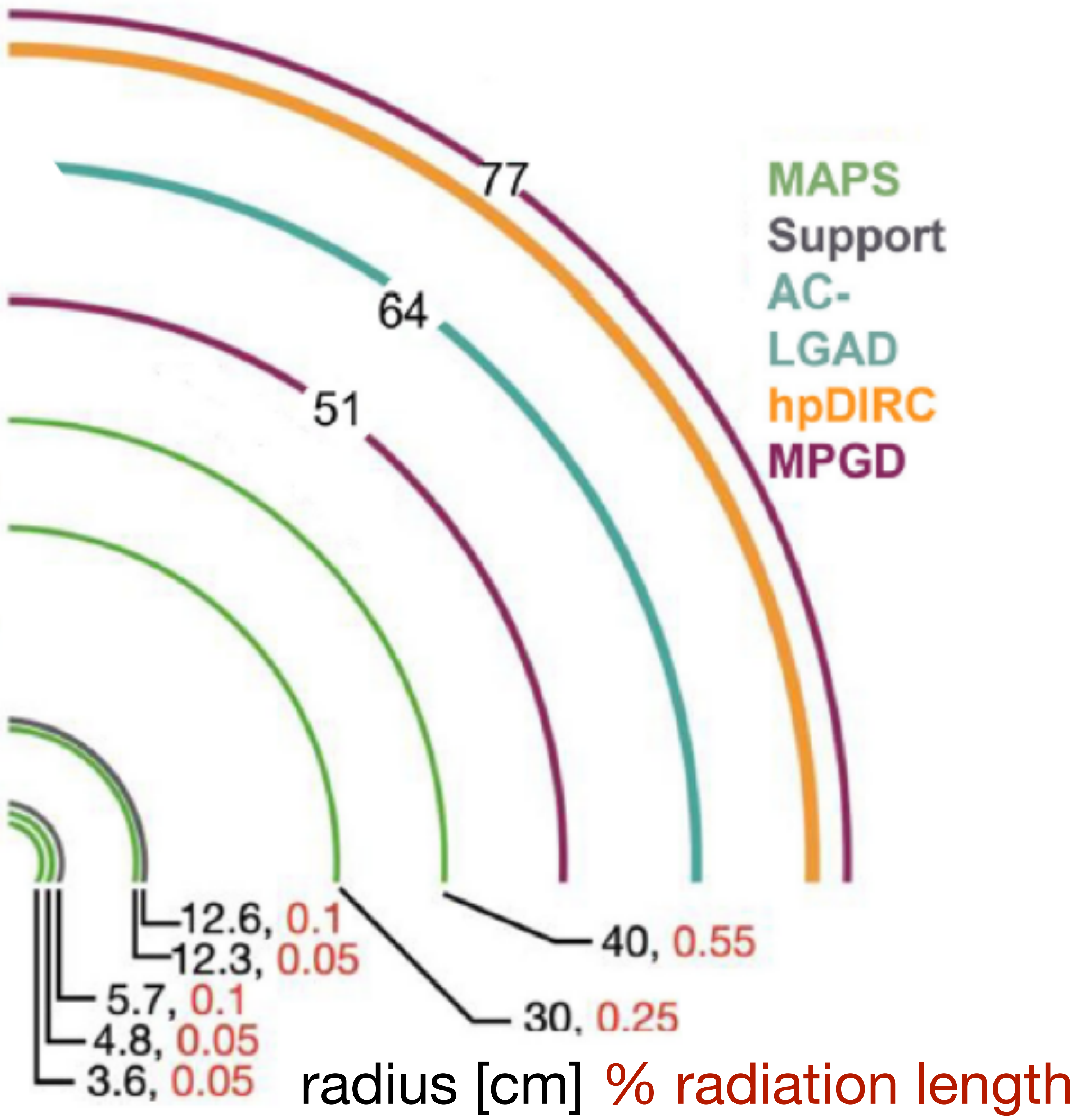

Tracking system

1.7 T magnet

- Monolithic Active Pixel Sensor (MAPS) Silicon vertexing/inner tracker
- Micro-pattern gaseous detectors

  μRWELL/microMegas:
  timing & pattern recognition
- AC-LGAD based TOF:
  PID & additional tracking point

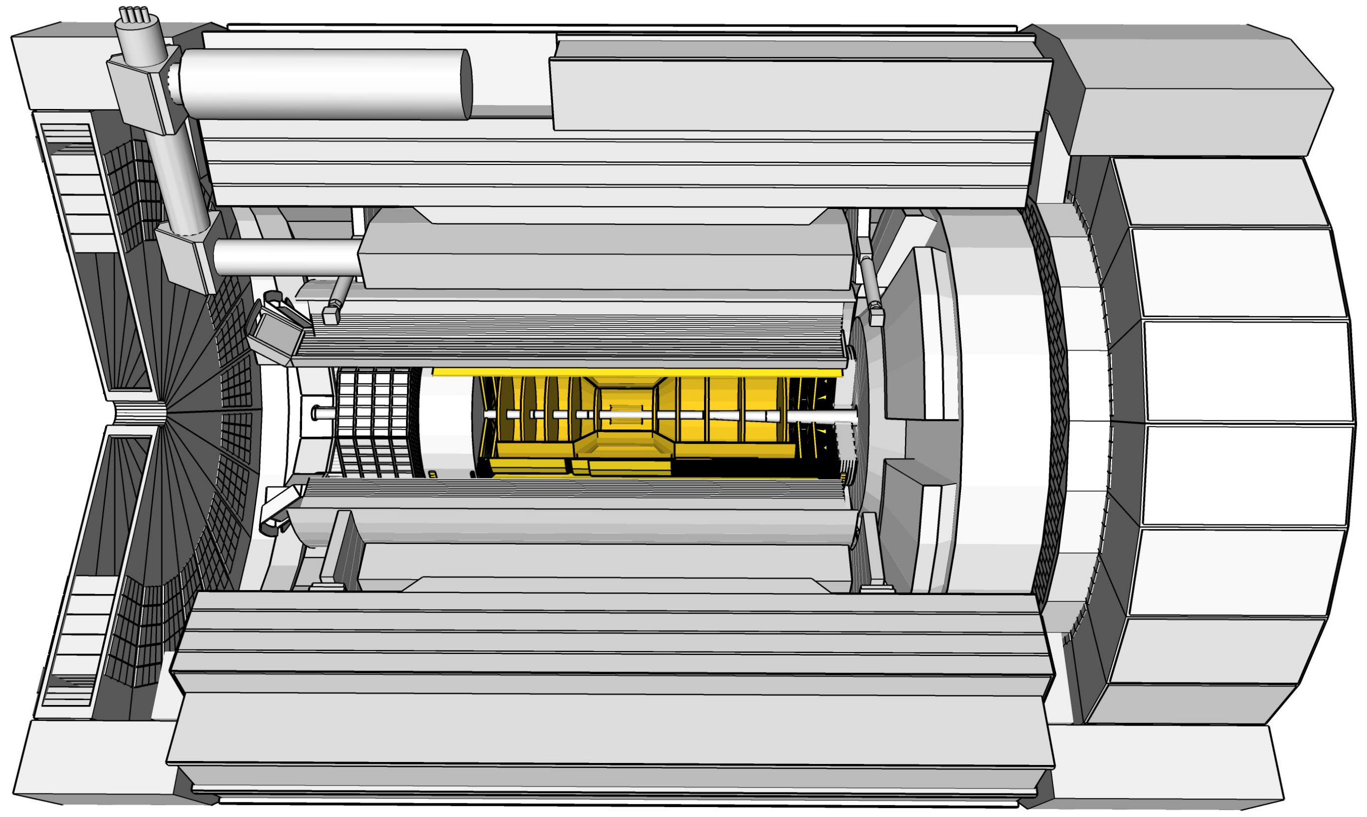

momentum resolution

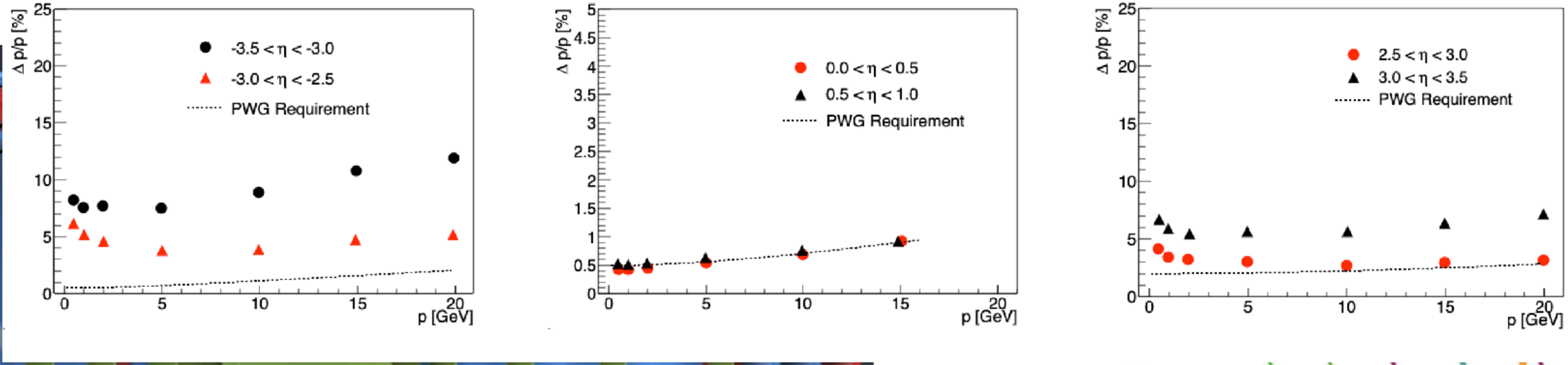

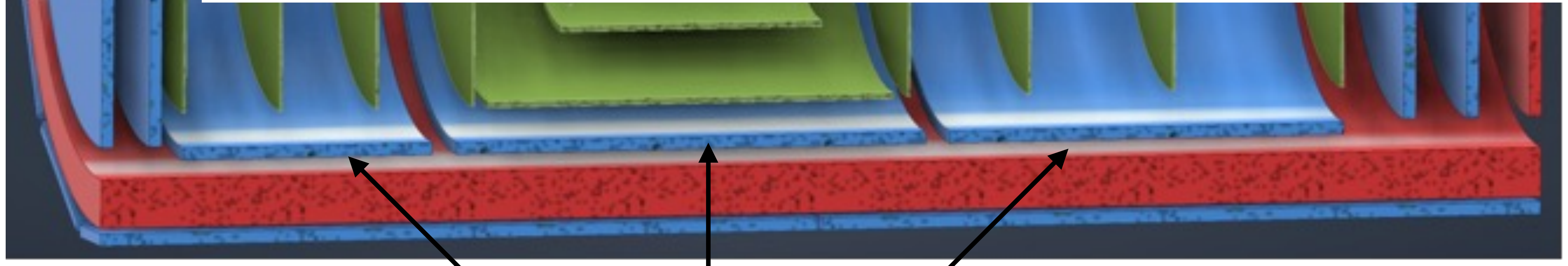

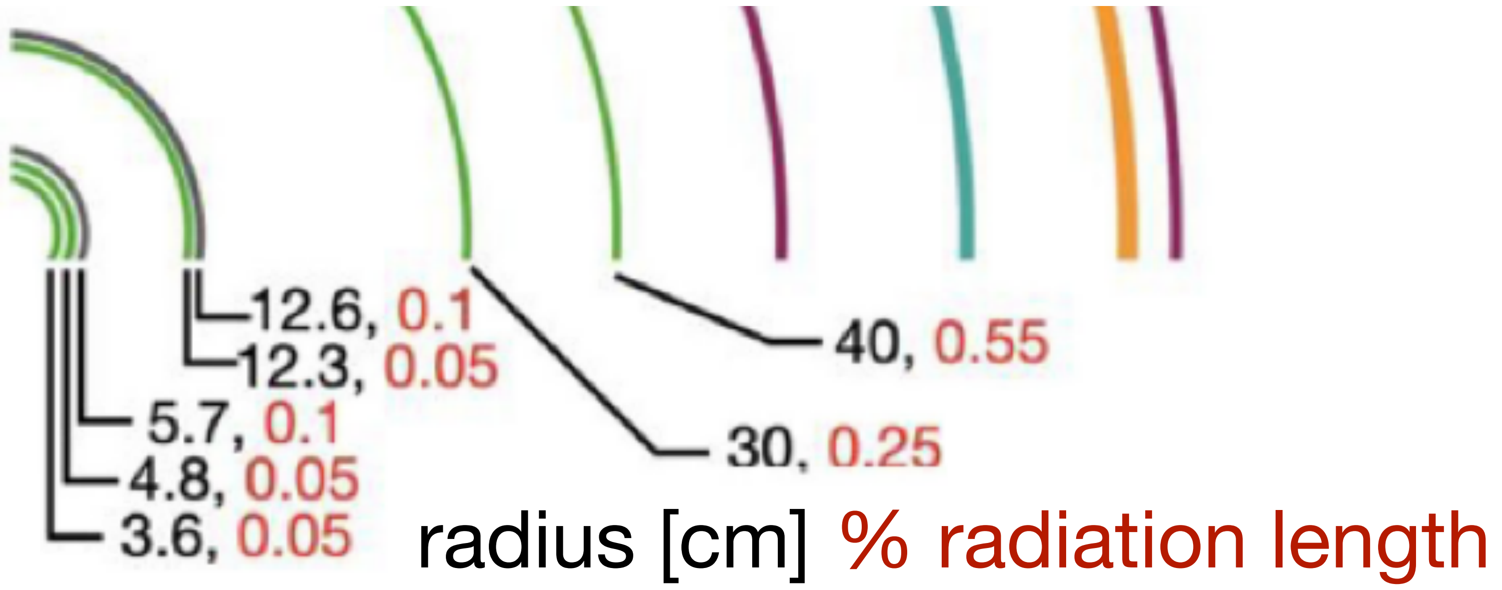

Tracking system

1.7 T magnet

- Monolithic Active Pixel Sensor (MAPS) Silicon vertexing/inner tracker
- Micro-pattern gaseous detectors

  µRWELL/microMegas:
  timing & pattern recognition
- AC-LGAD based TOF:
  PID & additional tracking point

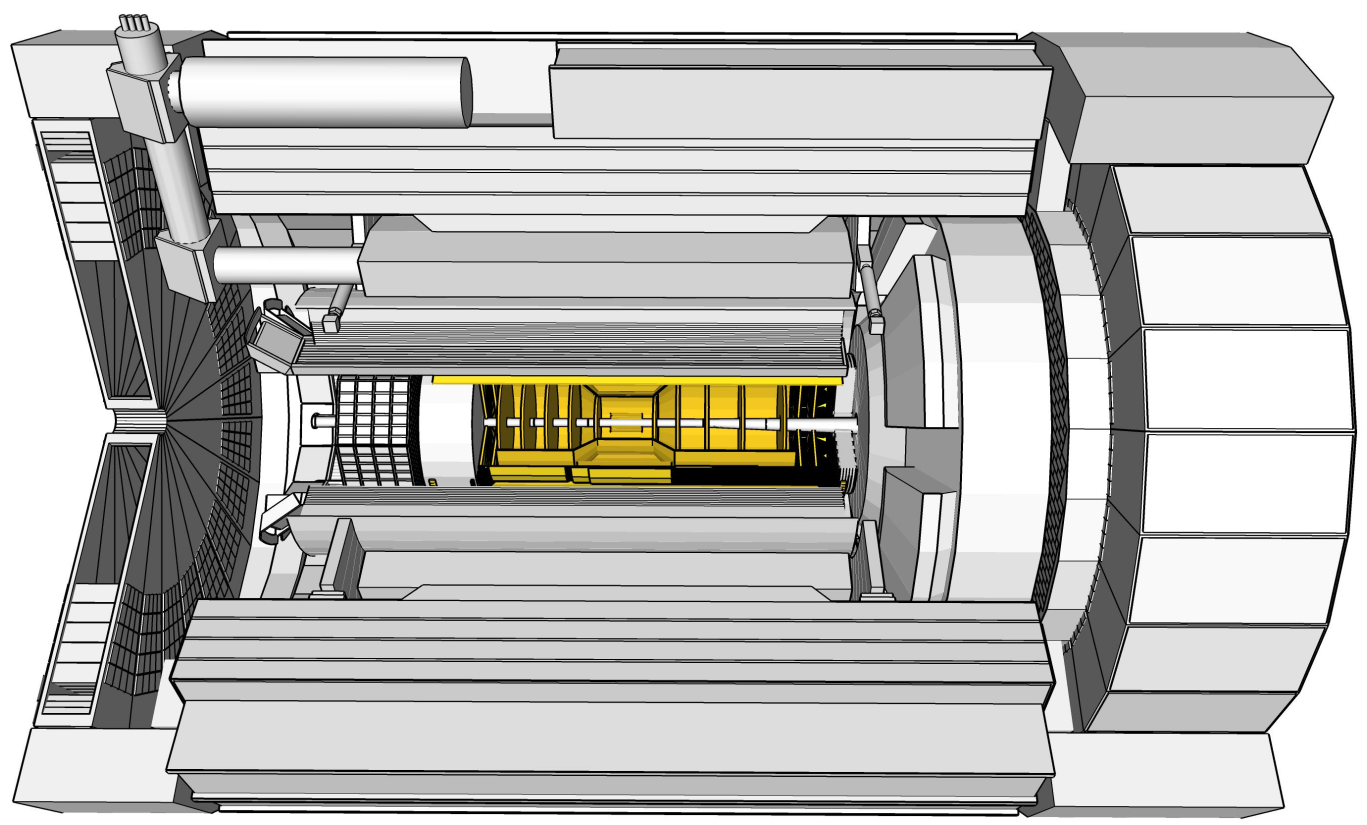

momentum resolution

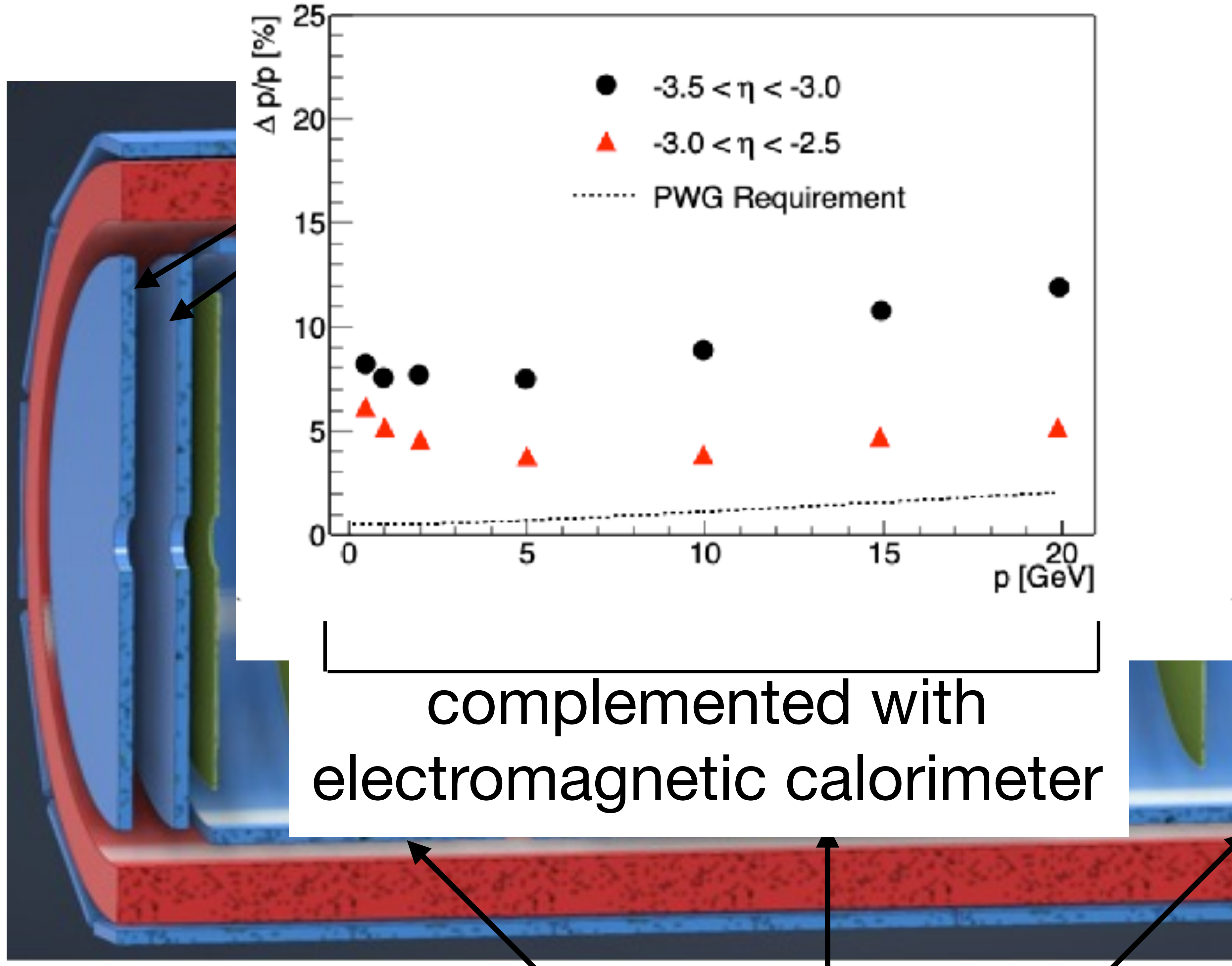

complemented with
electromagnetic calorimeter

microMegas

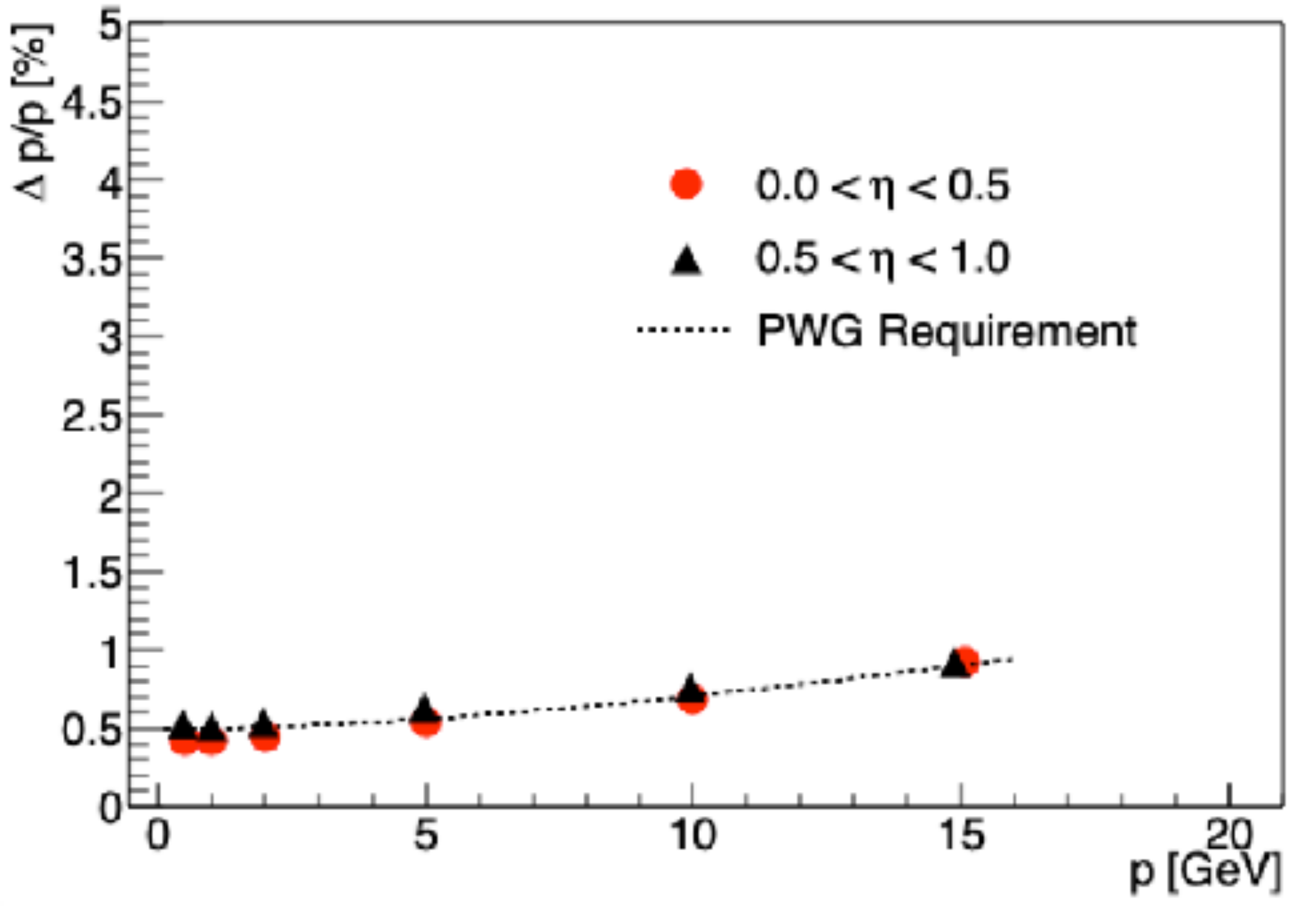

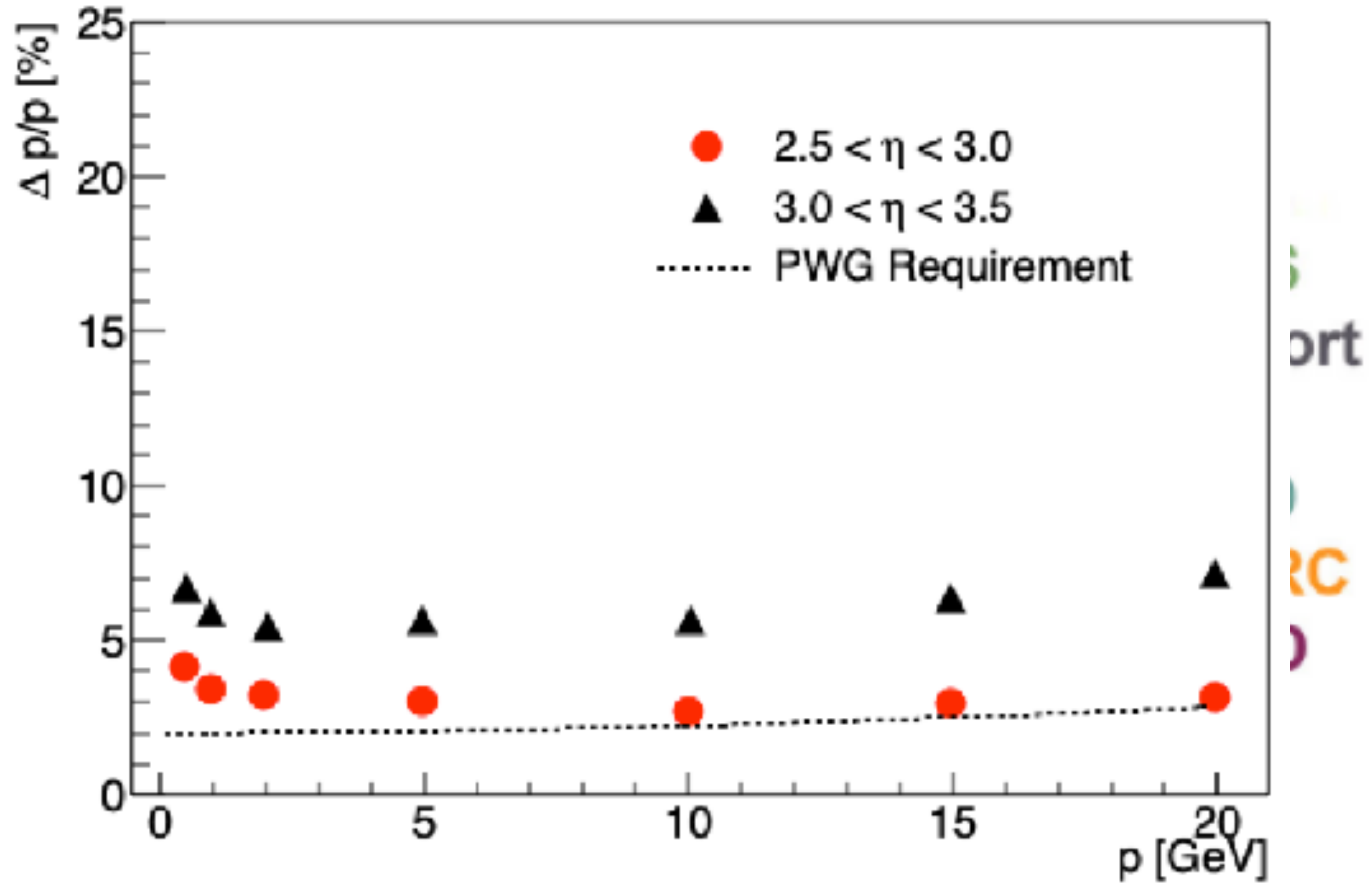

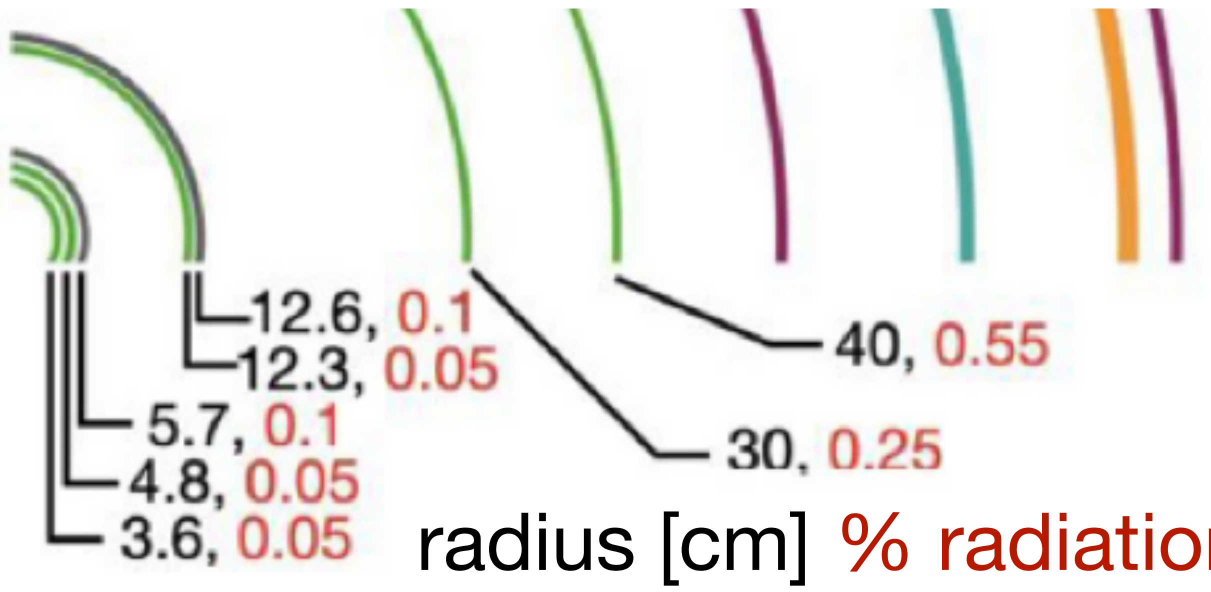

radius [cm] % radiation length

Electromagnetic calorimeter

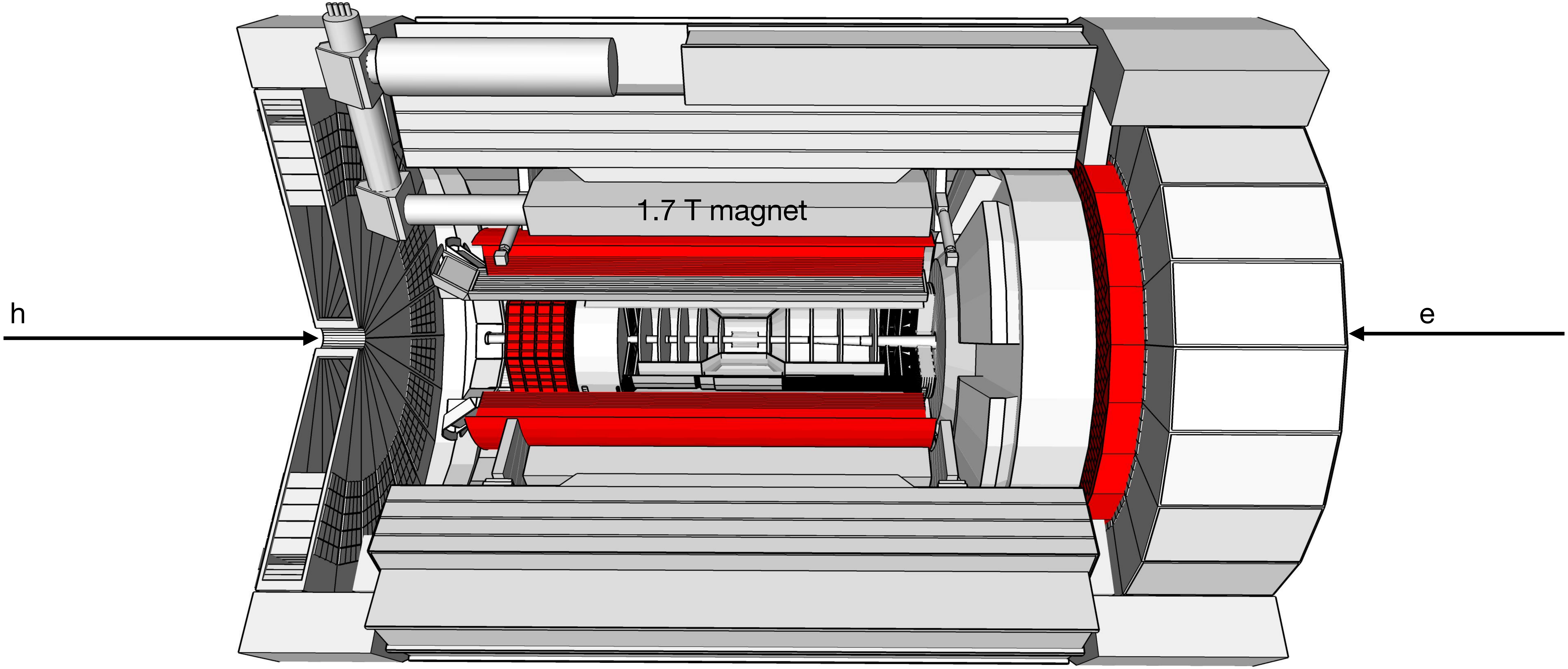

Electromagnetic calorimeter

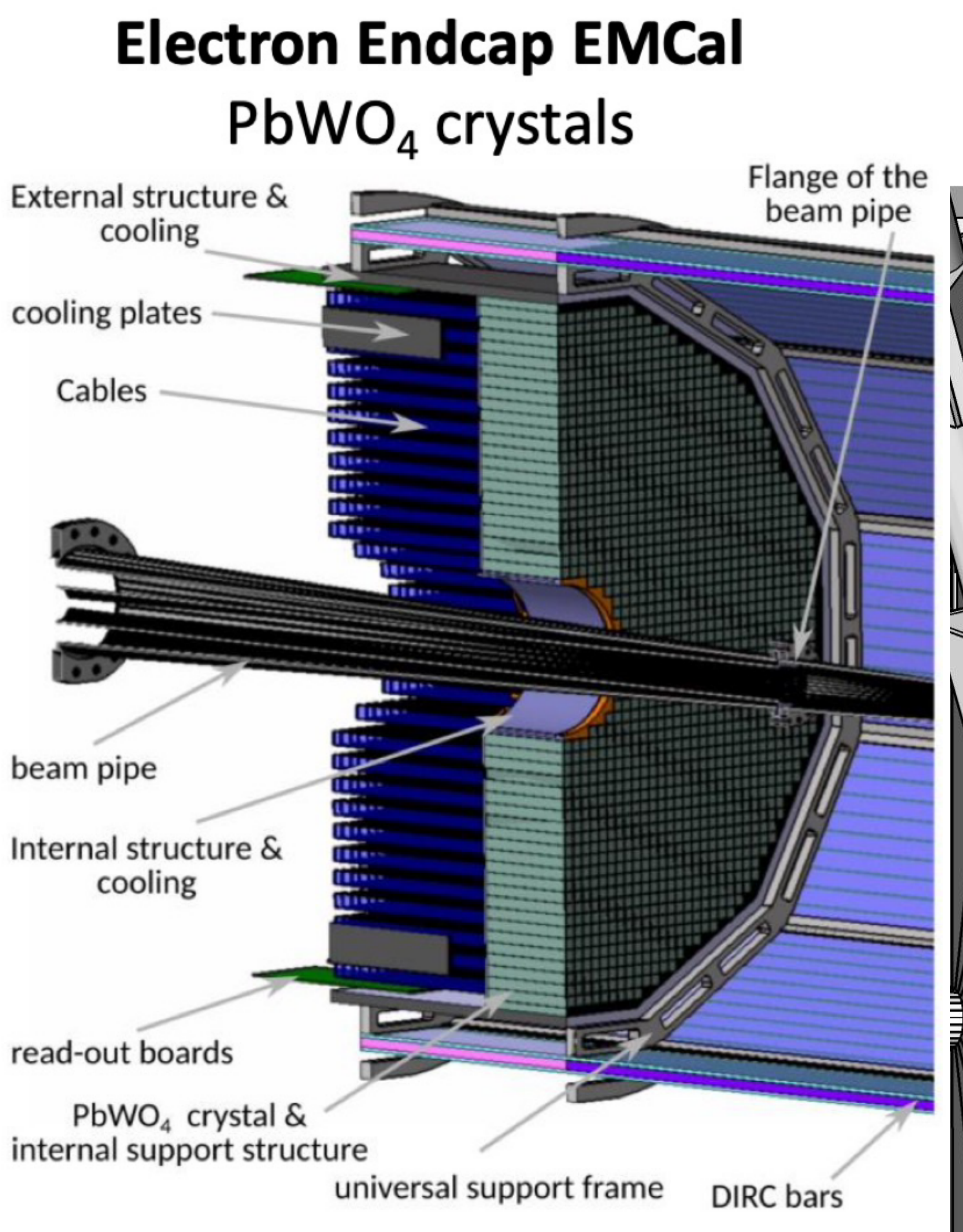

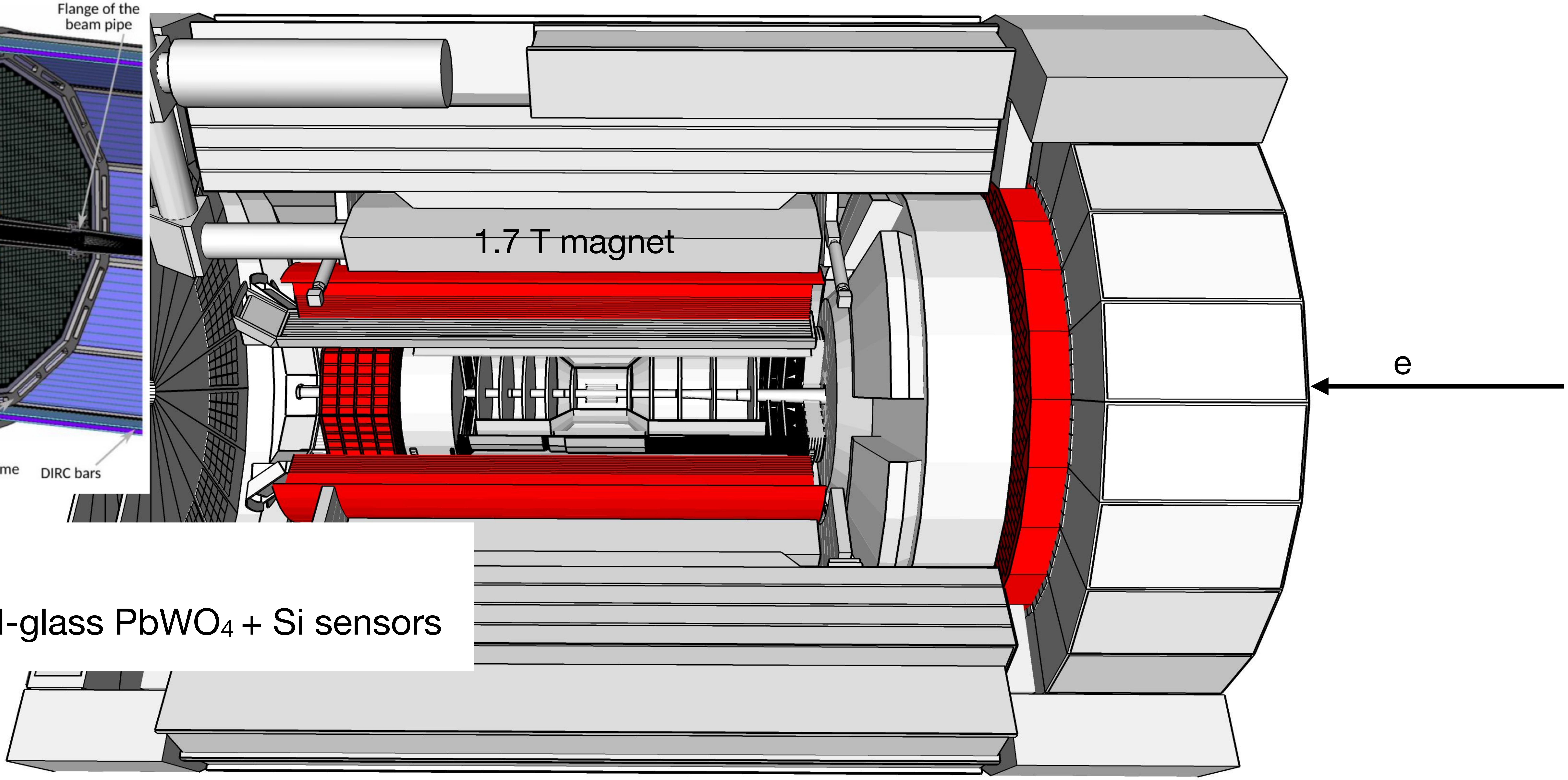

- Backward EMCAL:
  high-precision lead-glass $PbWO_4$ + Si sensors

Electromagnetic calorimeter

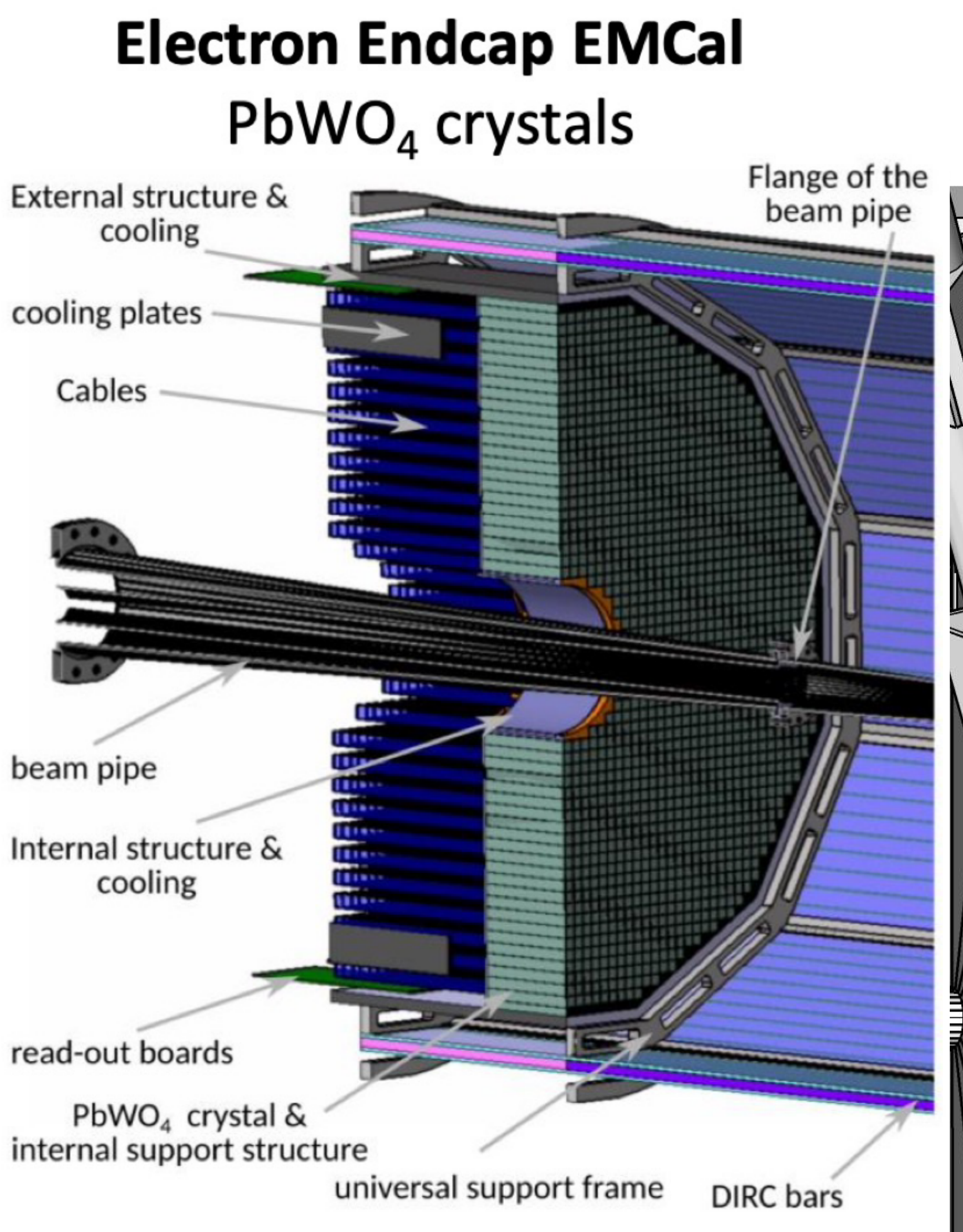

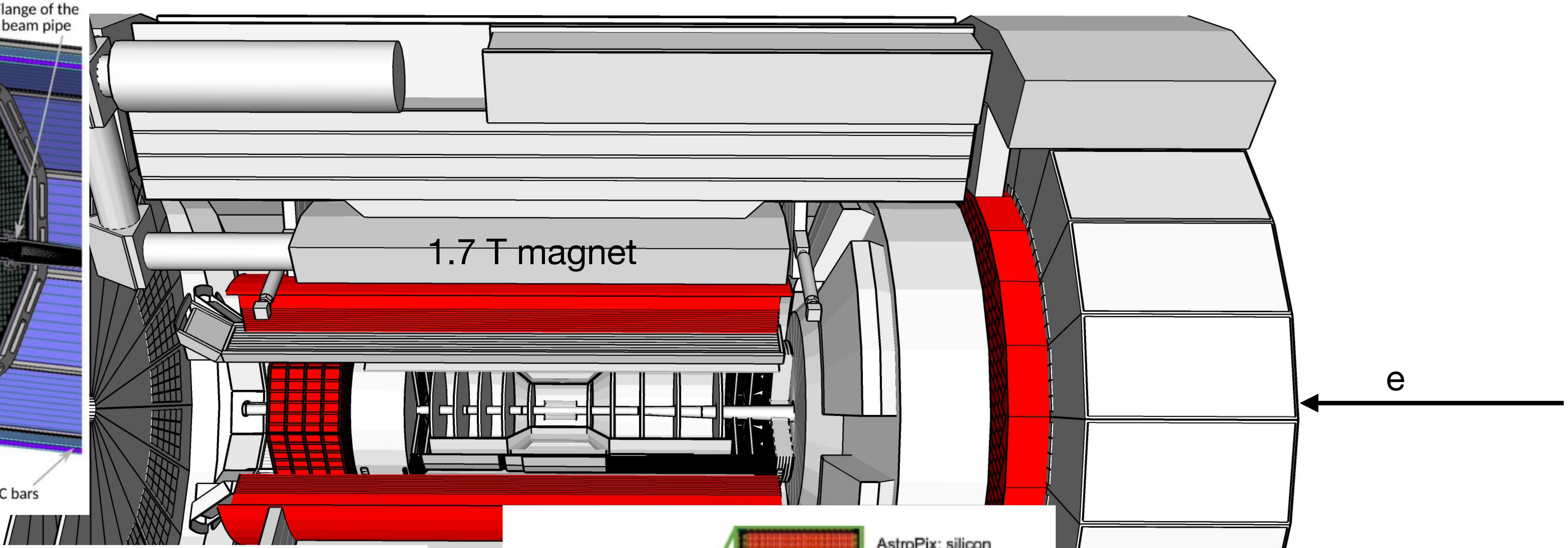

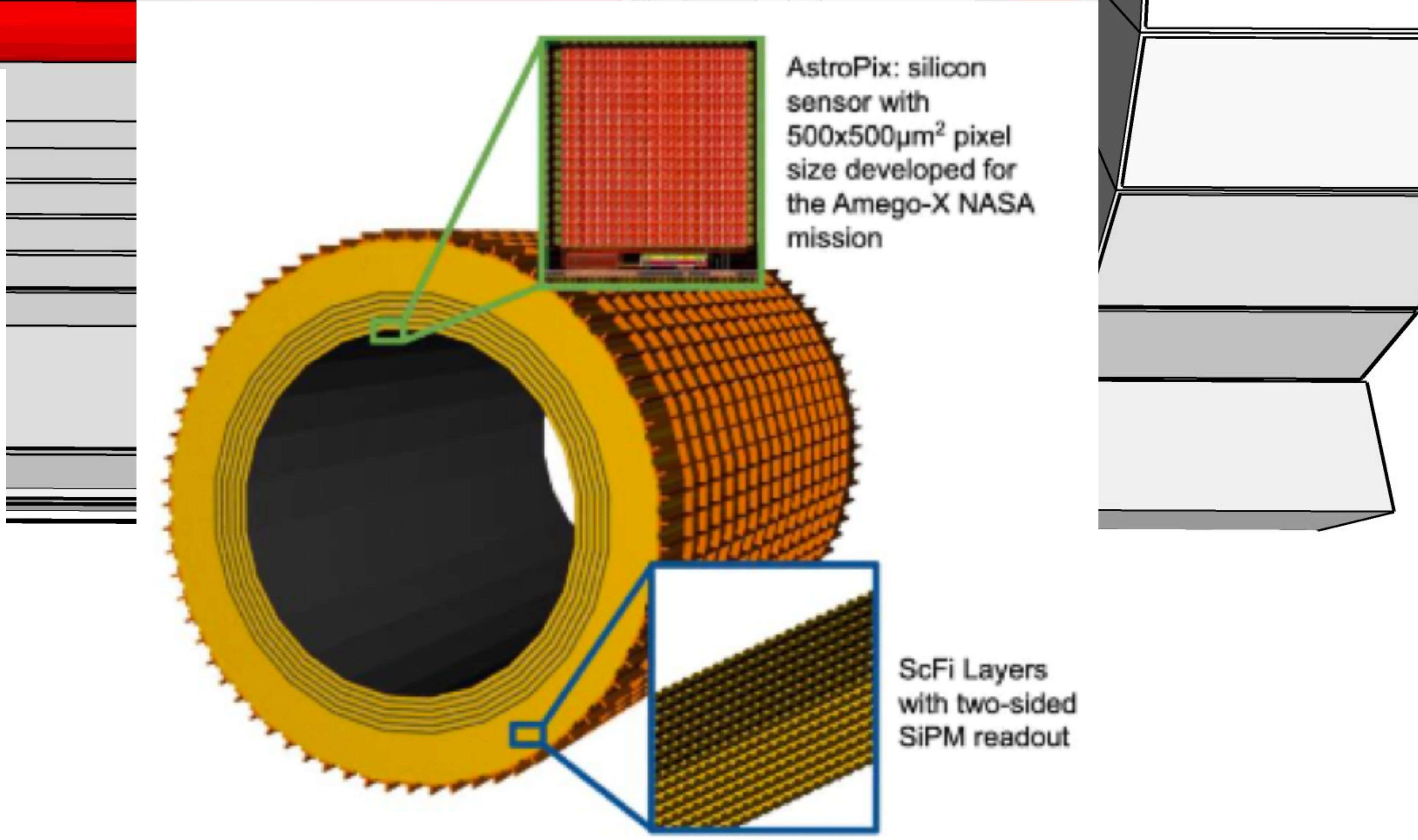

- Backward EMCAL:
  high-precision lead-glass $PbWO_4$ + Si sensors
- Barrel EMCAL:
  3D imaging with MAPS and sampling Pb/ scintillating fibres with Si sensors

Electromagnetic calorimeter

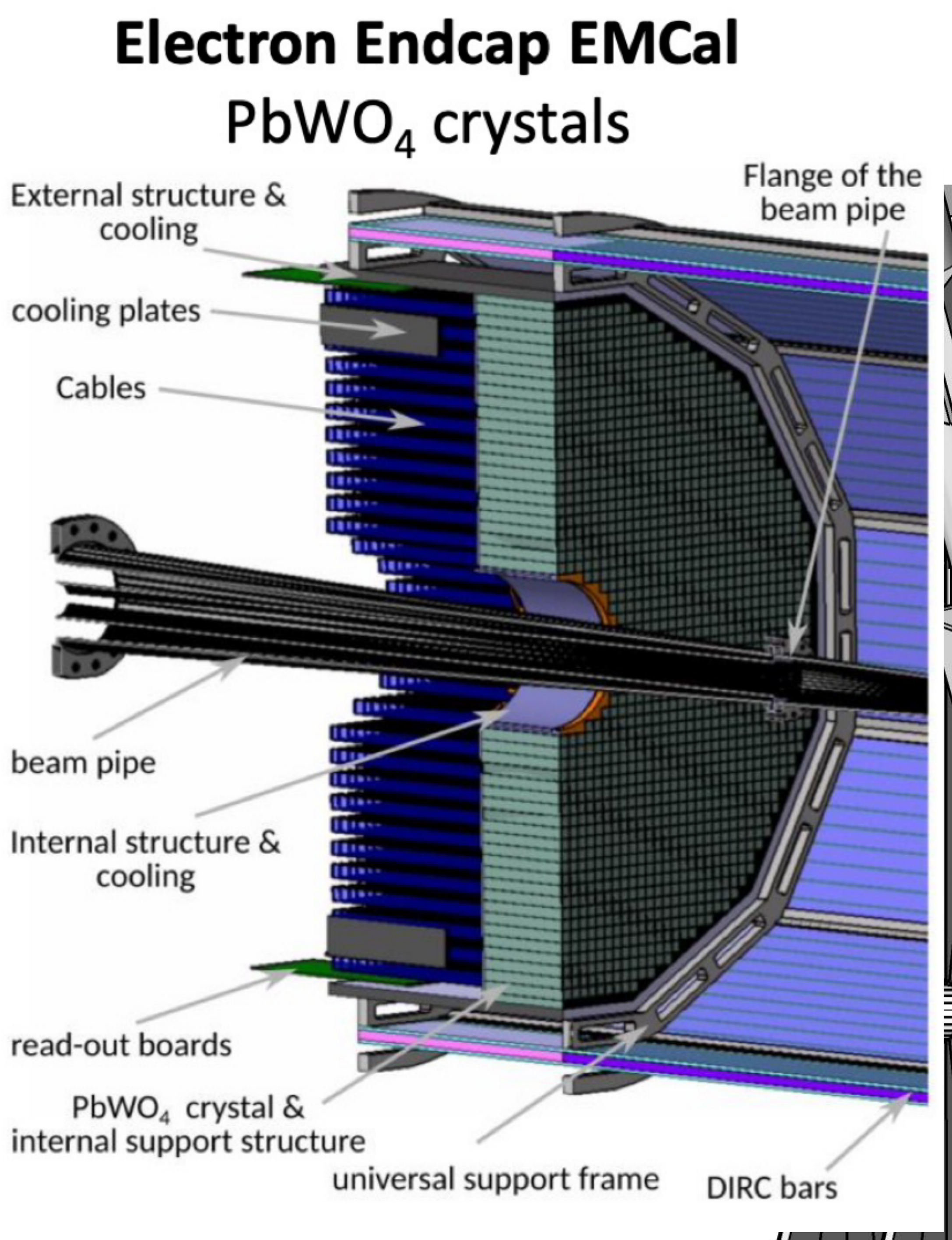

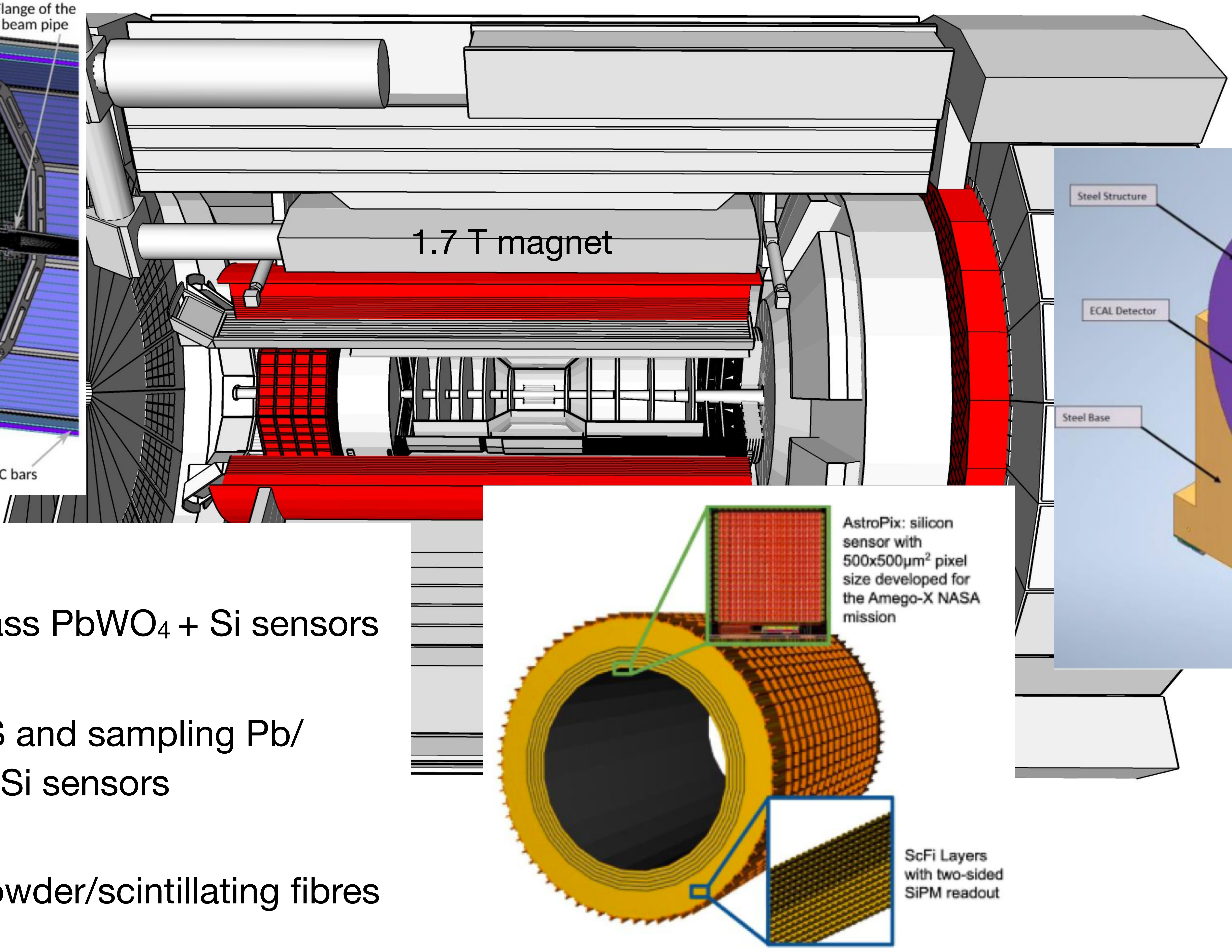

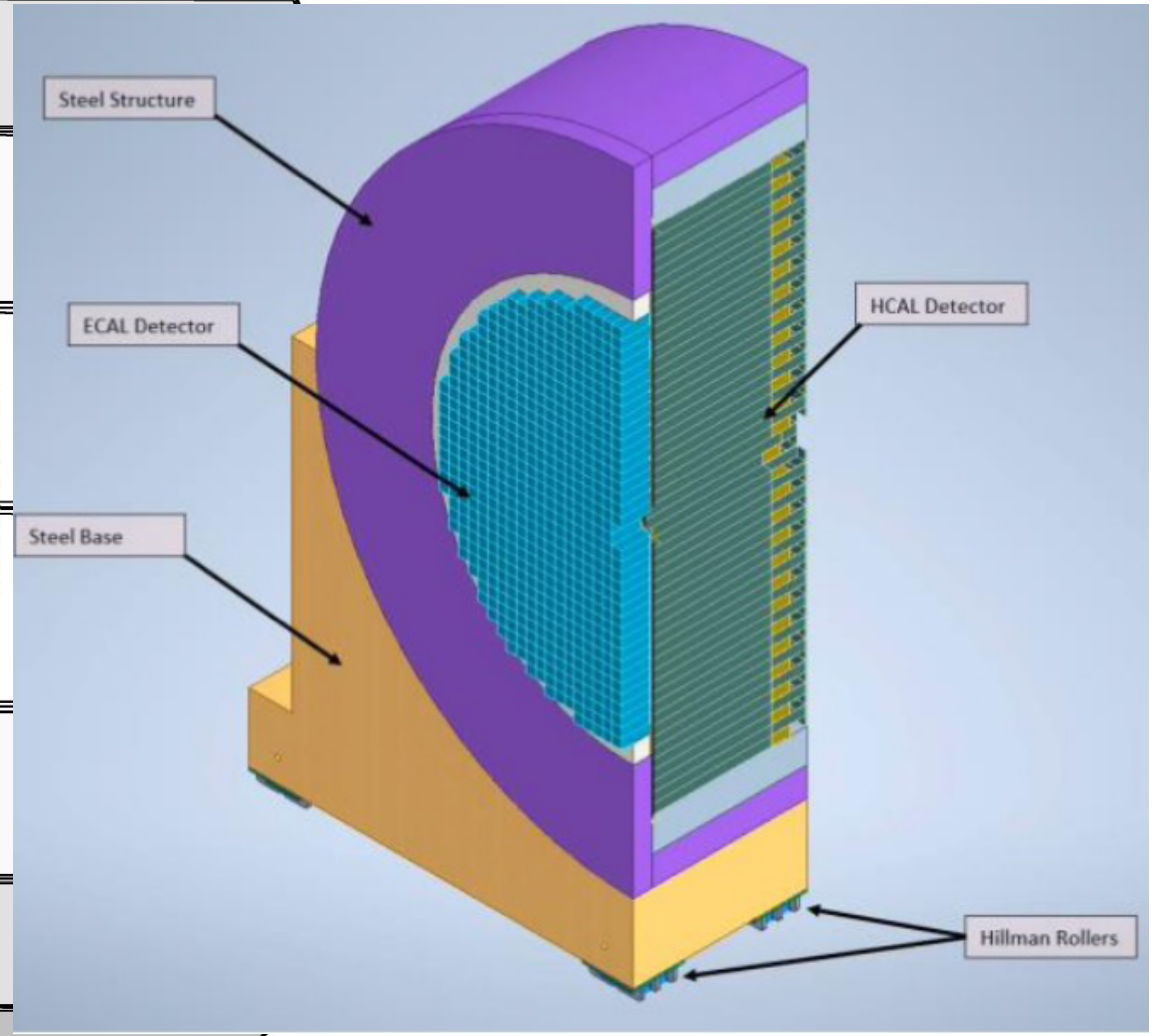

- Backward EMCAL:
  high-precision lead-glass $PbWO_4$ + Si sensors
- Barrel EMCAL:
  3D imaging with MAPS and sampling Pb/scintillating fibres with Si sensors
- Forward EMCAL:
  finely segmented W powder/scintillating fibres

Hadronic calorimeter

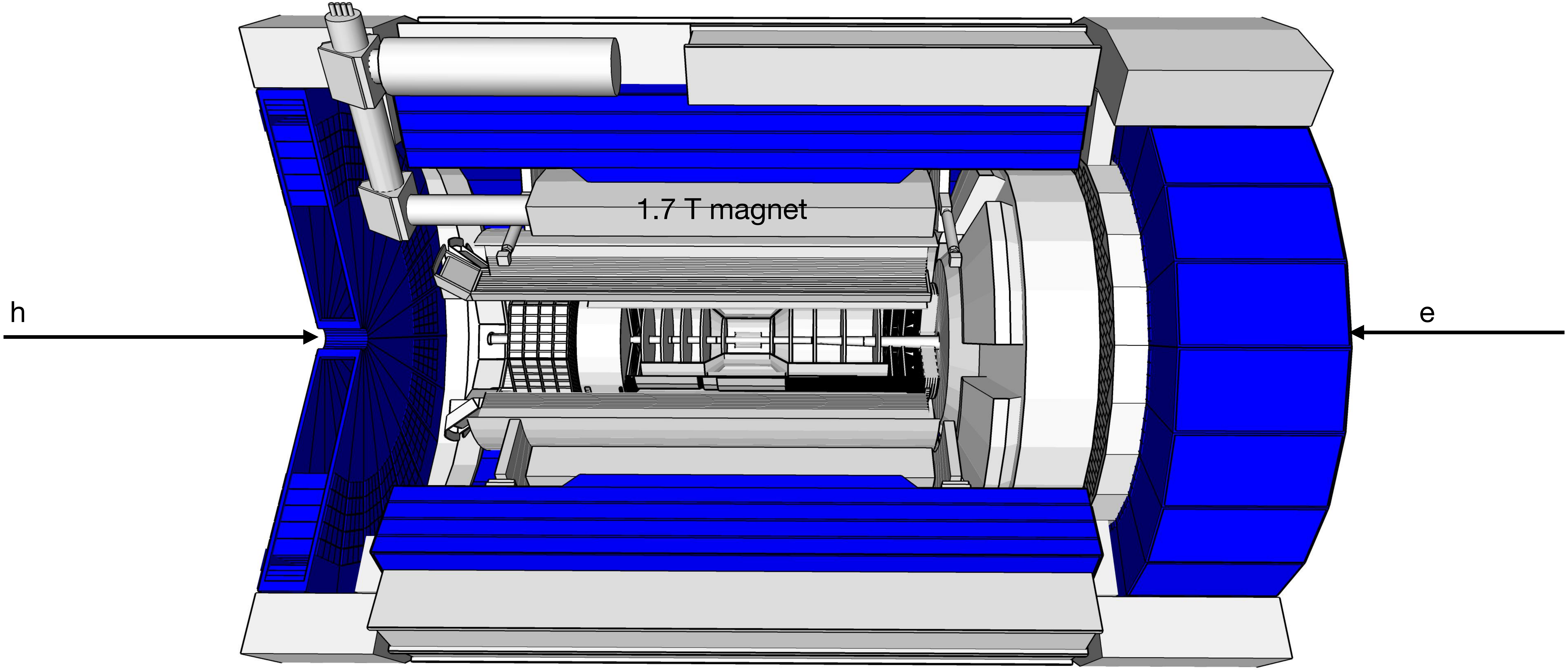

Hadronic calorimeter

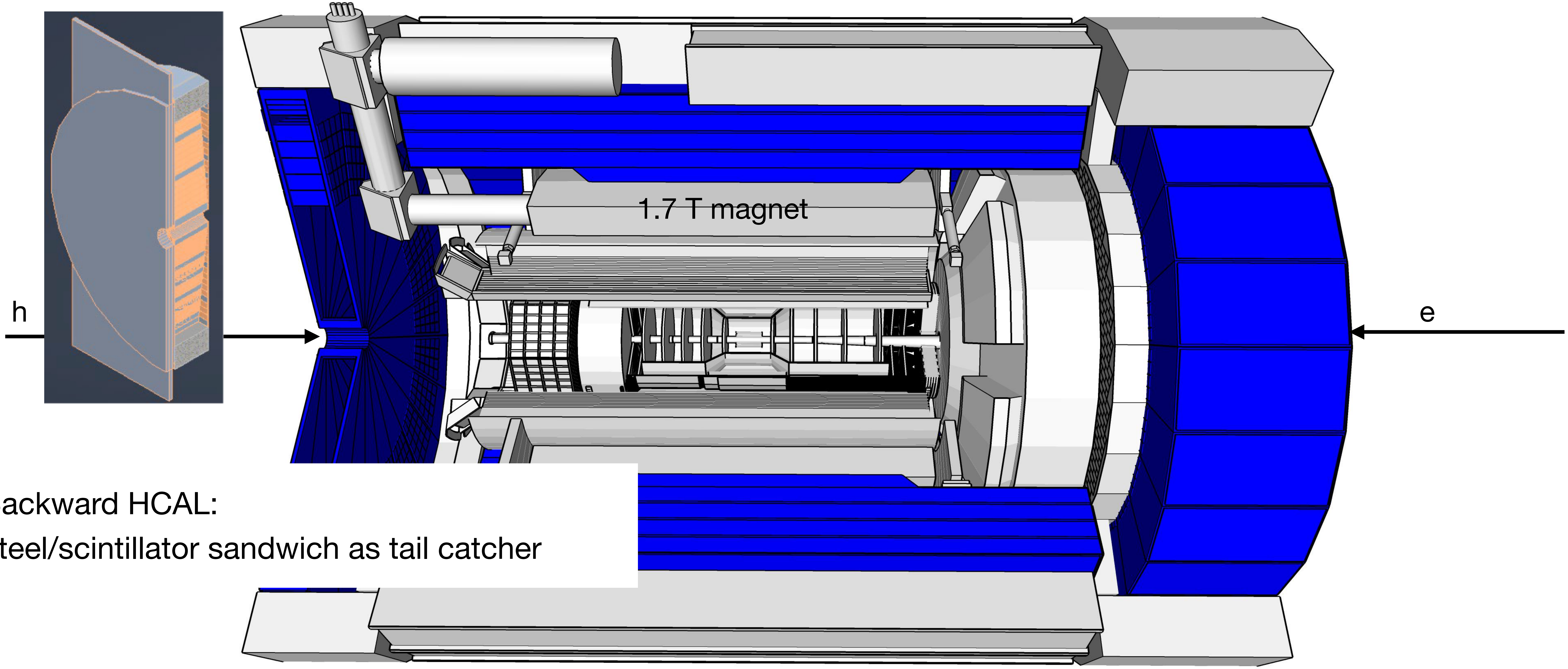

- Backward HCAL:
  steel/scintillator sandwich as tail catcher

Hadronic calorimeter

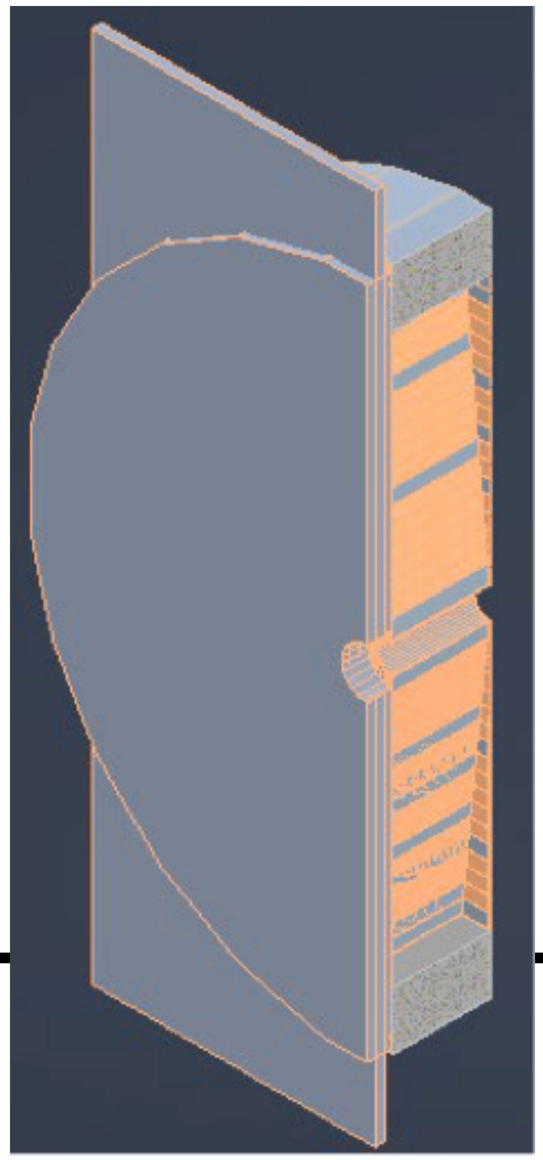

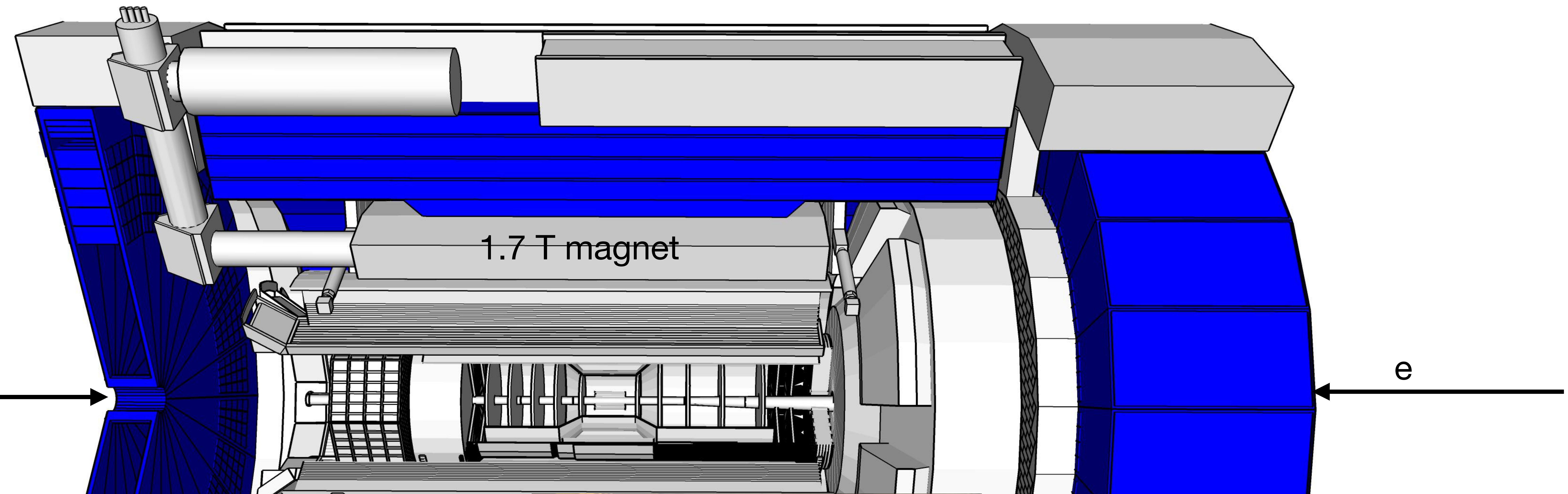

- Backward HCAL:
  steel/scintillator sandwich as tail catcher
- Barrel HCAL:
  Fe/scintillator sandwich: detection of neutrals

Hadronic calorimeter

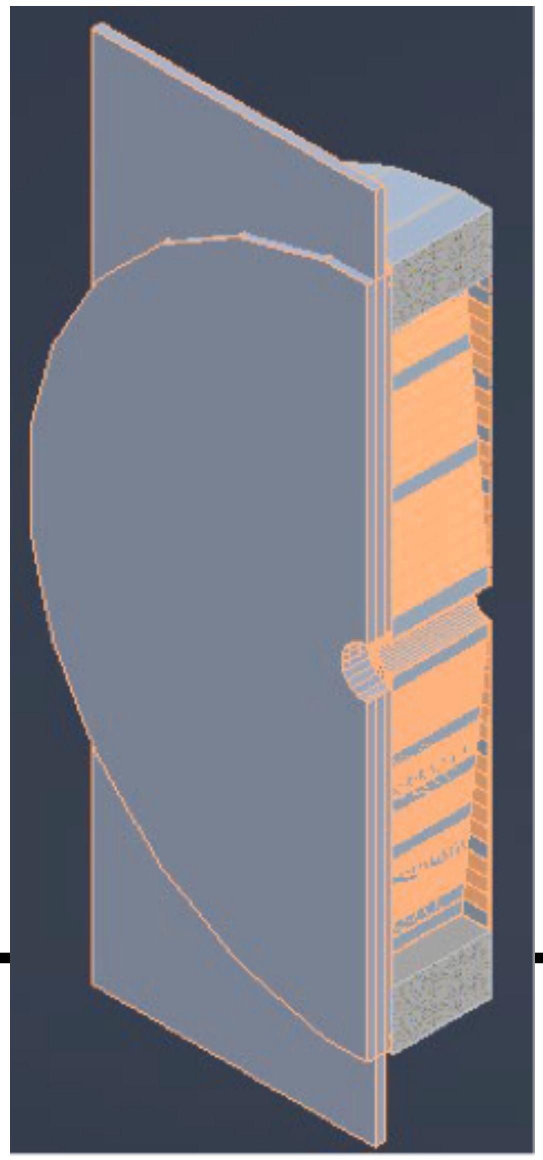

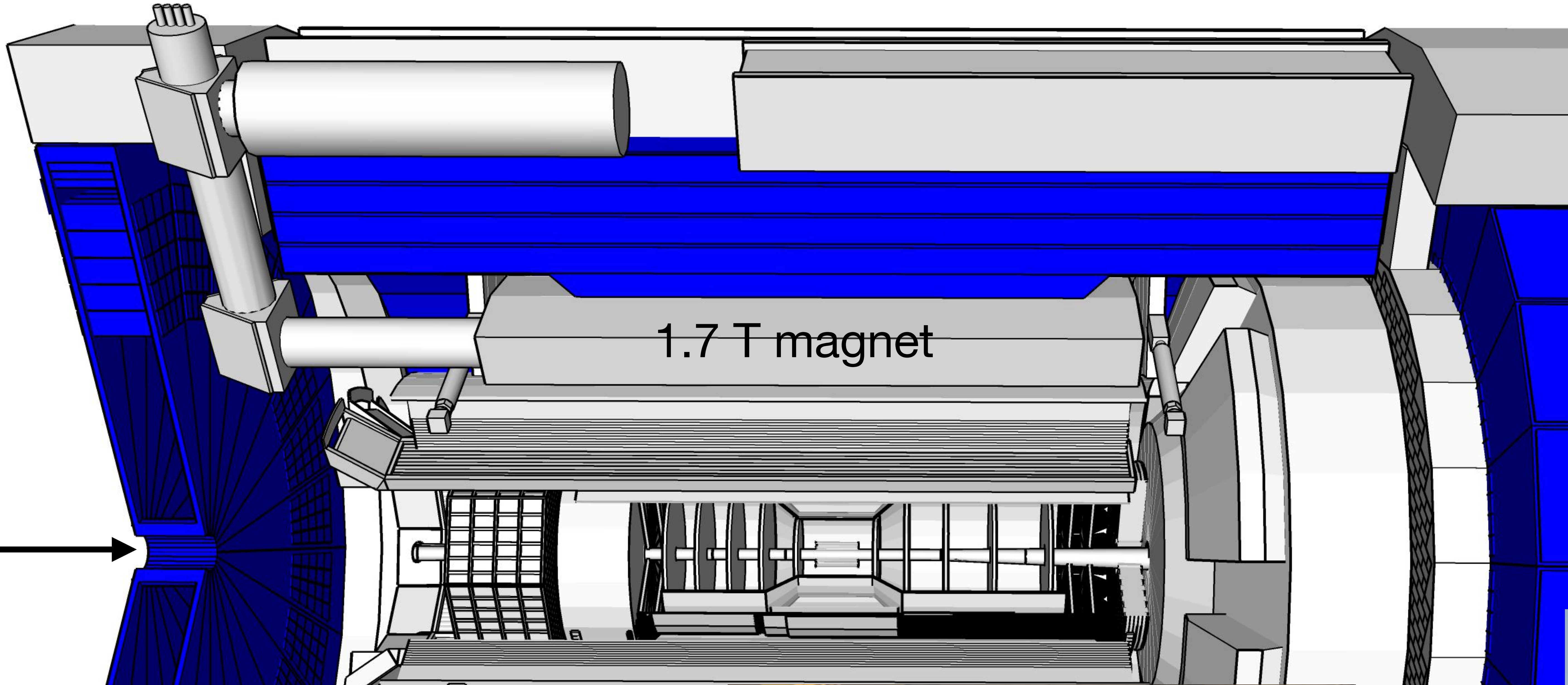

- Backward HCAL:
  steel/scintillator sandwich as tail catcher
- Barrel HCAL:
  Fe/scintillator sandwich: detection of neutrals
- Forward HCAL:
  W/scintillator sandwich longitudinally segmented, high granularity: good E resolution

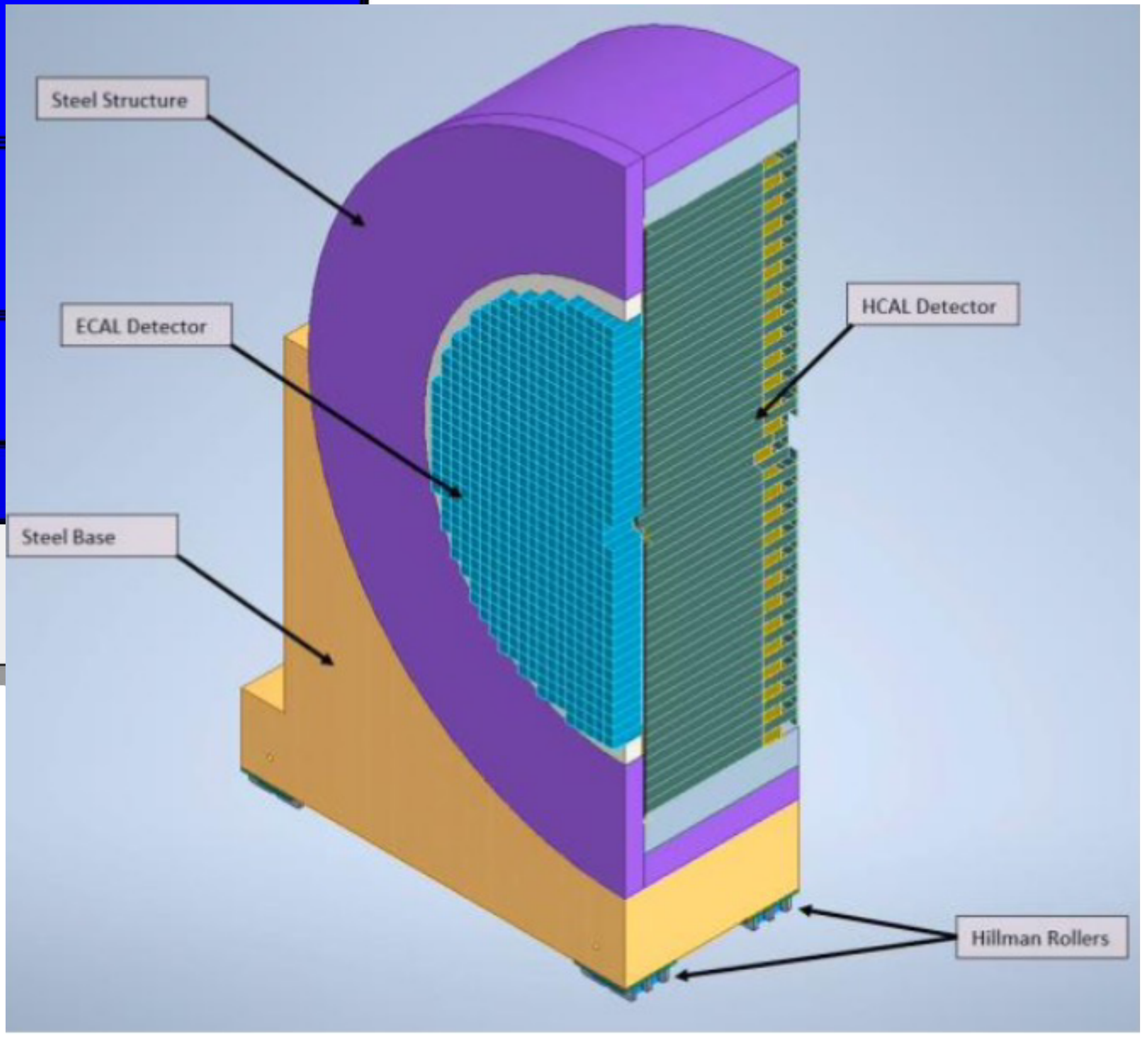

Particle identification

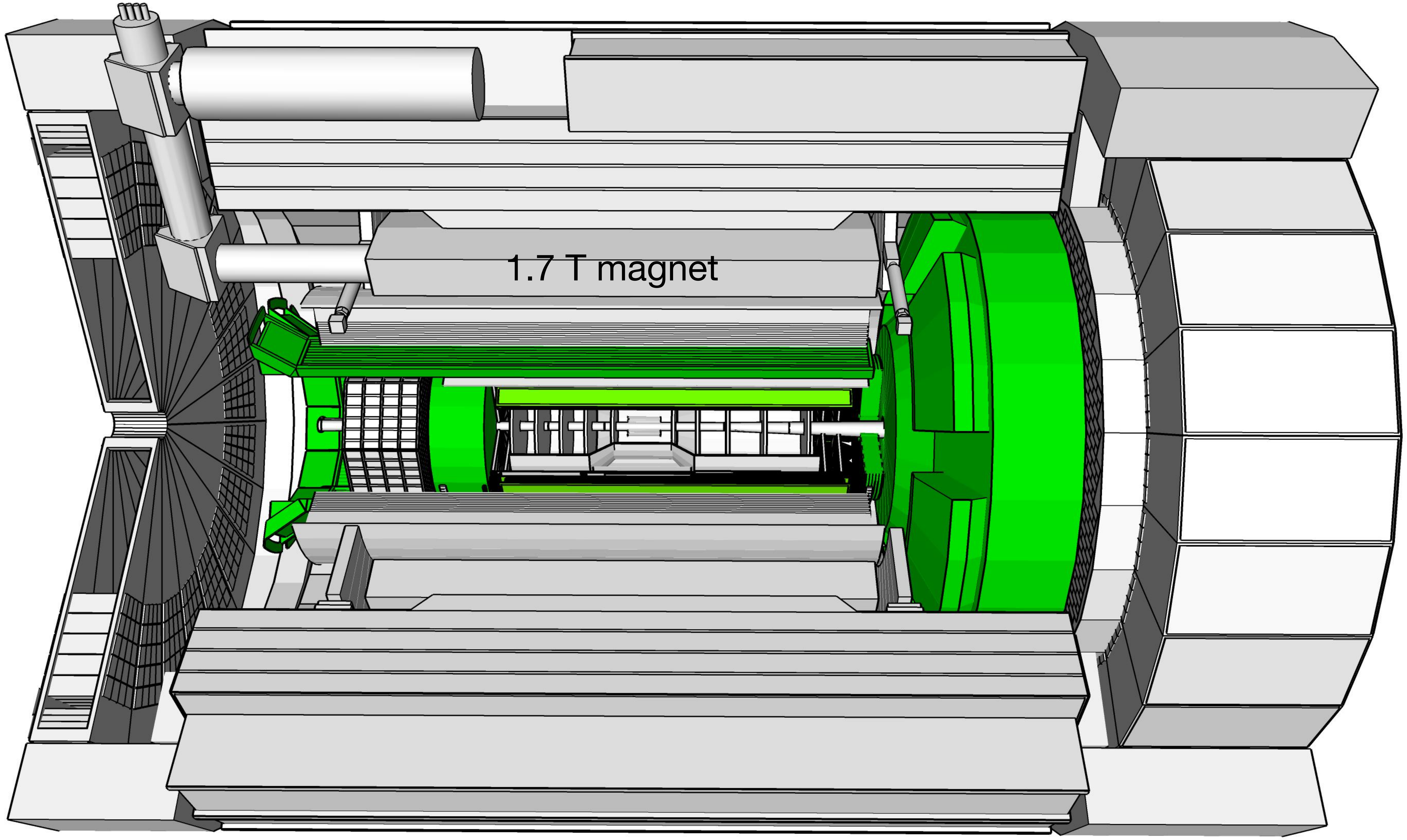

Particle identification

detectors based on
Cherenkov radiation
for 1 GeV/c<p<50 GeV/c

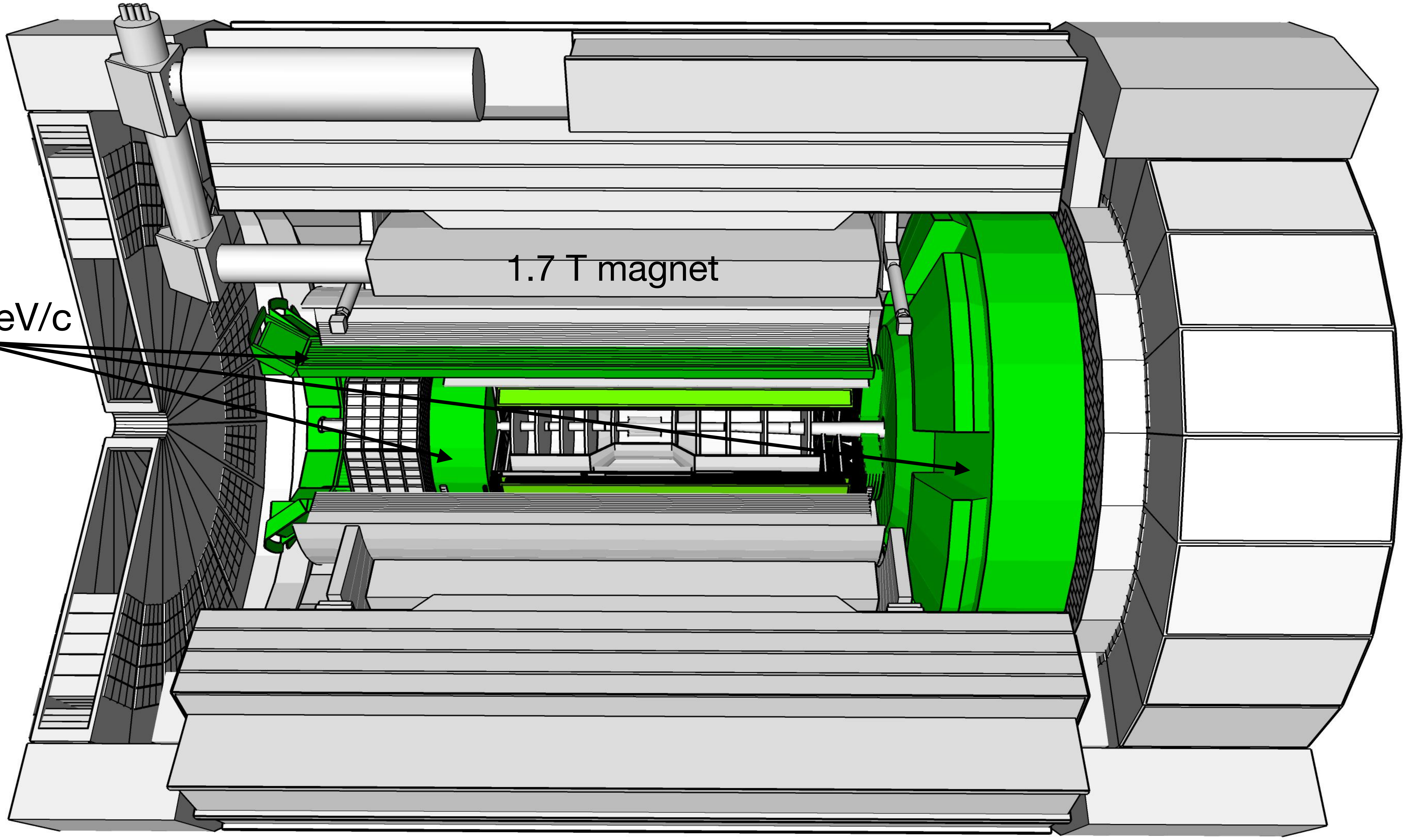

Particle identification

detectors based on
Cherenkov radiation
for 1 GeV/c<p<50 GeV/c

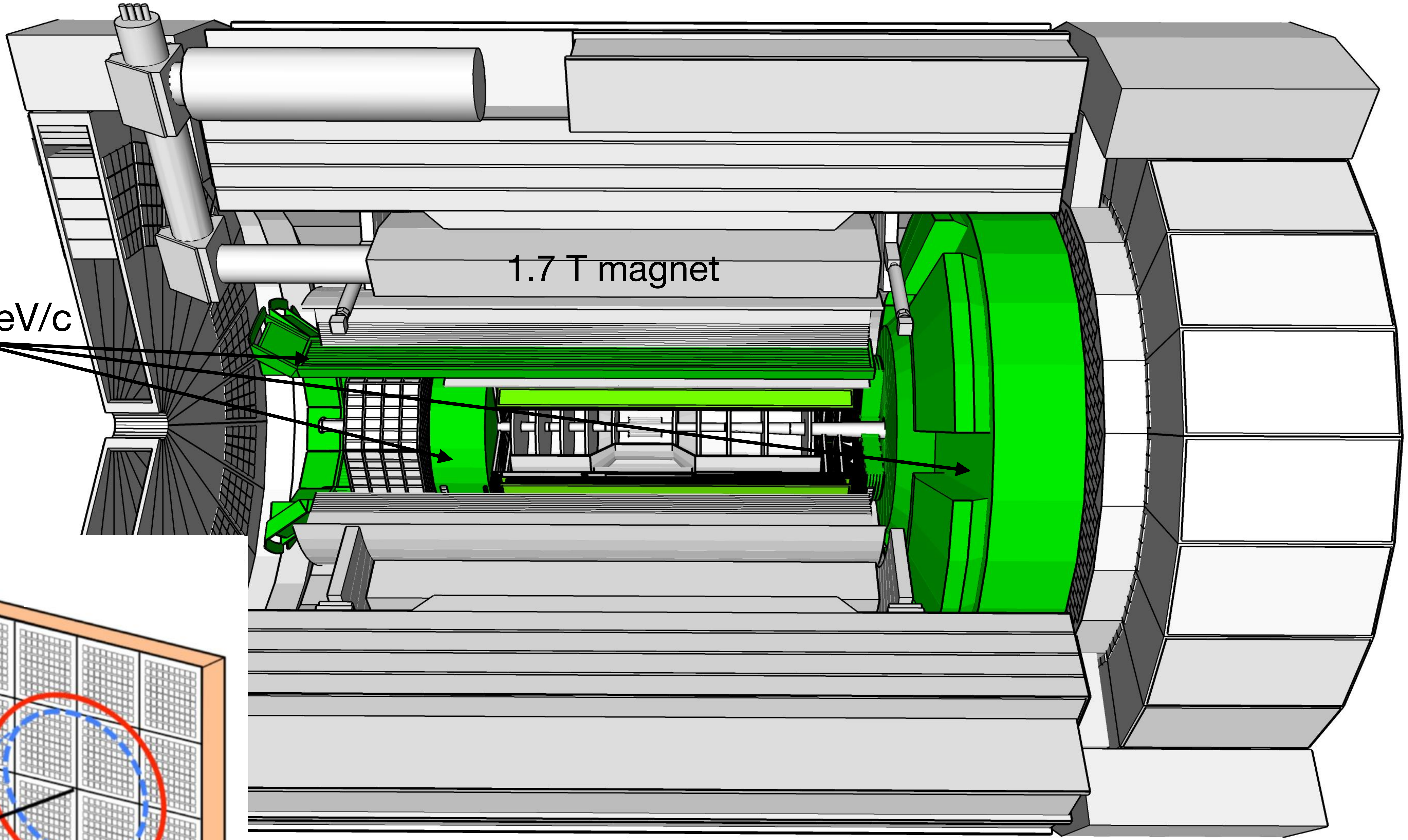

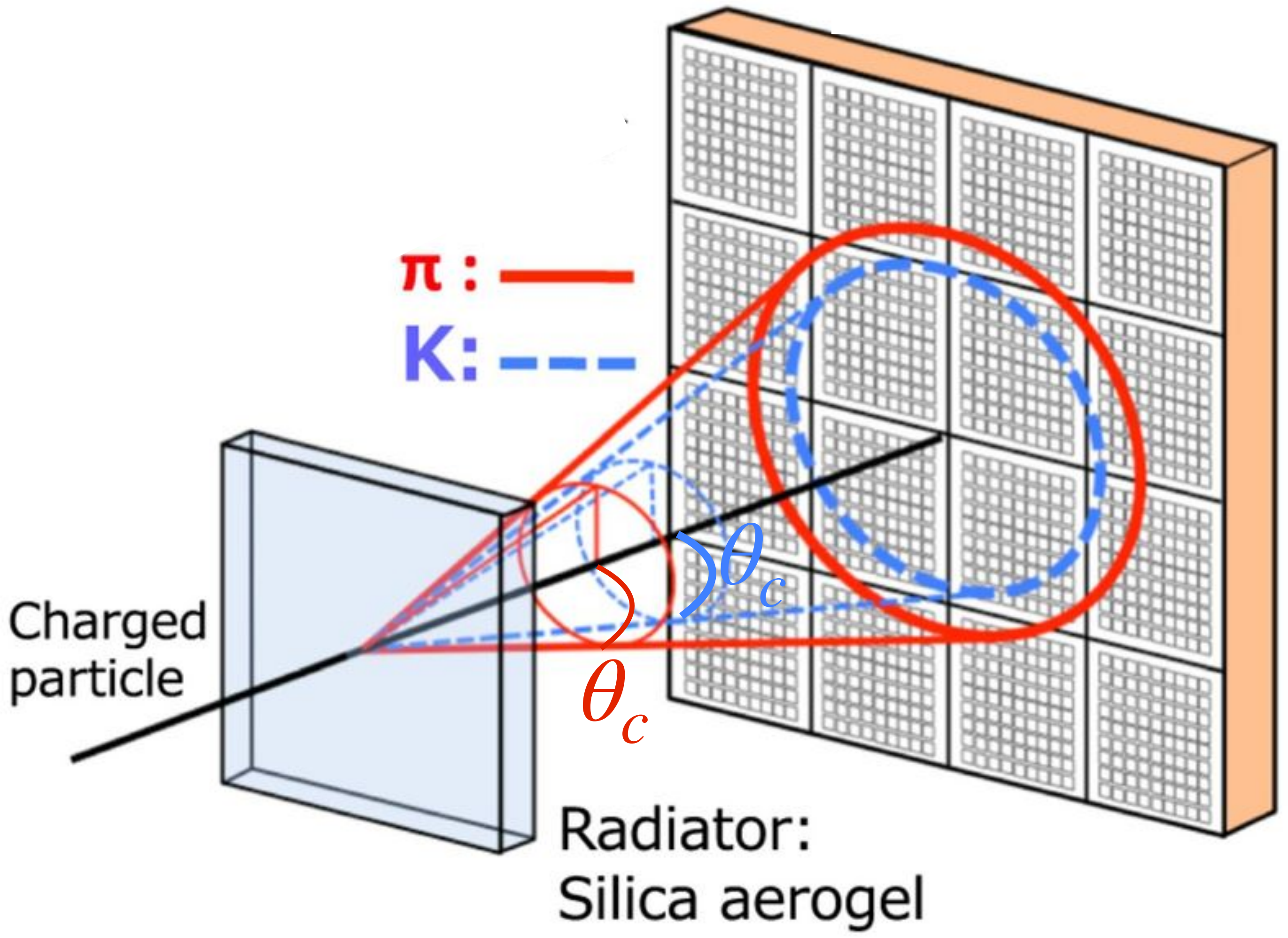

$$\cos\theta_c \propto \frac{1}{v}$$

Particle identification

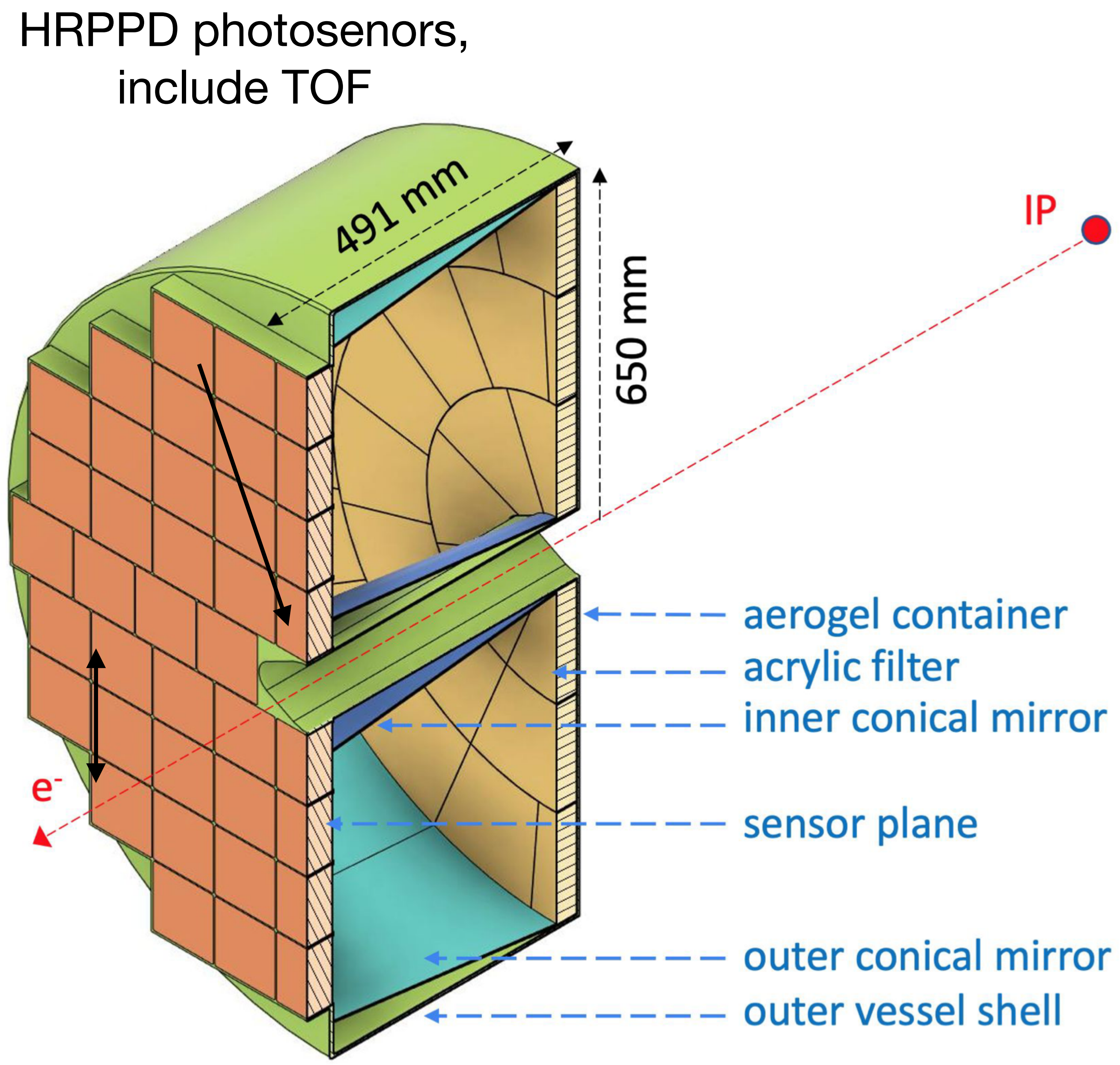

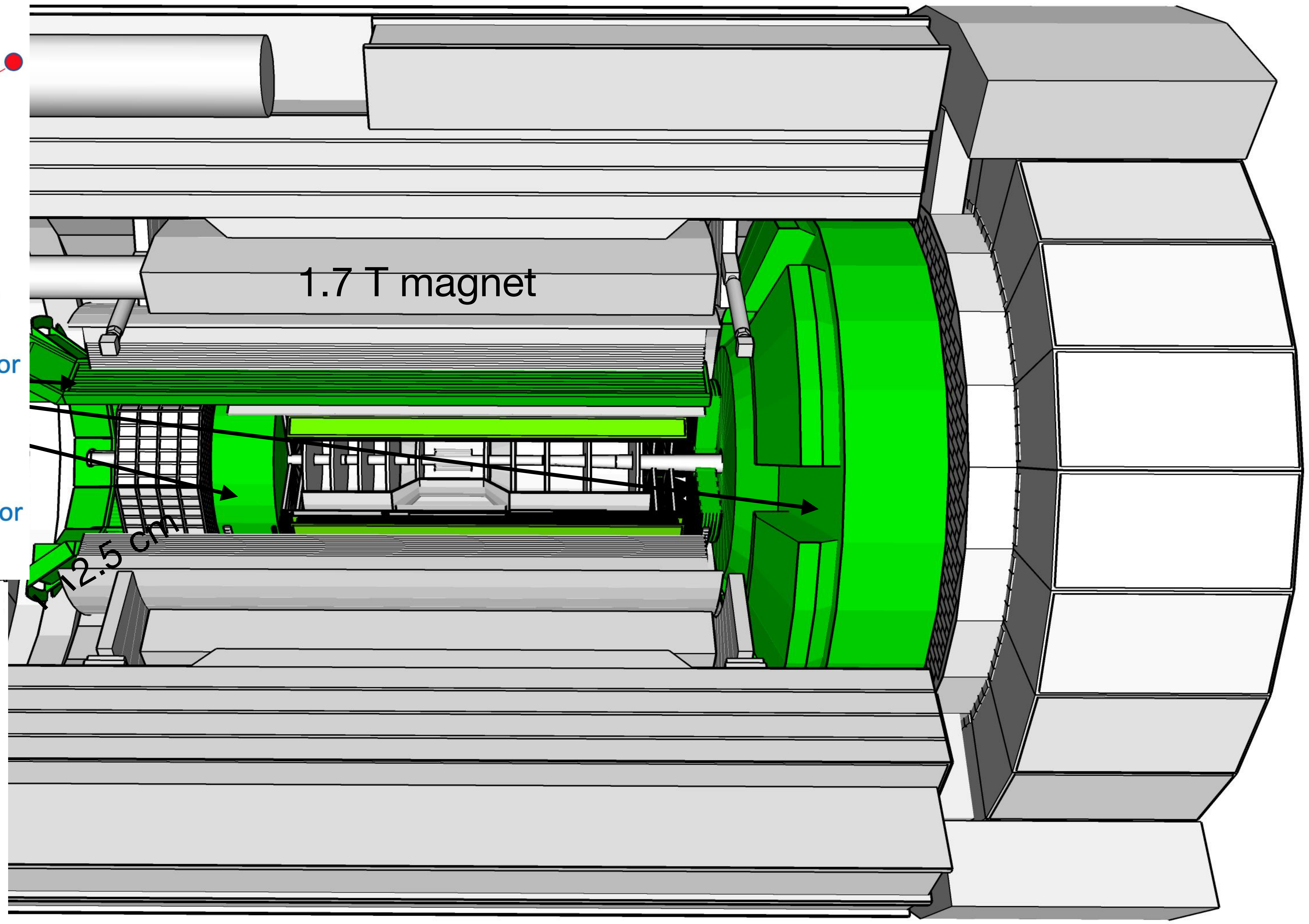

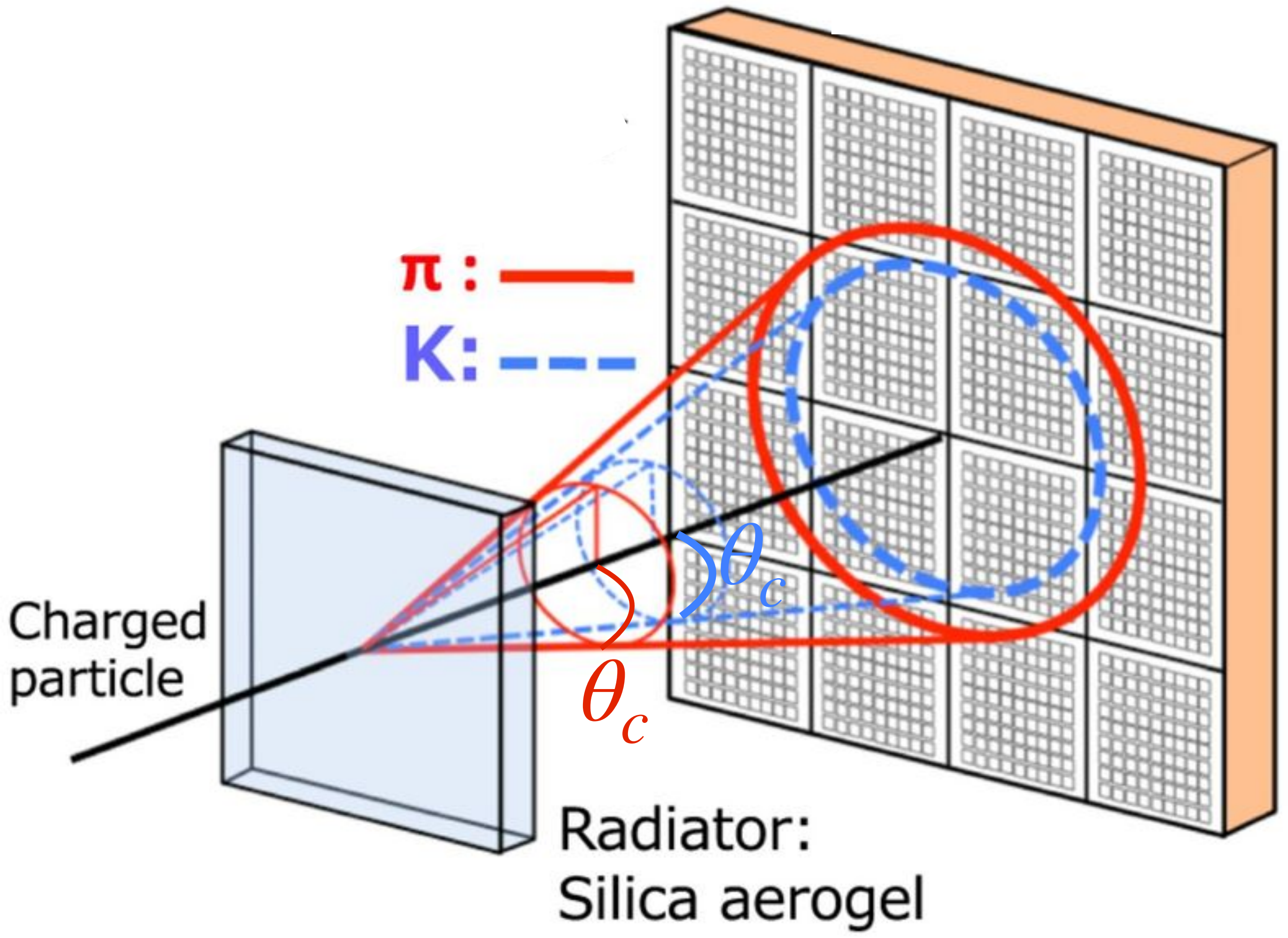

$$\cos\theta_c \propto \frac{1}{v}$$

Particle identification

HRPPD photosenors,
include TOF

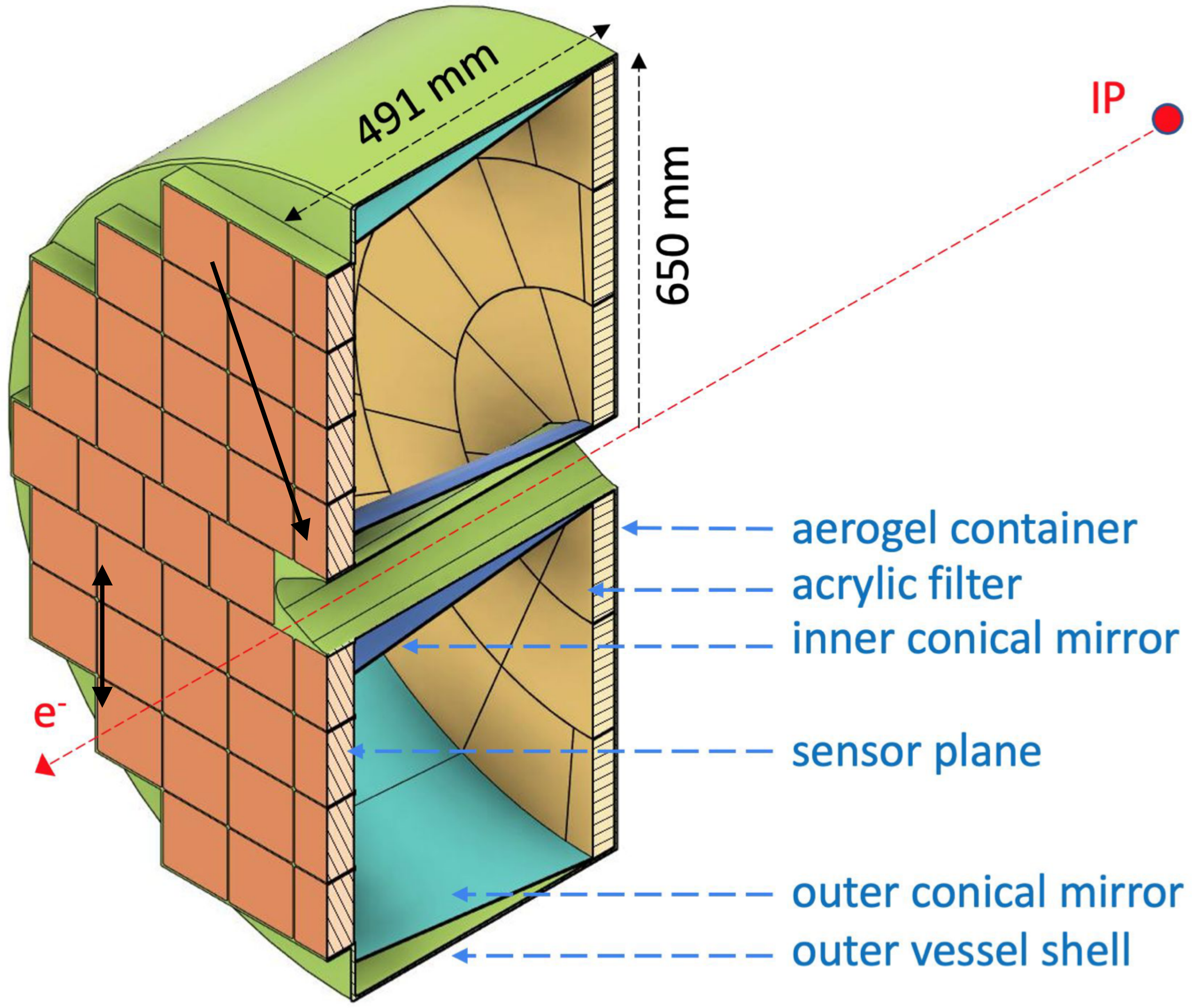

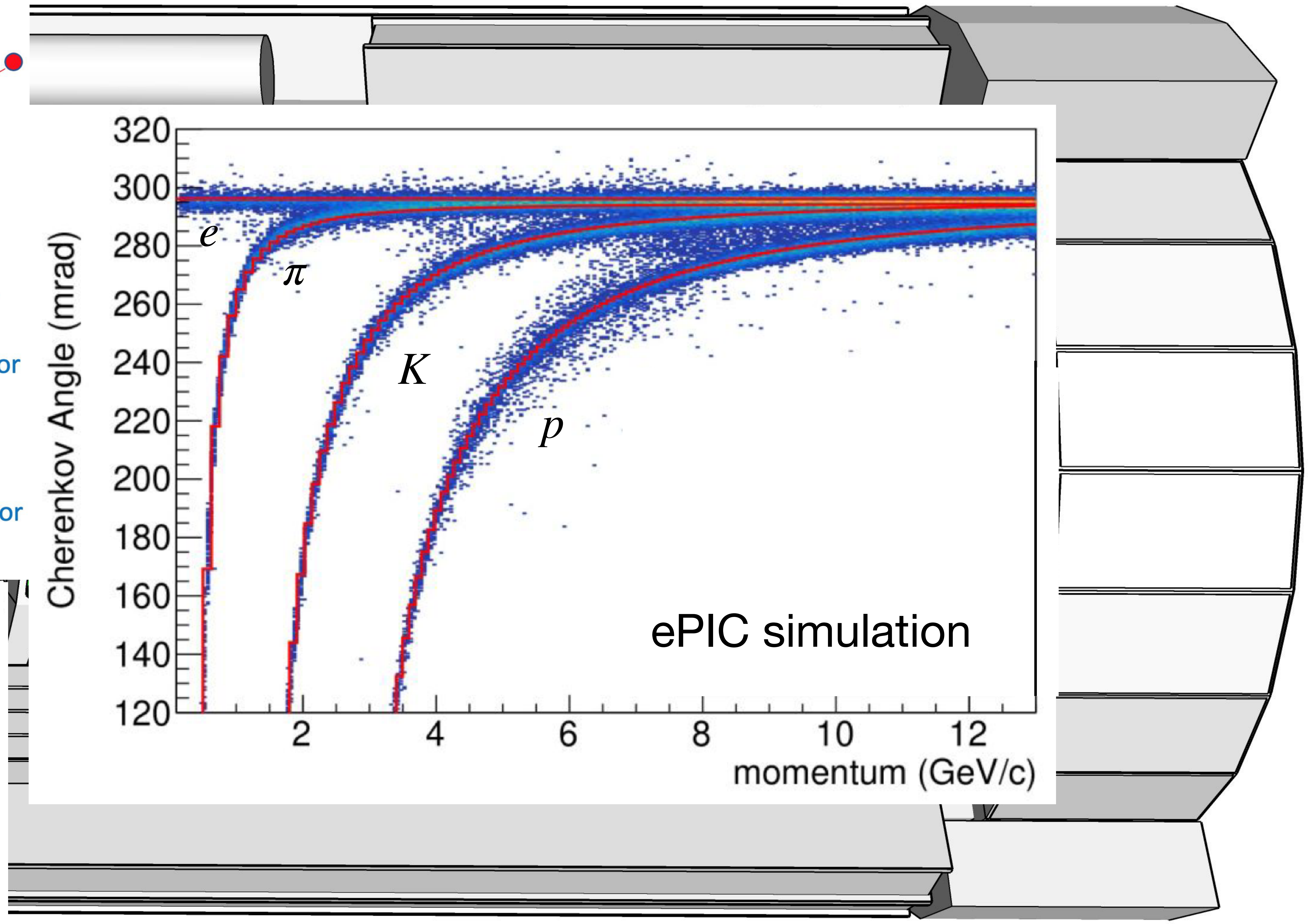

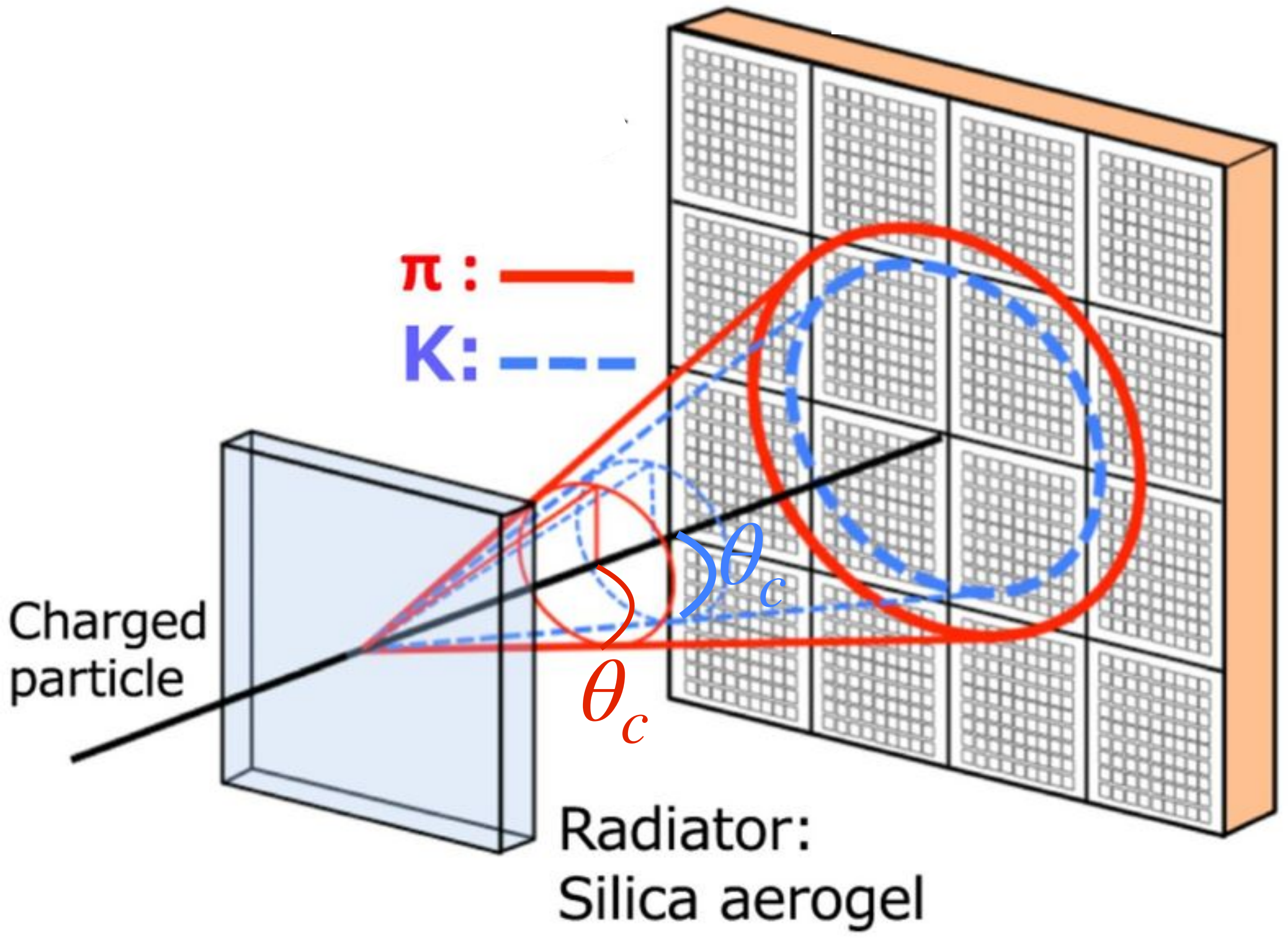

$$\cos\theta_c \propto \frac{1}{v}$$

Particle identification

detectors based on
Cherenkov radiation
for 1 GeV/c<p<50 GeV/c

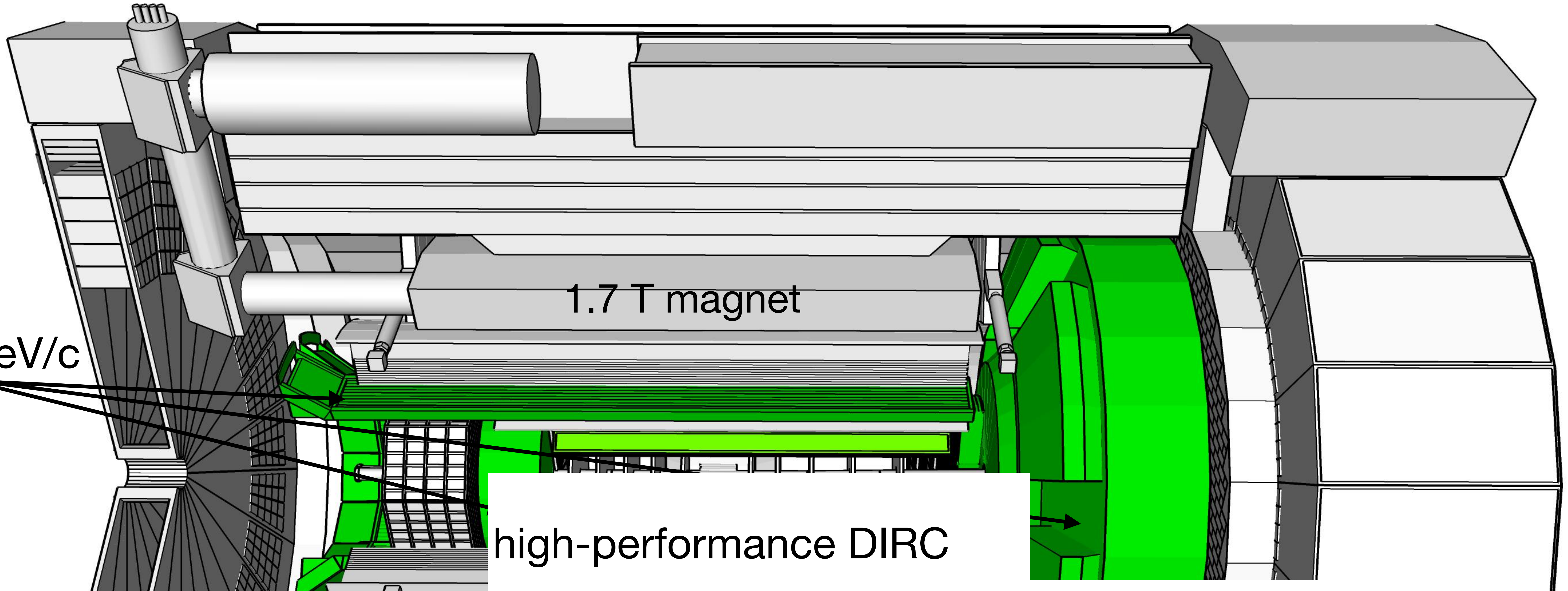

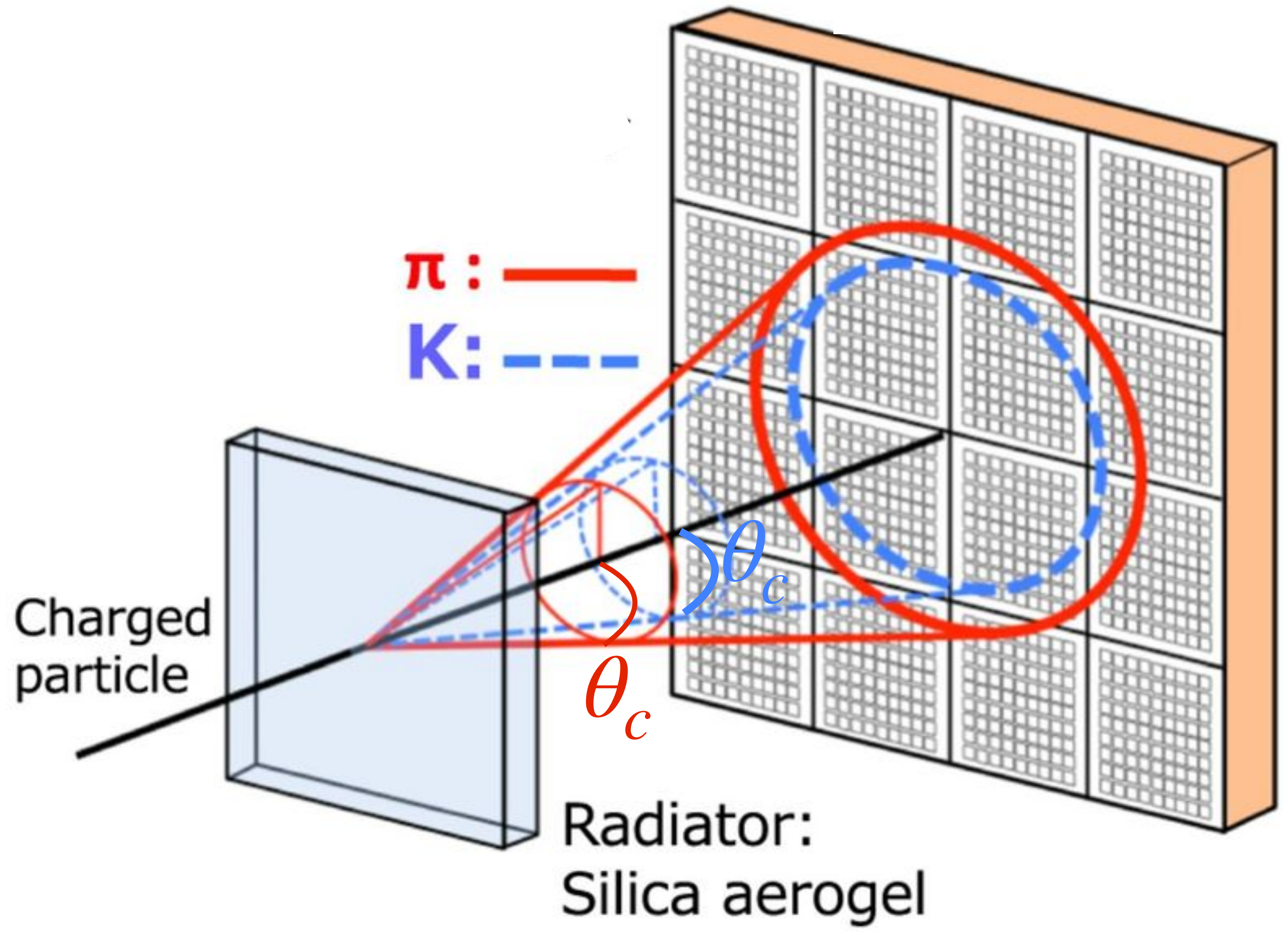

$$\cos\theta_c \propto \frac{1}{v}$$

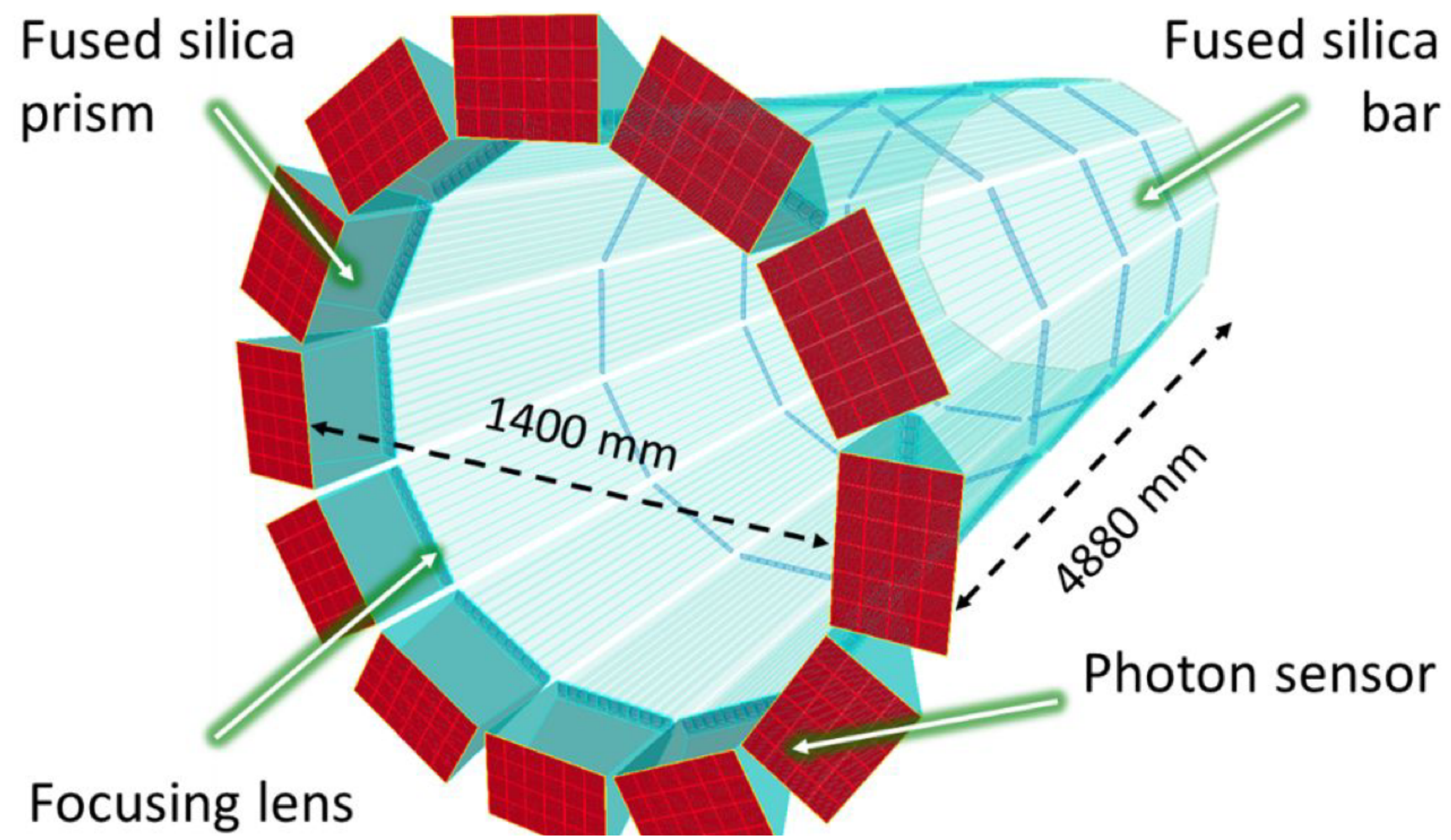

Particle identification

detectors based on Cherenkov radiation for 1 GeV/c<p<50 GeV/c

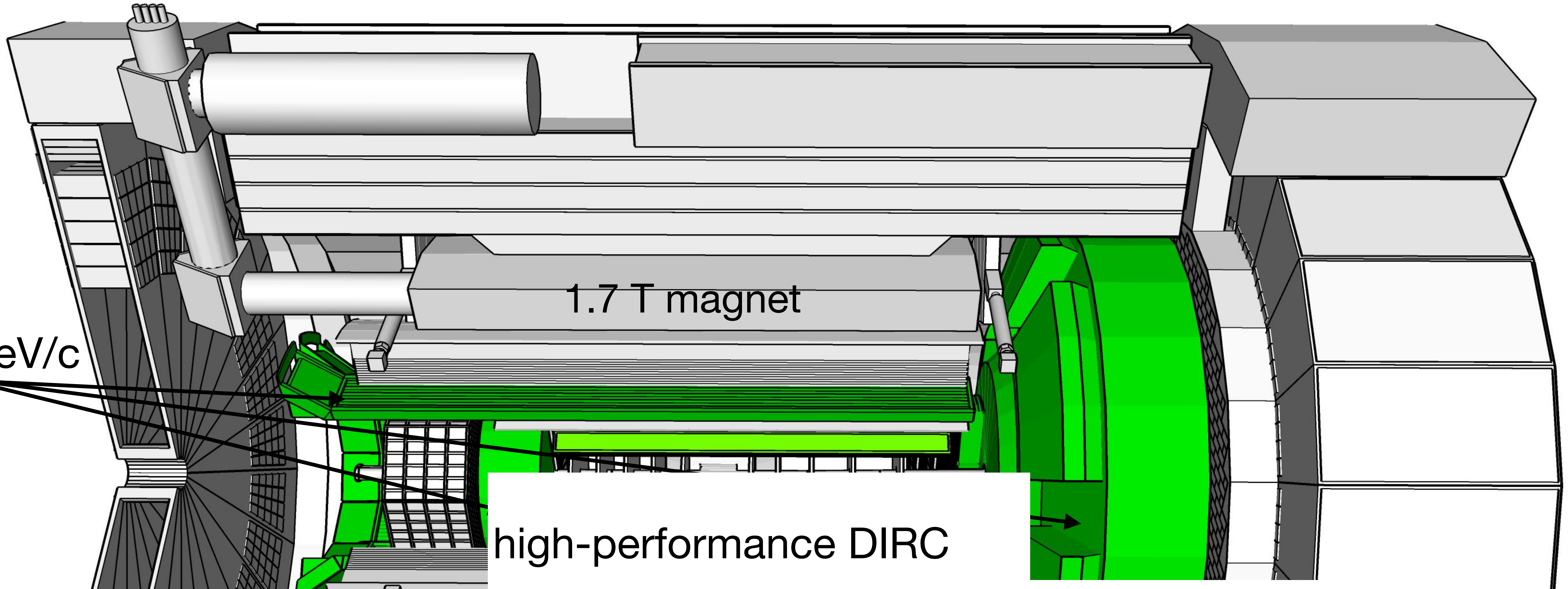

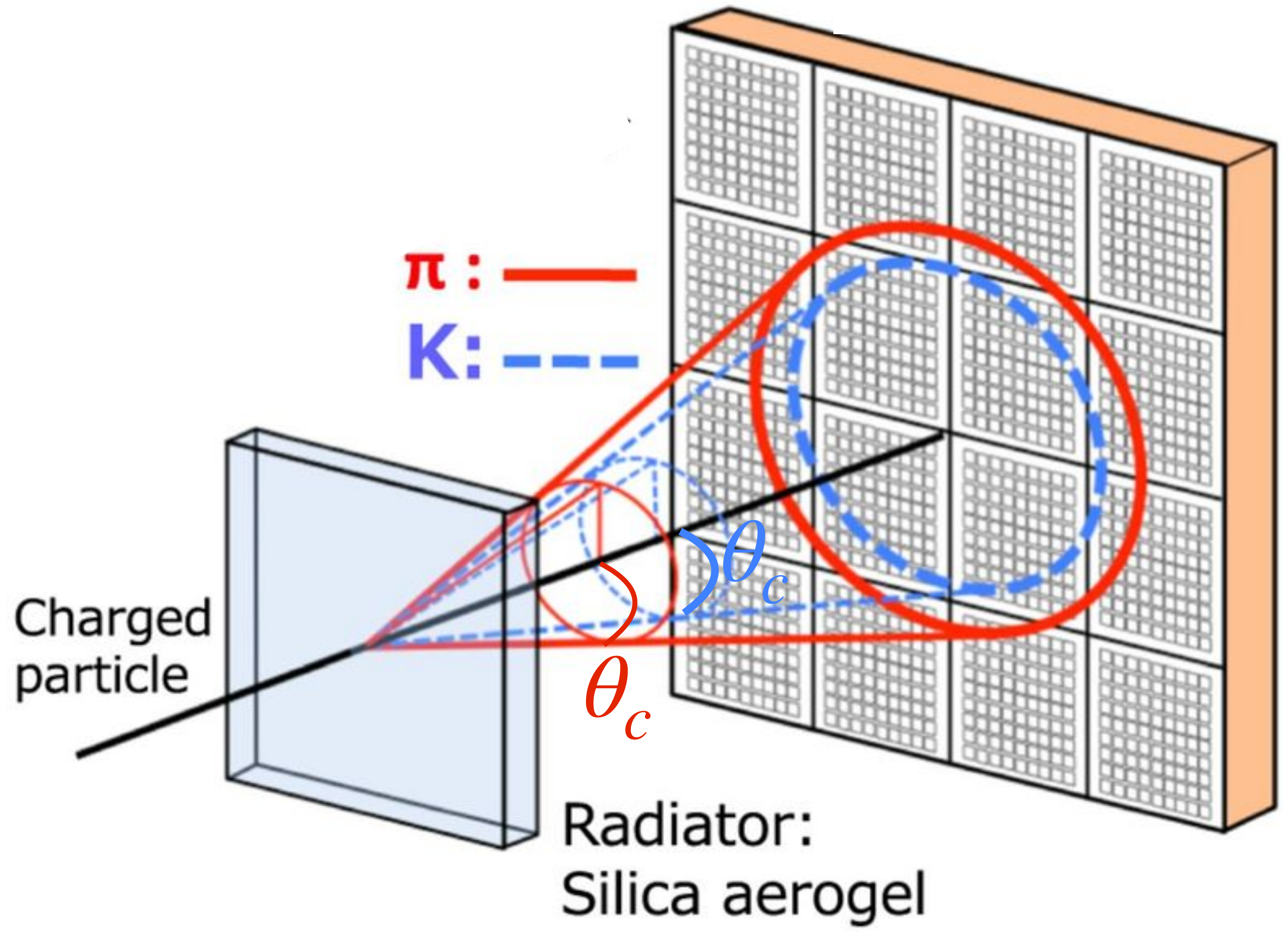

$$\cos\theta_c \propto \frac{1}{v}$$

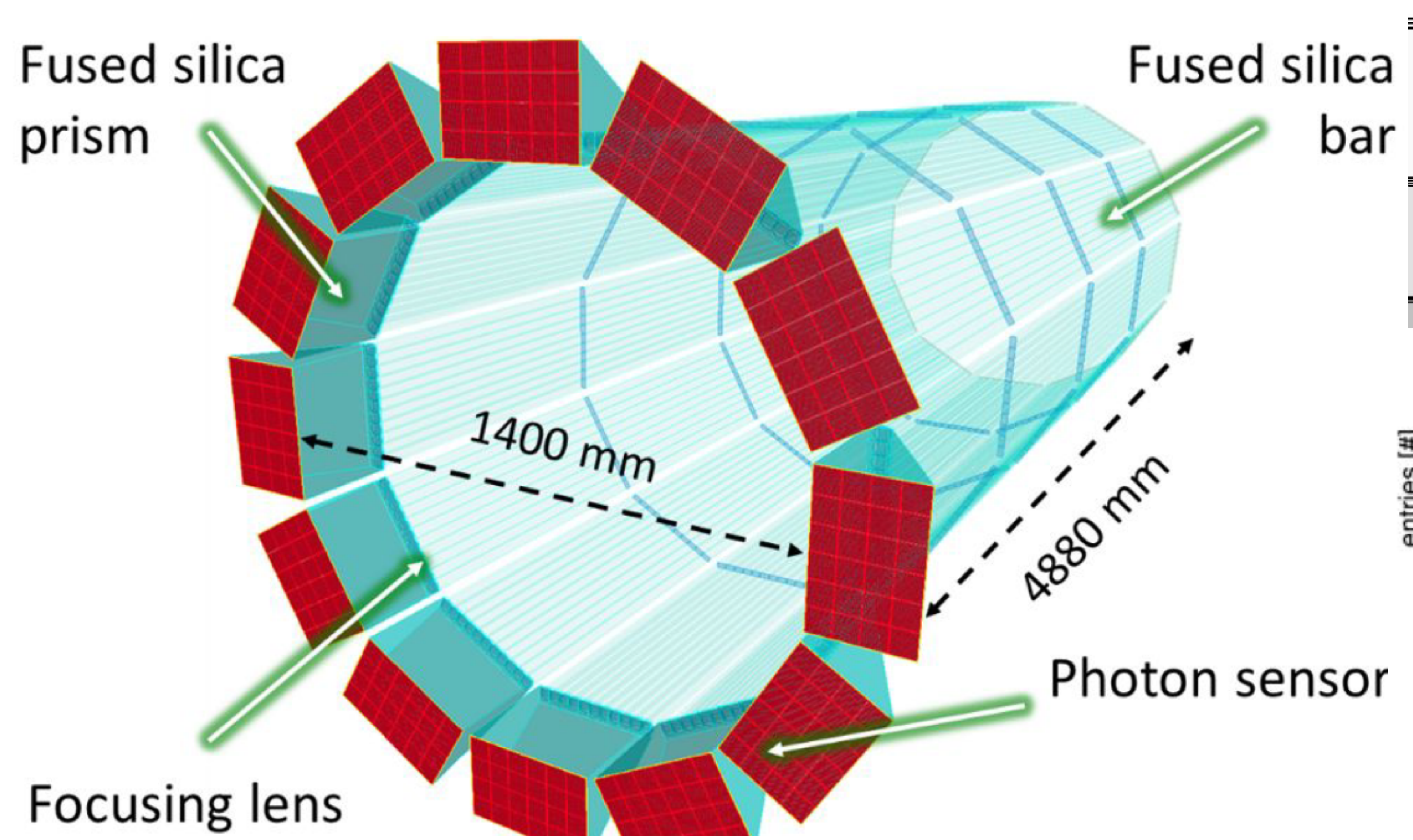

π/p separation power at 7 GeV/c

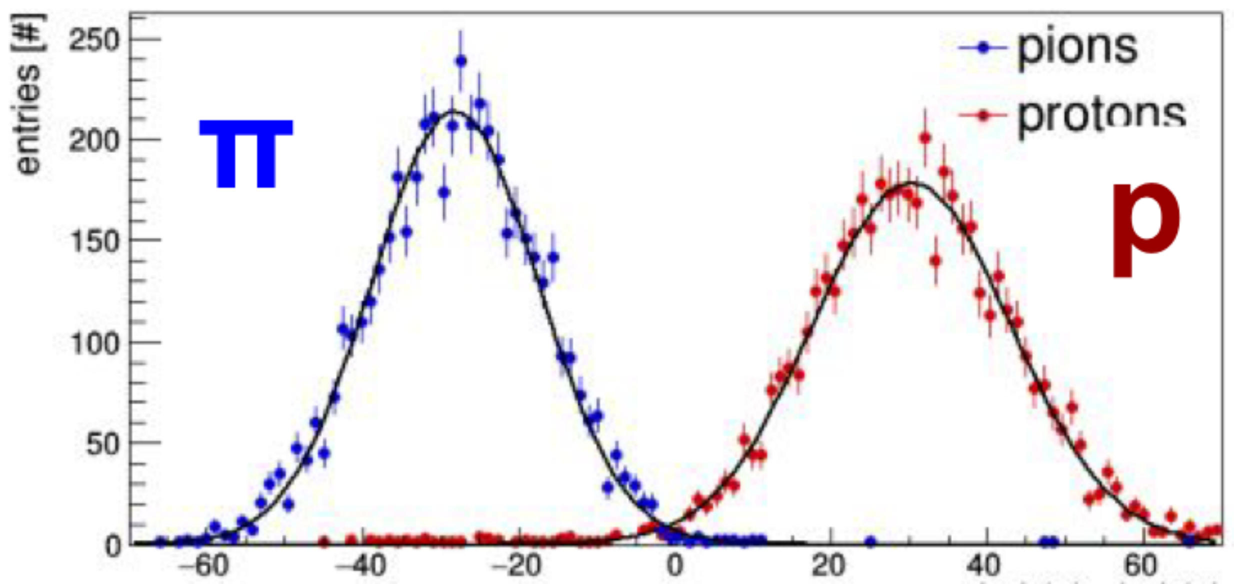

Particle identification

detectors based on Cherenkov radiation for 1 GeV/c<p<50 GeV/c

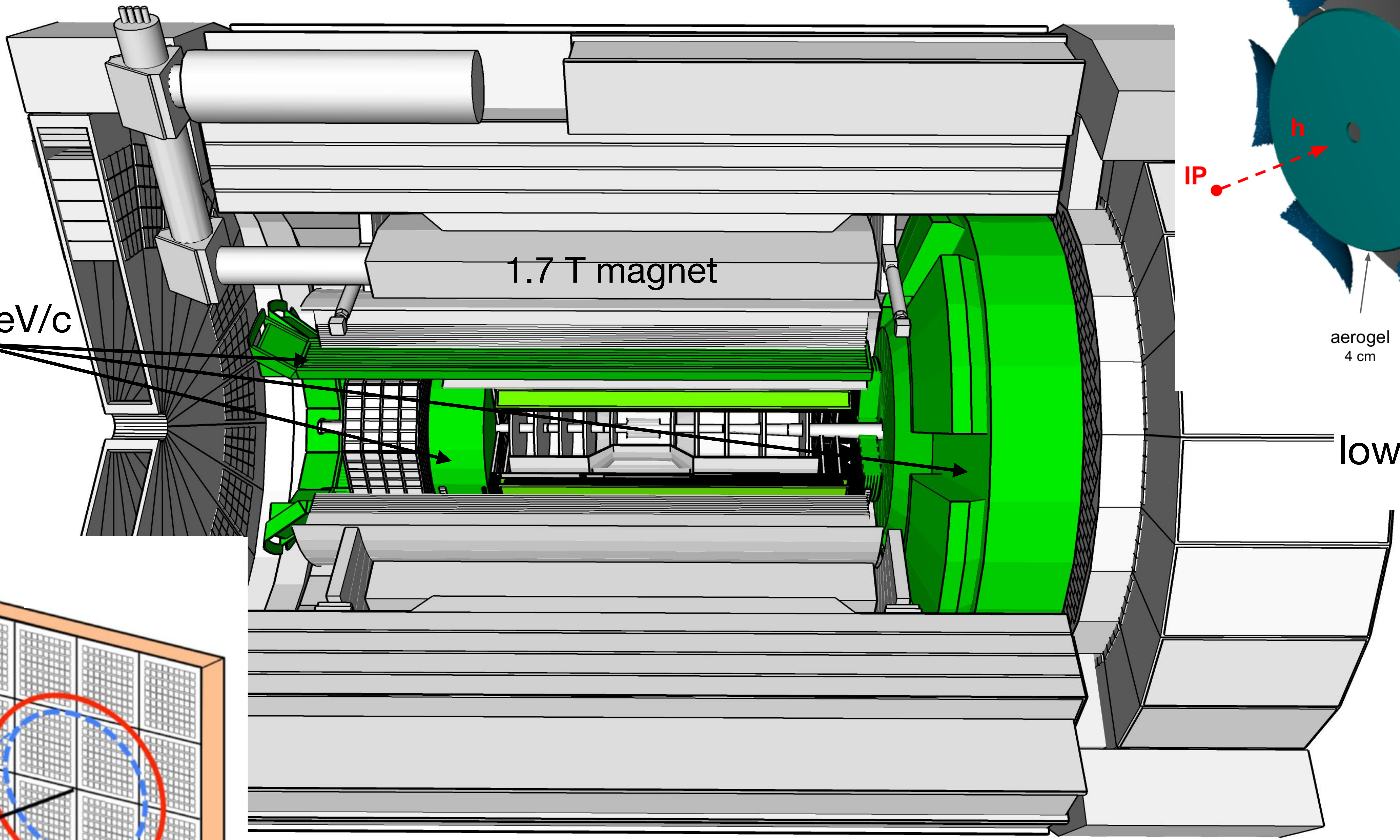

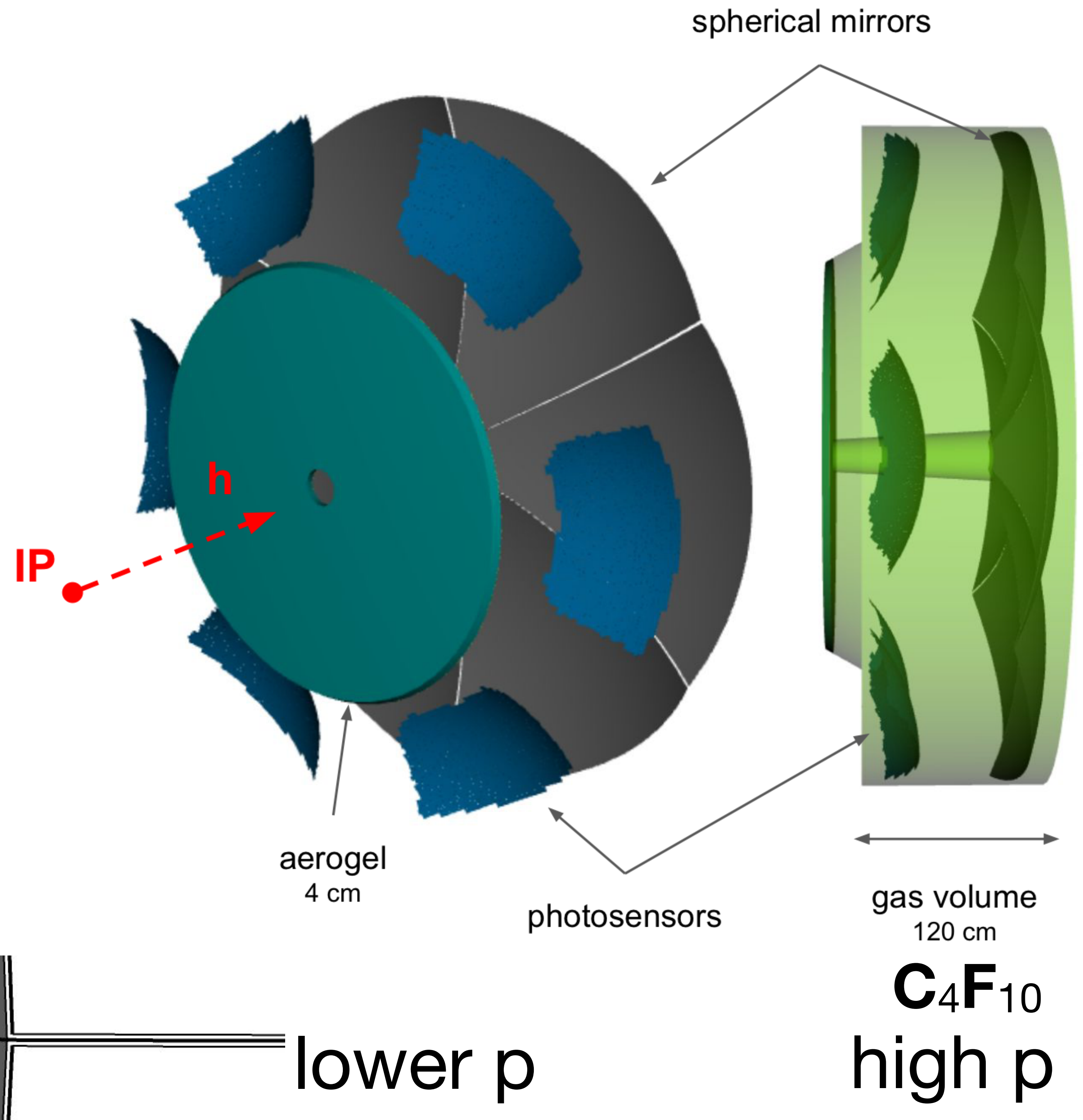

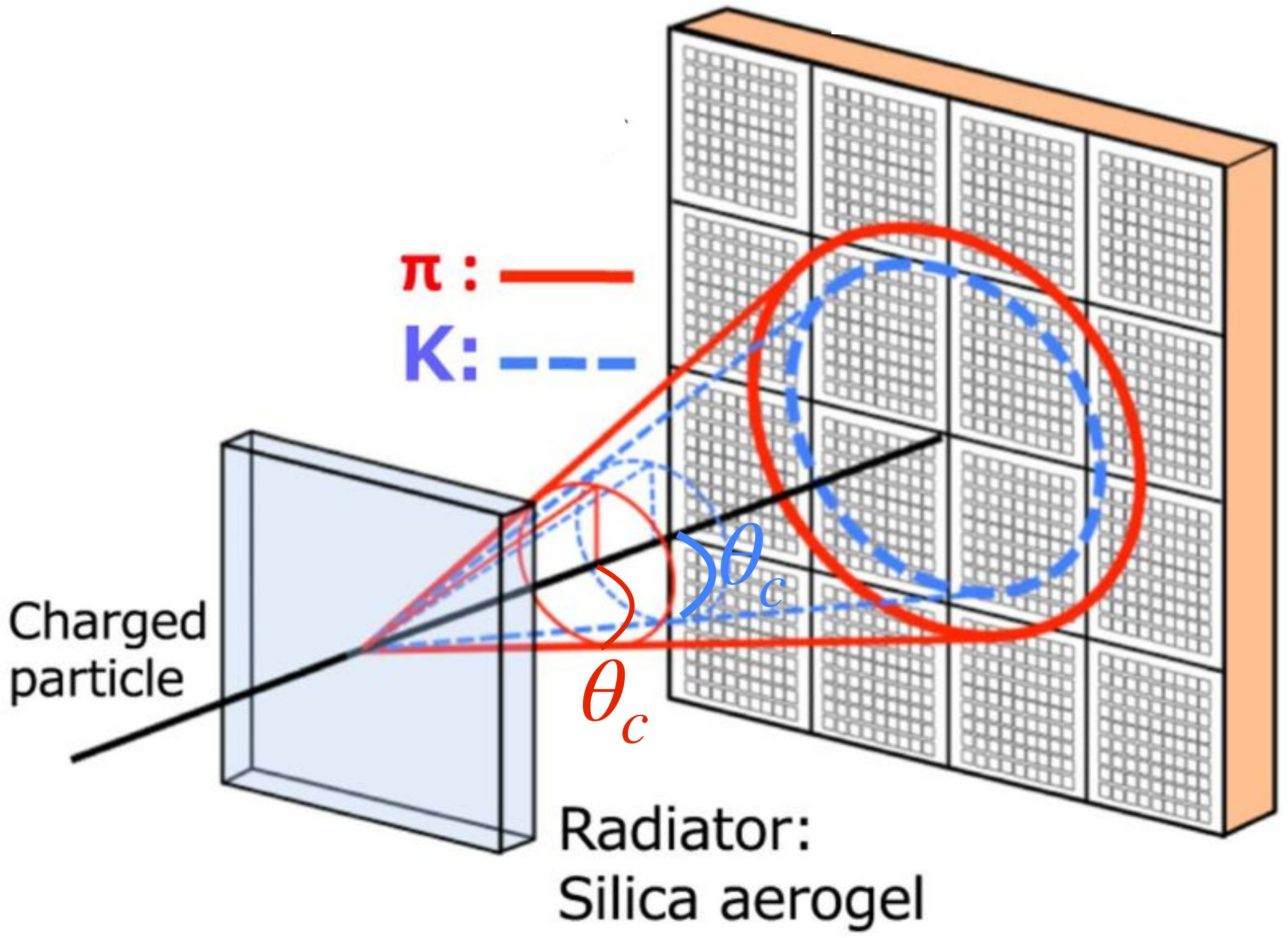

$$\cos\theta_c \propto \frac{1}{v}$$

Particle identification

detectors based on Cherenkov radiation for 1 GeV/c<p<50 GeV/c

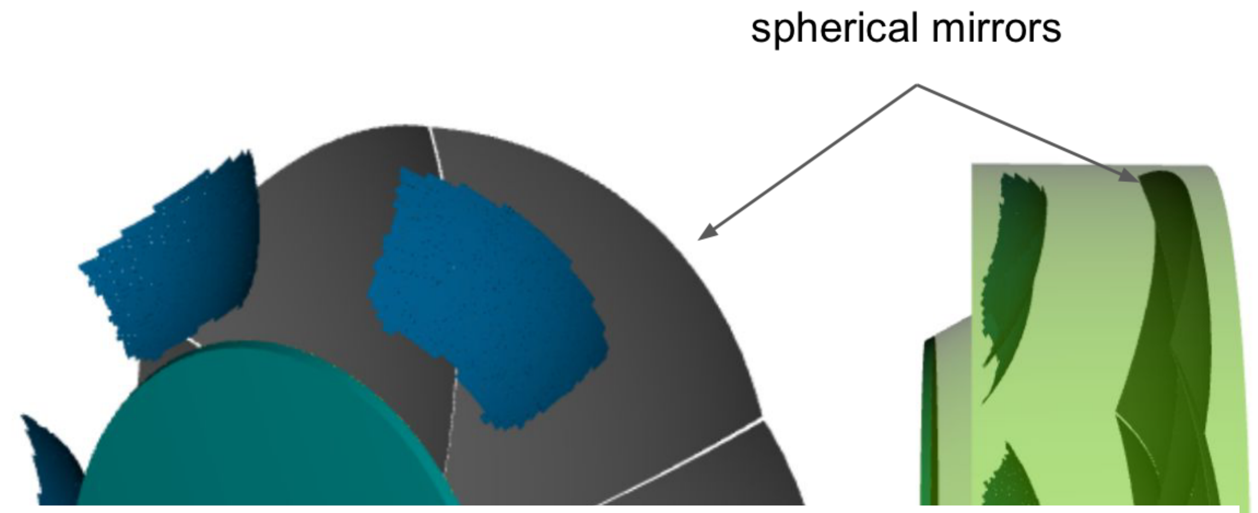

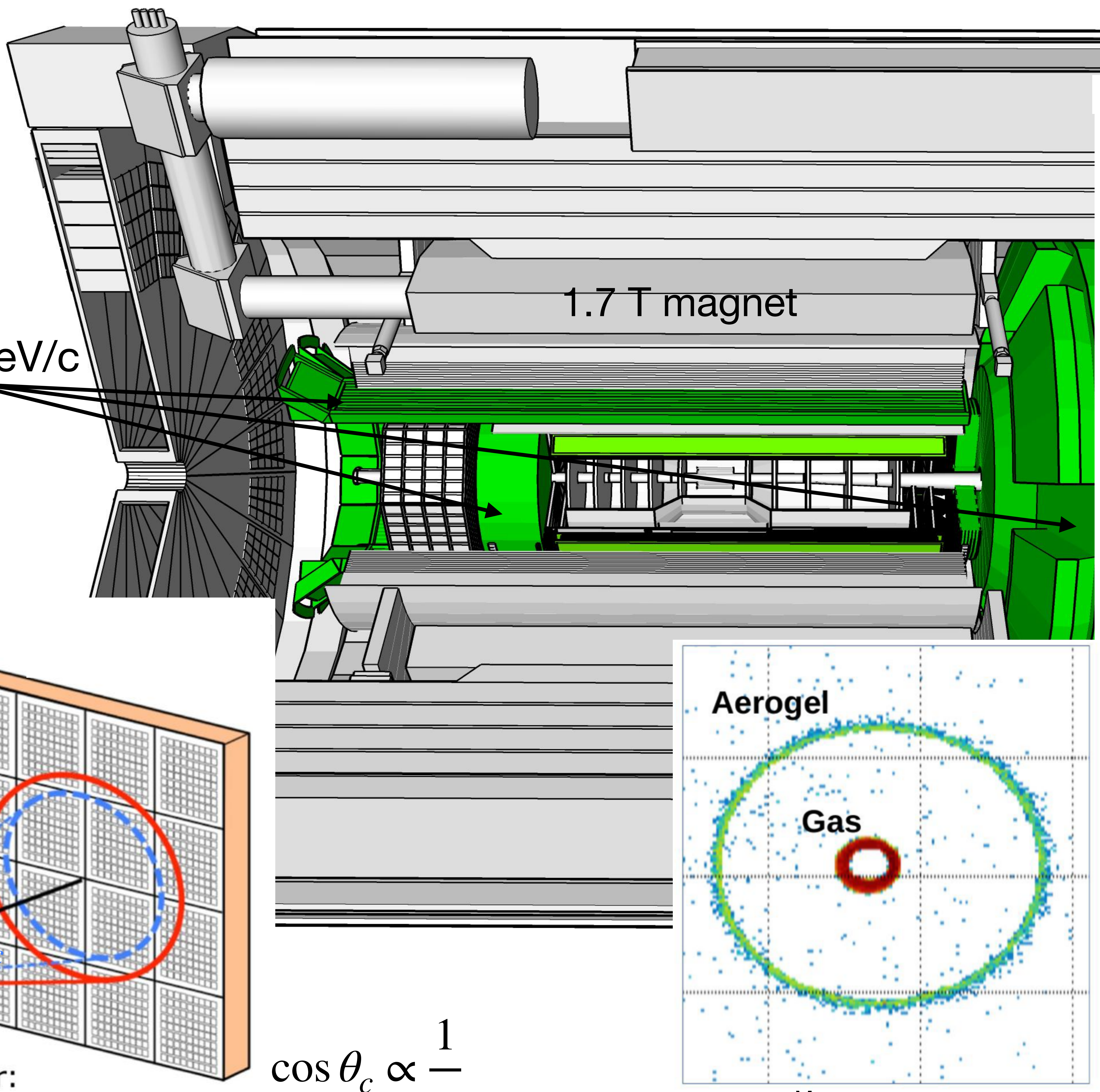

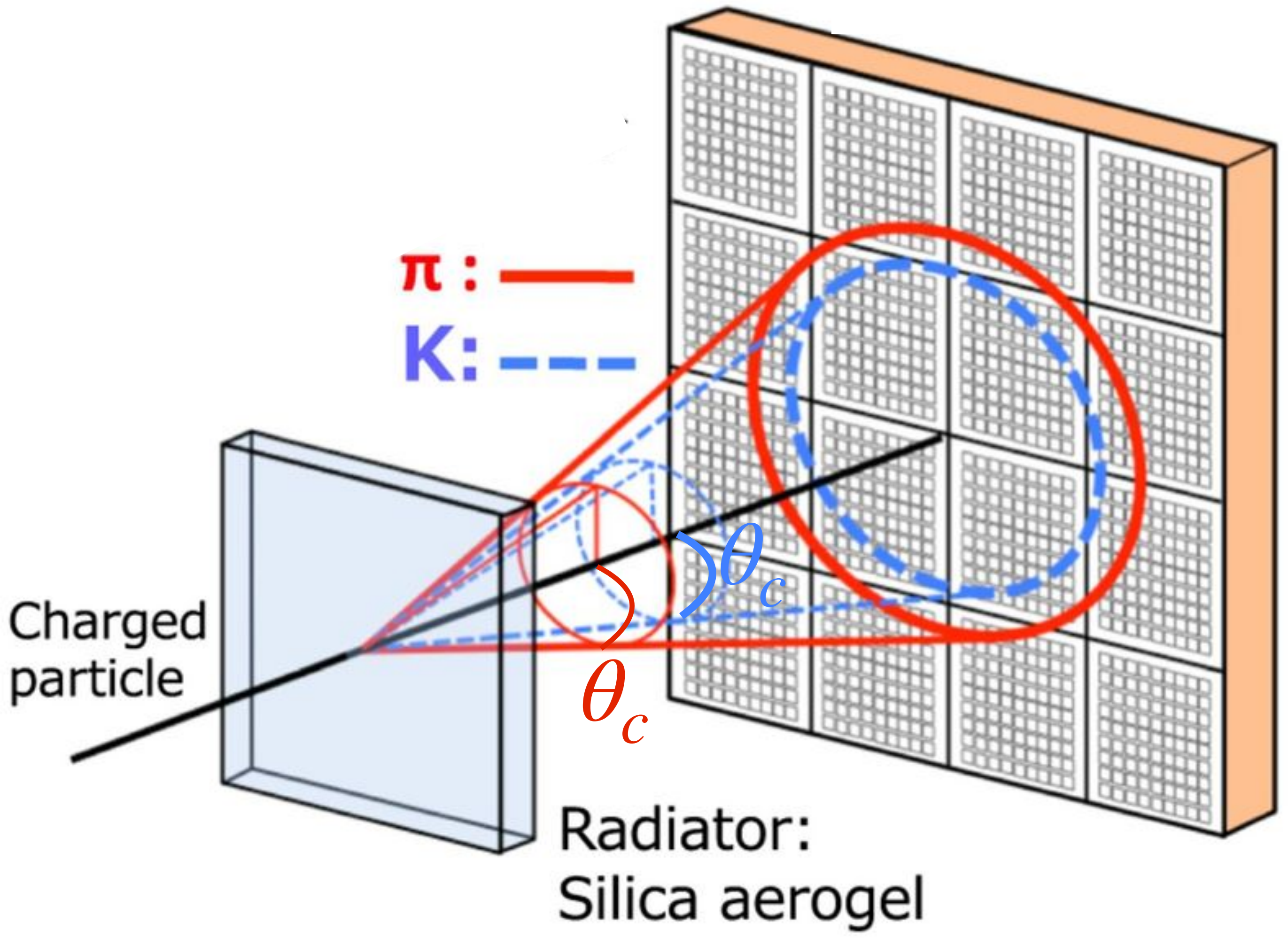

$$\cos\theta_c \propto \frac{1}{v}$$

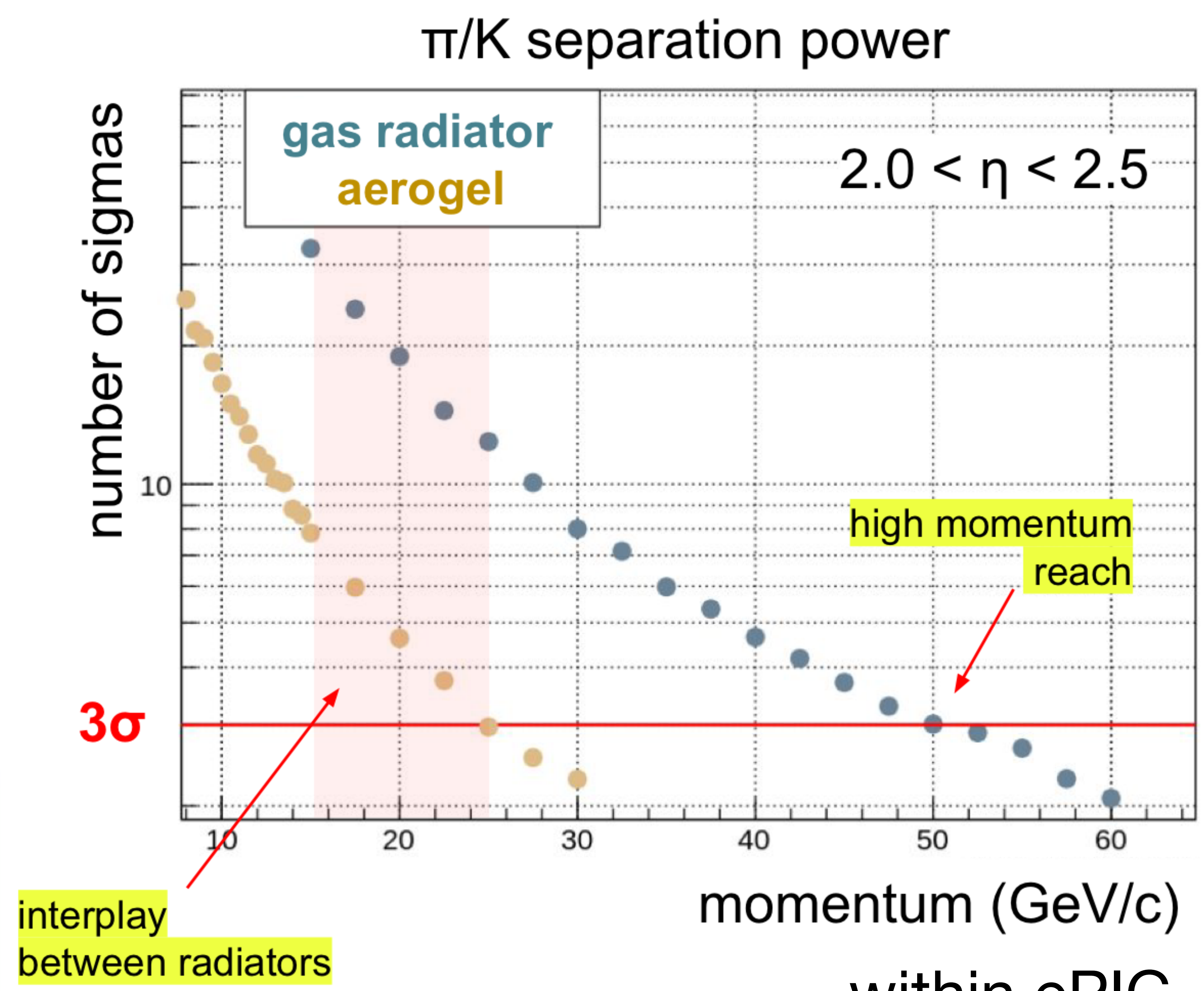

within ePIC simulation framework

Far-backward region

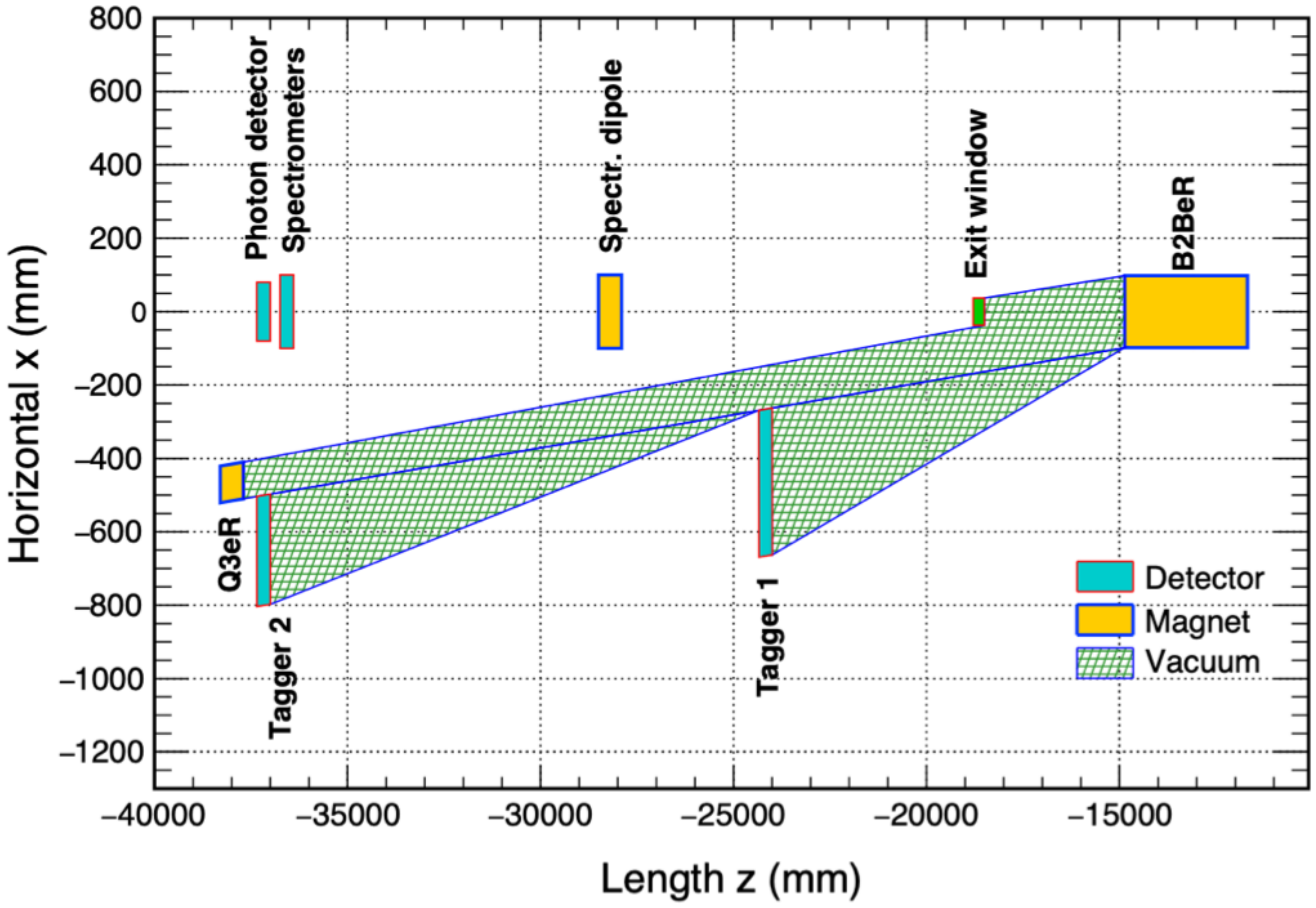

Far-backward region

low-Q² taggers

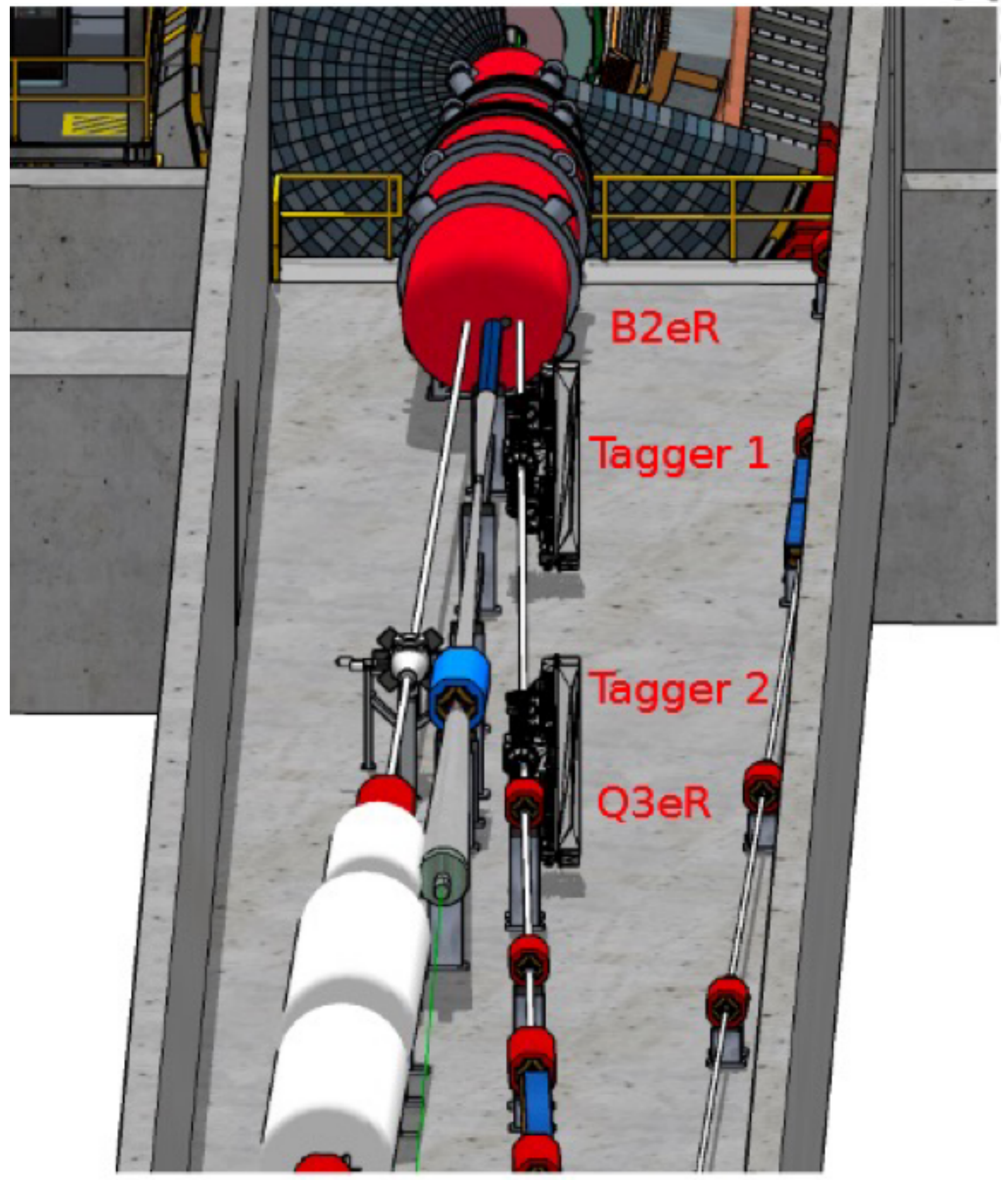

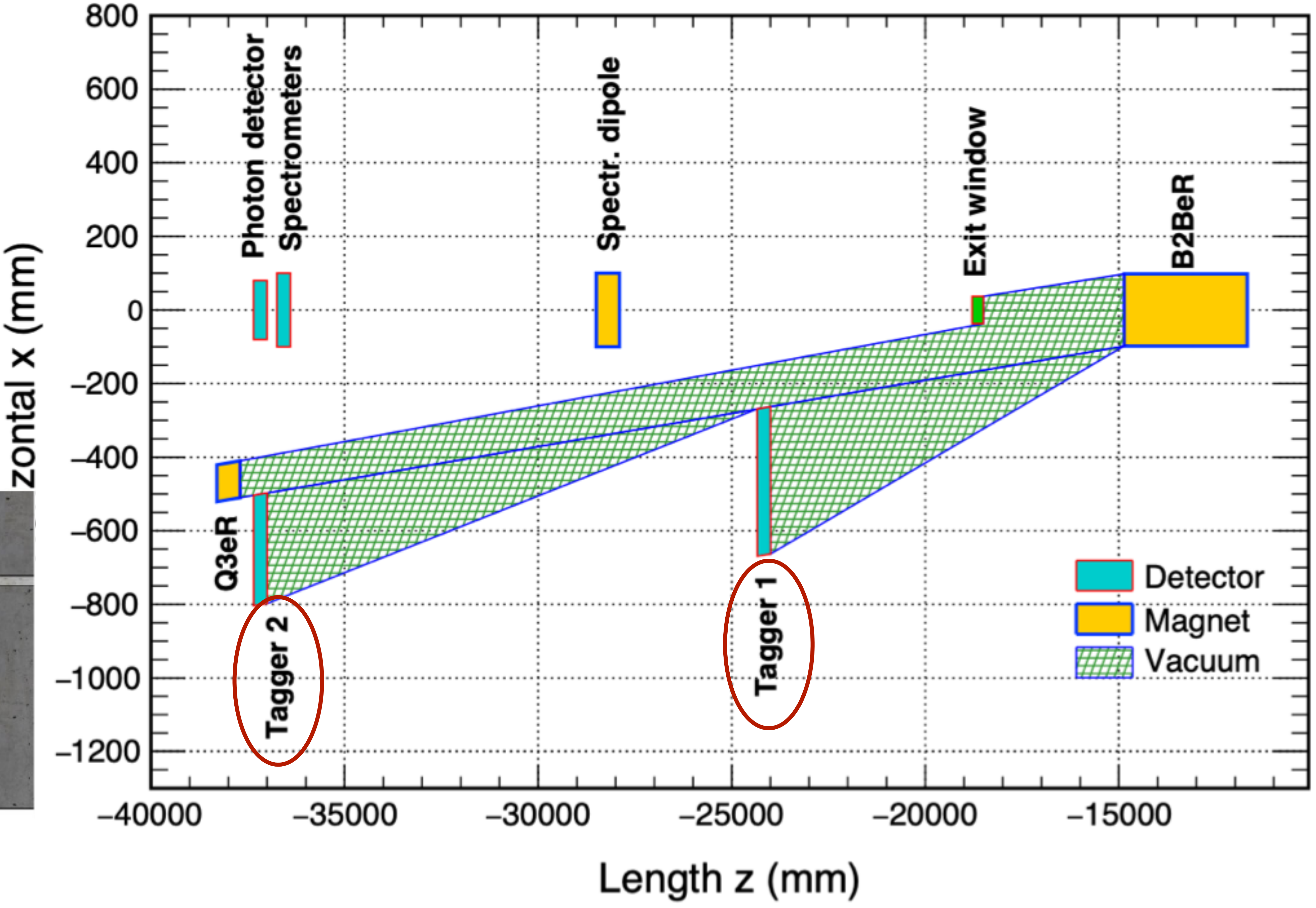

Far-backward region

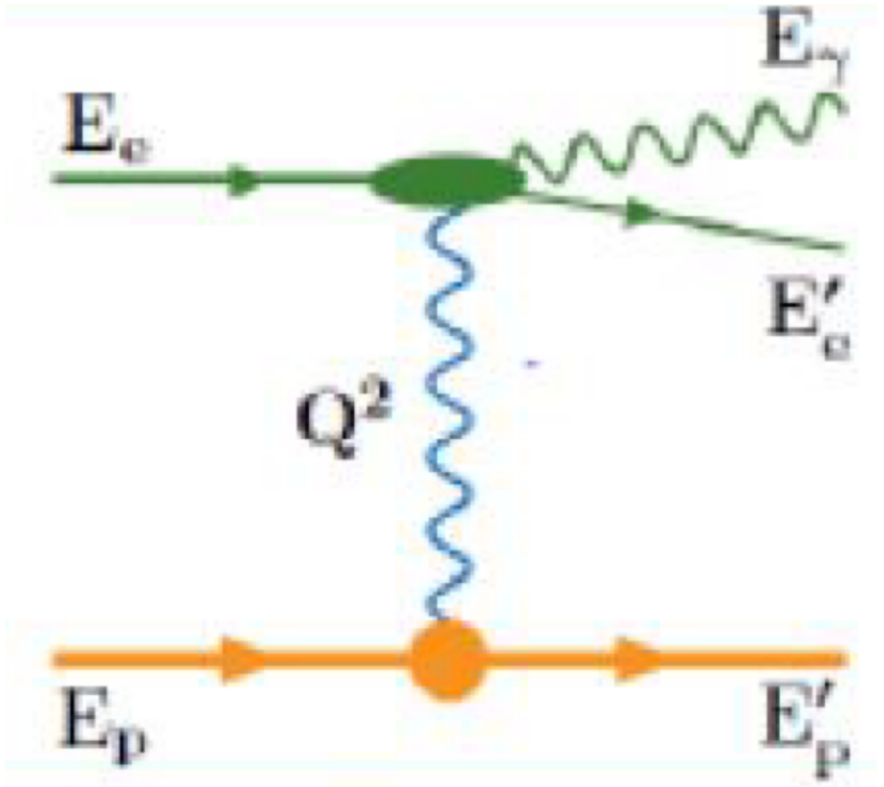

luminosity monitor

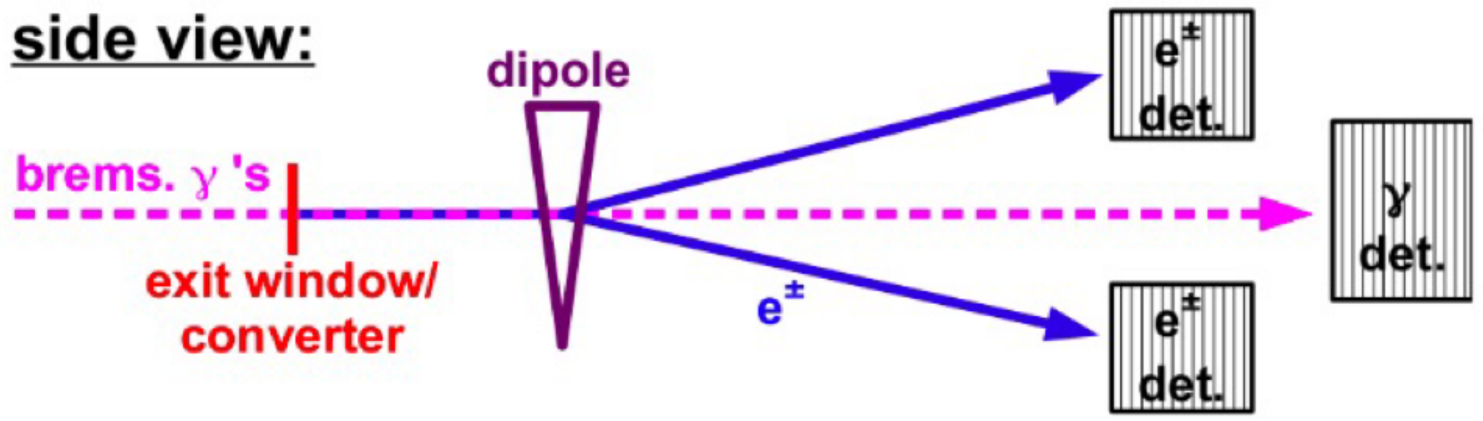

required absolute precision: 1%
required relative precision: 0.01%

low-Q² taggers

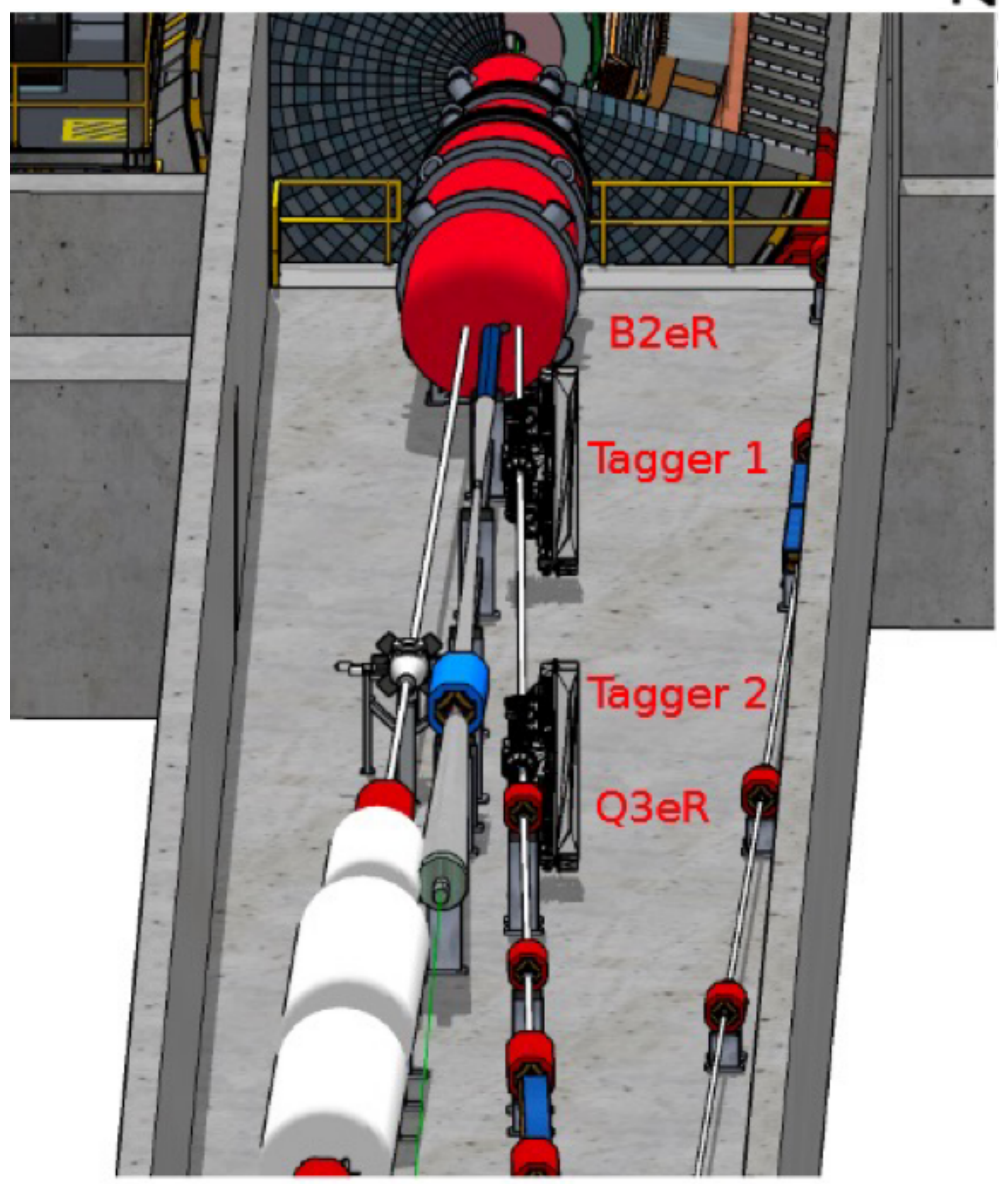

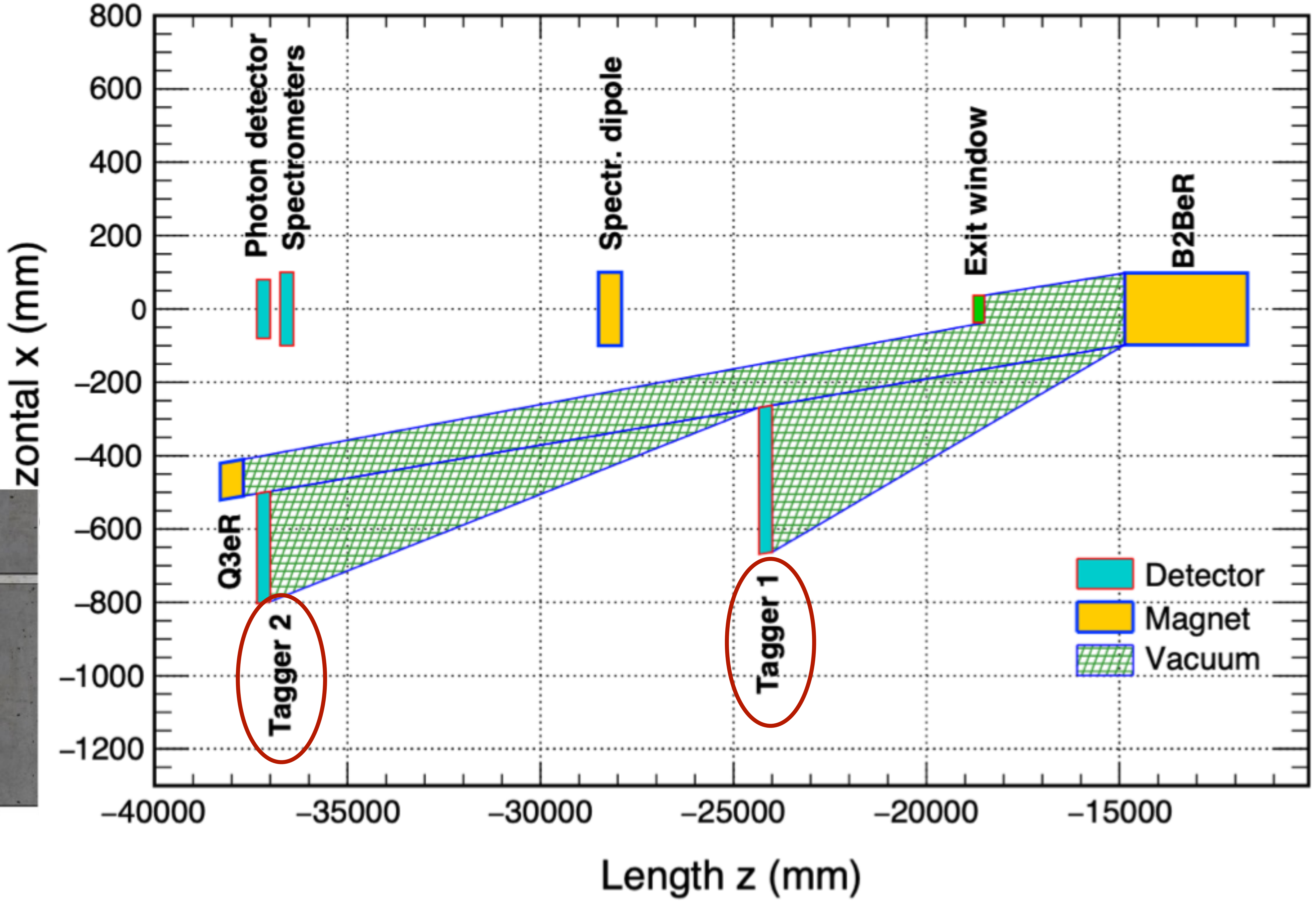

Far-forward region

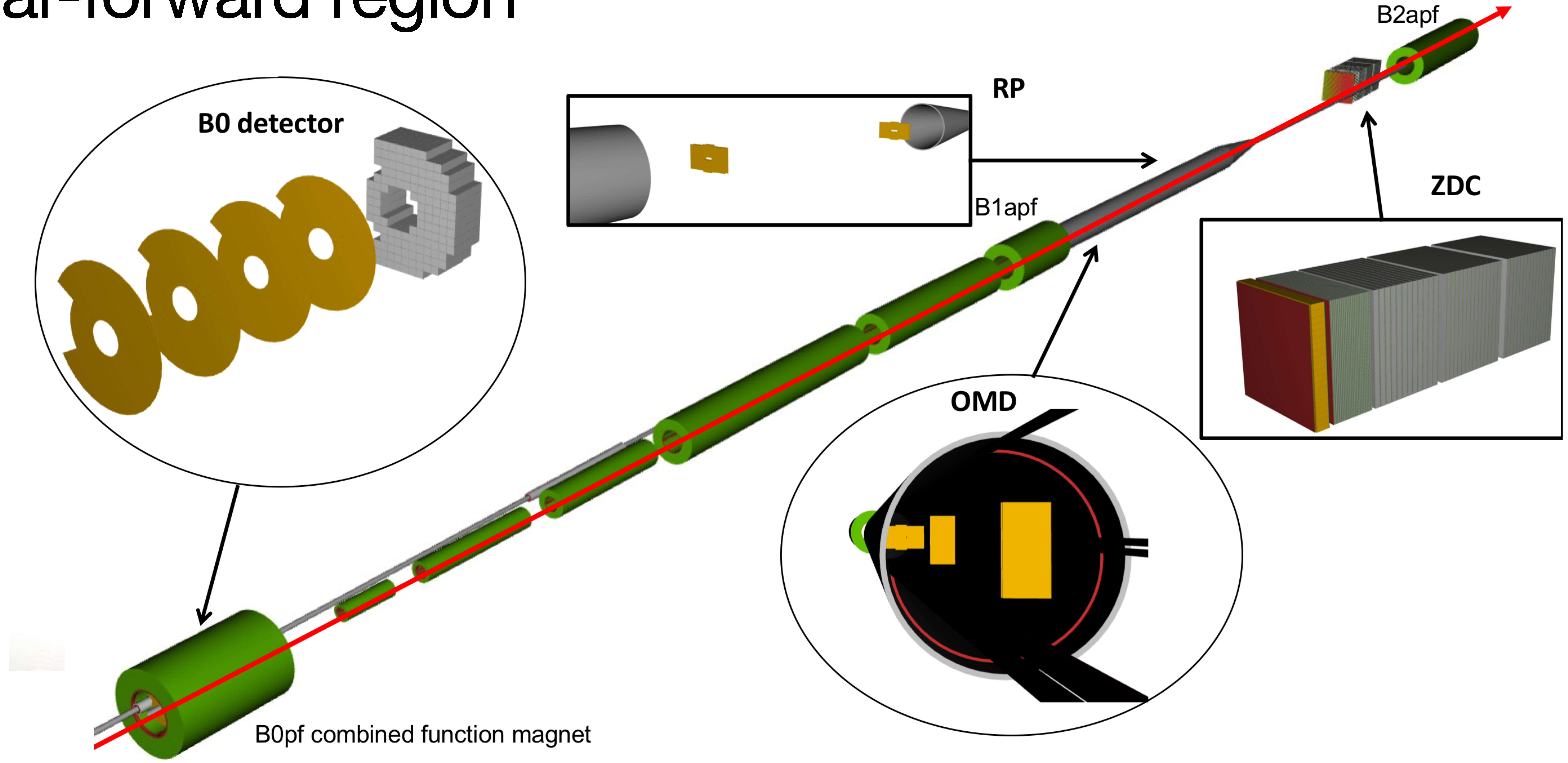

Far-forward region

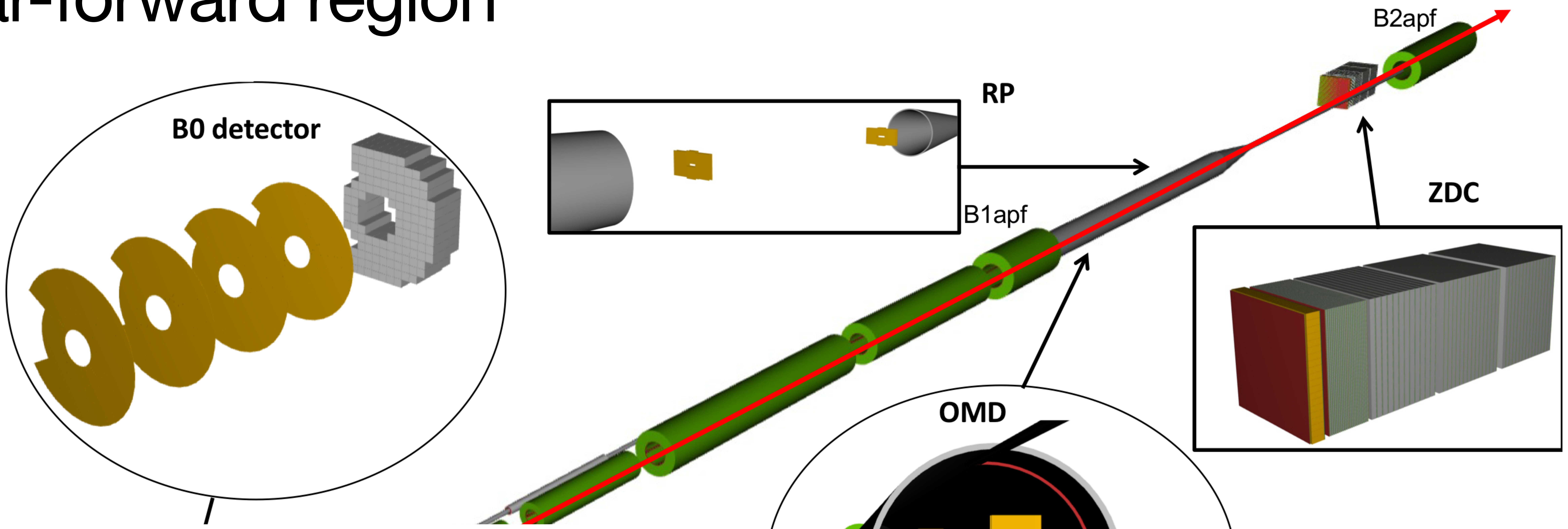

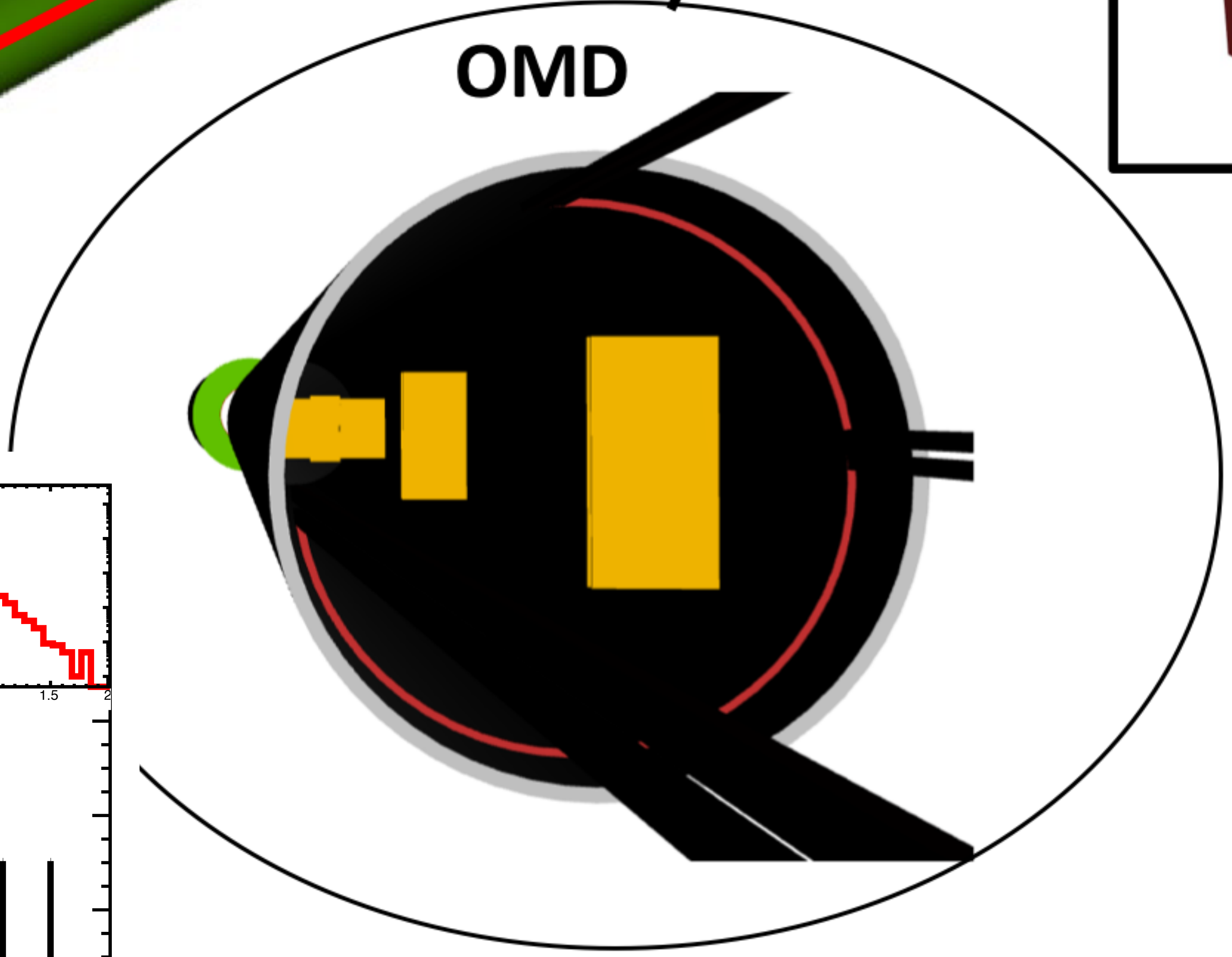

ECCE

Exclusive production on proton

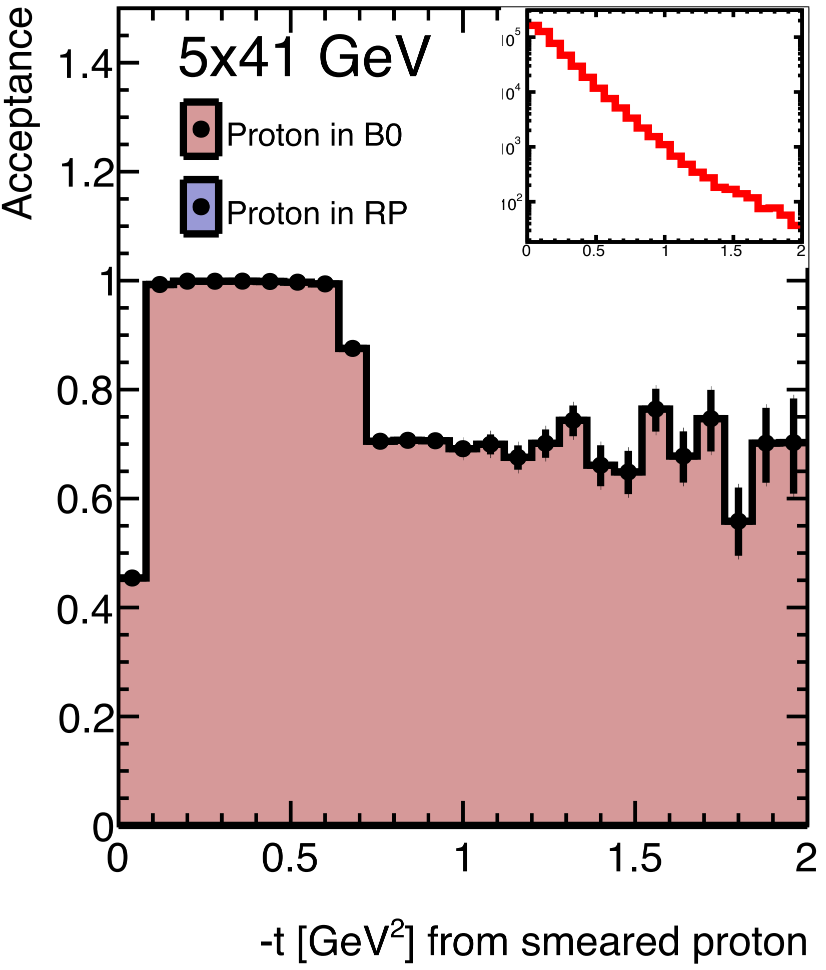

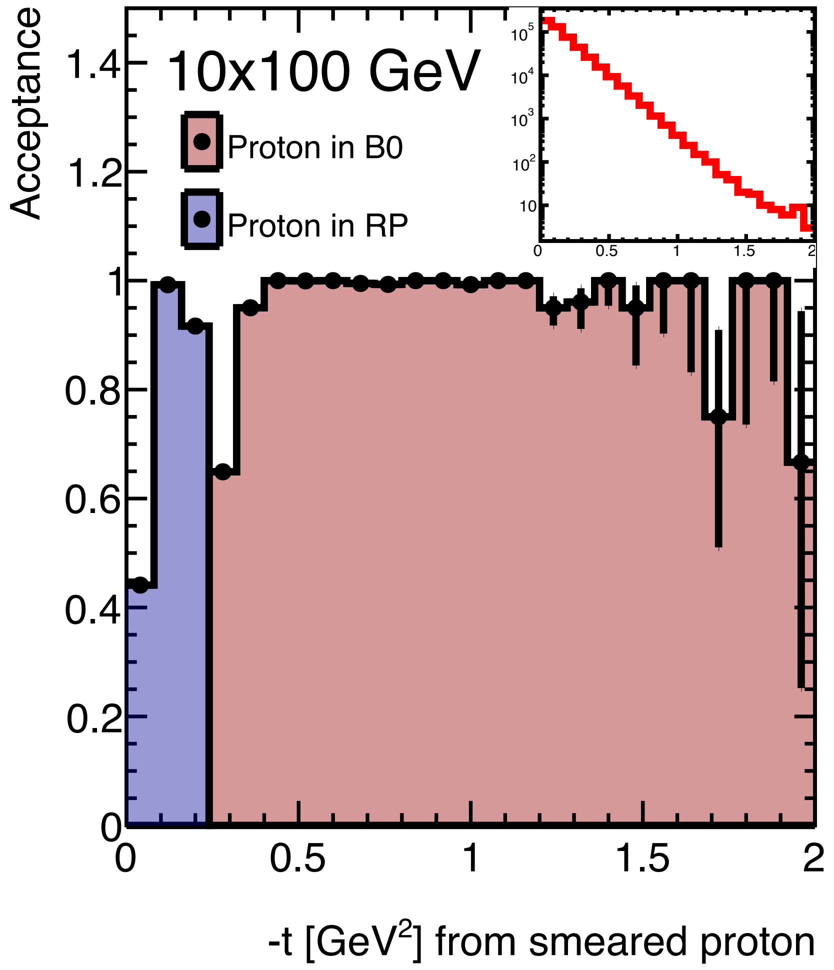

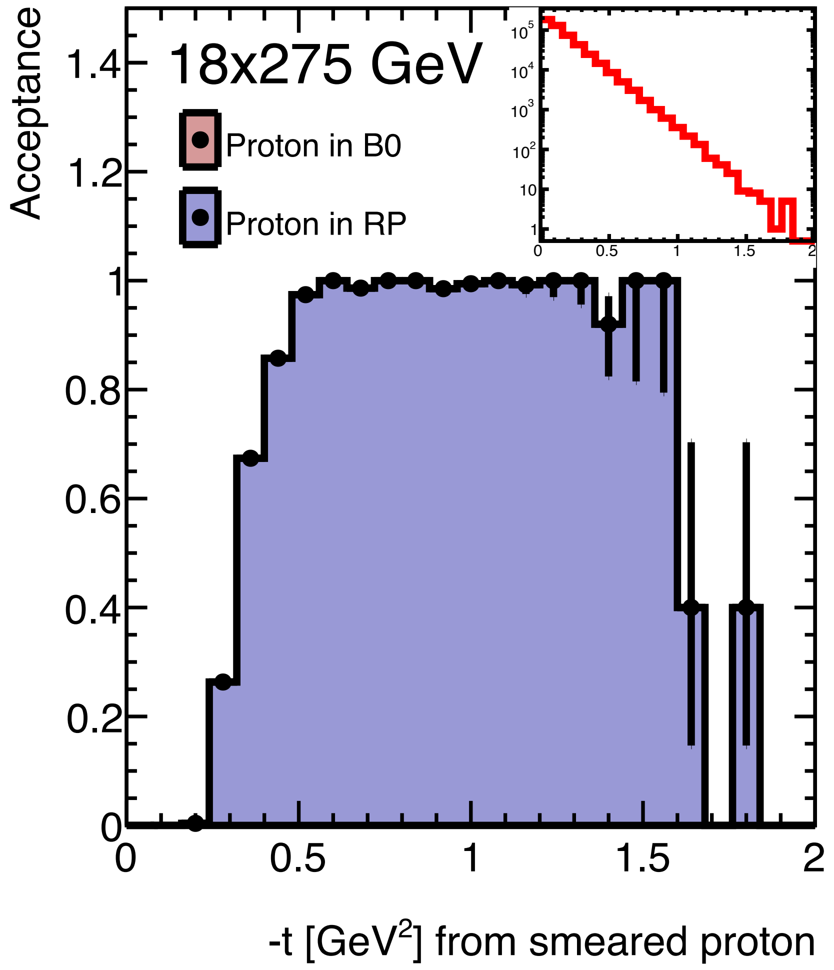

Why and electron-ion collider

nucleon spin

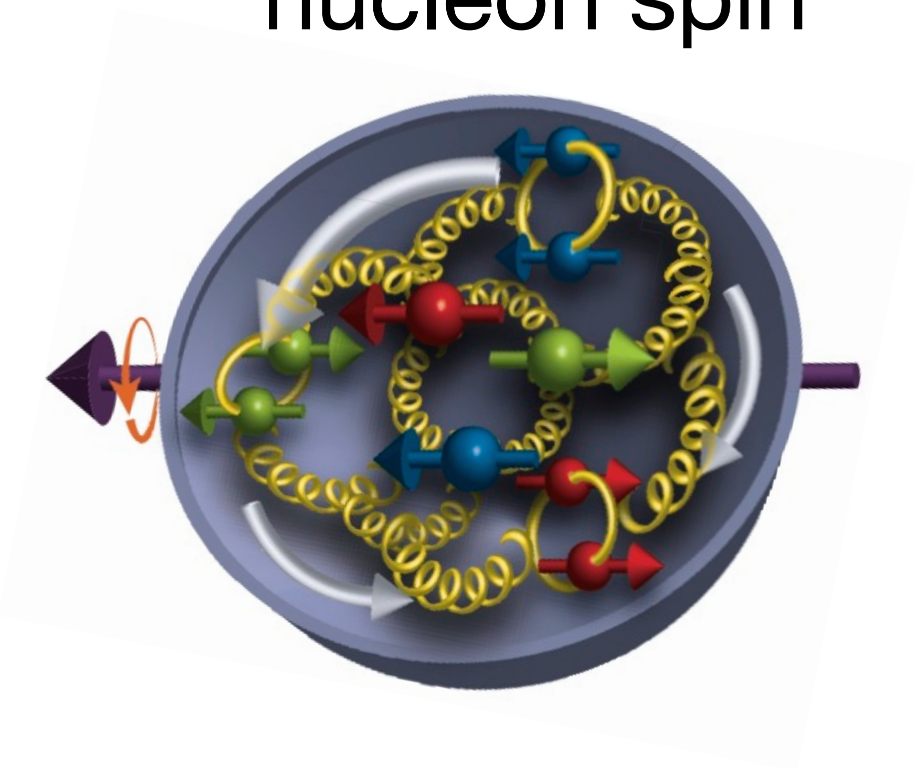

Why and electron-ion collider

nucleon spin

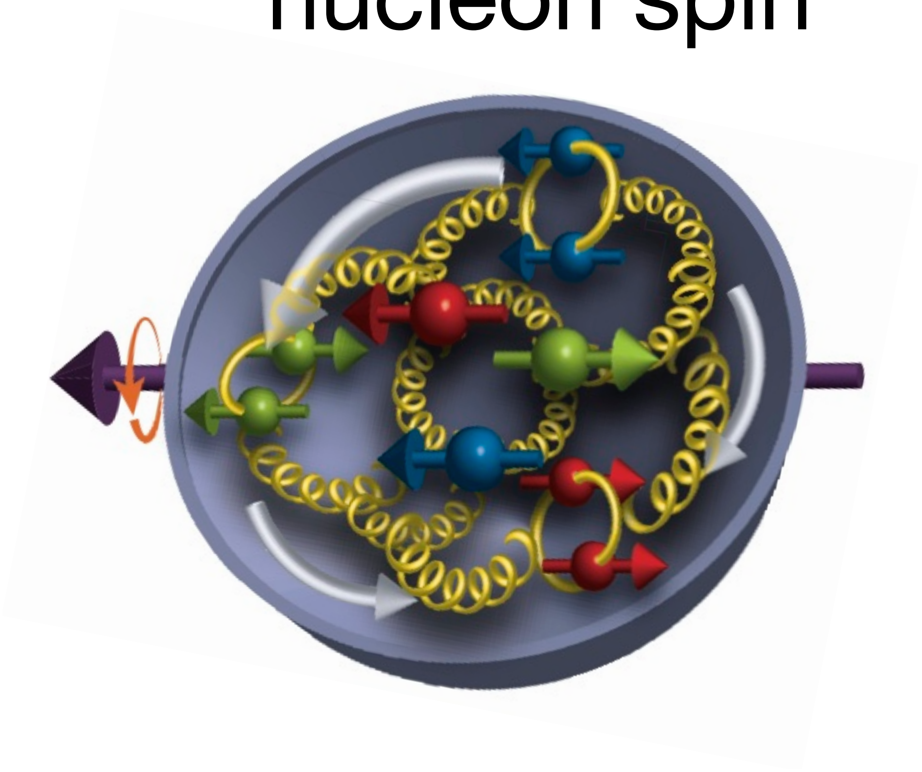

spin-dependent nucleon multi-dimensional structure

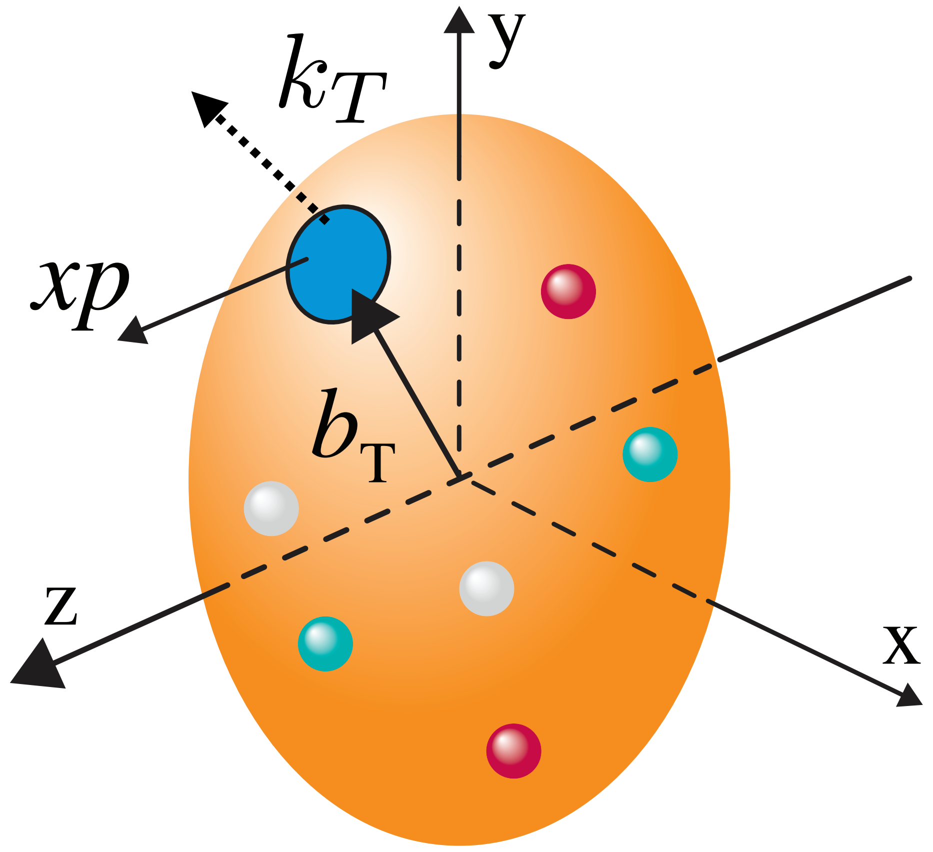

Why and electron-ion collider

nucleon spin

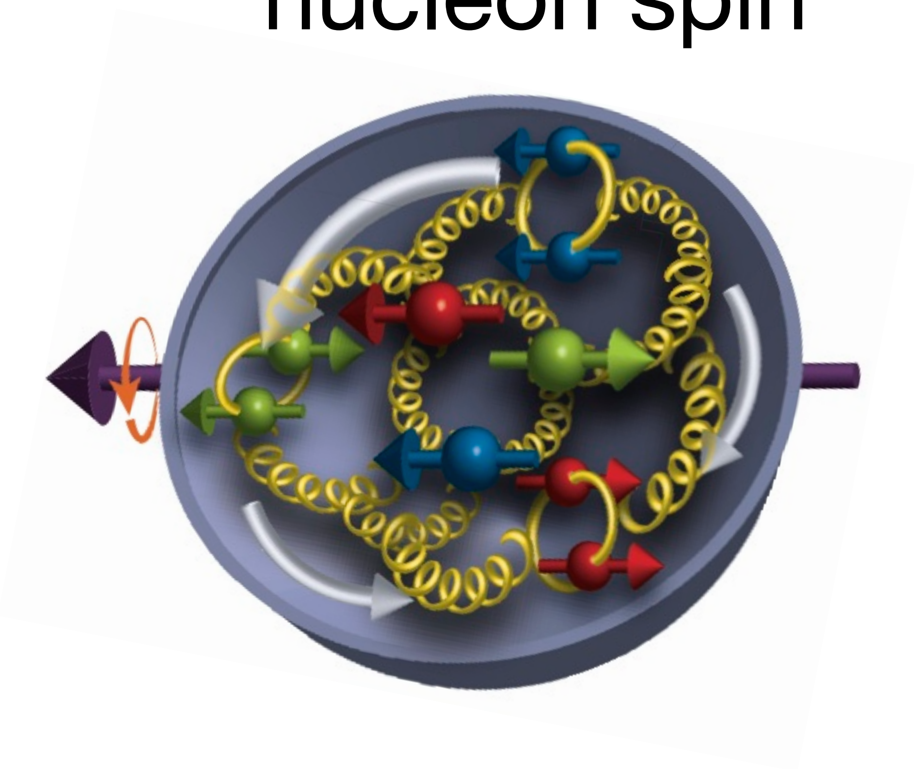

probing saturation

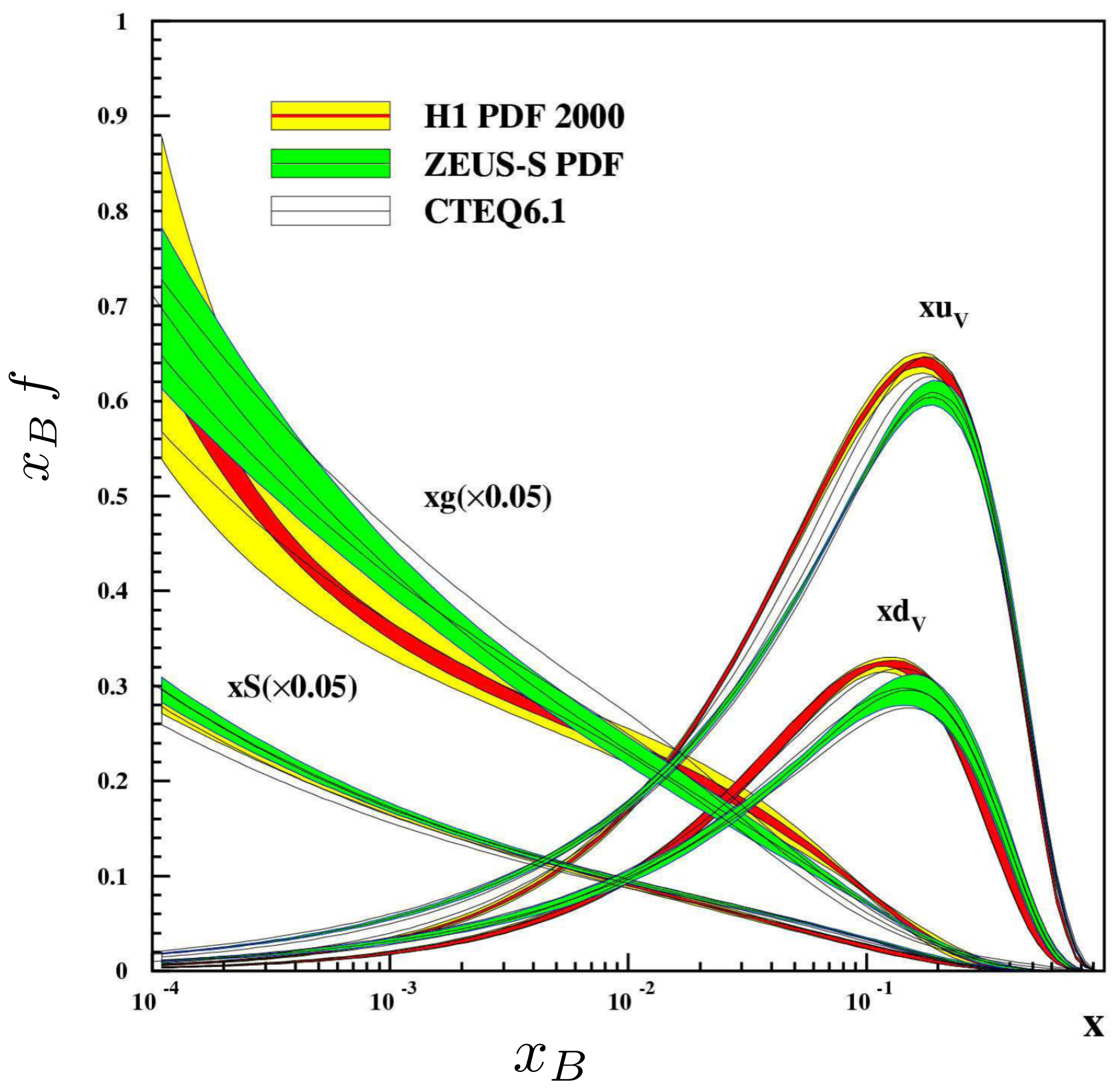

spin-dependent nucleon multi-dimensional structure

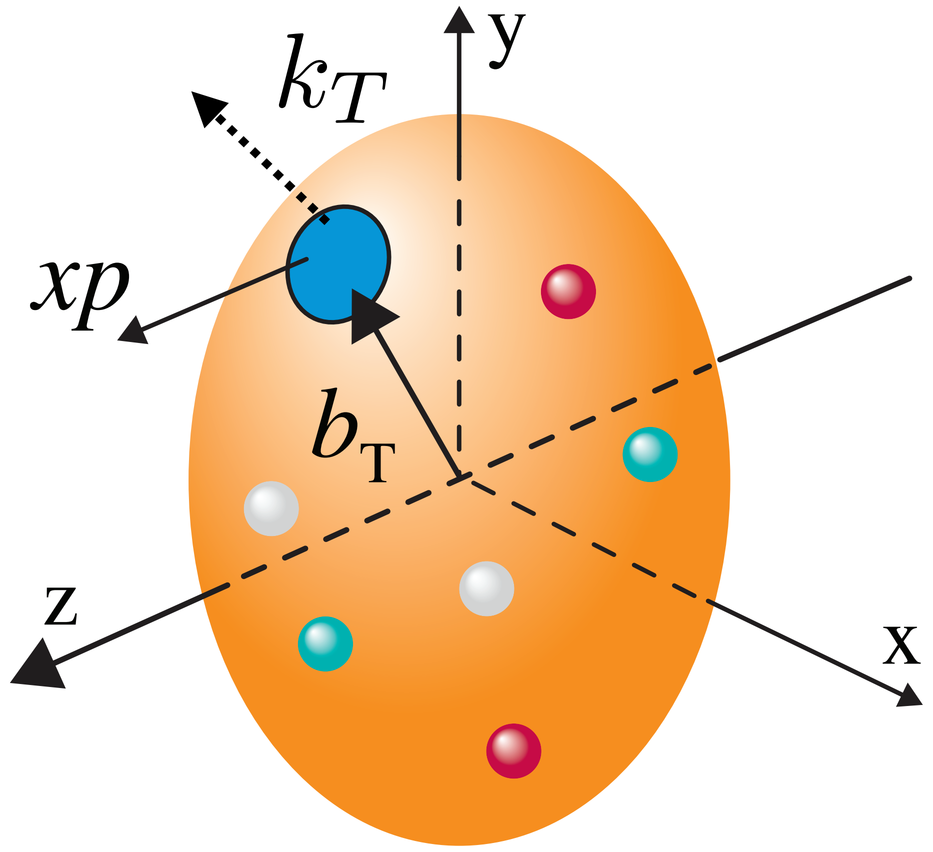

Why and electron-ion collider

nucleon spin

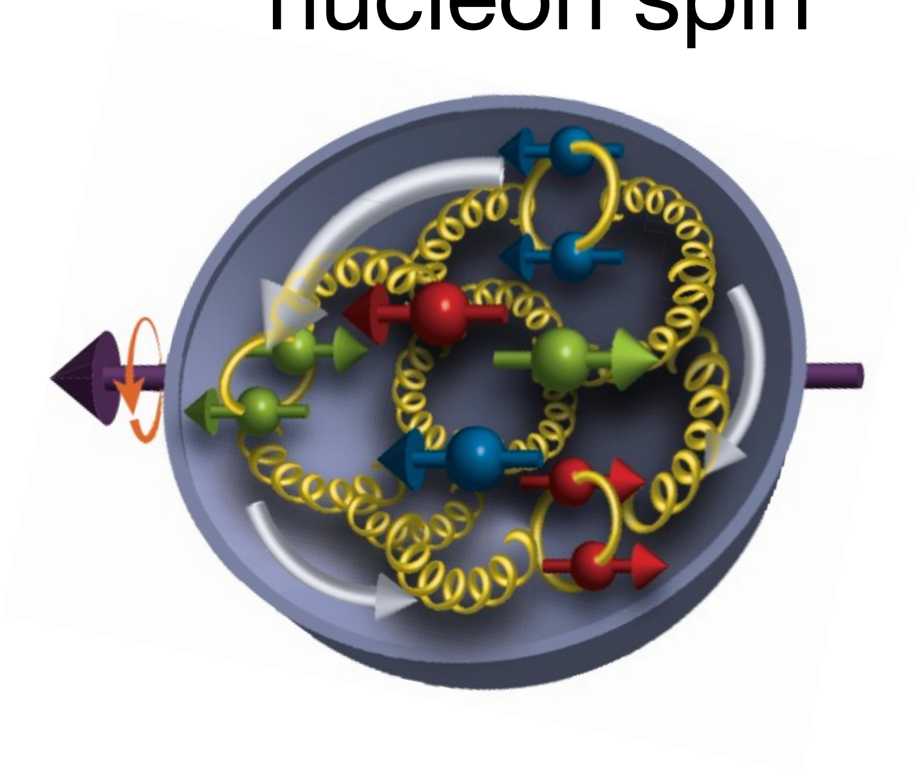

probing saturation

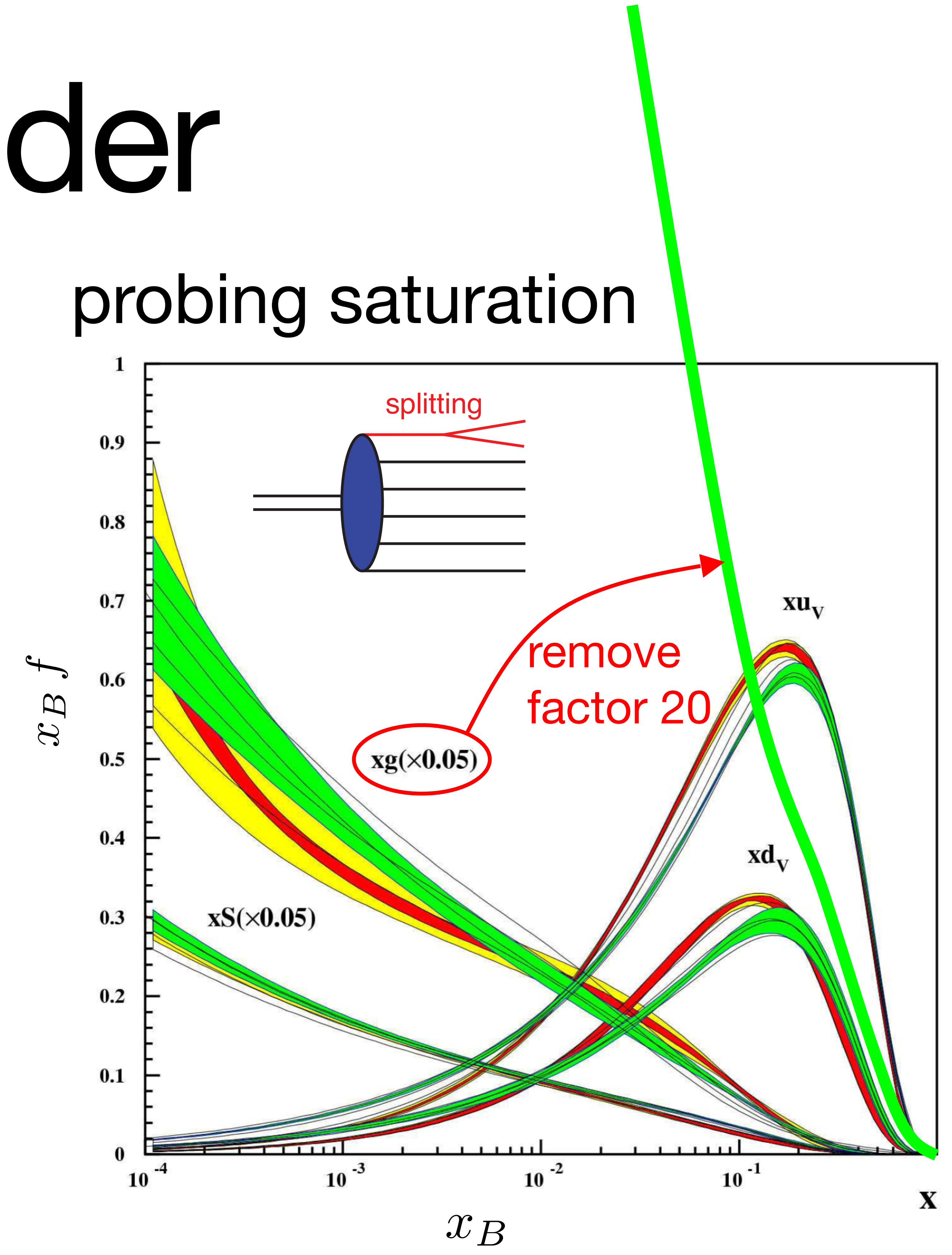

spin-dependent nucleon multi-dimensional structure

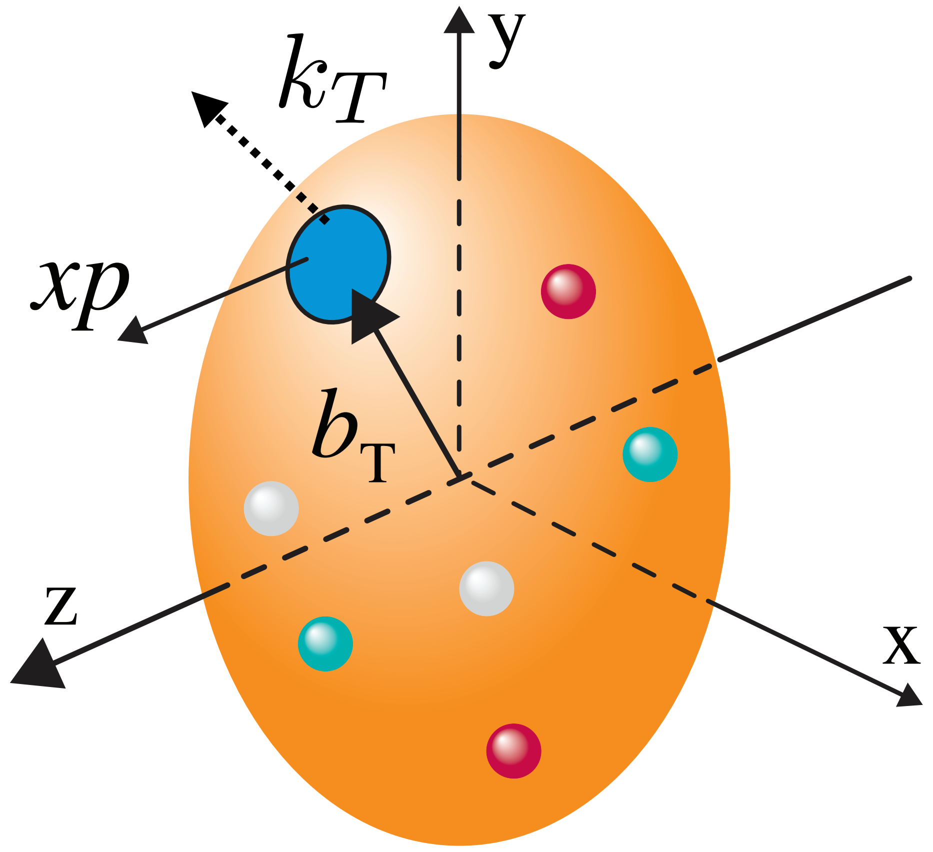

Why and electron-ion collider

nucleon spin

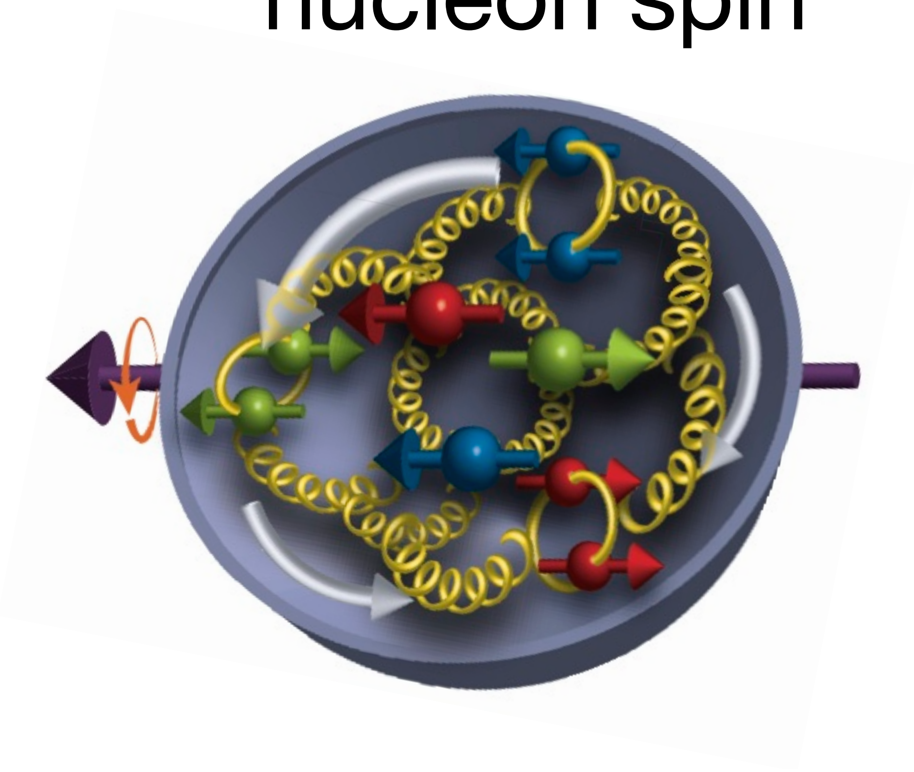

probing saturation

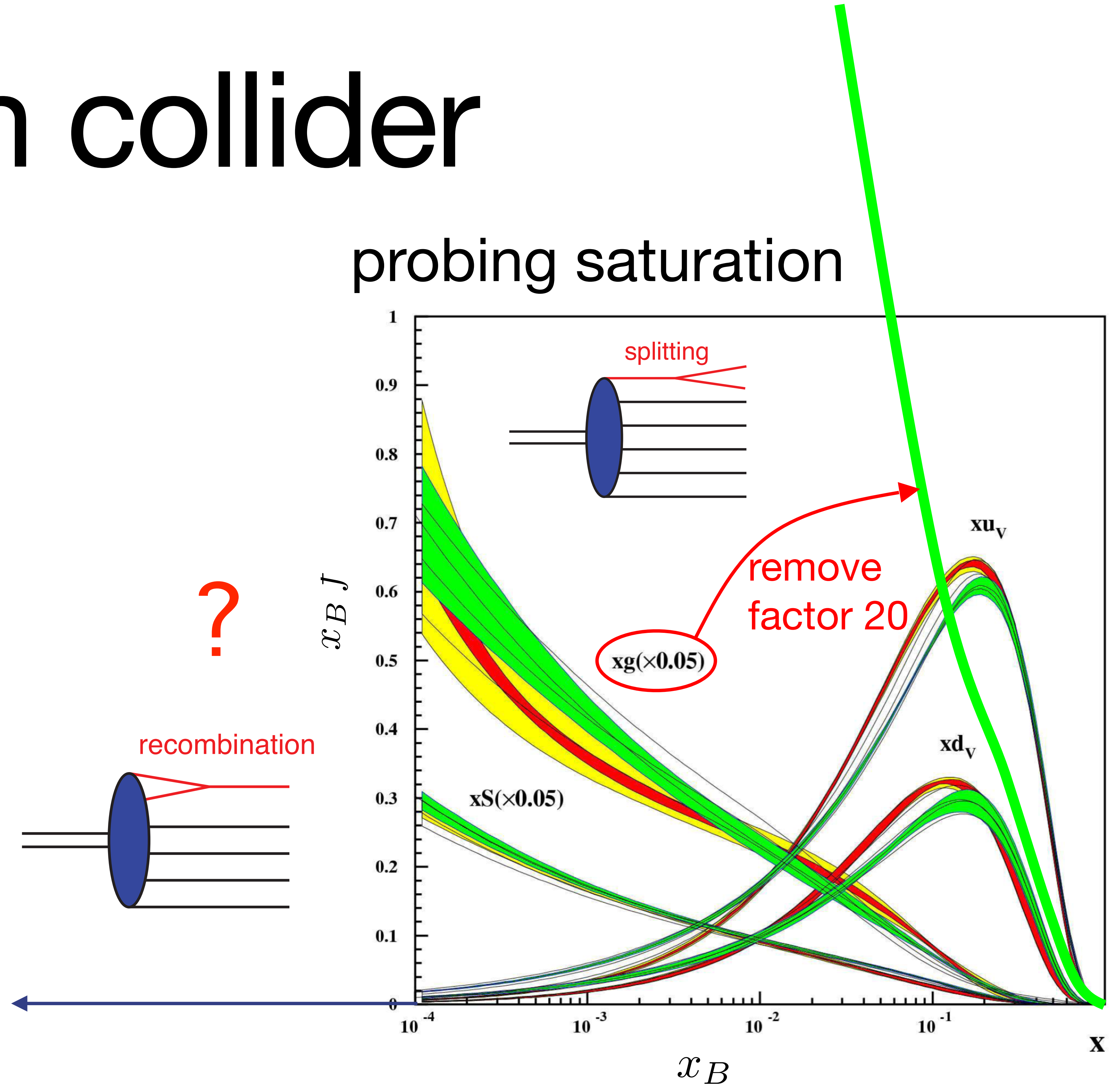

spin-dependent nucleon multi-dimensional structure

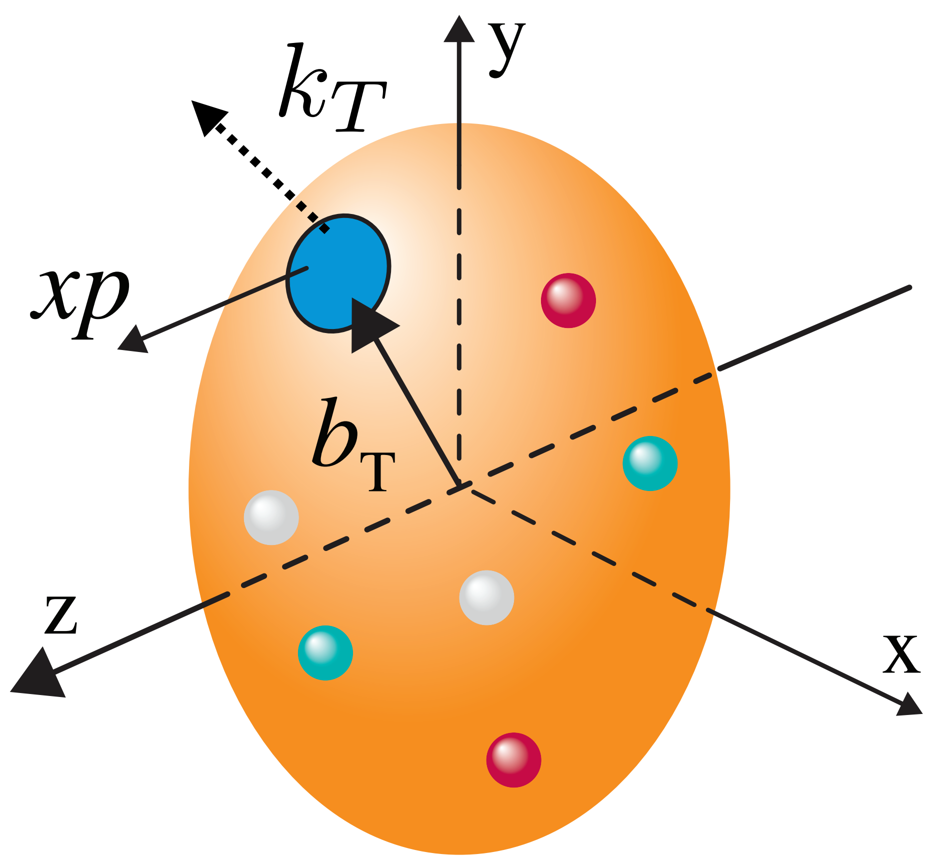

Why and electron-ion collider

probing saturation

nucleon spin

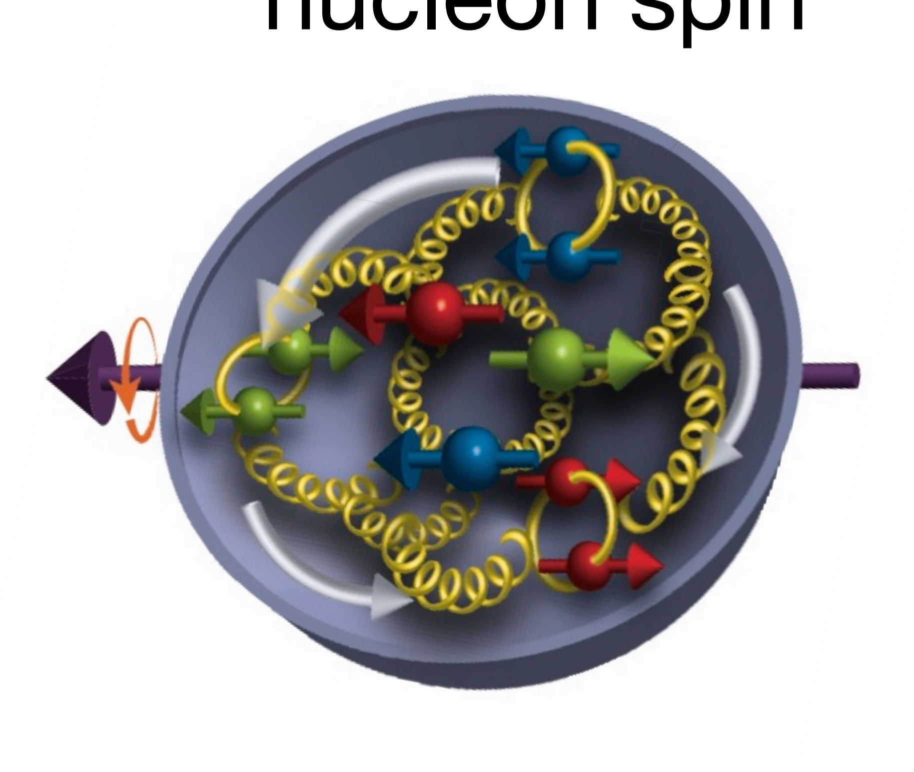

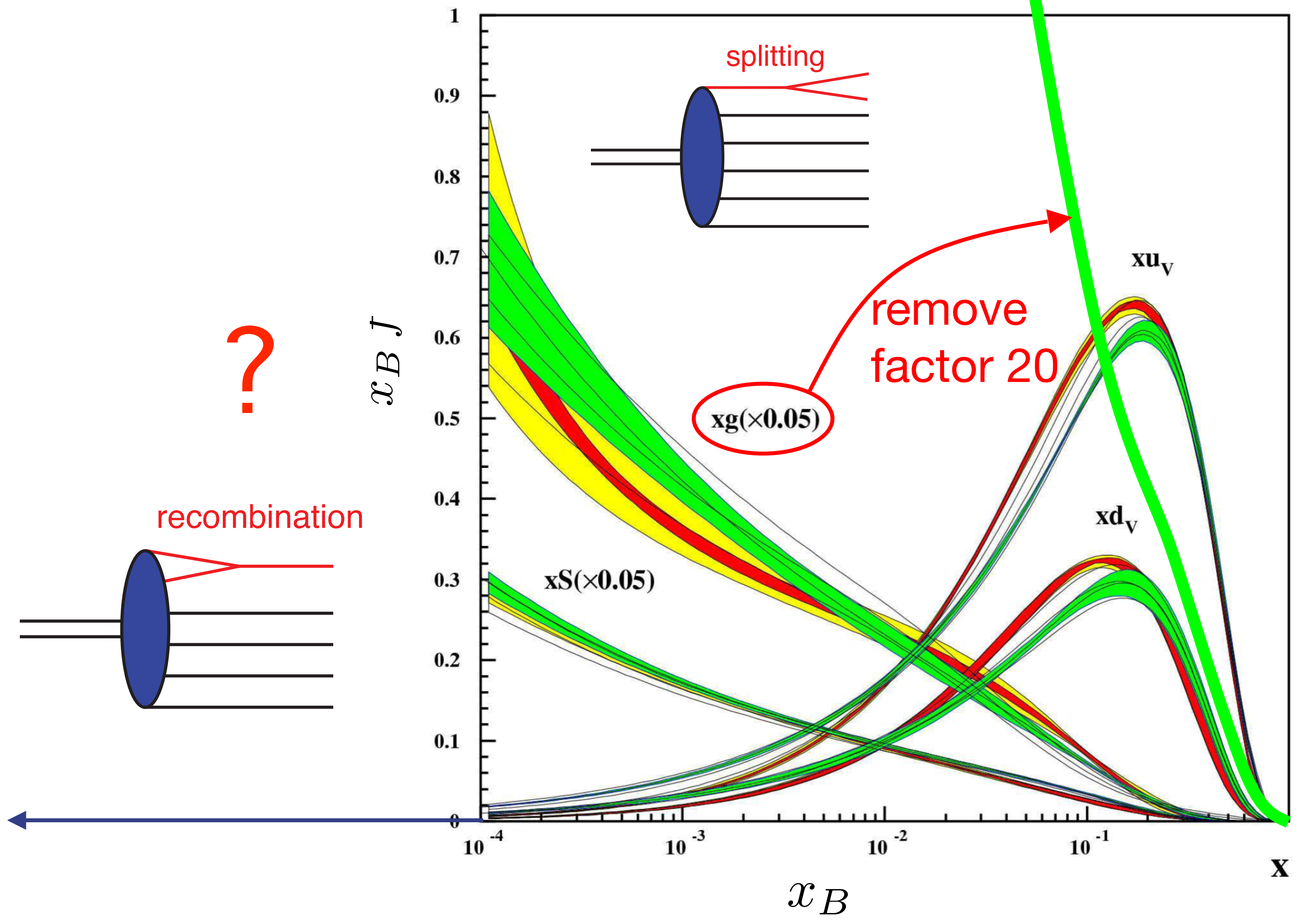

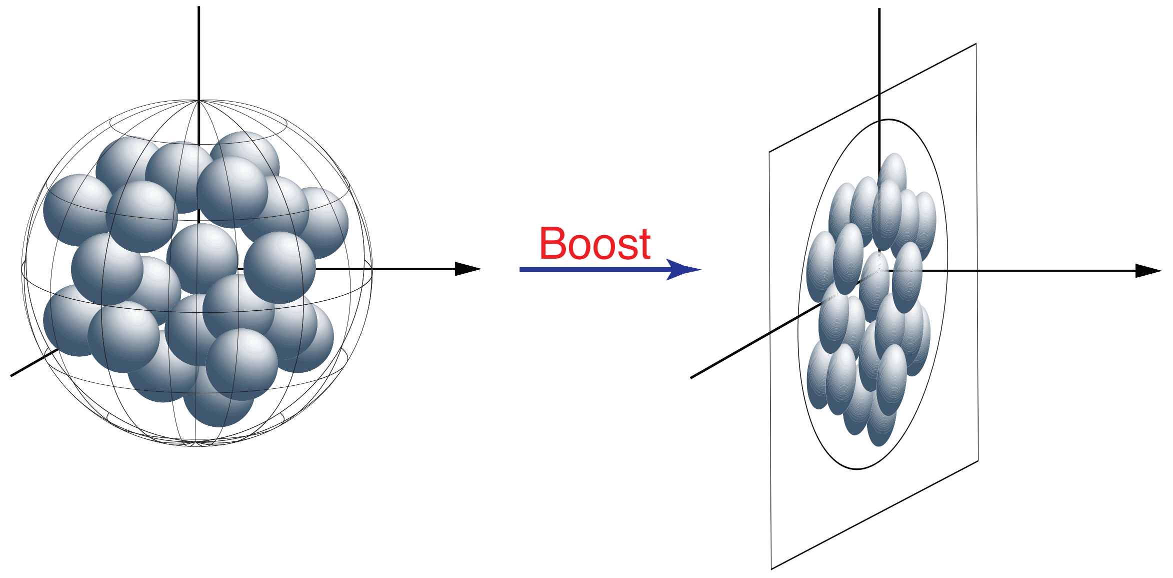

$A^{1/3}$ enhancement
of saturation effect for ions

spin-dependent nucleon multi-dimensional structure

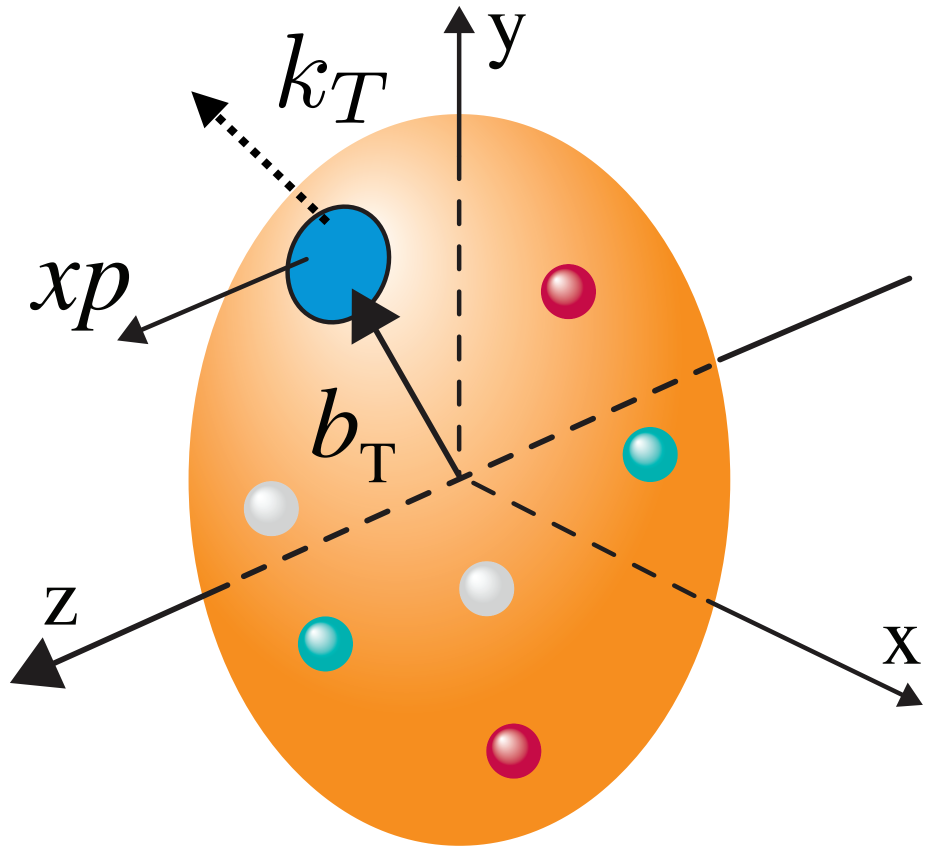

Why and electron-ion collider

nucleon spin

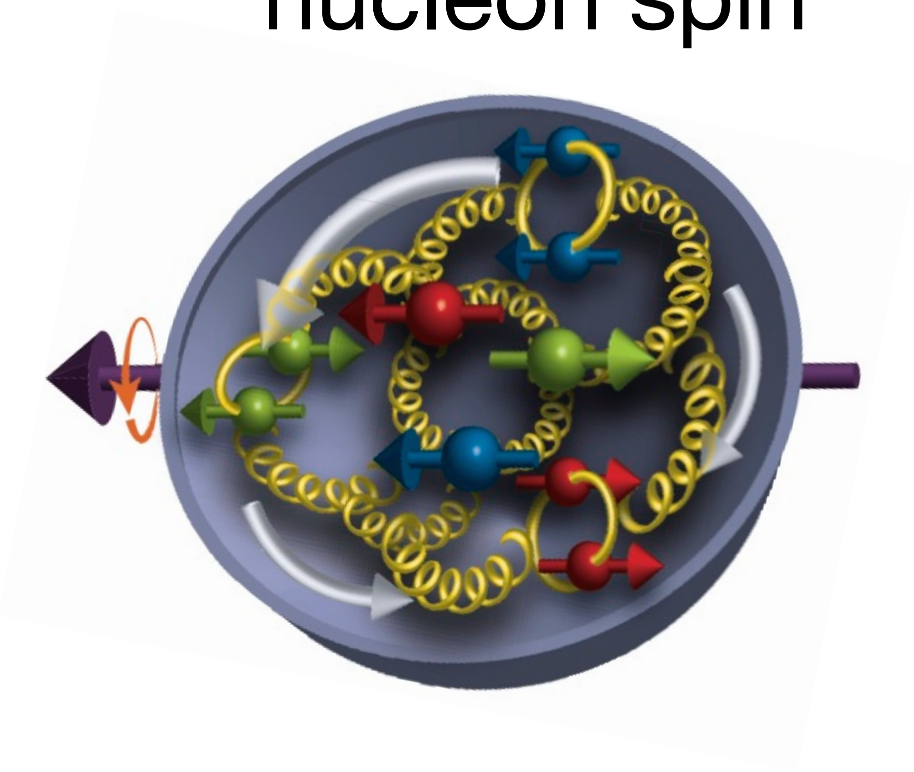

probing saturation

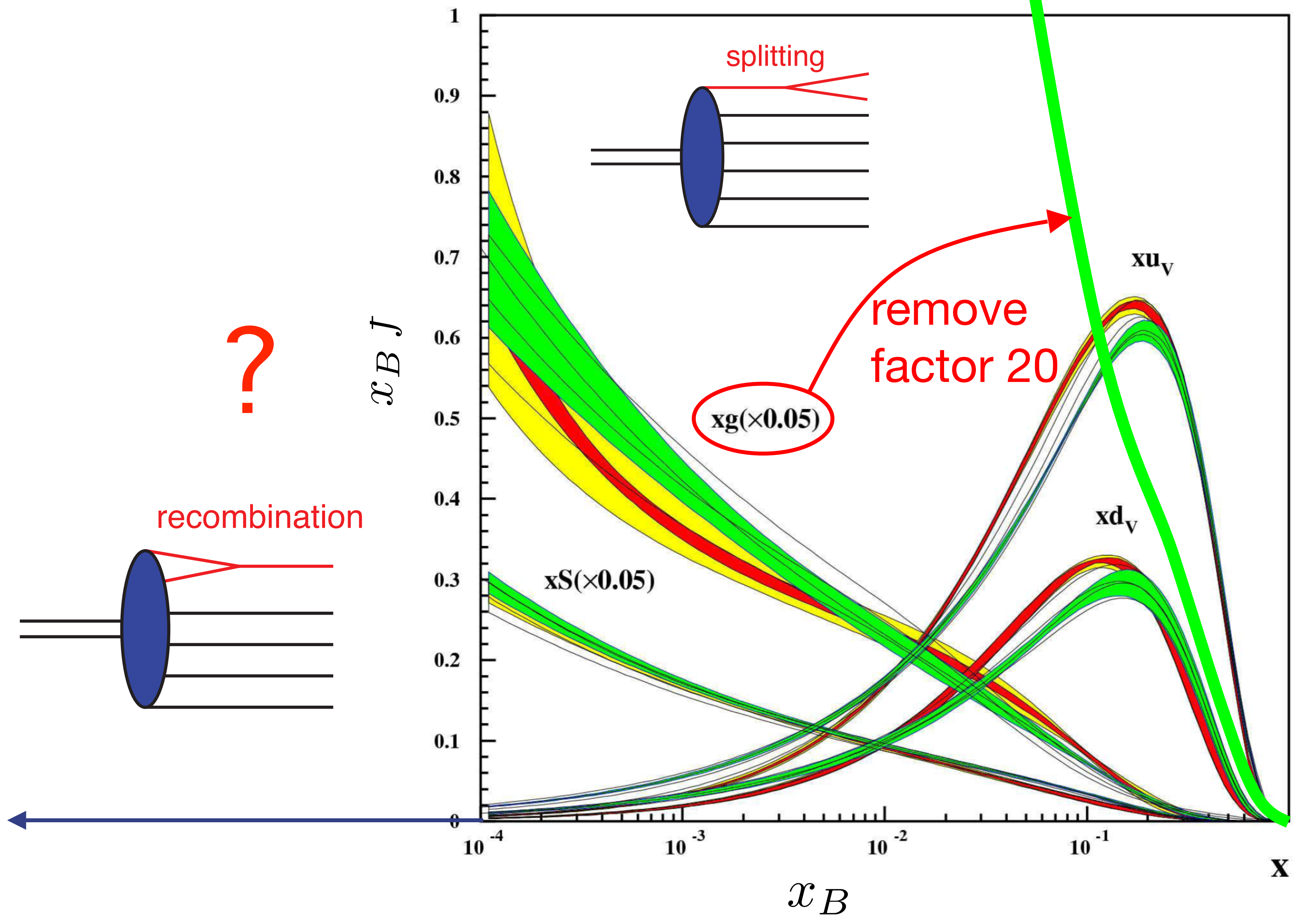

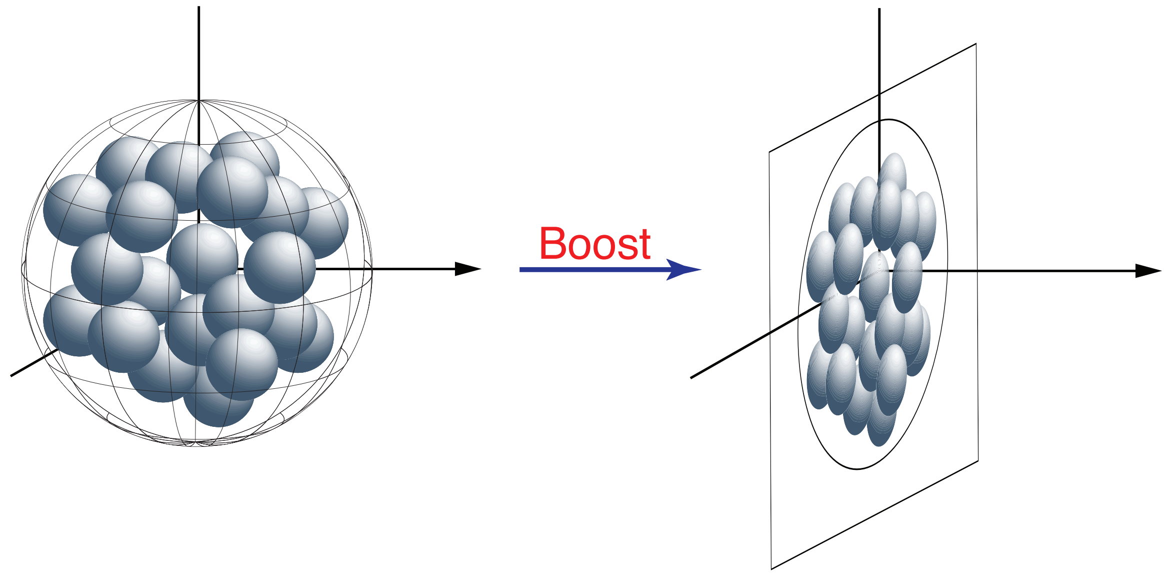

$A^{1/3}$ enhancement
of saturation effect for ions

spin-dependent nucleon multi-dimensional structure

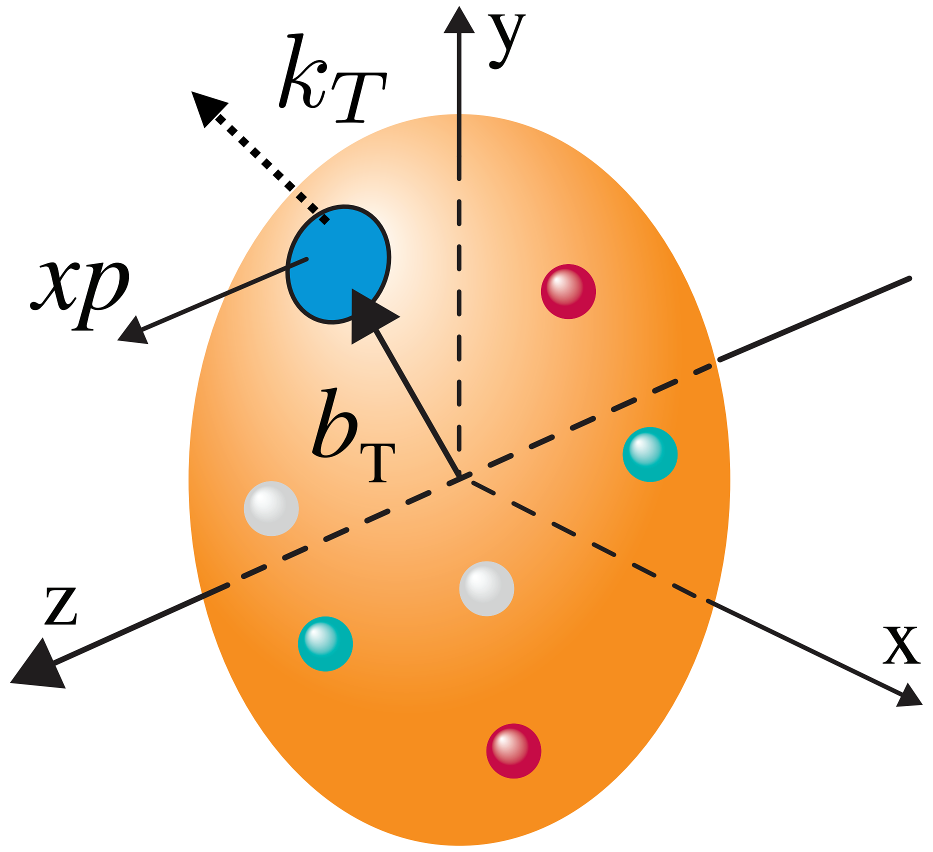

hadronisation

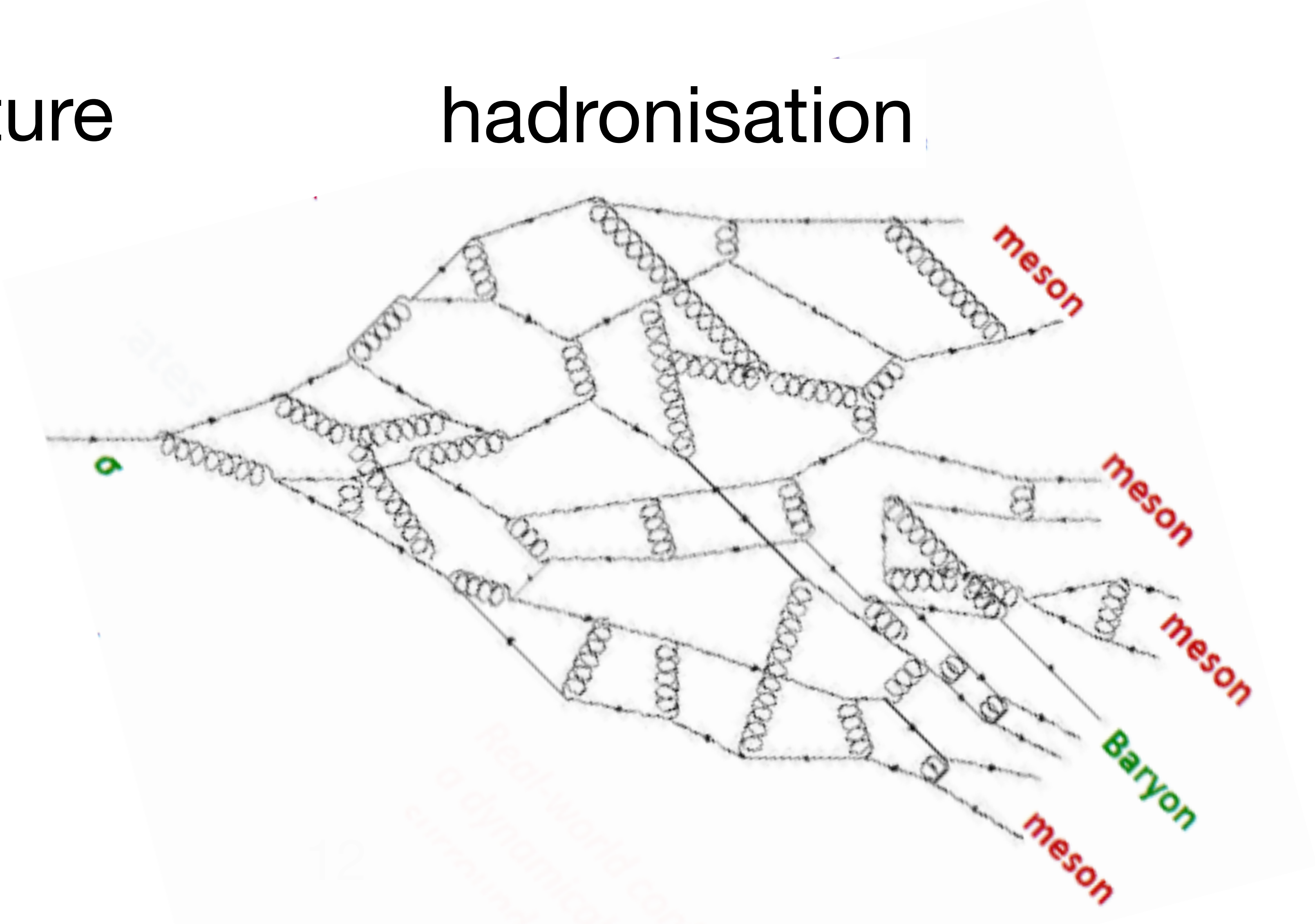

Why and electron-ion collider

nucleon spin

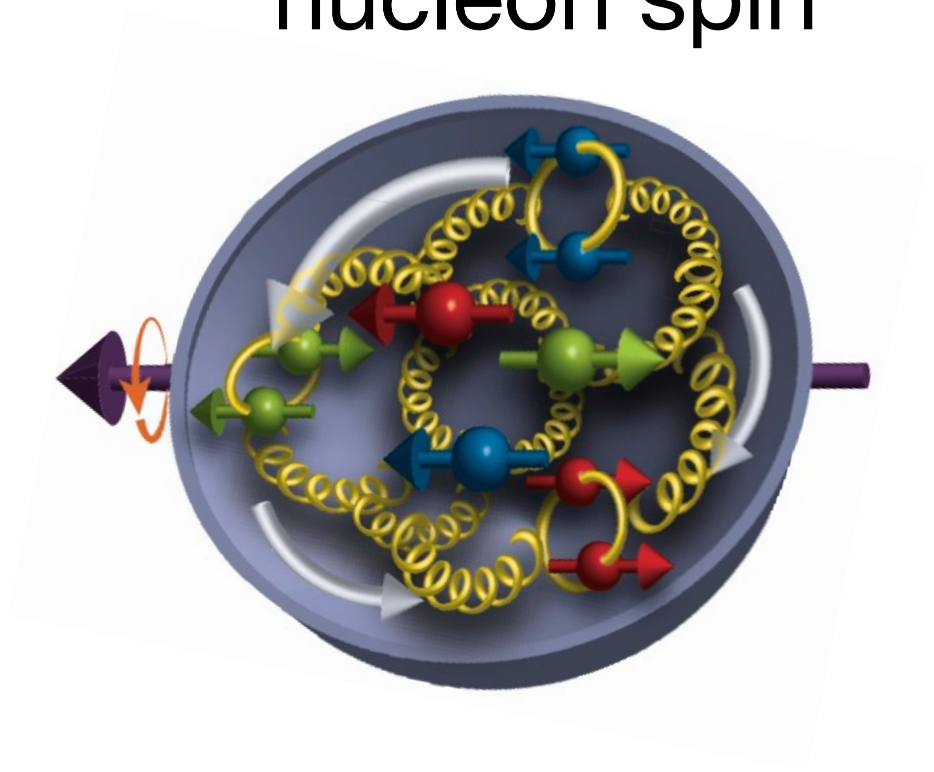

probing saturation

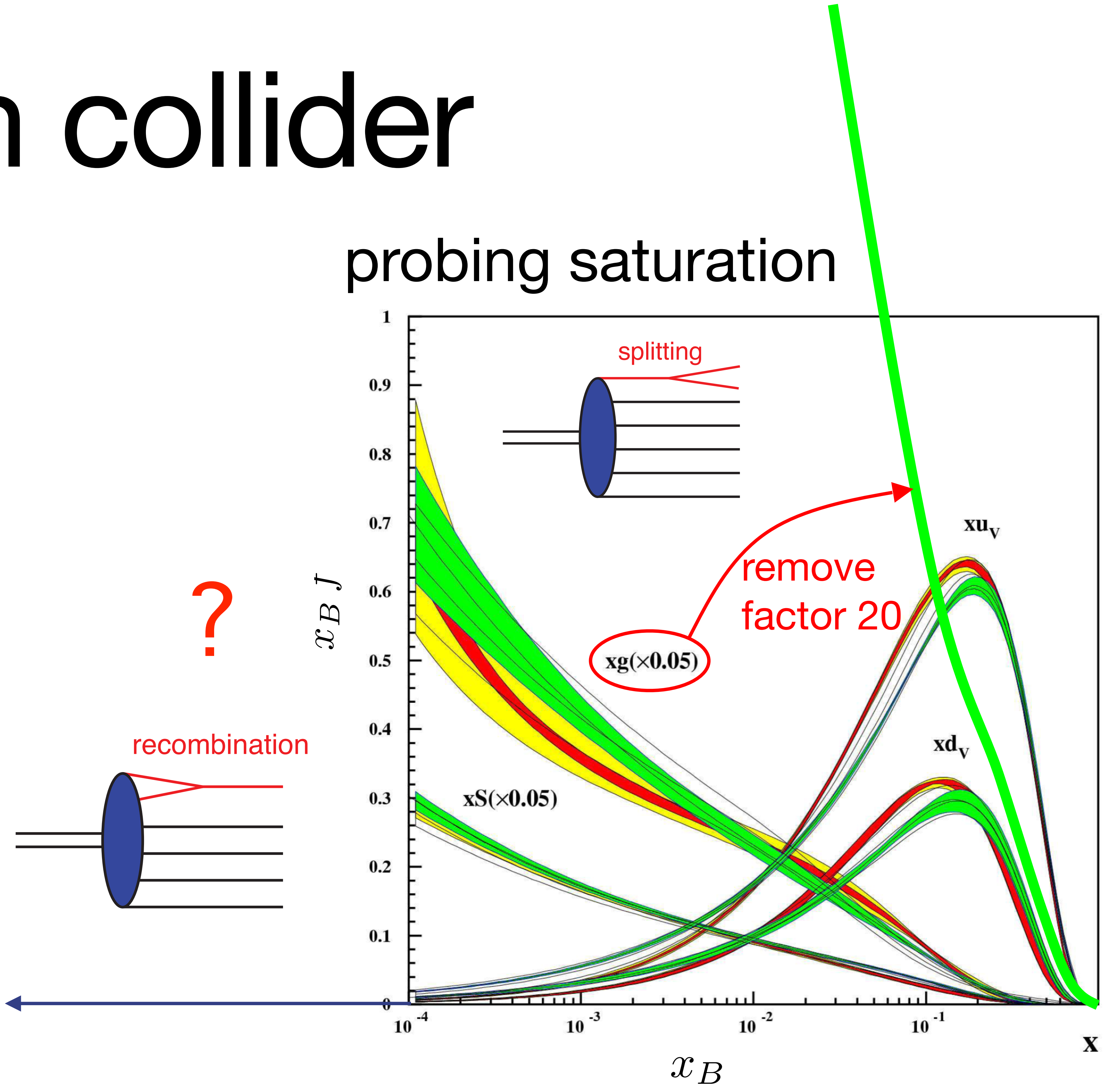

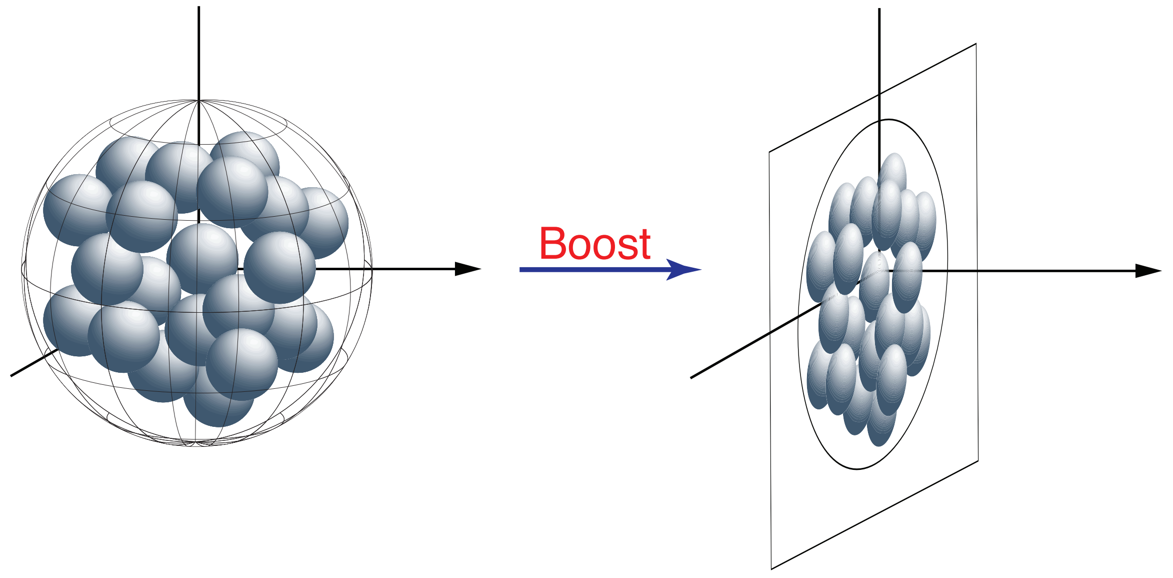

$A^{1/3}$ enhancement
of saturation effect for ions

spin-dependent nucleon multi-dimensional structure

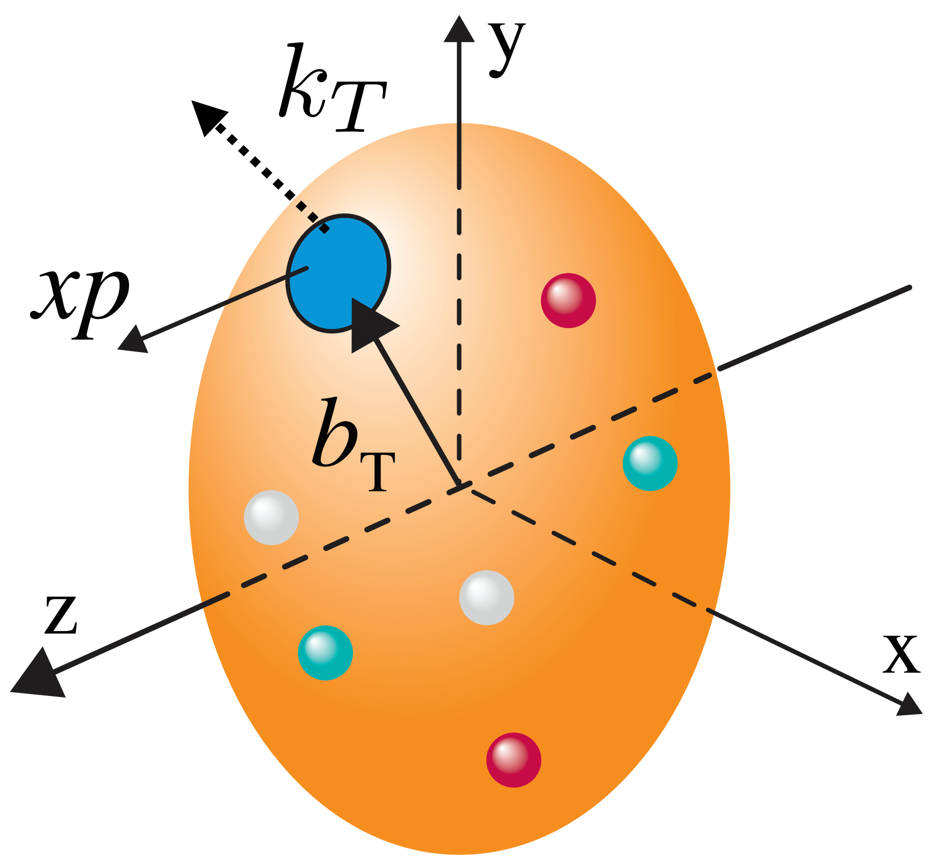

hadronisation

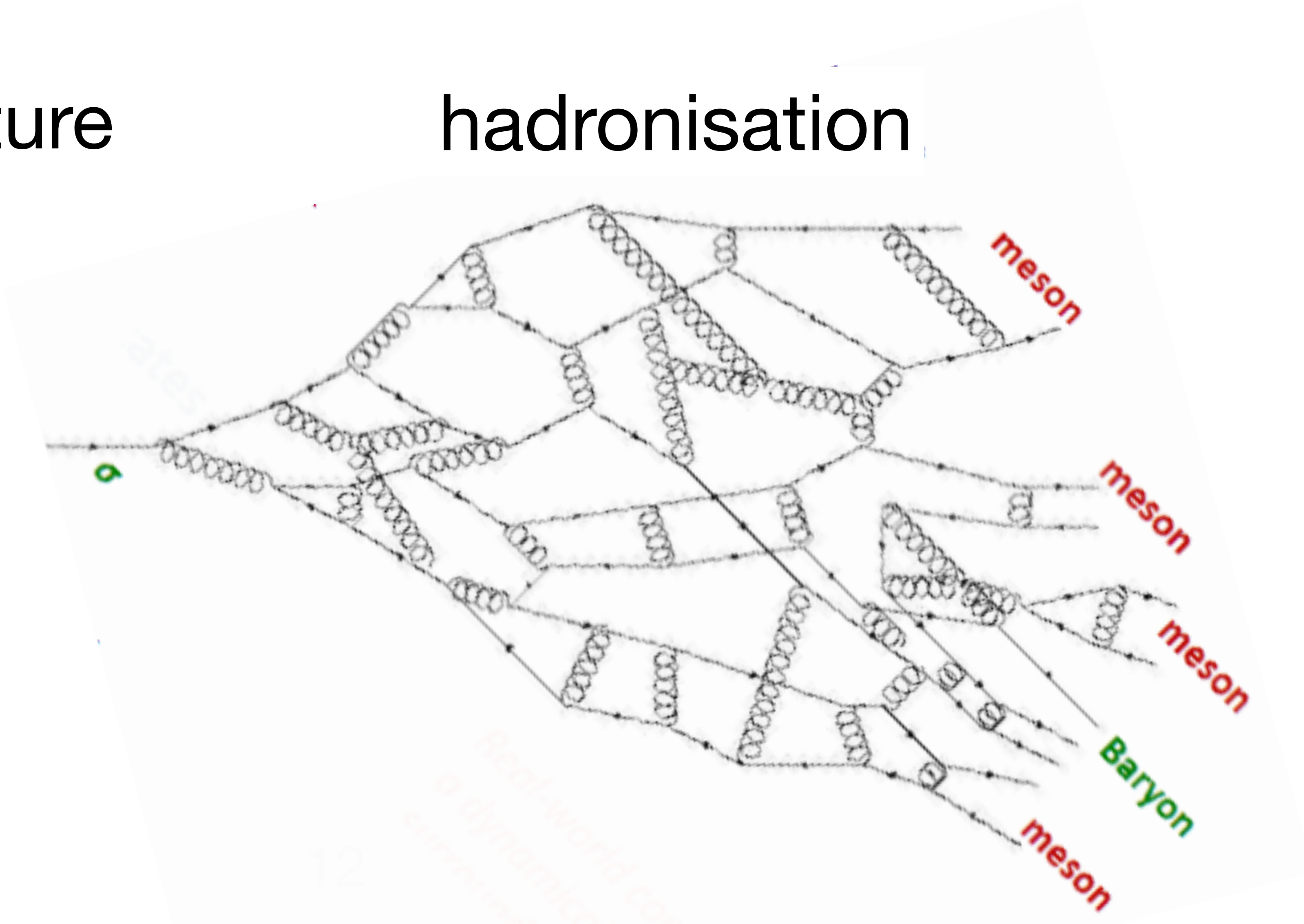

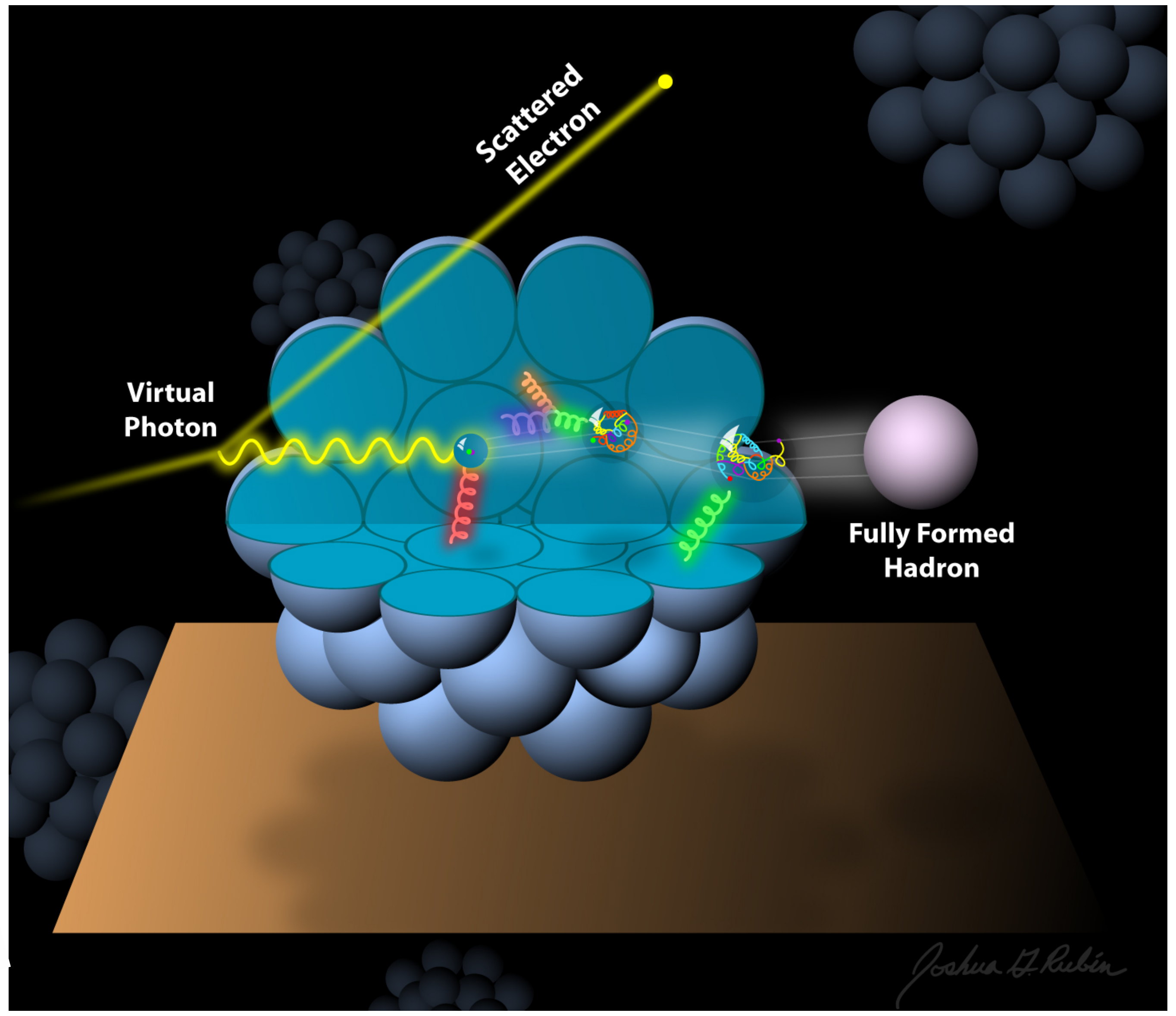

Luminosity and COM E needs for physics topics

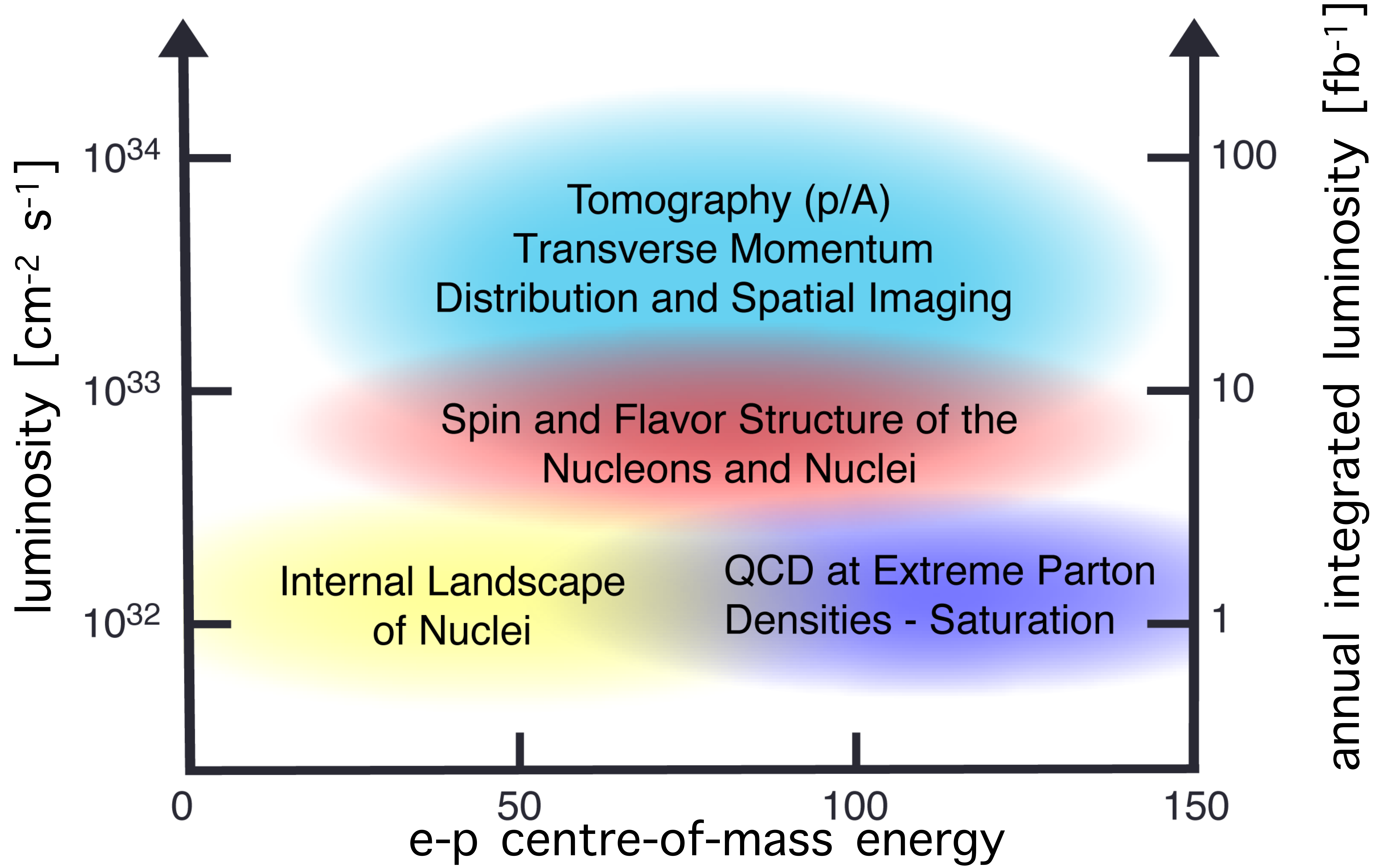

Kinematic coverage at the EIC

ATHENA, JINST **17** (2022) 10, P10019

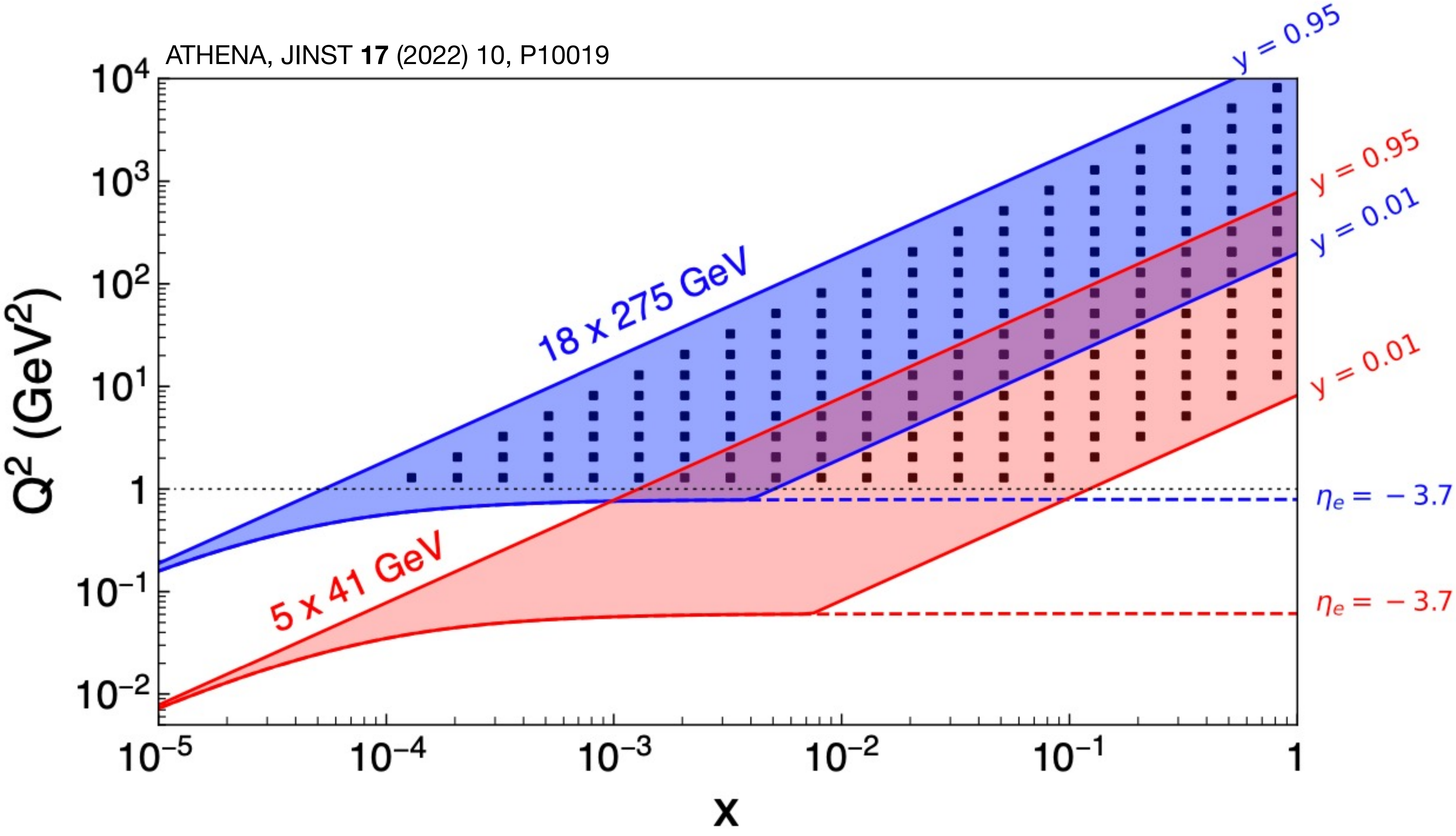

Helicity structure of the nucleon: gluons

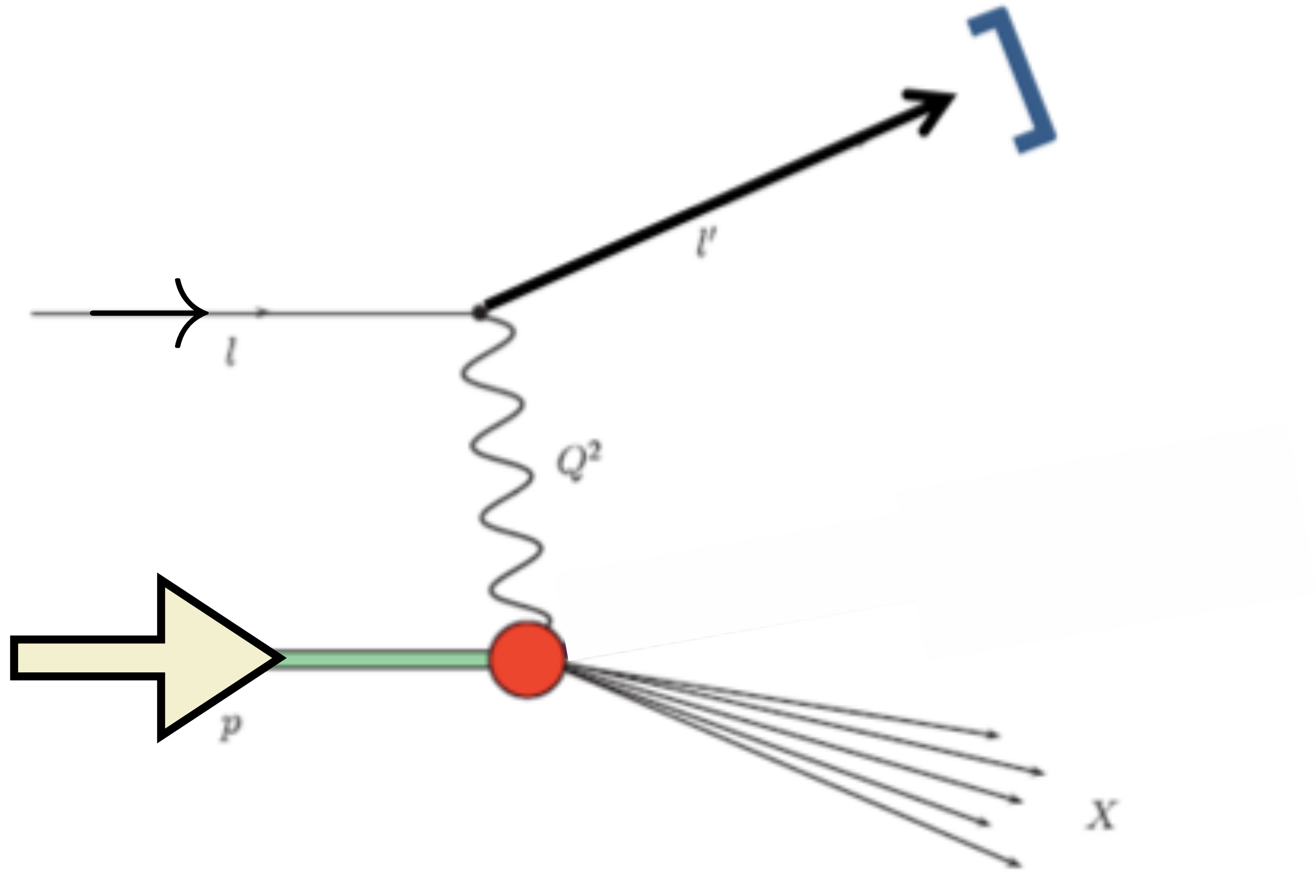

Inclusive measurements
→ access to gluon spin

scaling violation from $g_1(x,Q^2)$

ECCE consortium, 10.5281/zenodo.6537587

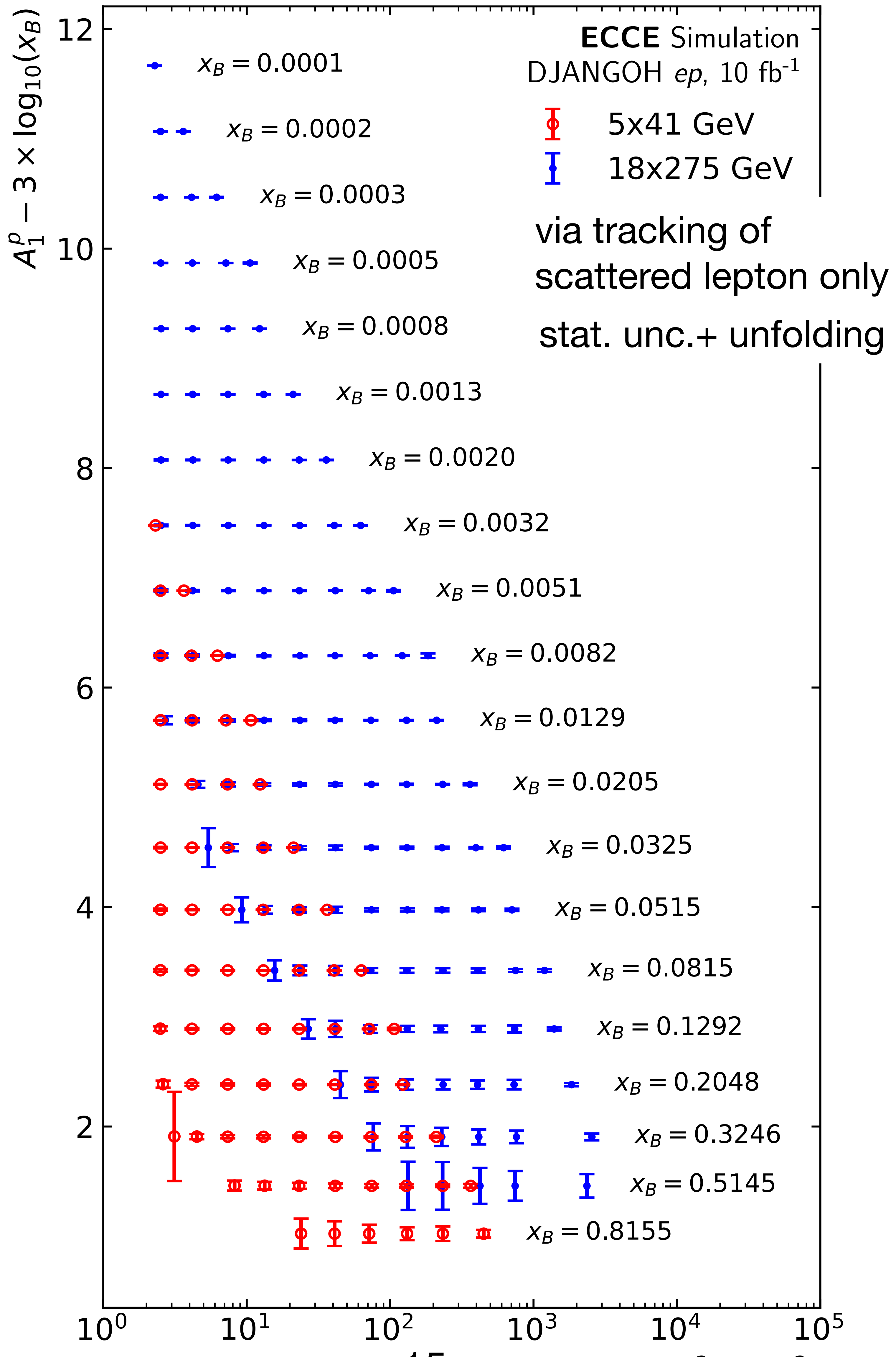

Helicity structure of the nucleon: gluons

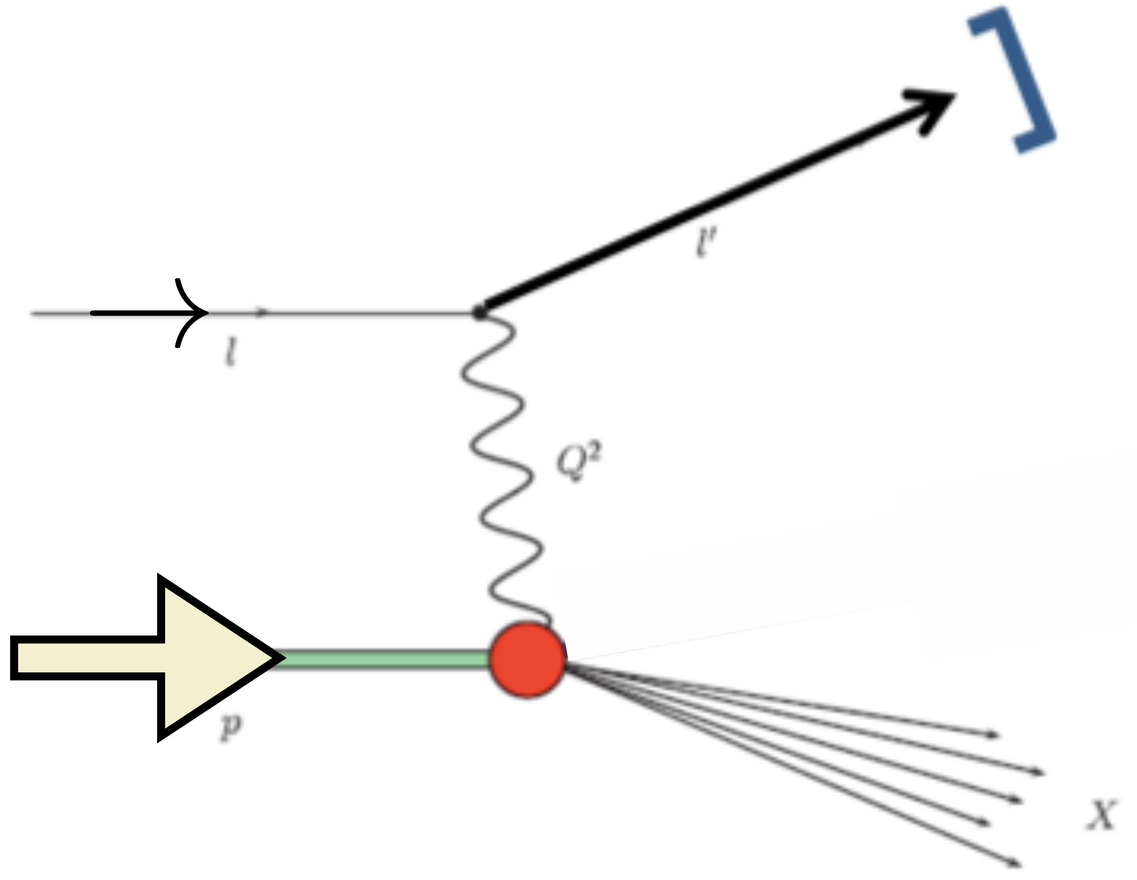

Inclusive measurements
→ access to gluon spin

scaling violation from $g_1(x,Q^2)$

ECCE consortium, 10.5281/zenodo.6537587

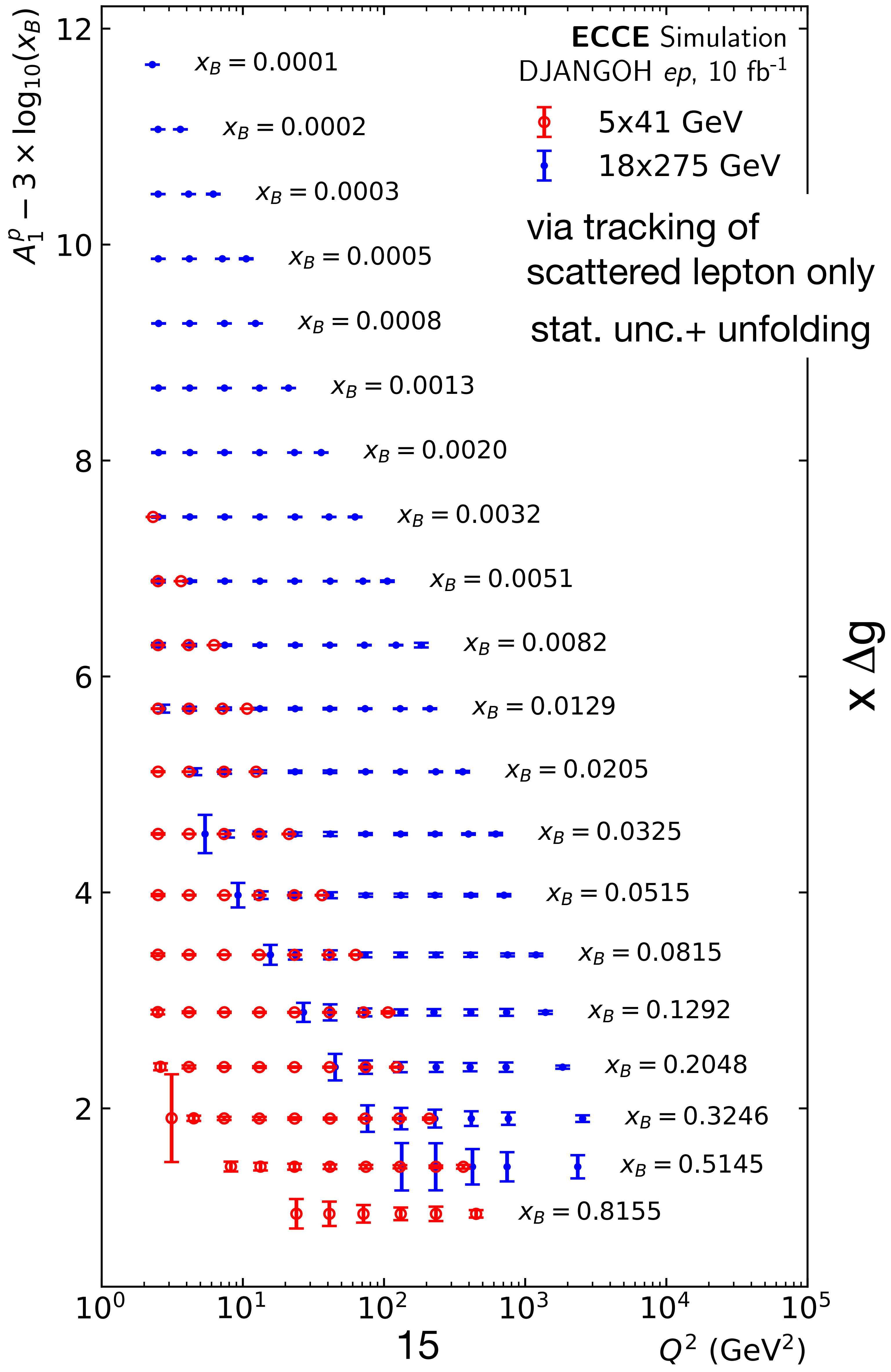

ATHENA, JINST **17** (2022) 10, P10019

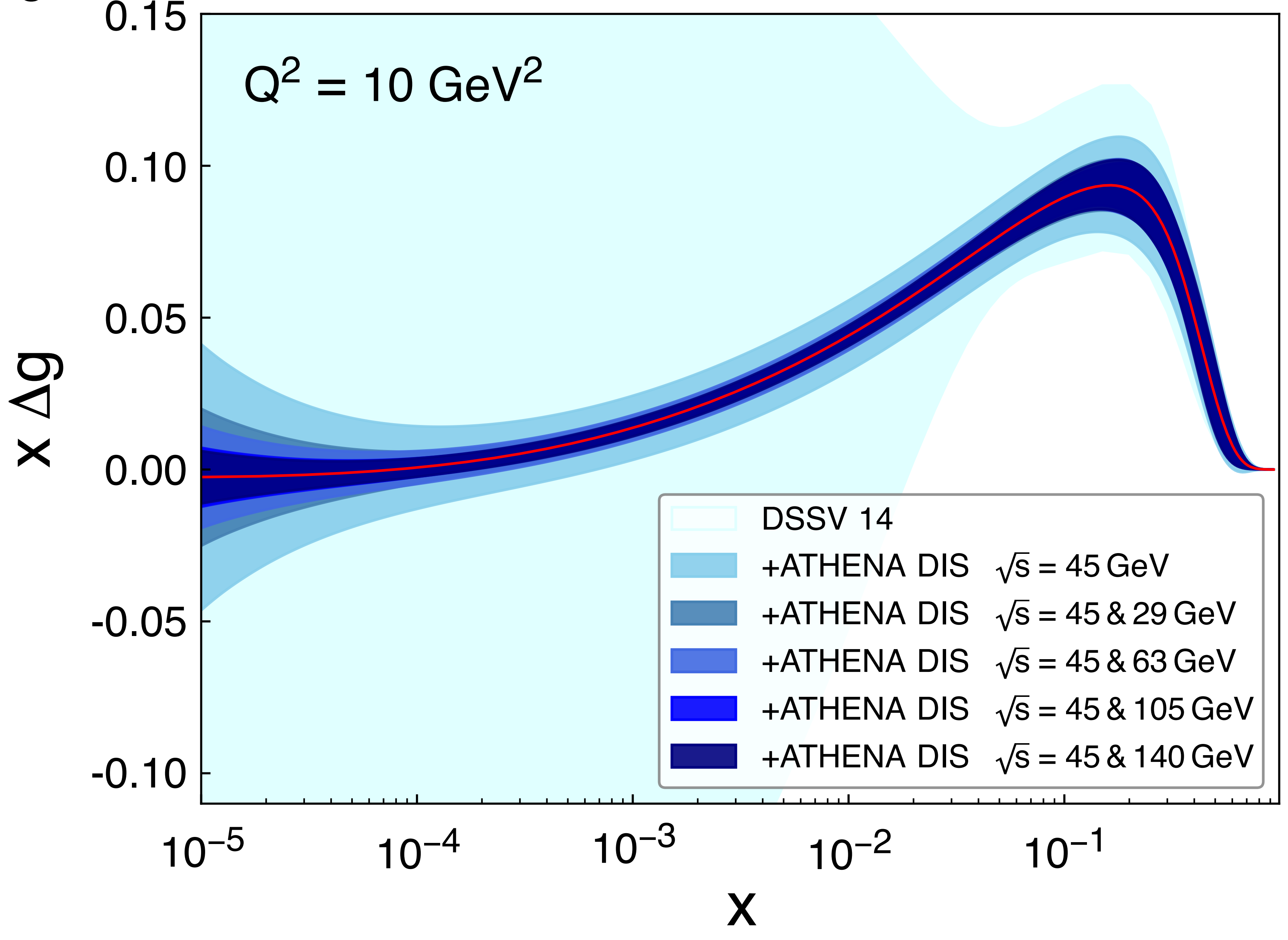

Helicity structure of the proton: sea quarks

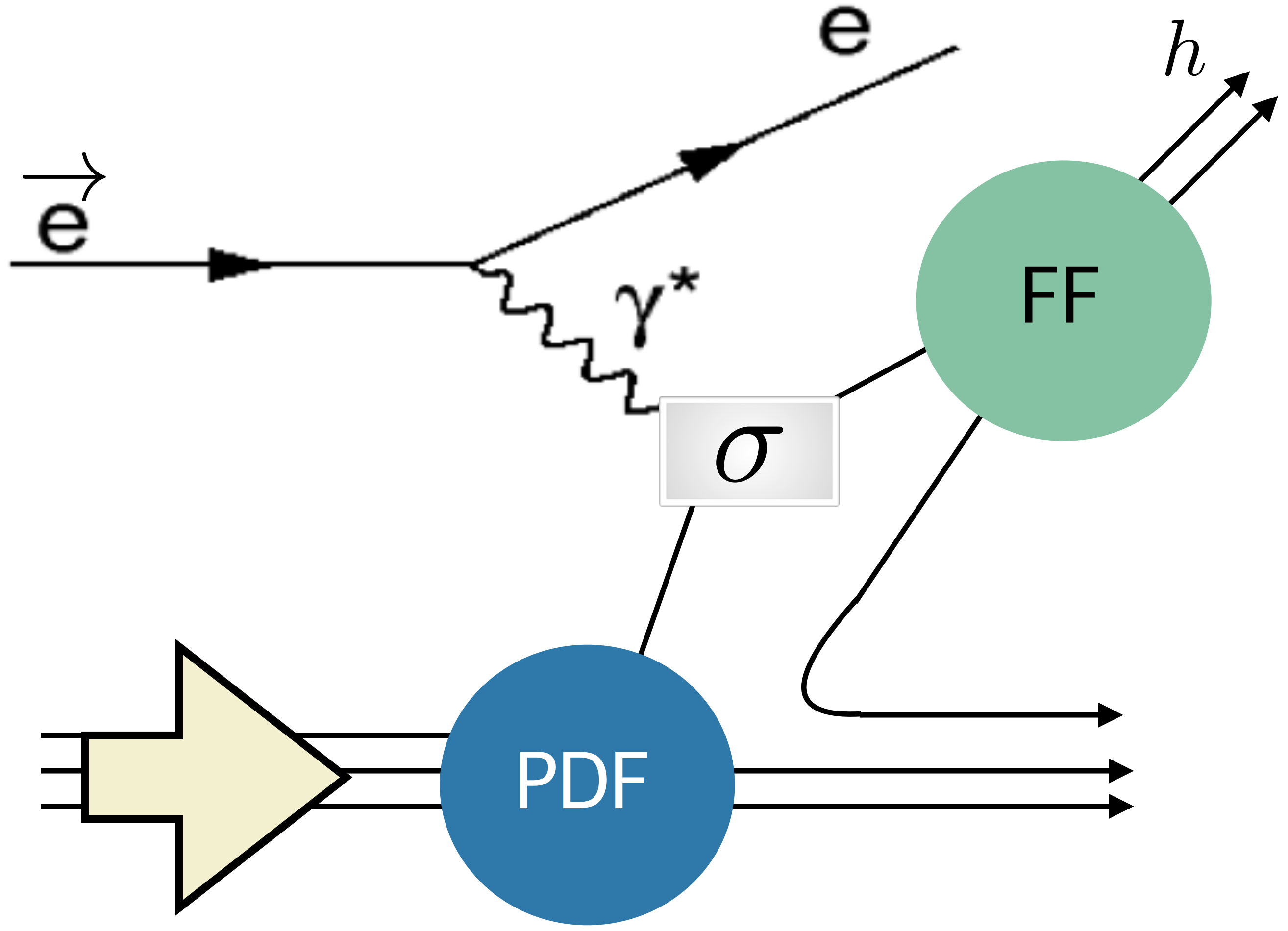

Semi-inclusive measurements, via good hadron PID
→ access to sea-quark spin

Helicity structure of the proton: sea quarks

CVH et al., NIM A 1056 (2023) 168563

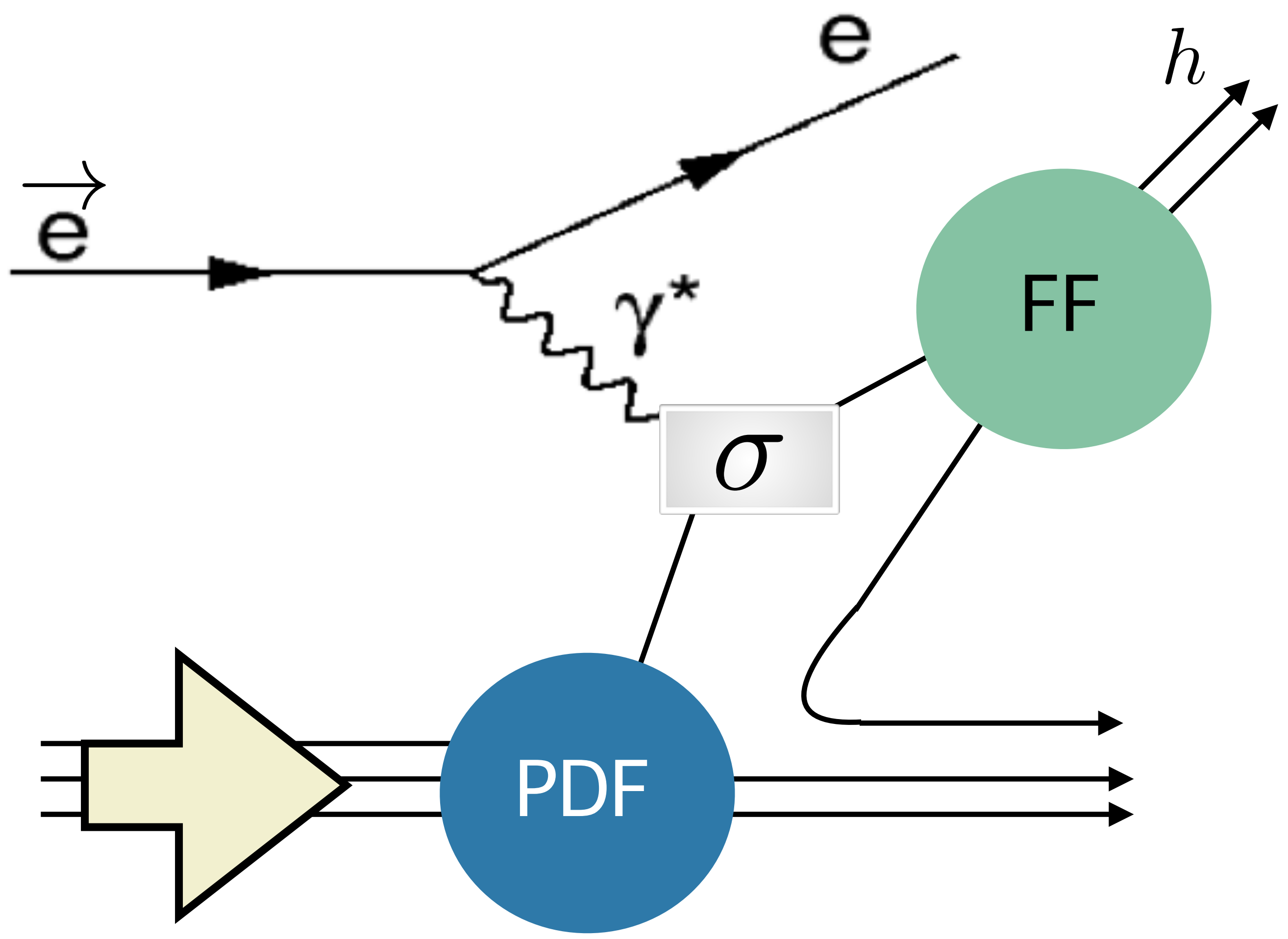

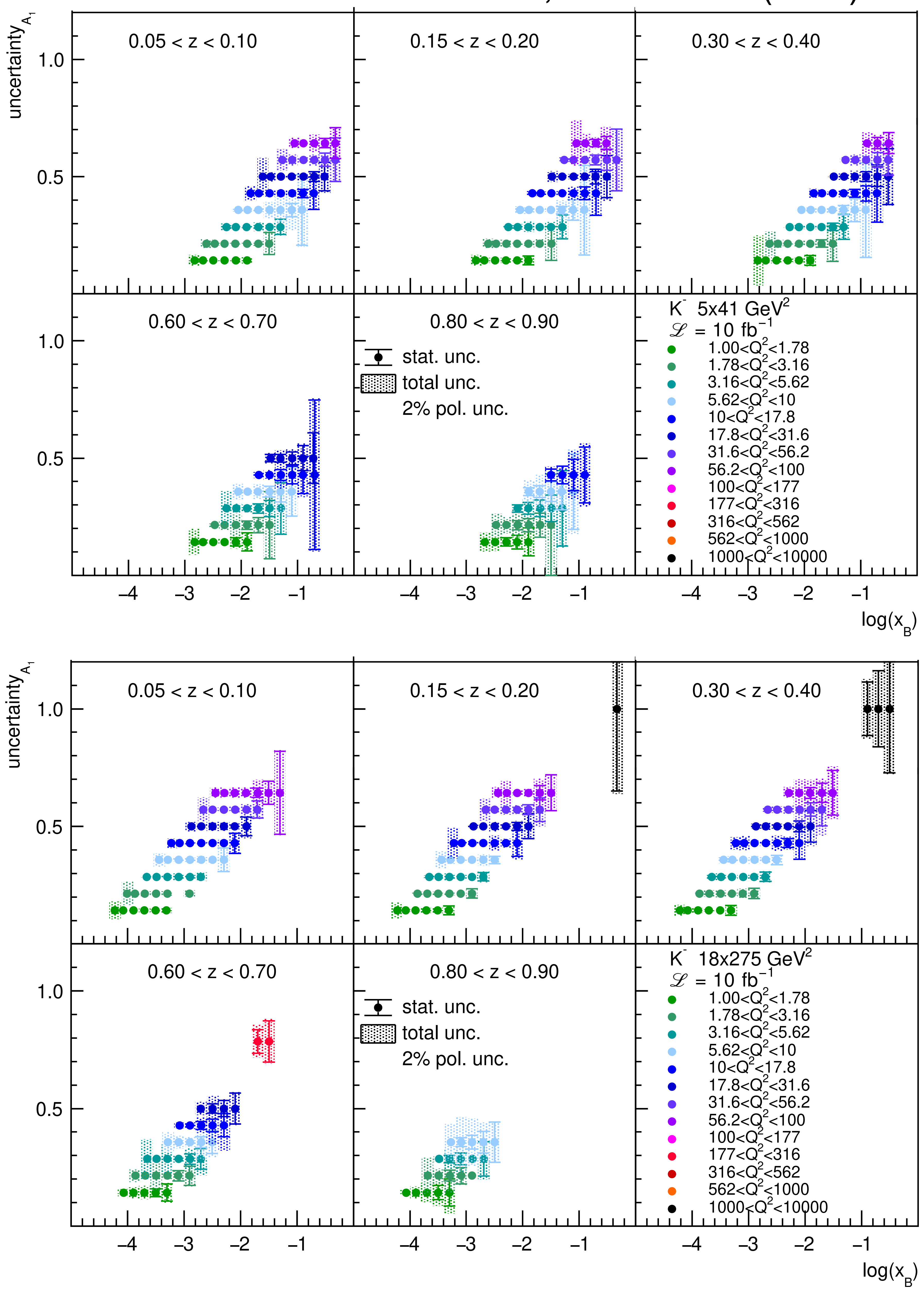

Semi-inclusive measurements, via good hadron PID
→ access to sea-quark spin

Helicity structure of the proton: sea quarks

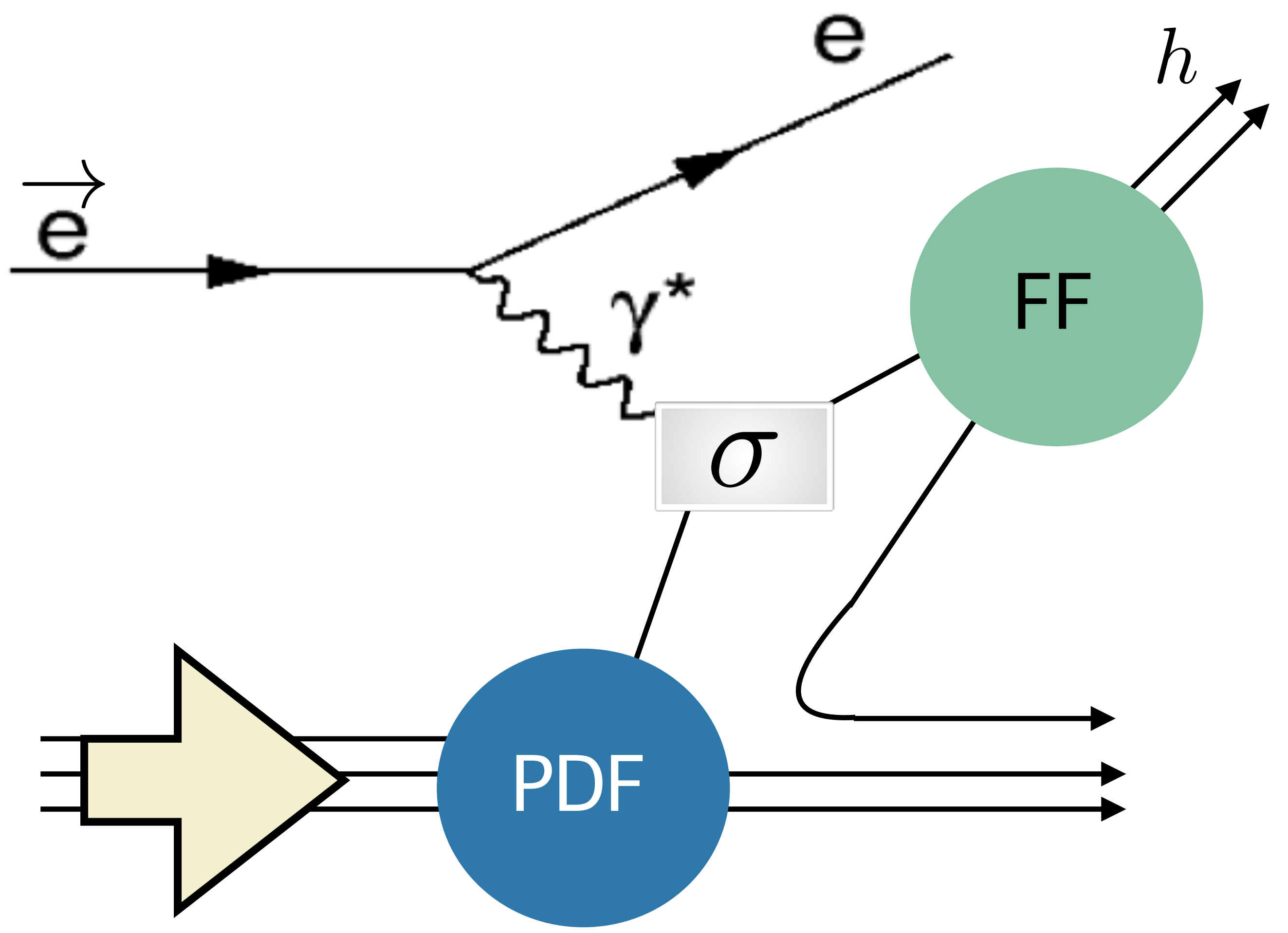

CVH et al., NIM A 1056 (2023) 168563

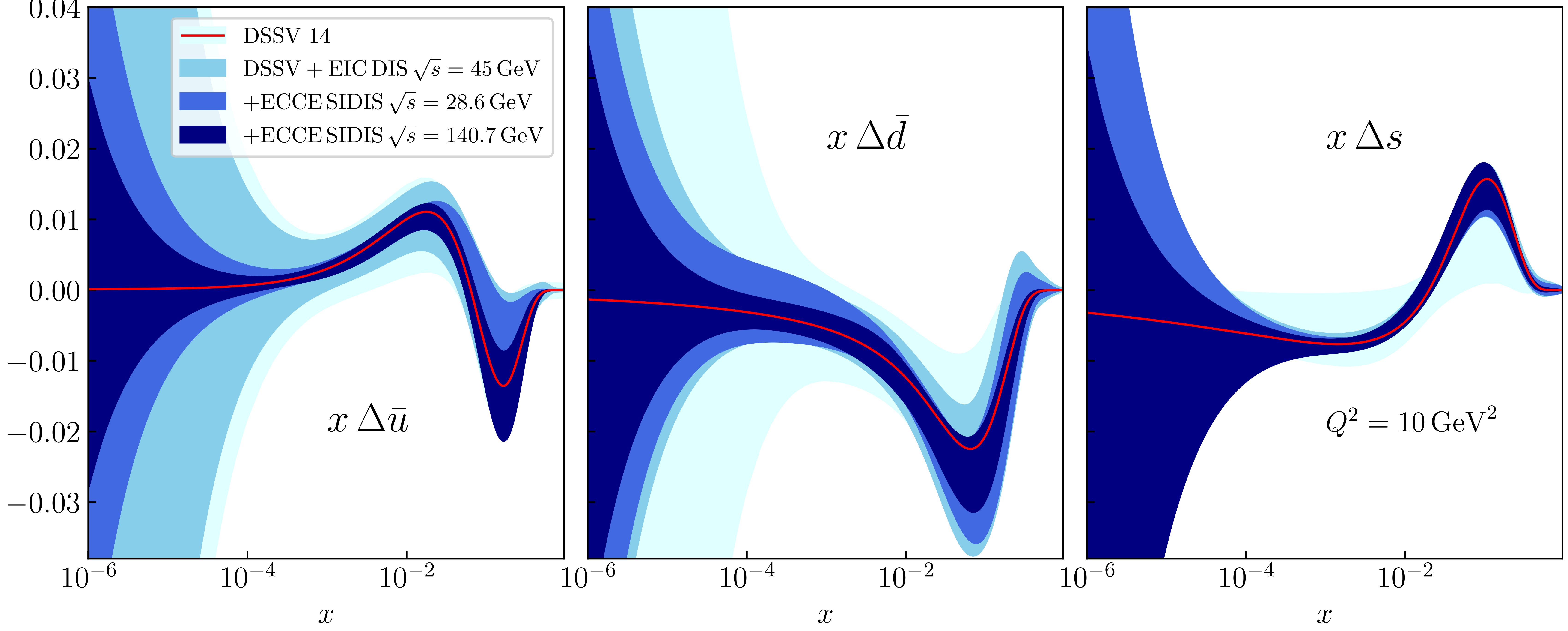

Semi-inclusive measurements, via good hadron PID
→ access to sea-quark spin

TMD PDFs: Sivers

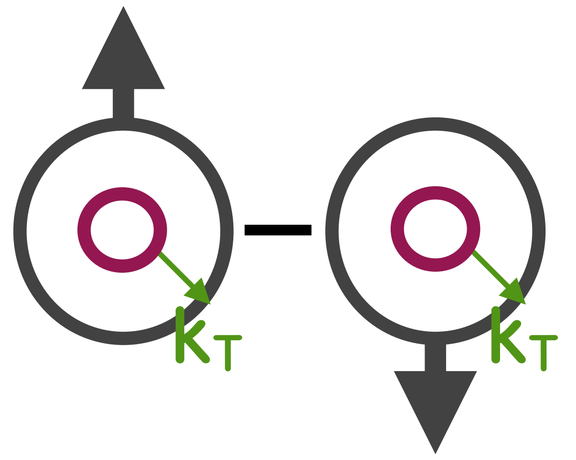

TMD PDFs: Sivers

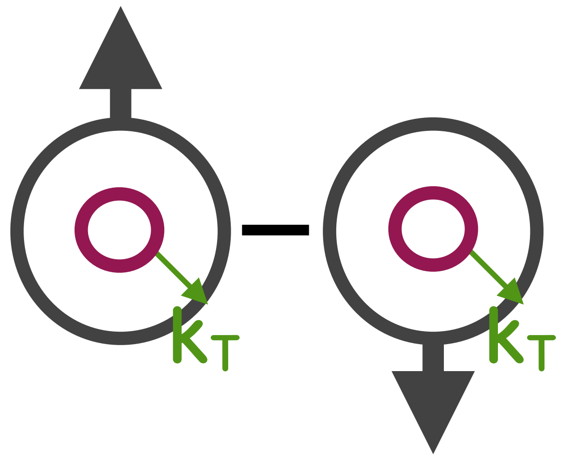

Sivers asymmetry

$$\sigma^h(\phi, \phi_S) \propto S_T\, 2\langle \sin(\phi - \phi_S)\rangle^h_{UT} \sin(\phi - \phi_S) \longrightarrow \mathcal{C}[f_{1T}^{\perp} \times D_1^{q\to h}]$$

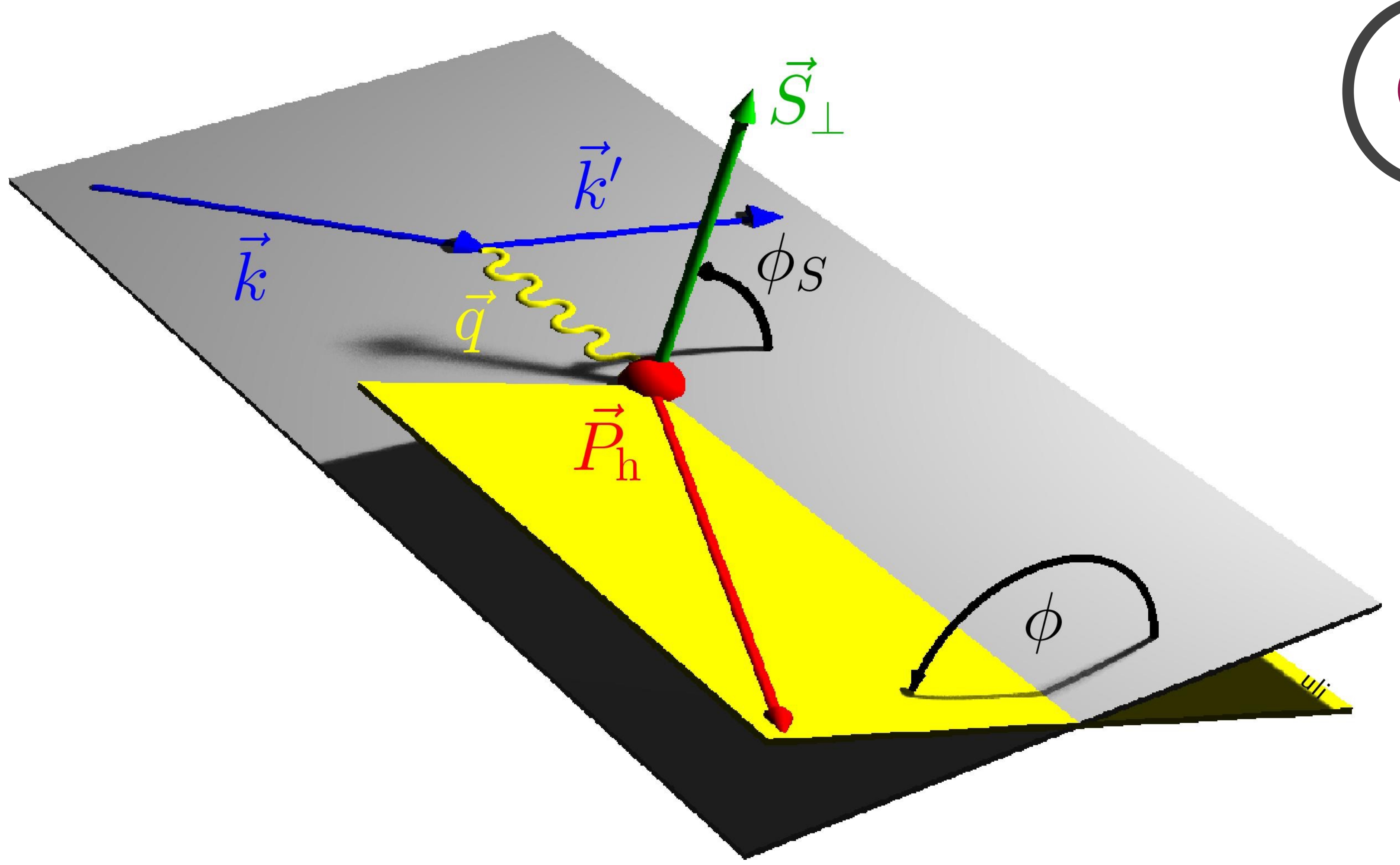

TMD PDFs: Sivers

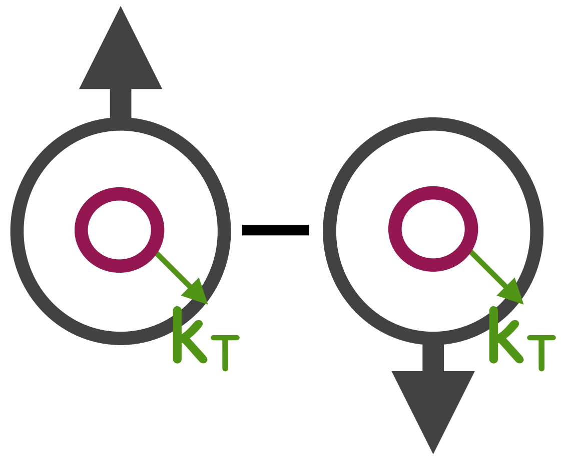

Sivers asymmetry

$$\sigma^h(\phi, \phi_S) \propto S_T \, 2\langle \sin(\phi - \phi_S)\rangle^h_{UT} \, \sin(\phi - \phi_S) \longrightarrow \mathcal{C}[f_{1T}^{\perp} \times D_1^{q\to h}]$$

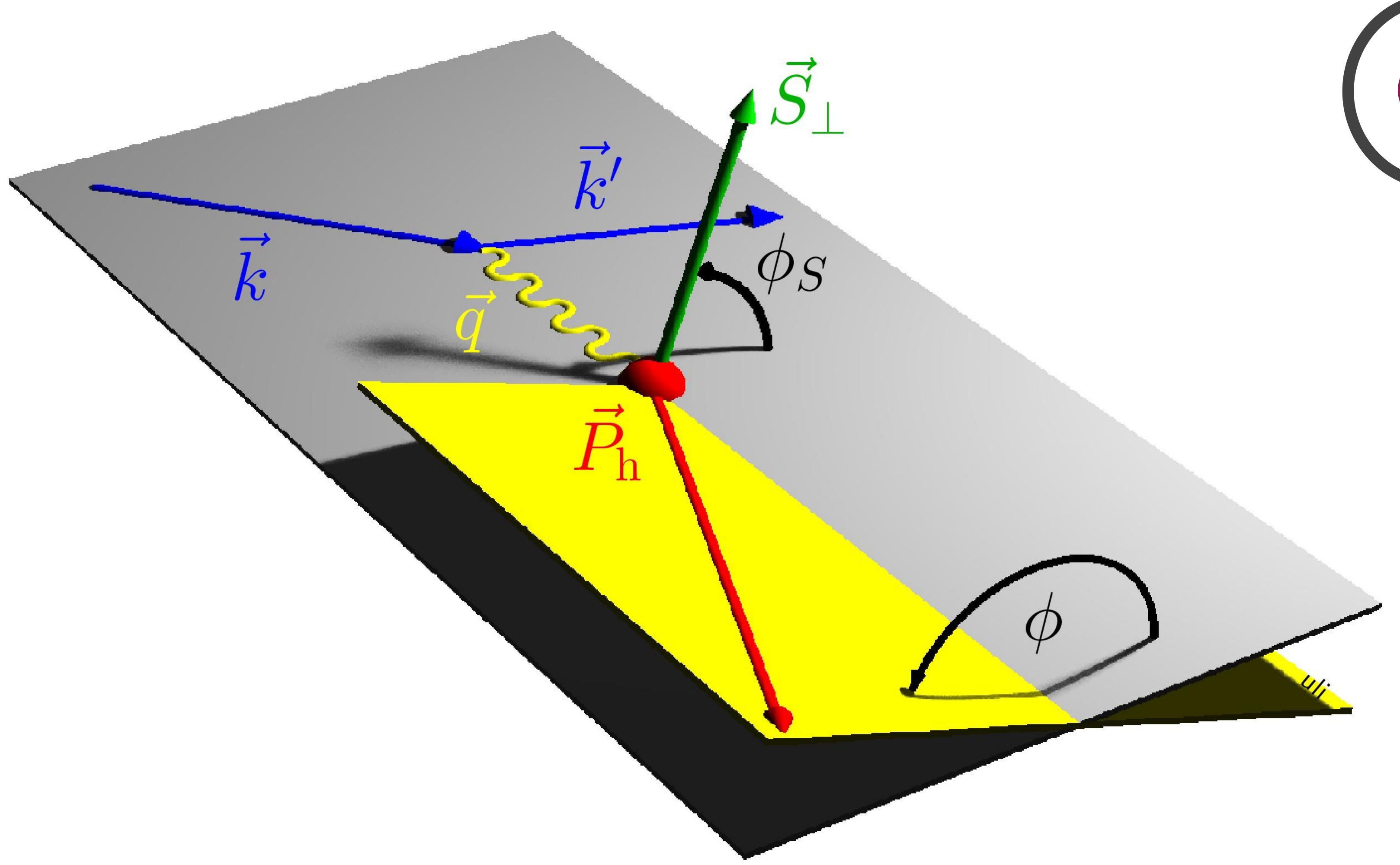

R. Seidl, A. Vladimirov et al., NIM A **1055** (2023) 168458

Parametrisation: M. Bury et al., JHEP **05** (2021)151

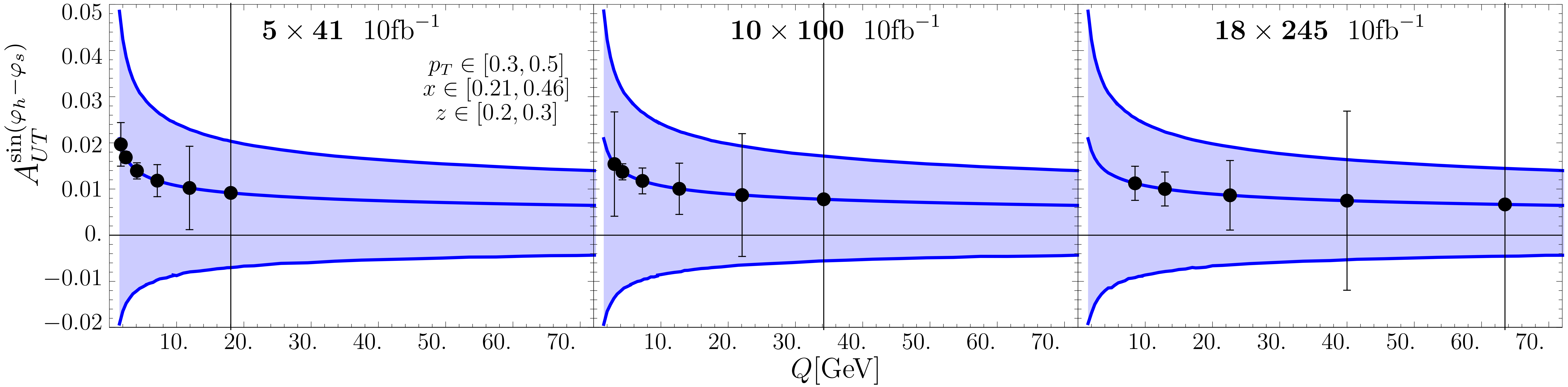

Decrease of asymmetry with increasing Q^2 → need high precision (<1%) to measure asymmetry at high Q^2

Impact of EIC on Sivers TMD PDF

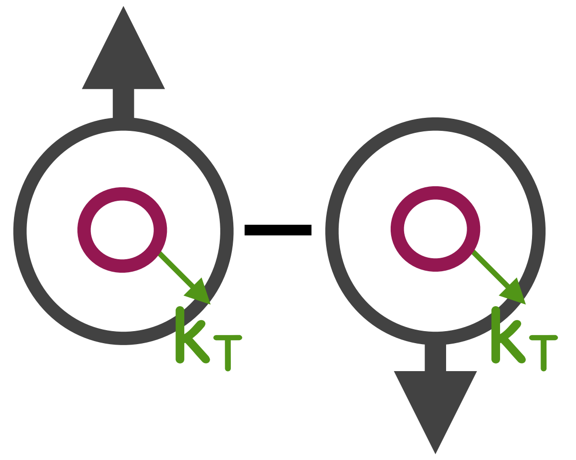

R. Seidl, A. Vladimirov et al., NIM A **1055** (2023) 168458

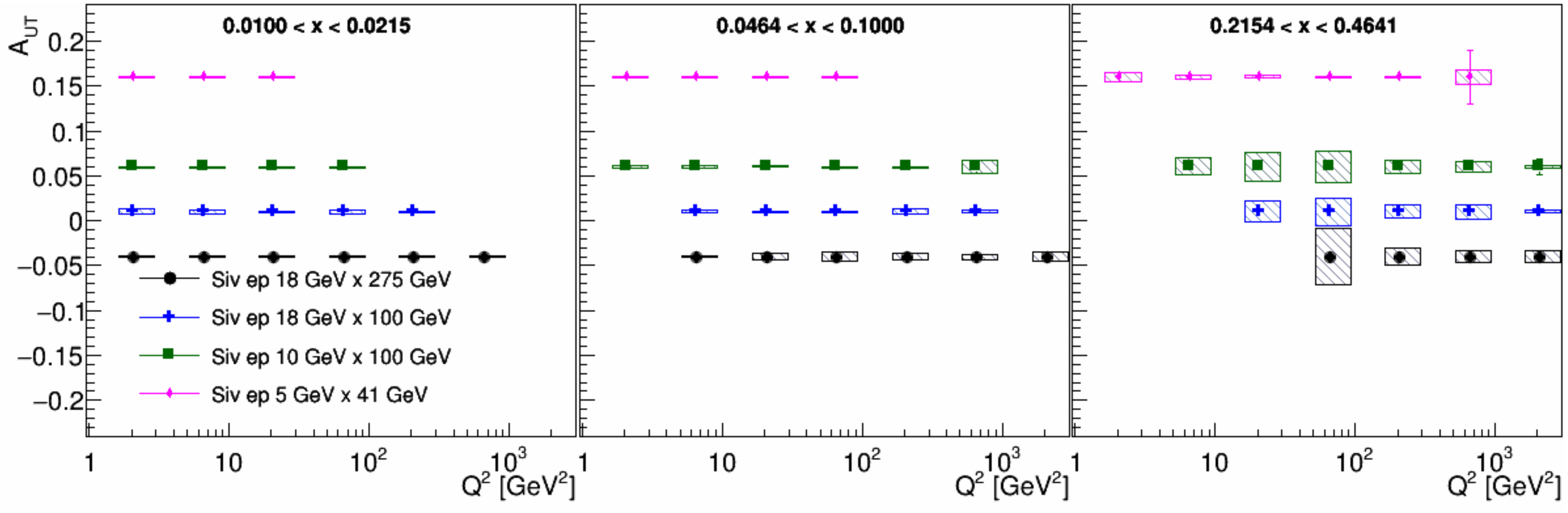

Impact of EIC on Sivers TMD PDF

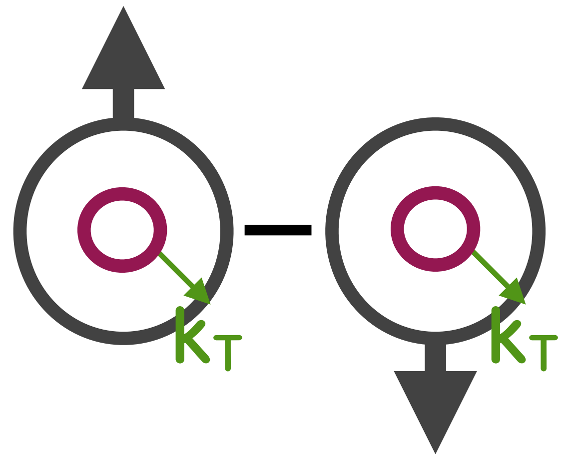

R. Seidl, A. Vladimirov et al., NIM A **1055** (2023) 168458

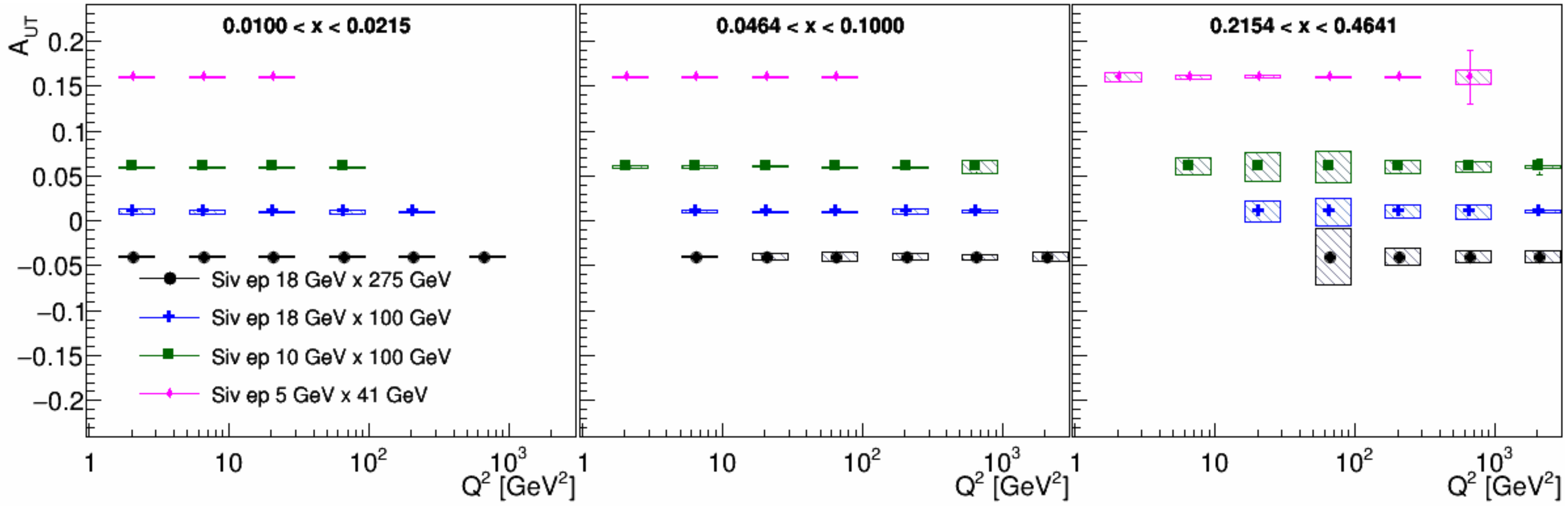

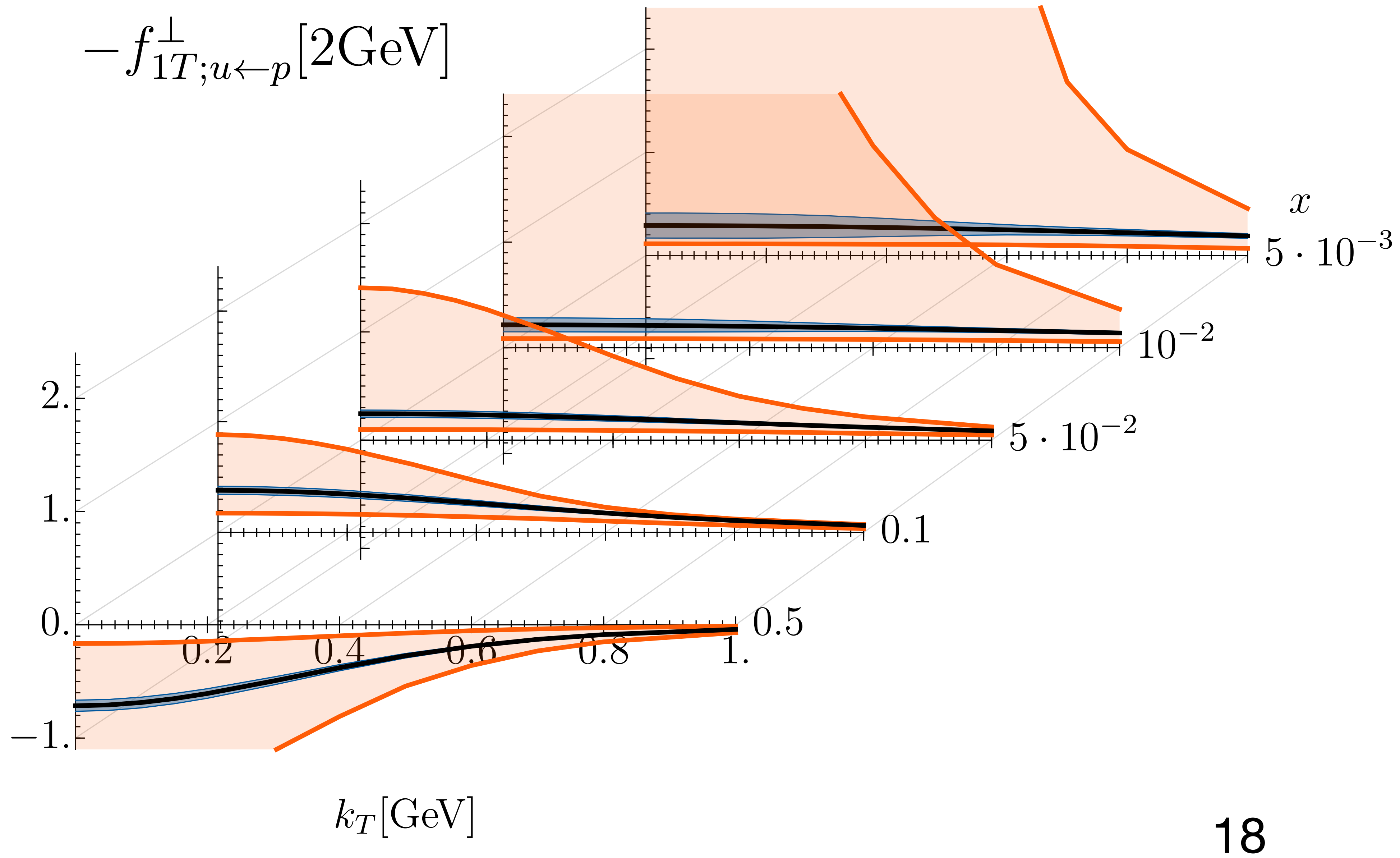

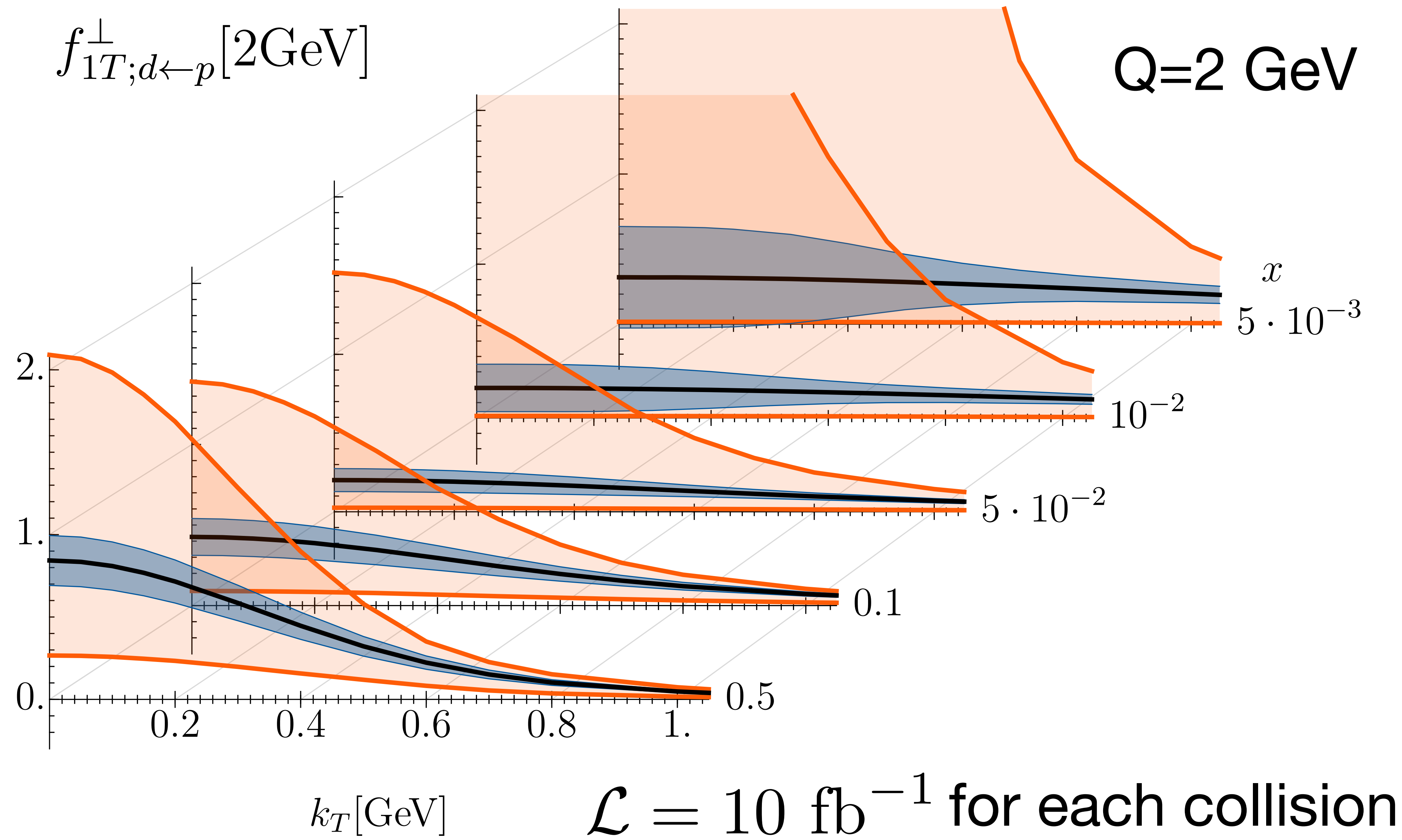

Q=2 GeV

$\mathcal{L} = 10\ \text{fb}^{-1}$ for each collision energy

Impact of EIC on Sivers TMD PDF

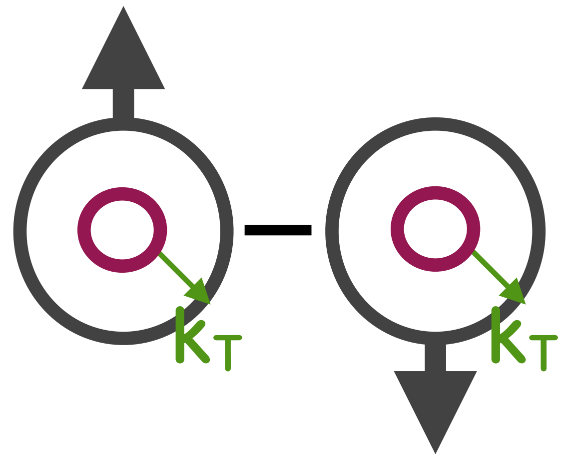

R. Seidl, A. Vladimirov et al., NIM A **1055** (2023) 168458

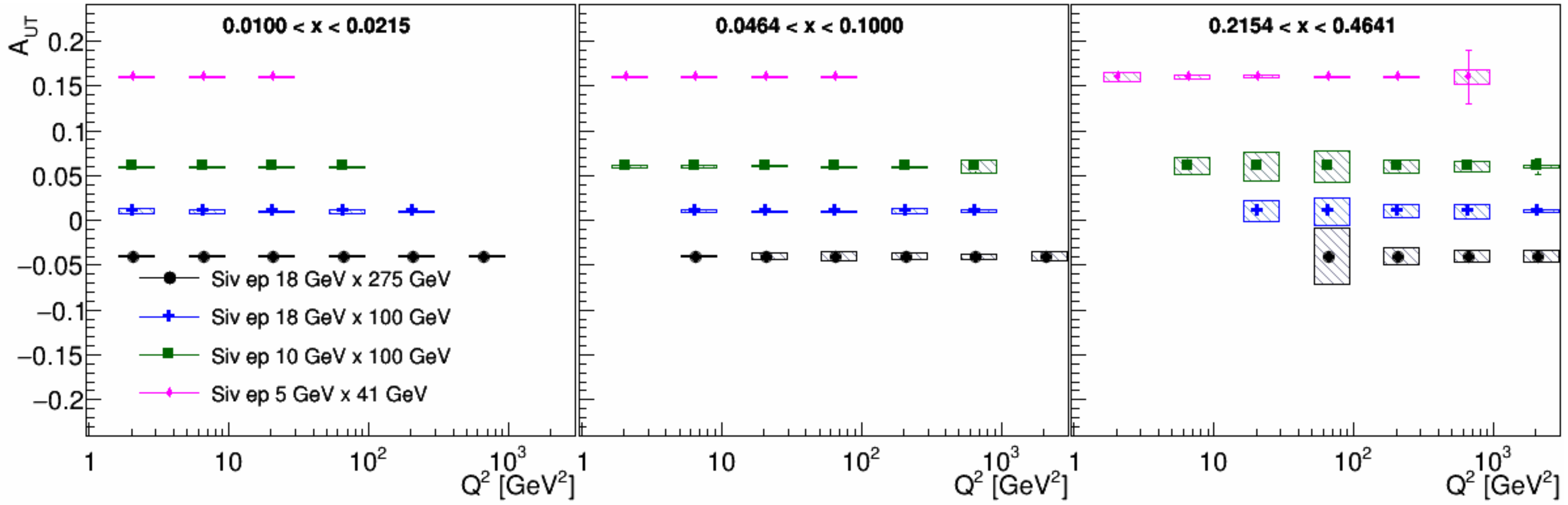

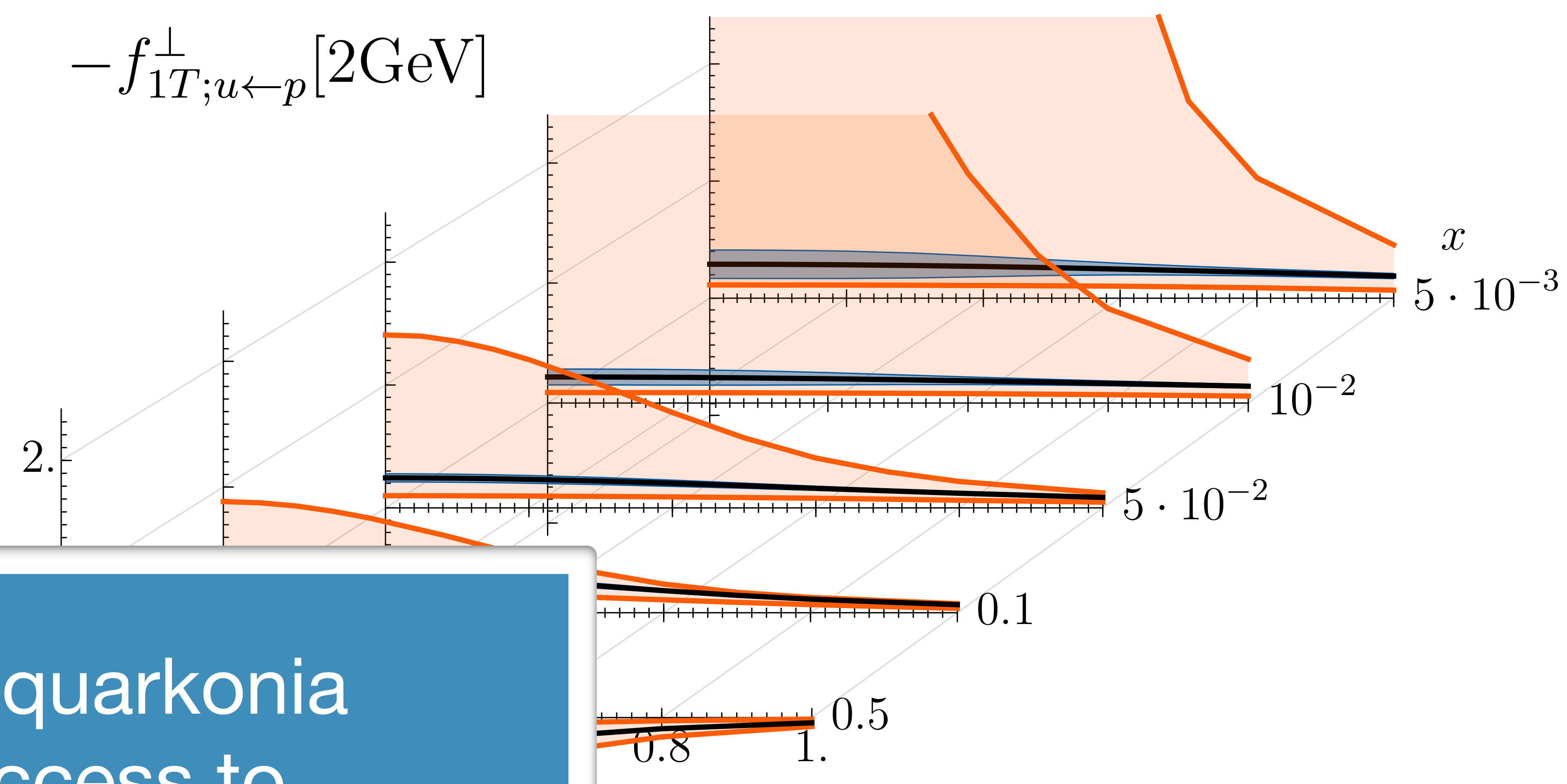

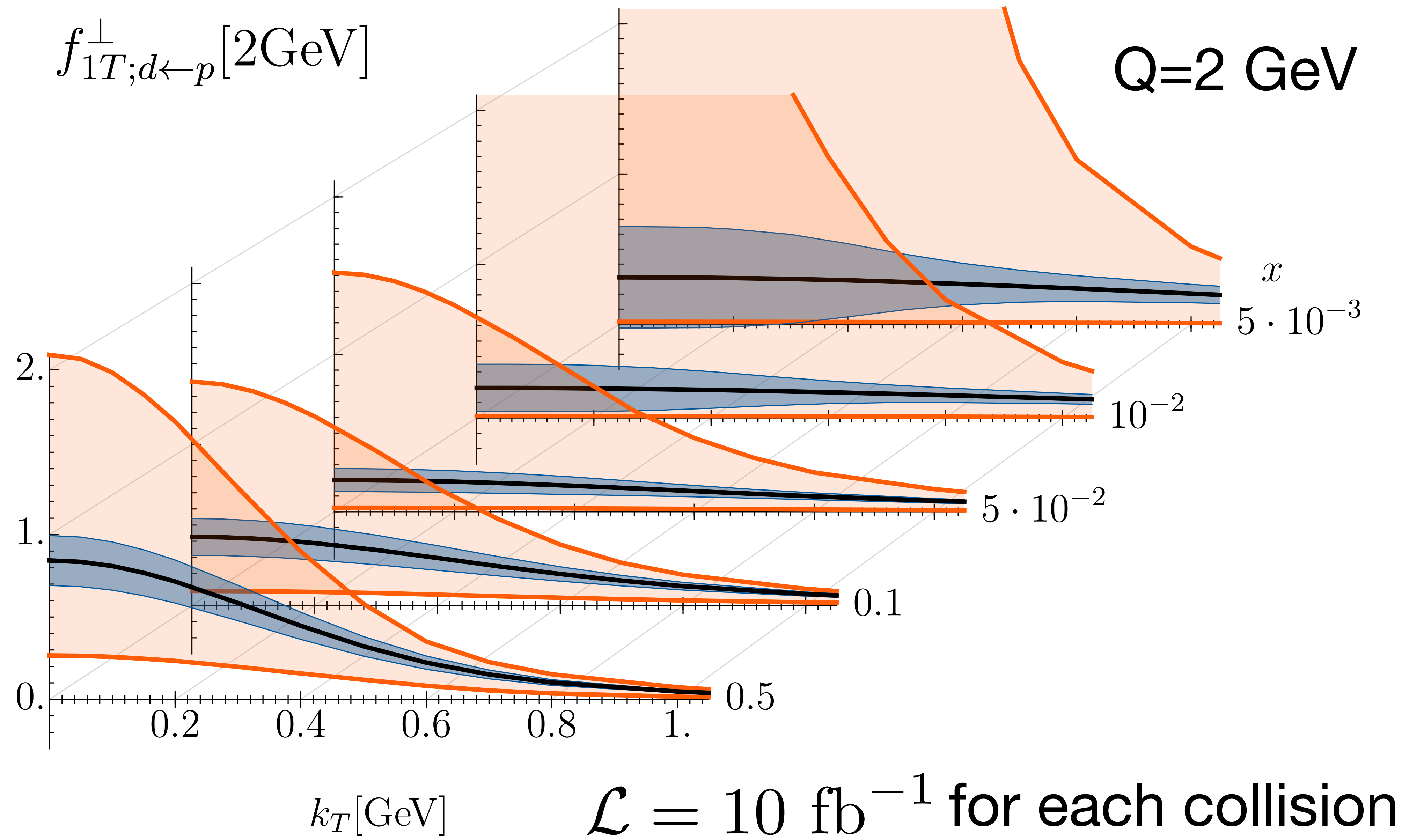

Q=2 GeV

Studies with quarkonia would give access to gluon TMD PDFs

$\mathcal{L} = 10\ \text{fb}^{-1}$ for each collision energy

Di-hadron production and jets in eA

- Complementarity region covered by dihadron and jet production

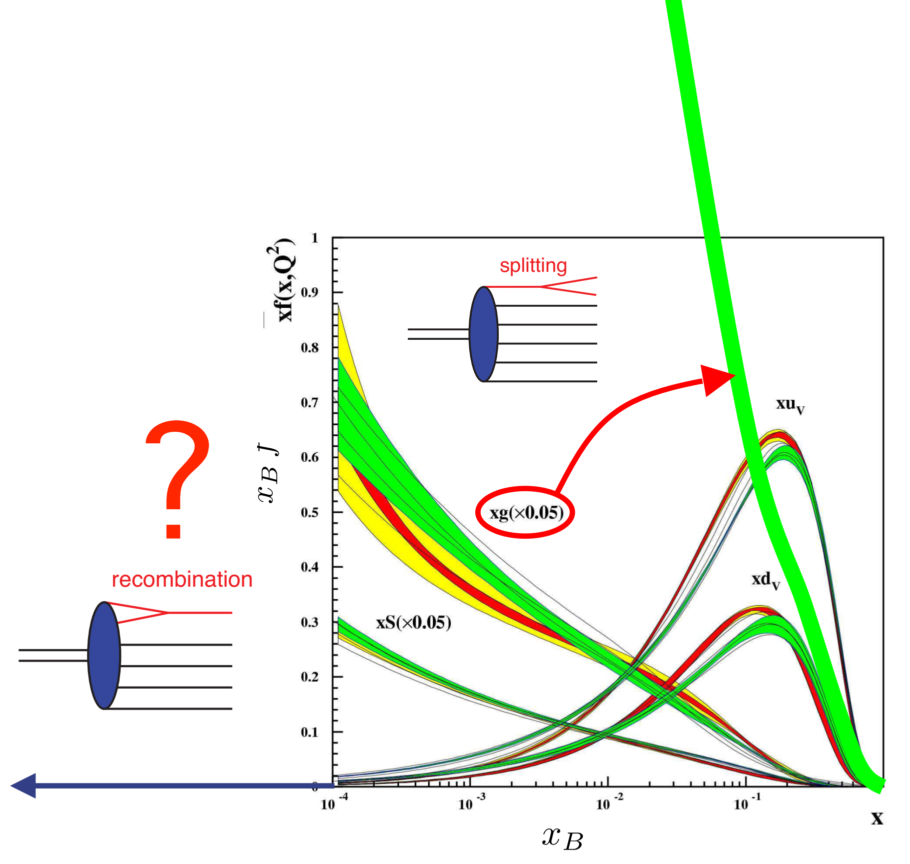

correlated back-to-back hadron pairs in e+Au/e+p scaled by $A^{1/3}$
Away-side suppression

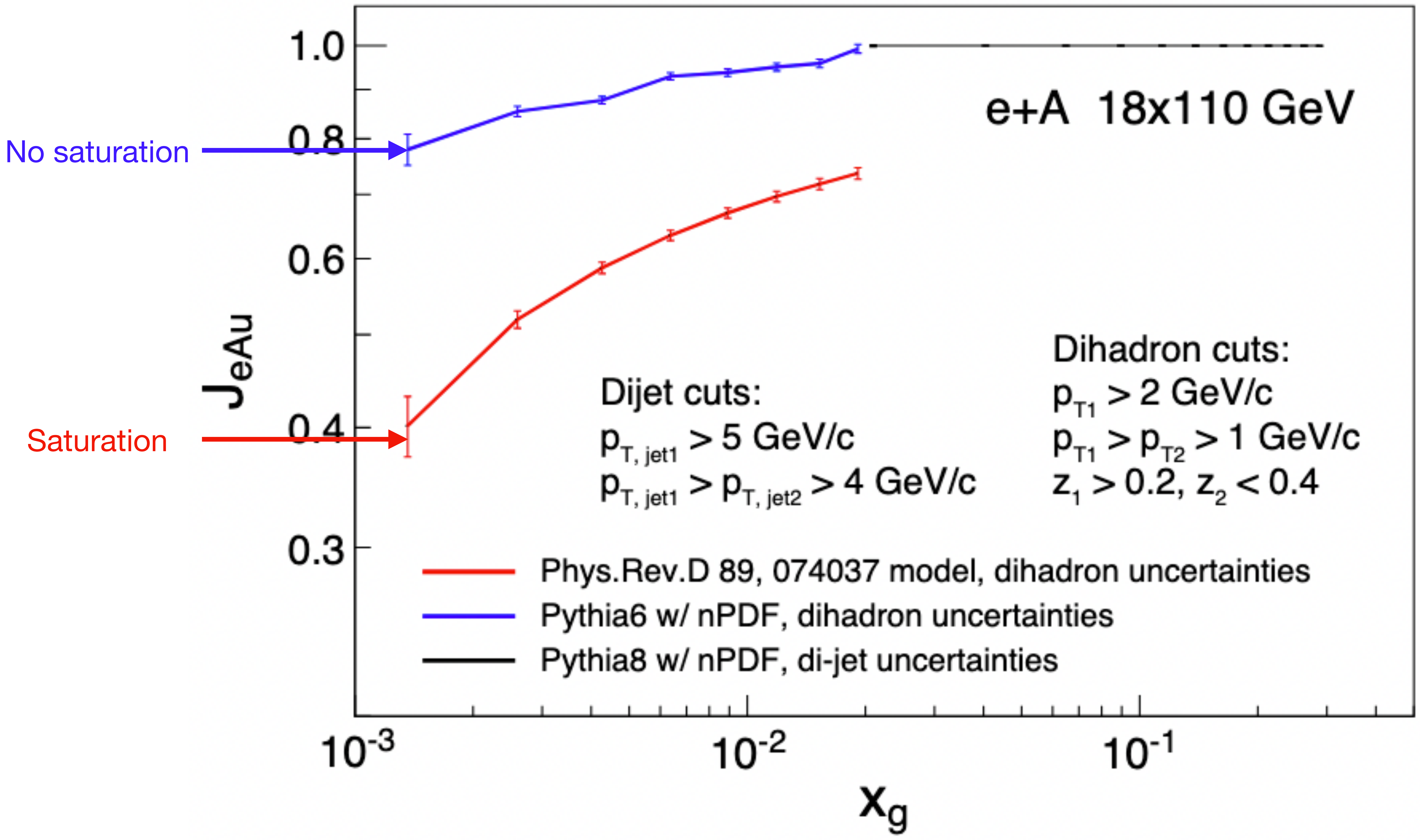

Exclusive measurements on p with the EIC

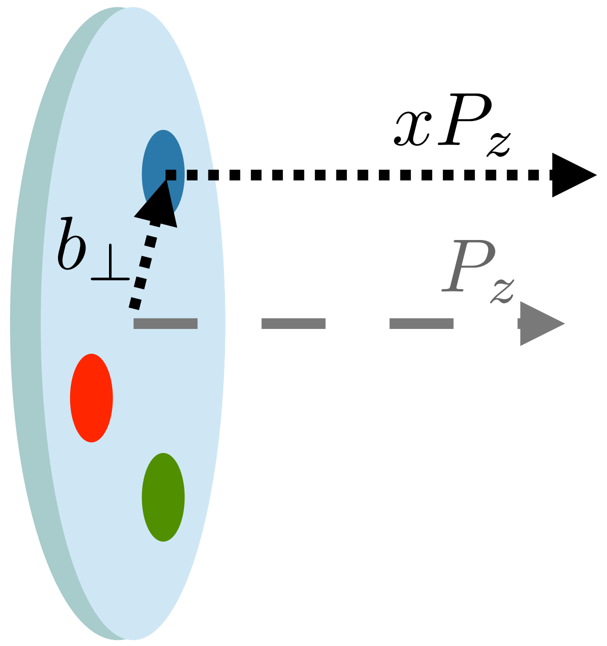

Deeply virtual Compton scattering
→ sensitive to quarks (and gluons)

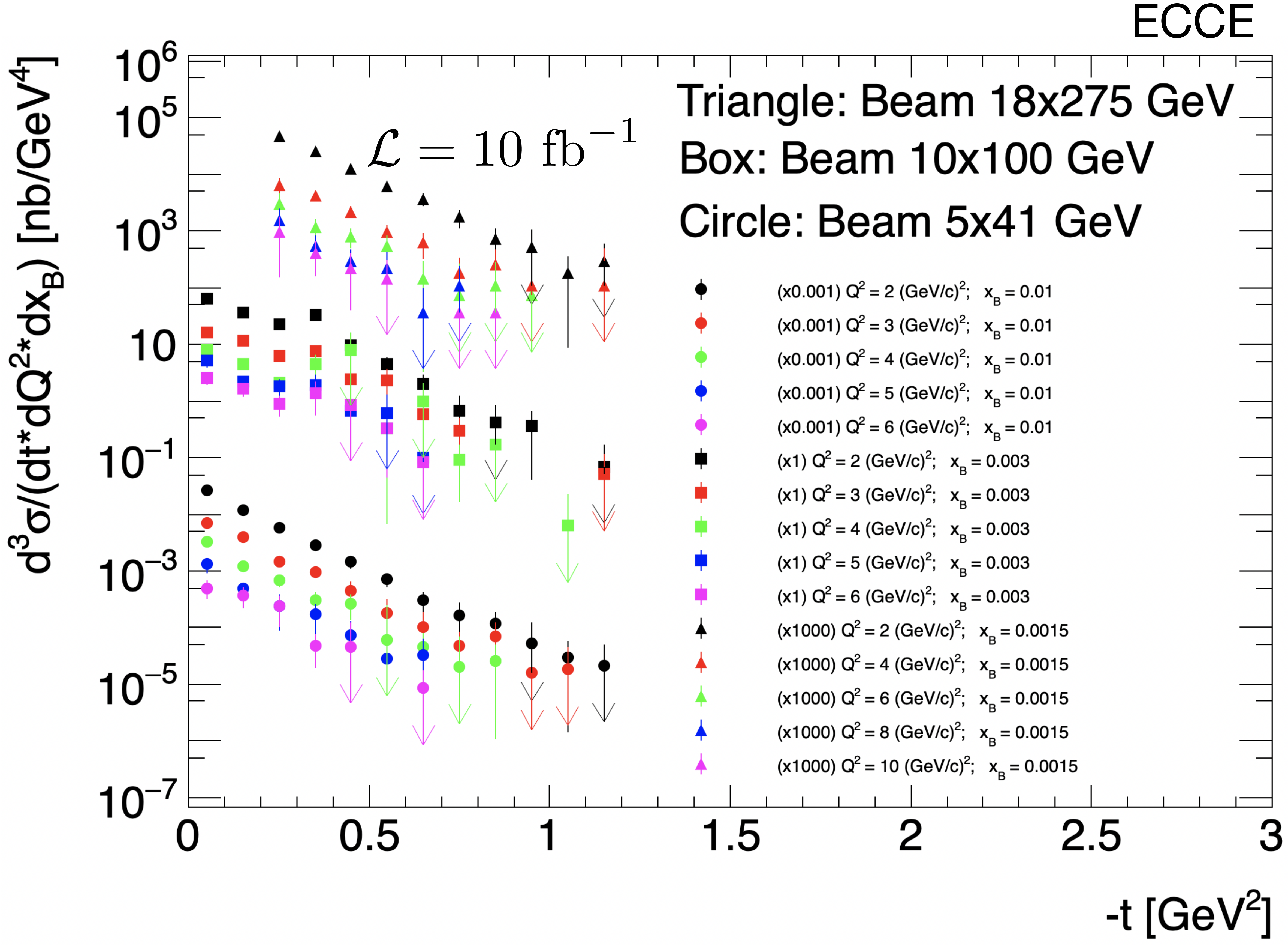

Exclusive J/ψ production
→ excellent to probe gluon GPDs

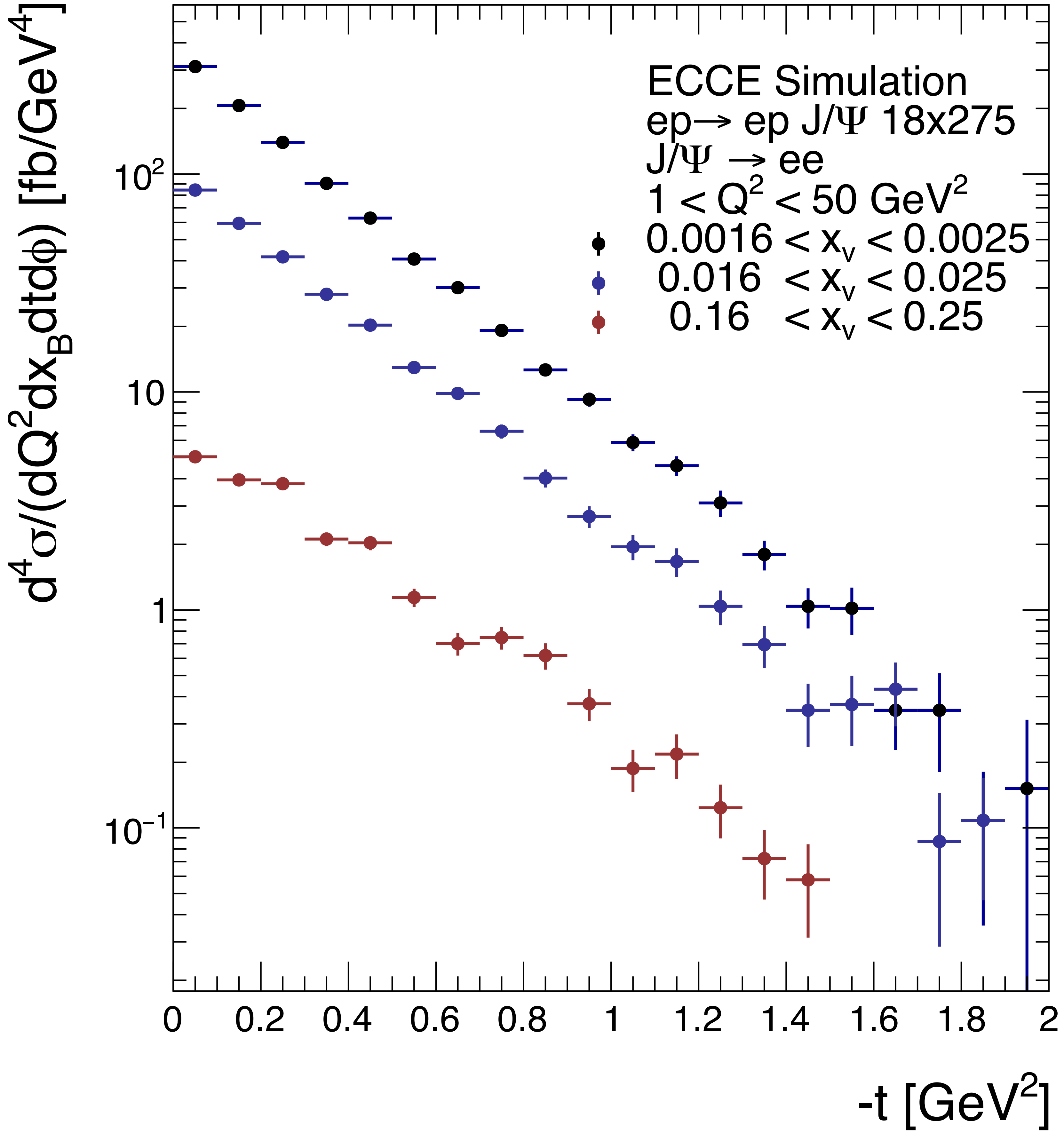

Exclusive measurements on nuclear targets

What object are we probing?

Exclusive measurements on nuclear targets

What object are we probing?

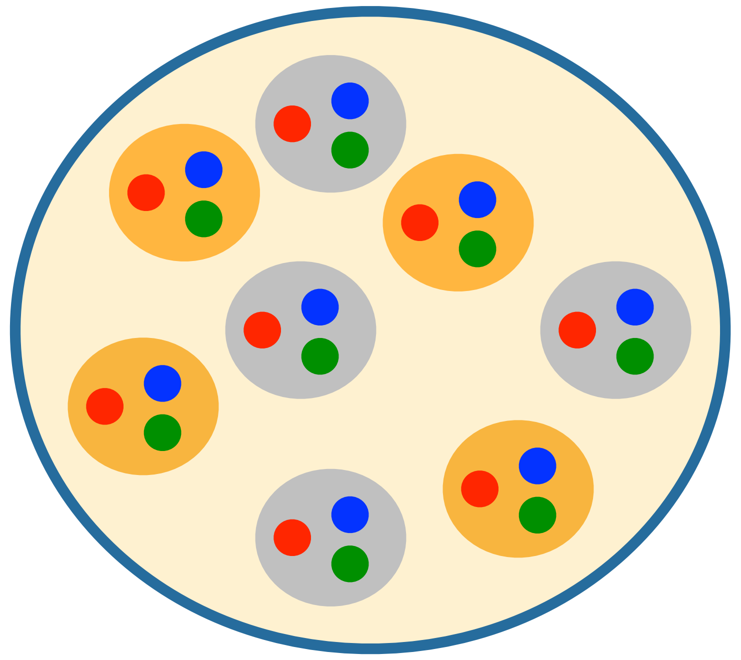

Exclusive measurements on nuclear targets

What object are we probing?

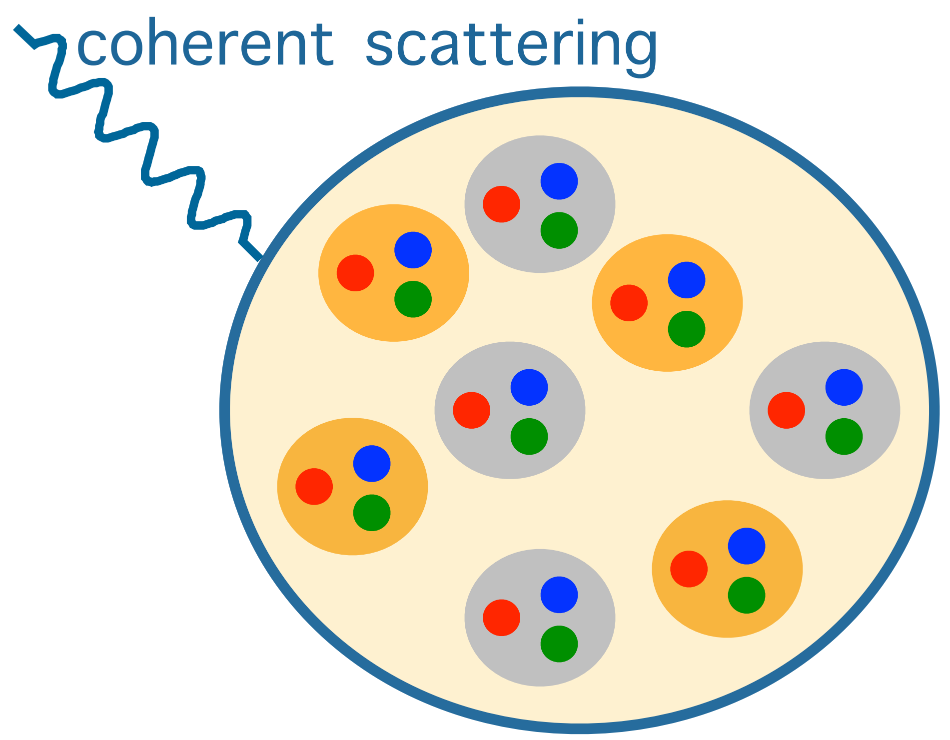

Coherent interaction: interaction with target as a whole.
~ target remains in same quantum state.

Exclusive measurements on nuclear targets

What object are we probing?

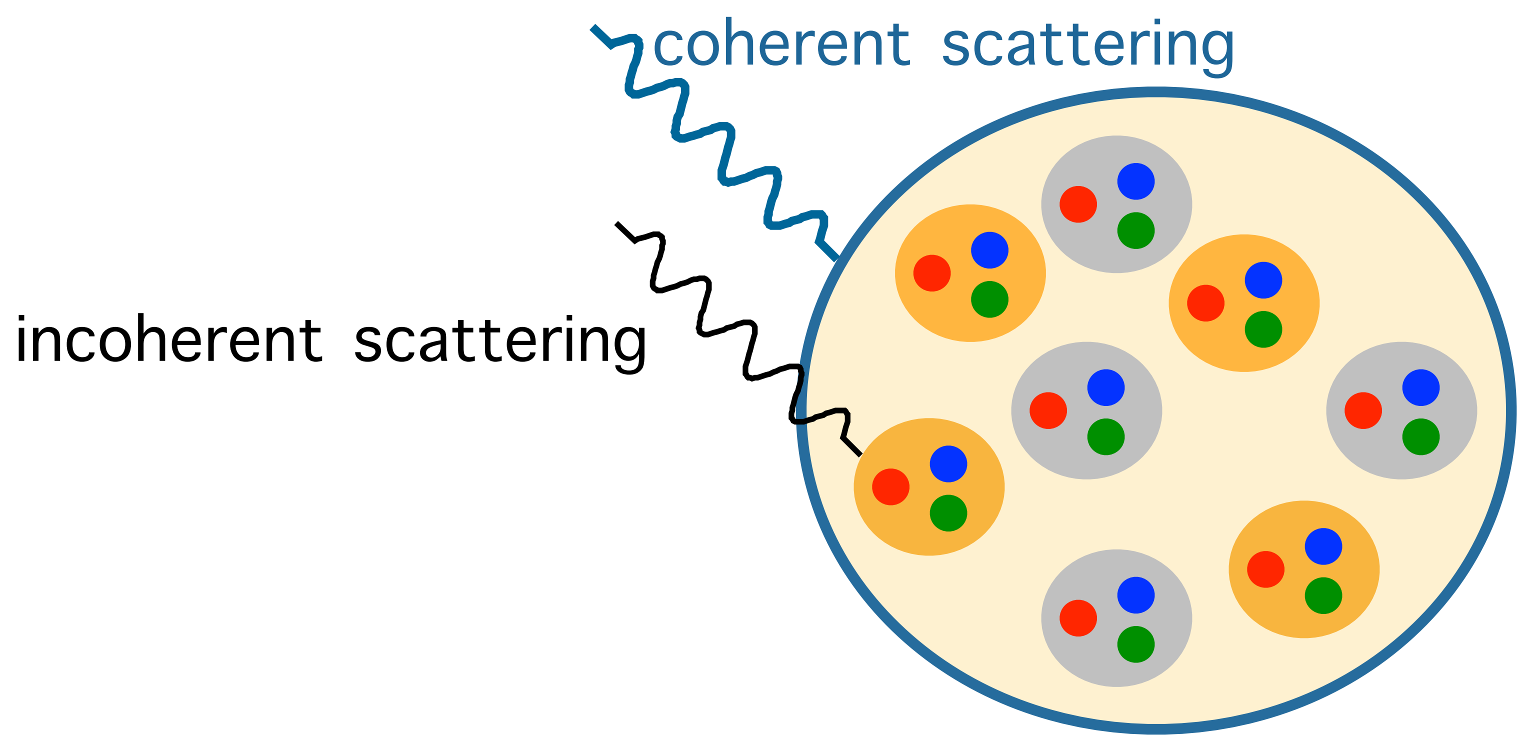

Coherent interaction: interaction with target as a whole.
~ target remains in same quantum state.

Incoherent interaction: interaction with constituents inside target.
~ target does not remain in same quantum state.
Ex.: target dissociation, excitation

Exclusive measurements on nuclear targets

What object are we probing?

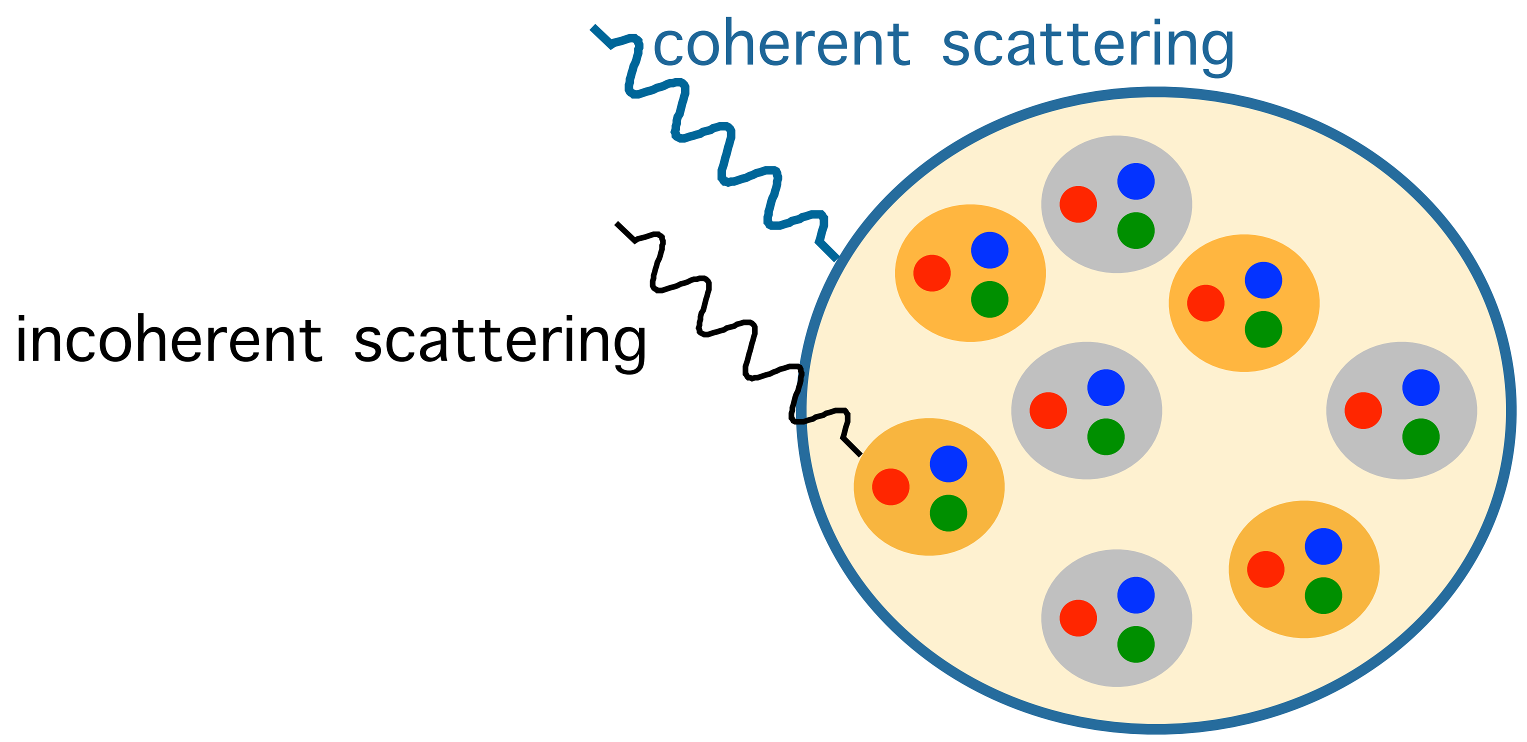

Coherent interaction: interaction with target as a whole.
~ target remains in same quantum state.

Incoherent interaction: interaction with constituents inside target.
~ target does not remain in same quantum state.
Ex.: target dissociation, excitation

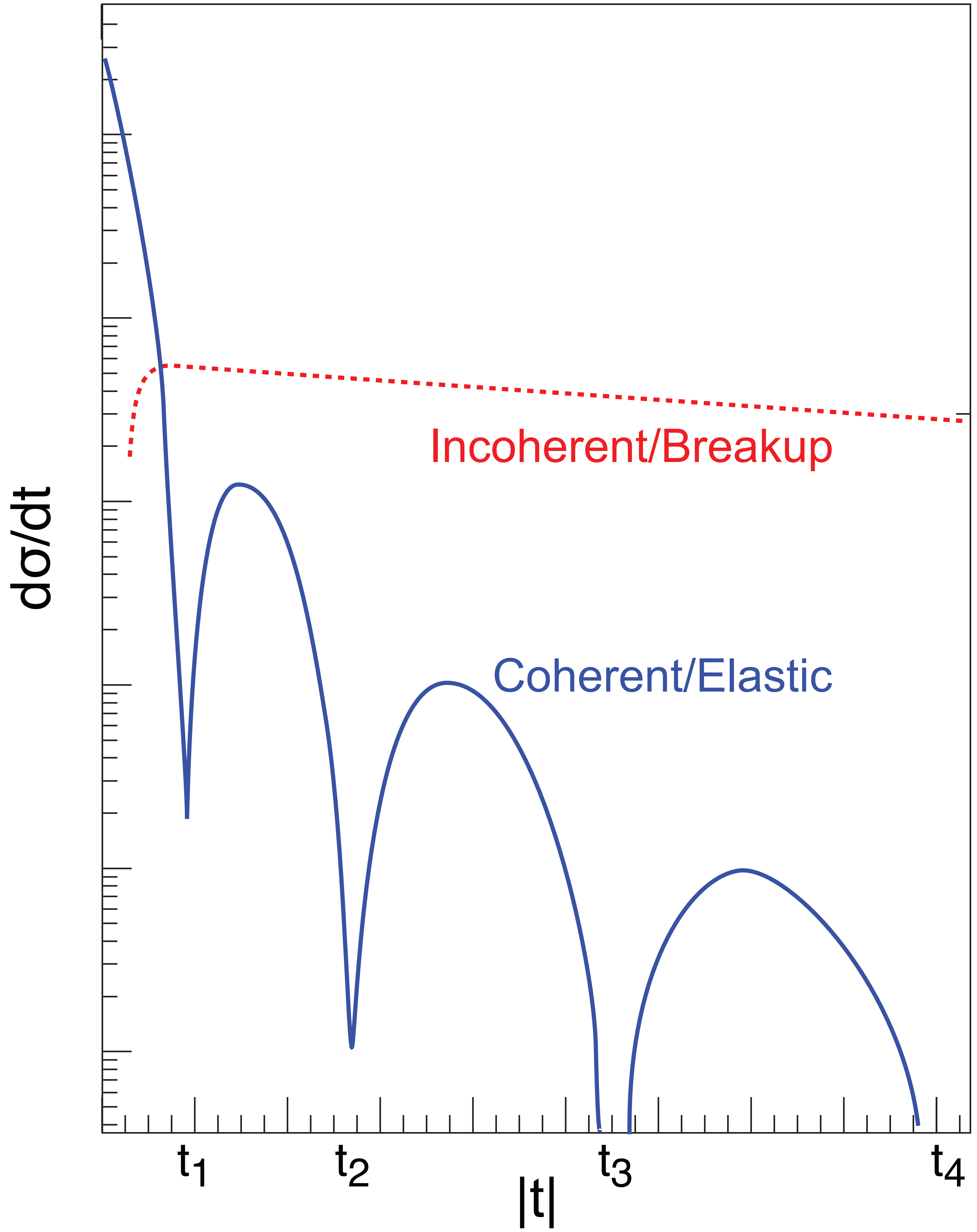

Coherent eA production

→ probe gluon saturation

→ nuclear imaging in position space:

$$\int_0^{\infty} d\Delta_\perp \; \mathrm{GPD}(x, 0, \Delta_\perp)\; e^{-ib_\perp \Delta_\perp}$$

Experimentally limited by maximum transverse momentum.
Need measured p_T range as extended as possible.
~third diffractive minimum.

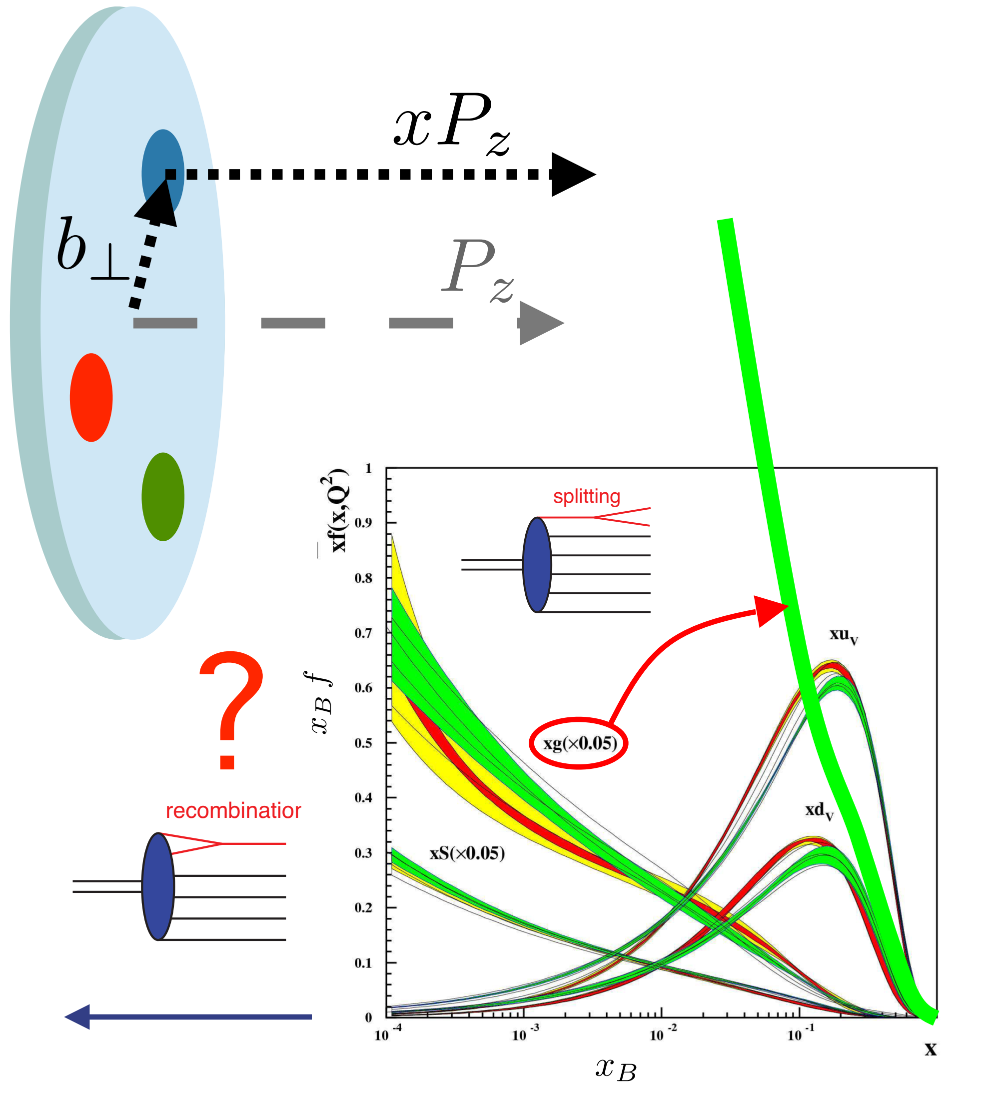

Coherent eA production

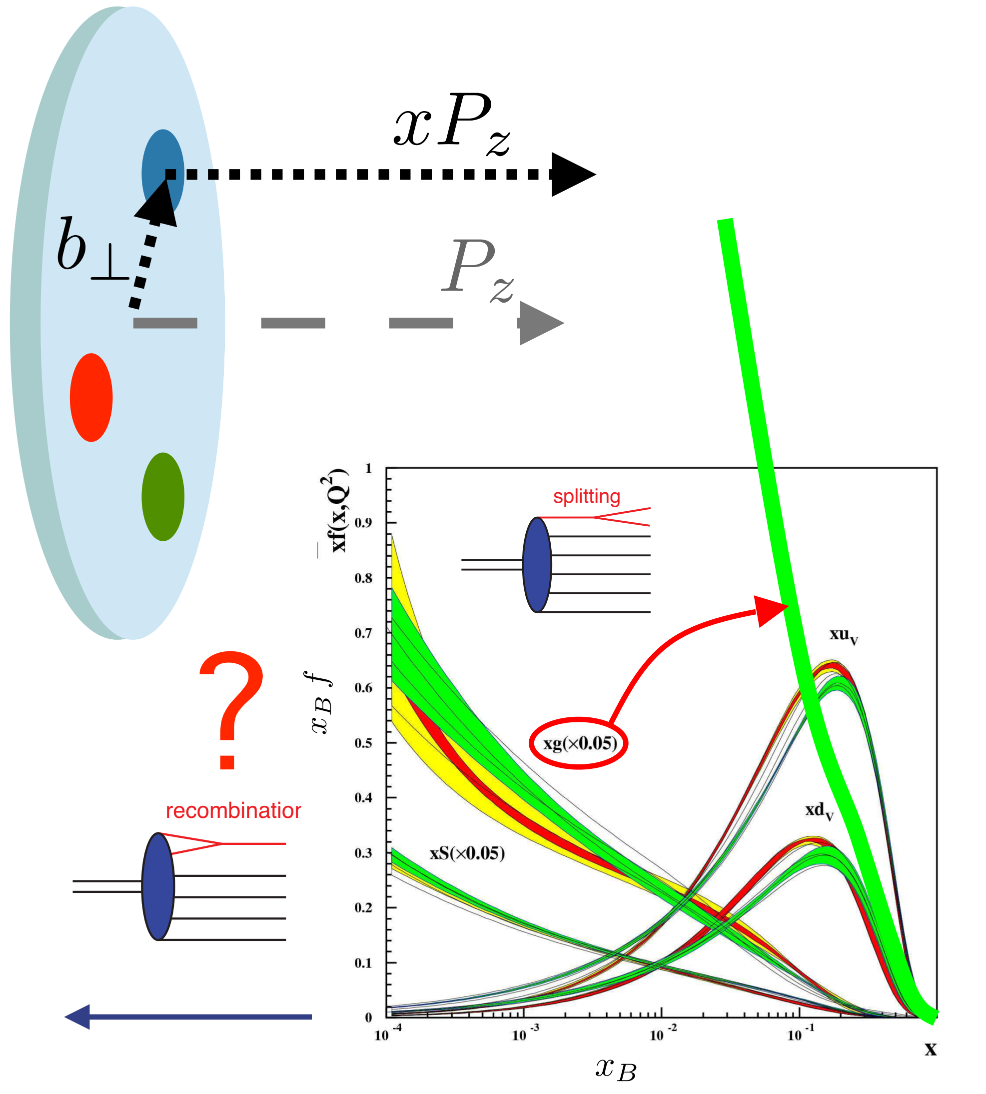

→ probe gluon saturation

→ nuclear imaging in position space:

$$\int_0^{\infty} d\Delta_\perp \; \mathrm{GPD}(x,0,\Delta_\perp)\; e^{-ib_\perp \Delta_\perp}$$

Experimentally limited by maximum transverse momentum.
Need measured p_T range as extended as possible.
~third diffractive minimum.

Toll, Ulrich, PRC **87** (13) 0249

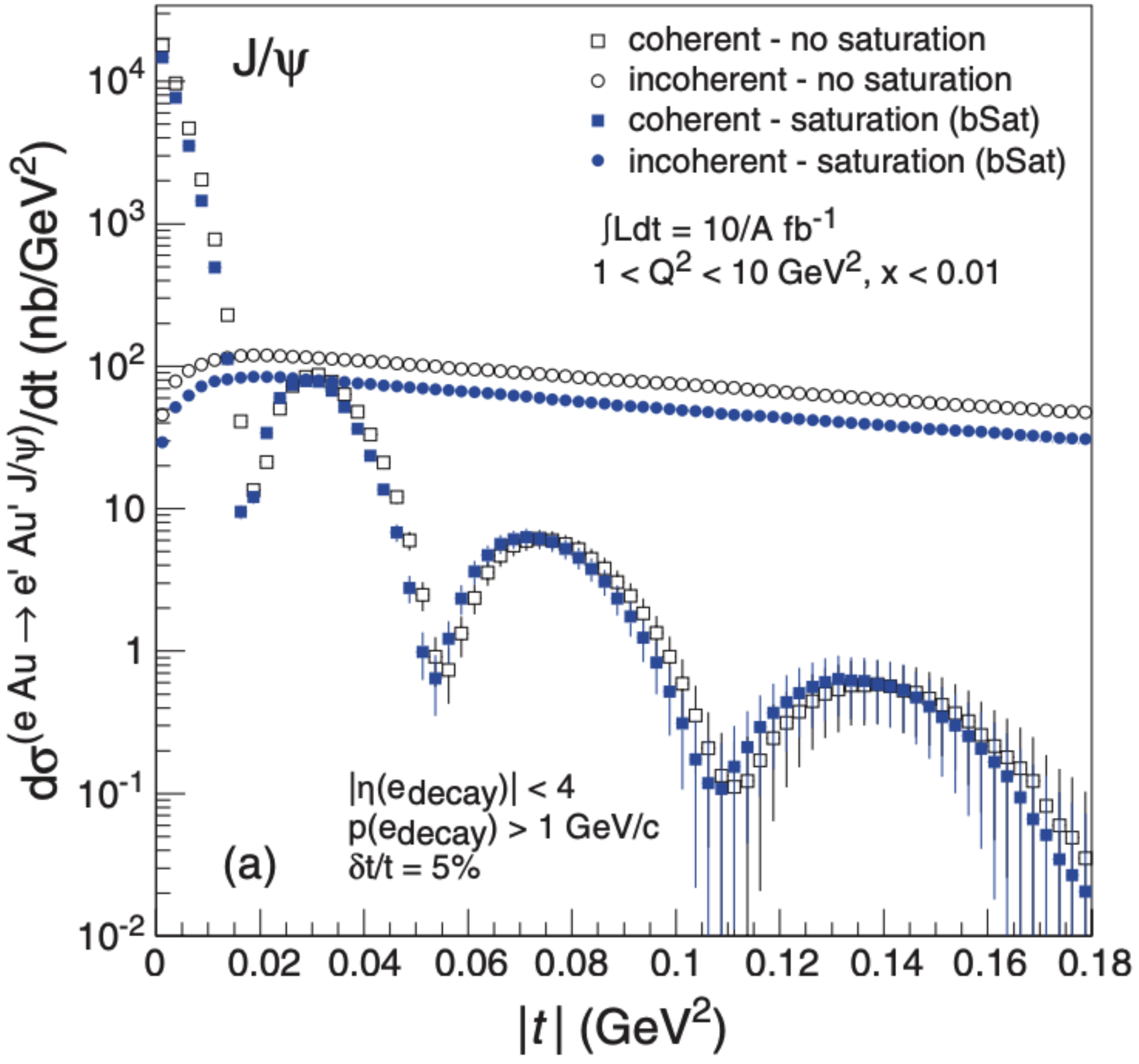

→ resolving minima is crucial

- Need 90%, 99%, and > 99.8% veto efficiency for incoherent production, for the respective minima at increasing t.

- veto of events where nuclei break up
  → use entire far-forward detector systems

- Need precise determination of t

- reconstruction via scattered lepton and exclusively produced vector meson/photon

Incoherent production

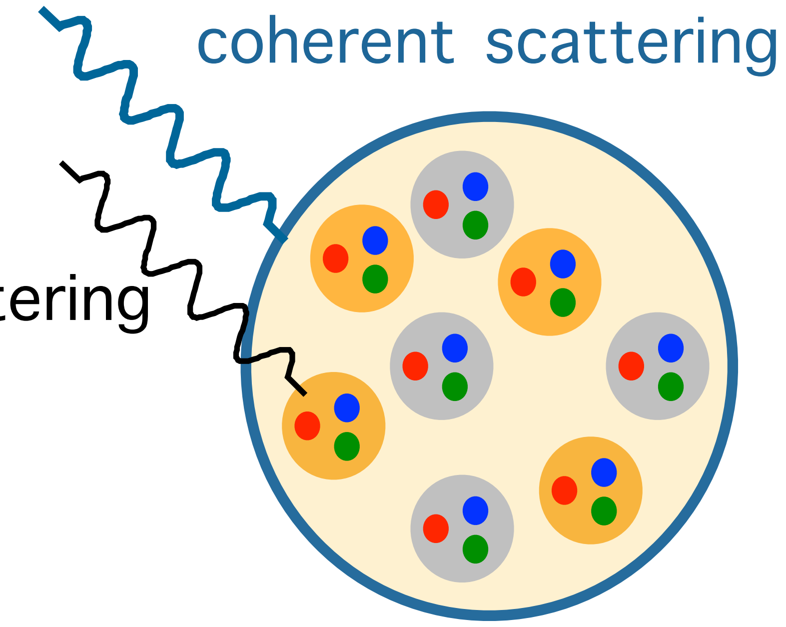

$$\sigma_{\text{tot}} \sim \langle |A|^2 \rangle$$

average over amplitudes squared

$$\sigma_{\text{coh}} \sim |\langle A \rangle|^2$$

average amplitude over target configurations:
probes average distributions

$$\sigma_{\text{incoh}} \sim \sum_{f \neq i} |\langle f|A|i\rangle|^2$$

$$= \sum_f \langle i|A|f\rangle^\dagger \langle f|A|i\rangle - \langle i|A|i\rangle^\dagger \langle i|A|i\rangle$$

$$= \left(\langle |A|^2 \rangle - |\langle A \rangle|^2 \right)$$

Incoherent
= difference between both:
probes event-by-event fluctuations

Incoherent production

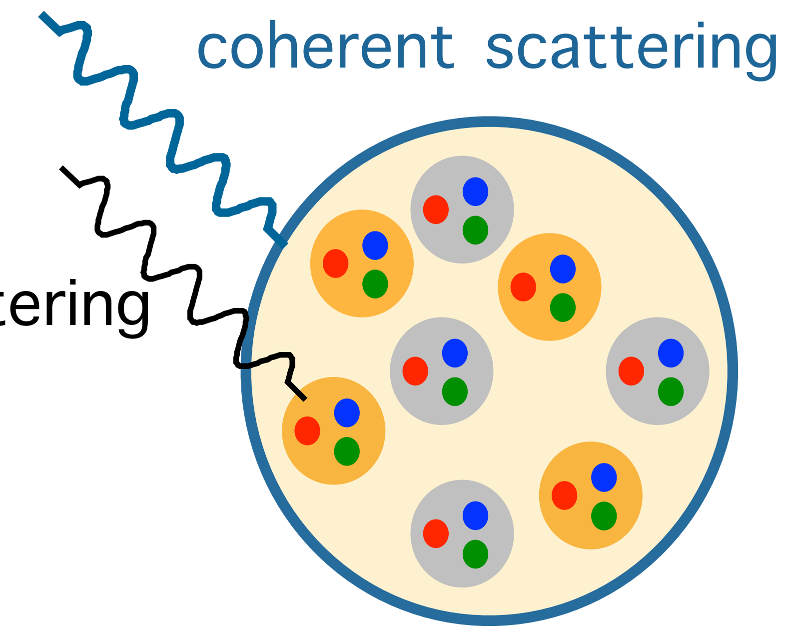

$$\sigma_{\rm tot} \sim \langle |A|^2 \rangle$$

average over amplitudes squared

$$\sigma_{\rm coh} \sim |\langle A \rangle|^2$$

average amplitude over target configurations:
probes average distributions

$$\sigma_{\rm incoh} \sim \sum_{f \neq i} |\langle f|A|i\rangle|^2$$

$$= \sum_f \langle i|A|f\rangle^\dagger \langle f|A|i\rangle - \langle i|A|i\rangle^\dagger \langle i|A|i\rangle$$

$$= \left(\langle |A|^2 \rangle - |\langle A \rangle|^2 \right)$$

Incoherent
= difference between both:
probes event-by-event fluctuations

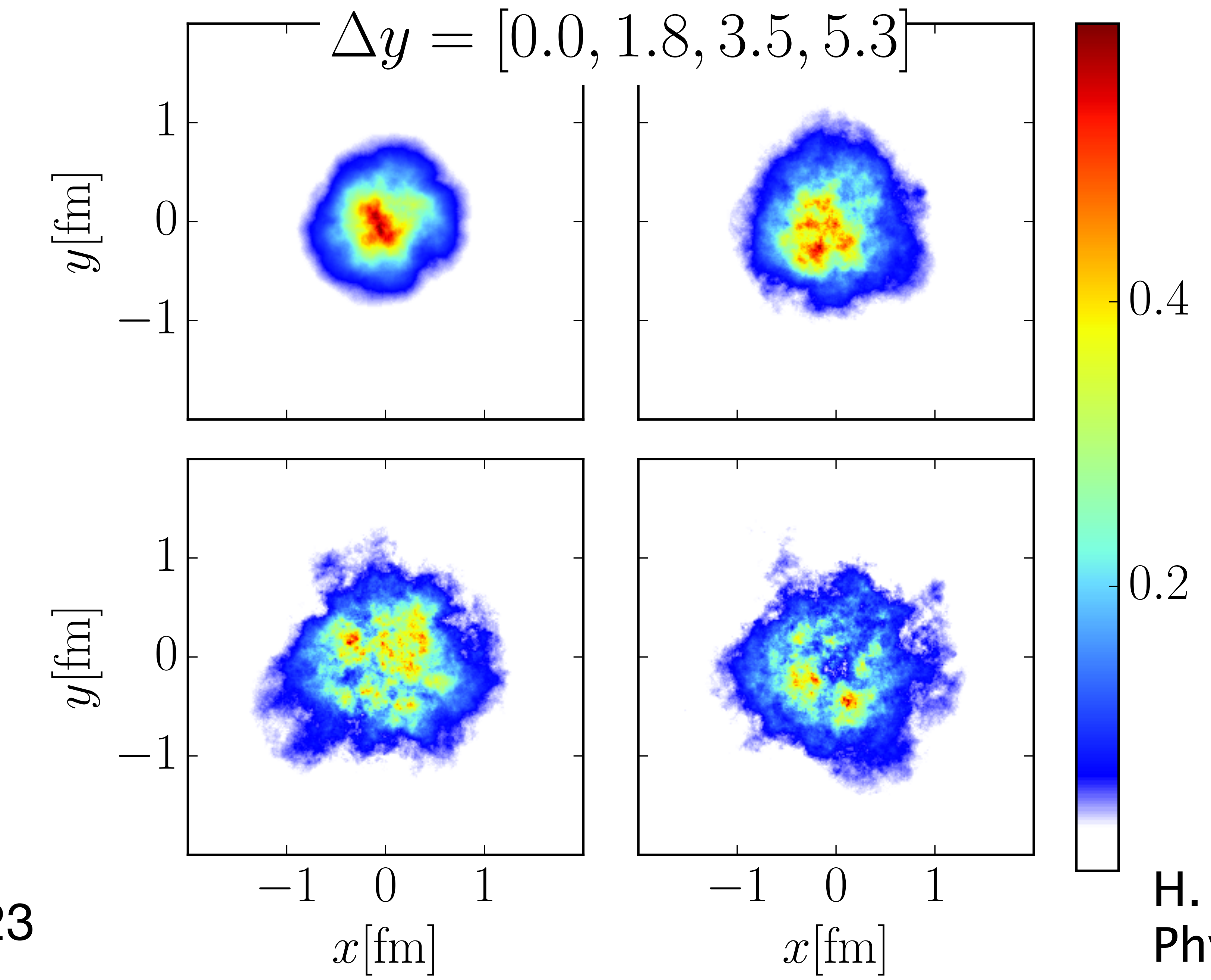

H. Mäntysaari and B. Schenke.
Phys. Rev. D 98, 034013 (2018)

Exclusive measurements on A with the EIC

K. Tu, DIS 2023

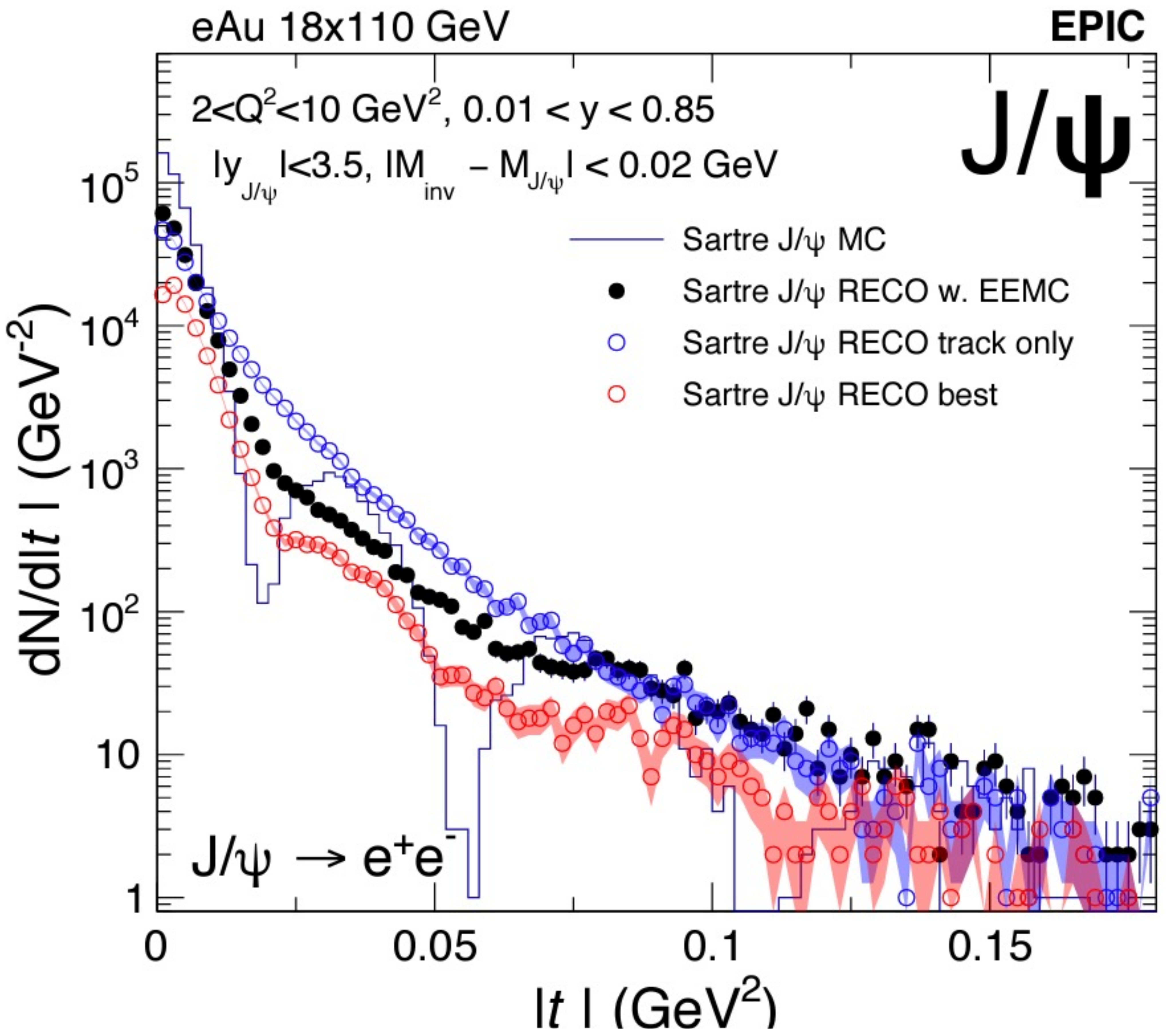

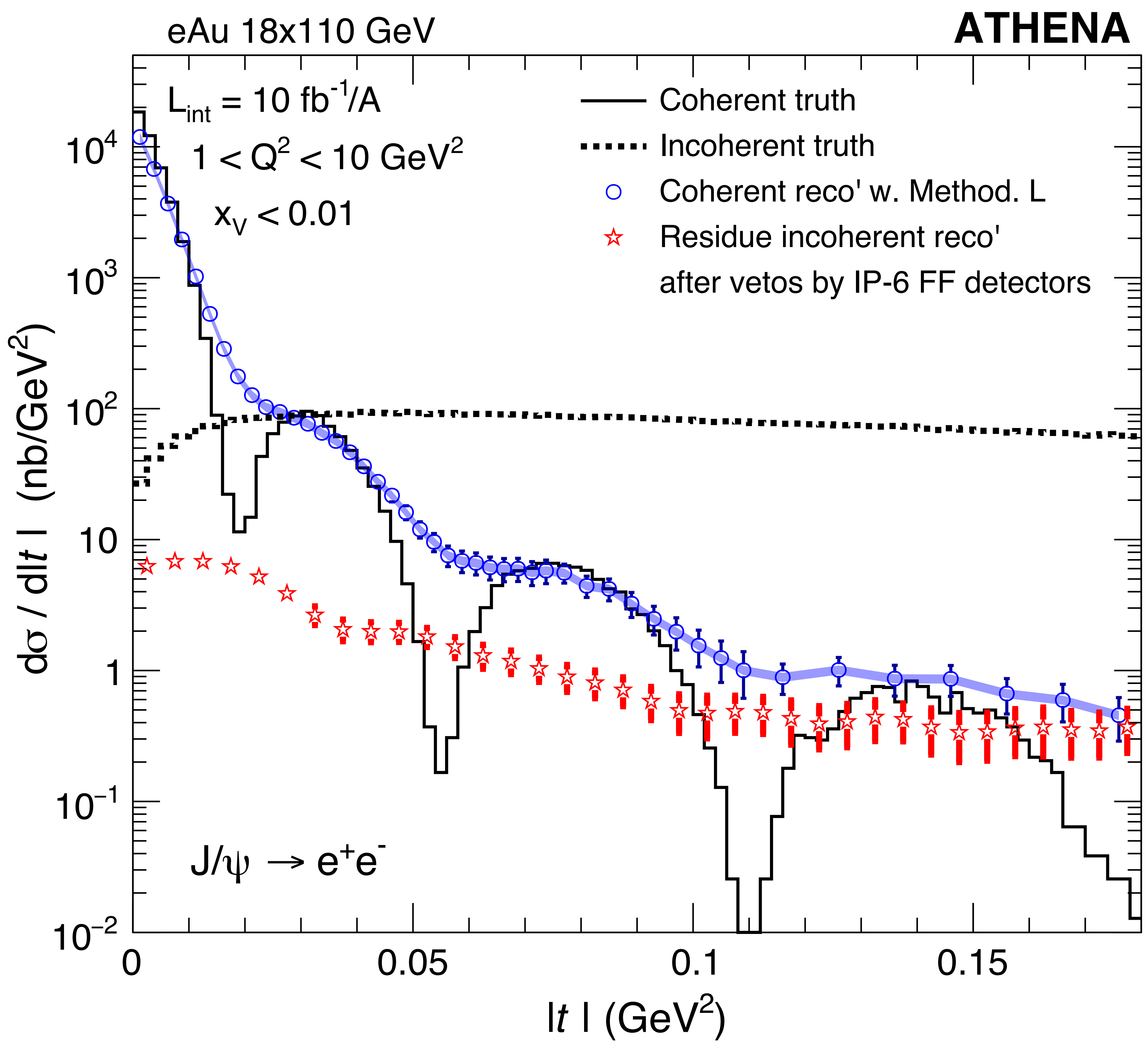

Summary

EIC with ePIC can address various aspects of the nucleon and nuclear structure through:

- Precise inclusive (spin-dependent) DIS measurements via high-resolution EM calorimeters.
- Measurements for 3D (spin-dependent) tomography in momentum space provided by good Cherenkov-based and TOF AC-LGAD hadron PID detectors and tracking.
- Exclusive measurements on protons, using the far-forward detector system
- Diffractive and exclusive measurements with coherent/incoherent separation via very precise EM calorimeters and far-forward detector system.
- Quarkonium production offers large possibility to study hadron structure and quarkonium production

⟶ Possibilities for ePIC with current design and muon detection for second detector need to be investigated!